

Large- and Microscale Community Structure and Abundance of Microalgae in the Coorong Lagoons, South Australia

Eloise Ann Prime

Bachelor of Science in Marine Biology (Hons)

Thesis submitted to the School of Biological Sciences, Faculty of Science and
Engineering, Flinders University in fulfilment of the requirements for the
degree of Doctor of Philosophy

September 2016



Flinders
UNIVERSITY

“Few objects are more beautiful than the minute siliceous cases of the diatomaceæ: were these created that they might be examined and admired under the higher powers of the microscope? The beauty in this latter case, and in many others, is apparently wholly due to symmetry of growth.”

- Charles Darwin
The Origin of Species (1872)

Table of Contents

Table of Contents	2
Summary.....	7
Declaration	9
Acknowledgements	10
List of Figures.....	11
List of Tables	14
Chapter 1: Introduction	15
<i>Microeukaryotes in Aquatic Environments.....</i>	<i>16</i>
Phytoplankton (Microalgae in the Water Column).....	16
Microphytobenthos (Microalgae of the Benthos).....	19
Diatoms	20
<i>Microscale Interactions</i>	<i>23</i>
<i>Study Site.....</i>	<i>24</i>
<i>Microbial Interaction Networks.....</i>	<i>25</i>
<i>Aims and Structure of the Thesis</i>	<i>26</i>
Chapter 2: Phytoplankton Dynamics under Drought Conditions in an Inverse Estuary	28

<i>Graphical Abstract</i>	29
<i>Abstract</i>	30
<i>Introduction</i>	31
<i>Methods</i>	33
Study Sites	33
Environmental Parameters	35
Dissolved Nutrient Analysis	35
Chlorophyll <i>a</i> Analysis	36
Phytoplankton Sampling and Abundance.....	36
Phytoplankton Diversity	36
Statistical Analysis.....	37
<i>Results</i>	38
Environmental Parameters	38
Dissolved Nutrients.....	42
Chlorophyll <i>a</i> Concentration.....	45
Phytoplankton Abundance	46
Phytoplankton Diversity	50
Correlations Between Communities of the North and South Lagoons.....	51
<i>Discussion</i>	54
The South Lagoon.....	54
The North Lagoon.....	56
<i>Conclusion</i>	58
<i>Chapter 2 Supplementary Material</i>	59

Chapter 3: Microscale Variation of Microbial Eukaryotic Communities Revealed by 18S Sequencing..... 62

Abstract..... 63

Introduction..... 64

Methods..... 65

 Study Site 65

 Sample Collection..... 67

 Bioinformatics and Data Analysis 69

Results..... 70

 Microscale OTUs 70

 Correlations with Chlorophyll 72

 Species Similarity between Microscale Sites 73

Discussion..... 77

 Comparison of Taxonomy and Chlorophyll Concentration..... 77

 Community Taxonomical Variations at the Microscale 78

Conclusion 80

Chapter 3 Supplementary Material 81

Chapter 4: Marine microbial benthic community interactions along a hypersaline microscale transect 120

Abstract..... 121

Introduction..... 122

<i>Results and Discussion</i>	124
<i>Chapter 4 Supplementary Material</i>	134

Chapter 5: Microscale Variation of Diatom Frustule Length in the Microphytobenthos
..... **141**

<i>Abstract</i>	142
<i>Introduction</i>	143
<i>Methods</i>	145
Study Site	145
Sample Collection.....	148
Chlorophyll Analysis	148
Microscopy	149
Statistical Analysis.....	149
Descriptive Statistics.....	149
Spatial Autocorrelation, Moran’s I	150
Spatial Autocorrelation, Geary’s C.....	151
Network Analysis.....	151
<i>Results</i>	152
Frustule Length	152
Chlorophyll Concentrations	158
Spatial Autocorrelation	158
Chlorophyll and Frustule Length Correlations	159
Network Analysis.....	161

<i>Discussion</i>	164
Chlorophyll Concentration Variation	164
Spatial Autocorrelation, Skewness and Kurtosis of Frustule Length	165
Network Analysis of Frustule Length.....	166
<i>Conclusion</i>	168
Chapter 6: Discussion	169
<i>Overview</i>	170
<i>Large Scale Phytoplankton</i>	171
<i>Microscale Microphytobenthos</i>	172
<i>Insights to the Microbial Community using Network Analysis</i>	175
<i>Future Directions</i>	176
<i>Conclusion</i>	176
Bibliography	178
Appendices	207
Appendix I	208
Appendix II.....	216

Summary

Microbial communities are composed of prokaryotic and eukaryotic organisms and form the basis of aquatic food webs. These microbial communities show seasonal patterns on spatial and temporal scales in the tens of metres to kilometres, known as the large scale. However, community interactions between these organisms occur on the micrometre to centimetre scale, known as the microscale. The dominant eukaryotes are phototrophic microalgae, commonly referred to as phytoplankton or, if on the bottom, the microphytobenthos. Of particular interest in this thesis are the diatoms, a ubiquitous and the most abundant group of eukaryotic phytoplankton which are characterised by their species specific shell-like structures, called frustules. Diatoms are of particular importance globally because they are estimated to produce up to 20% of global oxygen. Additionally, changes in species composition and abundances provide a reliable indication of ecosystem structure and have been used to assess changes in water quality on time scales, from seasonal to decadal.

The primary focus of this thesis is to investigate the variation in phytoplanktonic communities at the large scale and microphytobenthic communities at the microscale in the Coorong Lagoons, South Australia. In Chapter 2, the environmental parameters that influence phytoplankton communities are determined across large scale temporal and spatial distances, taking into account the impact of wind. It was shown that within the south lagoon phytoplankton composition were influenced by wind speed and in the north lagoon were influenced by water parameters such as pH and concentration of dissolved nutrients. Microscale variation of the microphytobenthos was also investigated. In Chapter 3, taxonomic analysis of the microphytobenthos was compared to chlorophyll concentrations at microscale distances. Here, it was found that haptophytes showed the only positive and significant relationship with chlorophyll *a*, suggesting that haptophytes are contributing to the

chlorophyll biomass. However, it is shown that it is the diatoms which show the strongest interactions with the ciliates and a group of unknown microeukaryote. Therefore, suggesting that the diatoms are a keystone group within the microbial community. These interactions in the microphytobenthos was further explored in Chapter 4 using metagenomics in order to take into account both the prokaryote and eukaryote populations to determine the key taxa influencing the communities. Network analysis was used to demonstrate that while bacteria show relative abundances that are up to one order of magnitude greater than the microeukaryotes, it is in fact the diatoms that provide crucial links between the anaerobic bacteria and other eukaryotes. A final study, Chapter 5, investigated how the frustule lengths of two diatom species vary over microscale distances. Using the concept of body length as an indicator of life stage or life cycle, variation in distribution frustule length distribution was assessed for the pennate diatoms *Amphora hyalina* and *Cocconeis costata*. The results for this chapter suggested that there is not only microscale variability of frustule length within populations of diatoms, but the changes in skewness of these populations indicate that this variability may be explained by predation, which is supported by the importance of ciliates and diatoms observed in Chapter 3.

The findings of this thesis provide insight to large- and microscale variation within eukaryotic communities. In the large scale study the importance of local environmental factors such as wind speed and nutrient concentration is revealed for the abundance and diversity of diatoms and dinoflagellates. Furthermore, microscale interactions in microbial eukaryotes show the impact of diatoms within microbial food webs, which are grazed upon by ciliates and other predatory protists, when assessing the taxa present. These findings were further supported by the heterogeneous distribution of diatom frustule lengths, showing patches that favour larger cell sizes which is suggested to be a direct result of predation.

Declaration

I certify that this thesis does not incorporate without acknowledgment any material previously submitted for a degree or diploma in any university; and that to the best of my knowledge and belief it does not contain any material previously published or written by another person except where due reference is made in the text.

Eloise Ann Prime

20 September 2016

Acknowledgements

First and foremost, I am extraordinarily grateful to my supervisors, Professor Jim Mitchell and Dr Sophie Leterme of Flinders University, South Australia. I would never have been able to start or finish without their guidance and support throughout my candidature.

Next, I wish to thank everyone from the Microbial Systems Lab, particularly those who helped me with all my field studies. These were long and intense days working in the Coorong that all turned out to be a lot of fun even when faced with winter storms. Your willingness to volunteer is appreciated without reserve. So many thanks go to Tamsyne Smith-Harding, Dr Kelly Newton, Dr James Paterson, Dr Virginie van Dongen-Vogels, Adrian Tableau, Delphine Rochais, Dr Thomas Jeffries, Kathryn Stoneburner, Dr Rachel Pillar, Dr Coraline Chapperon, Karina Winn and Carolyn Dannaoui. I wish to add a special thank you to Jody McKerral, whose help with network analysis has been more appreciate than I can say. Likewise to Dr Renee Smith and Dr Shanan Tobe, your help with sequencing was invaluable.

I wish to thank those from the lab who have helped to keep me going throughout the trials and tribulations that come with researching for a PhD. I am proud to count you as friends. Thank you especially to: Dr Lisa Dann, Jessica Carlson-Jones and Tamsyne Smith-Harding.

Finally, I need to thank my family and friends who have helped me through. I particularly want to thank my parents, Colin and Elisa, and my aunty, Rose. I also want to thank my big sister, Carolyn, and by extension, Rami and Azure. Last, but certainly never least, a big thank you to my best friend, Rhiannon. All of you have not only helped me through my PhD, but you have also helped me cope when I was diagnosed with a brain tumour during my candidature. In many ways it became as big a part of my life as my research. In more ways than one you have kept me sane through my treatment, recovery and PhD research, as well as putting up with my numerous mood swings, whether these were related to my PhD, tumour or both.

List of Figures

Chapter 1

Figure 1. Extant lineages of microeukaryotes.	17
Figure 2. Life cycle of pennate diatoms.....	22

Chapter 2

Graphical Abstract: used for submission to Estuarine, Coastal and Shelf Research	29
Figure 1. Map of Large Scale study sites, Coorong Lagoons, South Australia.....	34
Figure 2. Environmental parameters at 5 Coorong study locations.....	39
Figure 3. Mean daily wind speed at 5 Coorong study locations.....	41
Figure 4. Mean dissolved nutrients concentration at 5 Coorong study locations	43
Figure 5. Chlorophyll <i>a</i> concentration at 5 Coorong study locations	46
Figure 6. Phytoplankton abundances at 5 Coorong study locations	49
Figure 7. Phytoplankton diversity index at 5 Coorong study locations.....	50
Figure 8. Principal Components Analysis of biotic and abiotic factors at 5 Coorong study locations	58

Chapter 3

Figure 1. Sampling location map for microscale study, Salt Creek, South Australia.....	66
Figure 2. Microscale sampling strategy diagram.....	68

Figure 3. Percentage contribution of selected Chromalveolata groups to microscale sampling locations	72
Figure 4. Principle Coordinate Analysis for identified microeukaryotes from 18S OTUs	74
Figure 5. Interaction Network Analysis for identified groups of microeukaryotes from 18S OTUs.....	76
Figure S3. Percentage contribution of Eukaryote kingdoms and protest supergroups to microscale sampling locations	117
Figure S4. Mean chlorophyll <i>a</i> , chlorophyll <i>c</i> and total chlorophyll concentration for microscale sampling locations	118
Figure S5. CLUSTER Analysis of 18S OTUs samples by Class at 10 microscale sampling locations	119

Chapter 4

Figure 1. Total chlorophyll concentration within a 1 m ² quadrat	125
Figure 2. Rank abundance from metagenomic sequencing of a microscale transect	128
Figure 3. Interaction network analysis of taxonomic classes from metagenomic sequencing of a microscale transect	131
Figure S1. Sampling location map for microscale study, Salt Creek, South Australia	135
Figure S2. Microscale sampling strategy for total chlorophyll concentration and metagenomic sequencing	136

Chapter 5

Figure 1. Sampling location map for microscale study, Salt Creek, South Australia.....	147
Figure 2. Contour map and Frequency distribution for <i>Amphora hyalina</i> frustule length	153
Figure 3. Contour map and Frequency distribution for <i>Cocconeis costata</i> frustule length	154
Figure 4. Skewness and kurtosis of <i>Amphora hyalina</i> frustule length	156
Figure 5. Skewness and kurtosis of <i>Cocconeis costata</i> frustule length	157
Figure 6. Contour map of mean chlorophyll <i>a</i> and chlorophyll <i>c</i> concentration.....	158
Figure 7. Contour map of Spearman correlation between frustule length and chlorophyll concentration.....	160
Figure 8. Interaction network analysis of frustules length descriptive statistics	162

List of Tables

Chapter 2

Table S1. Mean dissolved nutrient concentration.....	60
--	----

Chapter 3

Table S1.18S sequence summary	82
Table S2.18S OTU absence/presence table	83

Chapter 4

Table S3. Metagenomics sequence summary	137
Table S4. Bacterial relative abundances	138
Table S5. Eukaryote relative abundances	139

CHAPTER 1

Introduction

Microeukaryotes in Aquatic Environments

Phytoplankton (Microalgae in the Water Column)

Phytoplankton is the term given to photosynthetic microeukaryotes which occupy the water column. These unicellular organisms are ubiquitous to aquatic environments where there are adequate light and dissolved nutrient concentrations (Whitman *et al.* 1998). Classes of phytoplanktonic include dinoflagellates, diatoms, ciliates and green algae from the Chromalveolates, in addition to chlorophytes and euglenoids (Figure 1).

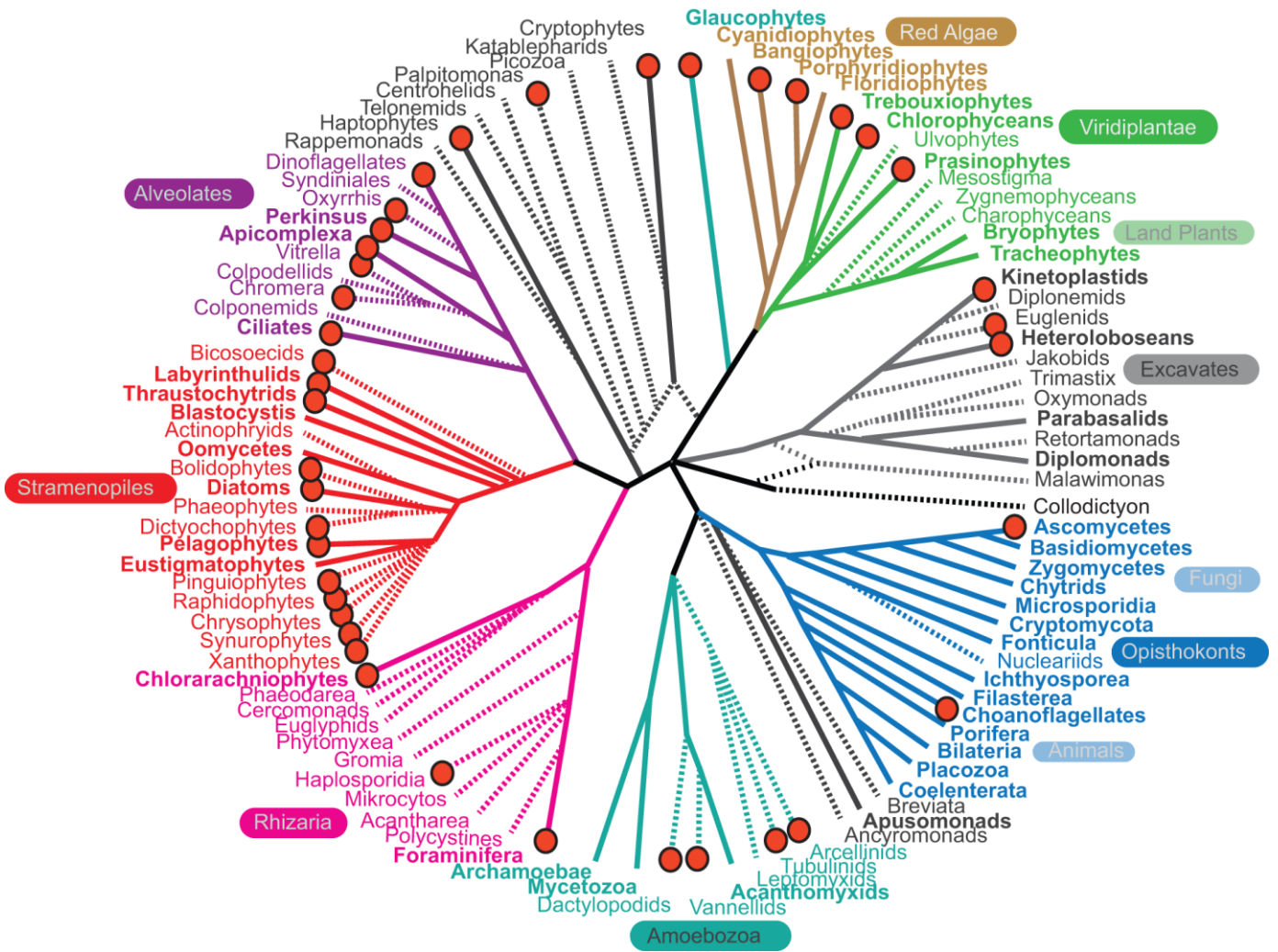


Figure 1. Schematic diagram of the major extant lineages of microeukaryotes obtained through sequencing, displaying the relationships between lineages from the Marine Microbial Eukaryote Transcriptome Sequencing Project (MMETSP). Solid line indicates lineages with complete genomic sequences according to the GOLD database, and incomplete sequences are indicated by dashed lines. Lineages from the MMETSP project where sequencing of the transcriptome is completed or underway at the time of publication is indicated with the red dots. **Source: Keeling *et al.* 2014.**

The structure and diversity of phytoplankton communities has been studied worldwide in a number of aquatic systems such as in estuaries (e.g. Buric *et al.* 2007, Jendyk *et al.* 2015), the open ocean (e.g. Meyer *et al.* 2016) and lakes (e.g. Kissman *et al.* 2013, Liu *et al.* 2013). Nutrient concentrations have been demonstrated to impact on the species abundance and composition of the phytoplankton communities (Kissman *et al.* 2013, Ly *et al.* 2014). Phytoplankton blooms are generally driven by high concentrations of phosphate and/or nitrogen (Domingues *et al.* 2015, Burson *et al.* 2016), and once the limiting nutrient is depleted the blooms recede (Jin *et al.* 2013). Additionally, Burson *et al.* (2016) demonstrated that different species of phytoplankton are limited by different nutrients, where reductions of phosphorous loads without reducing nitrogen loads suppress *Phaeocystis* blooms. However, nutrients are not the only limiting factor of phytoplankton communities.

Comparison between different environments and locations shows that community composition and bloom dynamics do not follow a general model, and are instead regulated by a number of site-specific biological and physical processes where species adapt to local changes in conditions (Thomas *et al.* 2012, Wyatt *et al.* 2014, Carstensen *et al.* 2015). Temperature and salinity are known to impact productivity and growth rate (Larson and Belovsky 2013, Quigg *et al.* 2013). In coastal ecosystems, freshwater discharge not only transports nutrients into the water column but also determines salinity, meaning that it is one of the primary influencers on local phytoplankton communities (Cloern and Dufford 2005, Thomas *et al.* 2012). However, it is possible that these parameters may induce species specific responses for individual species (Carstensen *et al.* 2015). Boyd *et al.* (2013) used species and strains isolated from various sites in the world's oceans, to show that there were differences at the genus and species level for the optimal temperature for cell growth and population abundances (Boyd *et al.* 2013). Carstensen *et al.* (2015) observed phytoplankton communities, including thirteen diatom species, at six different coastal locations in Europe

and North America. They found that diatom species thrived and bloomed across a range of salinity, 8 – 28 PSU, and temperatures, 5 – 24°C with species such as *Skeletonema costatum* providing niche partitions between the different temperatures. In being able to more accurately predict phytoplankton communities responses on larger, global scales, a greater understanding of local processes and species interactions is needed but requires increased sampling effort and meta-analysis of local parameters (Garrido *et al.* 2016, Carstensen *et al.* 2015). This is particularly important to keep in mind, in Chapter 2 of this thesis which assessed the large-scale spatial distribution of phytoplankton communities.

Microphytobenthos (Microalgae of the Benthos)

The microphytobenthos forms a vital component of coastal ecosystems, contributing processes such as sediment stabilisation and trophic fluxes (MacIntyre *et al.* 1996, Spilmont *et al.* 2006). These communities consist of benthic autophototrophs that occupy the upper few millimetres of sediment (Kireta *et al.* 2012). Particularly in shallow water communities, there are a number of species that exist in the water column as phytoplankton or on the sediment. This contributes to the microphytobenthos diversity but adds ambiguity about the physical boundaries between water and sediment (Pan *et al.* 2013). Particularly in shallow water communities, where water depth is less than 2 m, the biomass of the microphytobenthos is often greater than that of the phytoplankton in the water column above (MacIntyre *et al.* 1996). A number of previous studies suggested that chlorophyll concentration, which may be used as an indicator of community biomass, and light availability are the primary factors which impact on benthic primary production (MacIntyre *et al.* 1996, Light and Beardall 2001, Araújo *et al.* 2013, Pan *et al.* 2013, Vieira *et al.* 2013, Pniewski *et al.* 2015). Within estuarine and coastal microphytobenthic communities, diatoms are often observed to be dominating the benthic communities (Pan *et al.* 2013). This is because diatoms are vital for the input of

energy into the microphytobenthos, primarily through their role as prey and production of polysaccharides (MacIntyre *et al.* 1996, Araújo *et al.* 2013). The latter is important to formation of biofilms on the sediment surface by diatoms, usually in conjunction with cyanobacteria and ciliate (Pan *et al.* 2013, Tekwani *et al.* 2013). In this thesis, the interactions between diatoms with other groups of taxa, including cyanobacteria and ciliates, is investigated in Chapters 3 and 4, which show the importance within the microphytobenthic community.

Diatoms

Diatoms, of the phylum Bacillariophyta and defined by the presence of a silica frustule, are ubiquitous to aquatic environments with adequate nutrients for growth, especially silica (Whitman *et al.* 1998). Ecologically diatoms are important on global scales. They are an important source of food for zooplankton grazers including ciliates (Straile 1997, Chang *et al.* 2014), and play a major role in the cycling of silica (Tréguer and De La Rocha 2013). With an estimated 30, 000 and 100, 000 species (Mann and Vanormelingen 2013) and responsible for 40% of oceanic primary productivity (Dugdale and Wilkerson 1998, Kamp *et al.* 2013), they are the most abundant and diverse group of aquatic algae (Armbrust *et al.* 2009).

Diatom frustules are made of two halves, the hypovalve, which originates from the parent cell, and the epivalve, which is formed after cell division (Round *et al.* 1990). The frustule surface also has fine architectural features, such as spines, channels and pores (Round *et al.* 1990). These morphological features are usually either genus or species specific and can therefore be used as diagnostic features for classification (Round *et al.* 1990). Moreover, diatoms cells undergo asexual and sexual reproduction; the latter is made necessary by the limitations the silica frustules impose on the size of an individual during cell division (Round *et al.* 1990, D'Alelio *et al.* 2010). From where the diatom has reached critical maximum size,

cells will asexually divide until reaching a critical minimum size where the cell then undergoes sexual reproduction once more (Figure 2). This progressive decrease in size over the life cycle occurs over approximately three to ten years for some species (D'Alelio *et al.* 2010) and therefore there is the potential to track diatom communities based on these size variations (Montresor and Lewis 2006). In this thesis, the ecological importance of diatoms in the microphytobenthos at the microscale is explored in Chapters 3 and 4, and in Chapter 5 this concept will be further explored by using the variation of frustule length as an indication of growth within the populations.

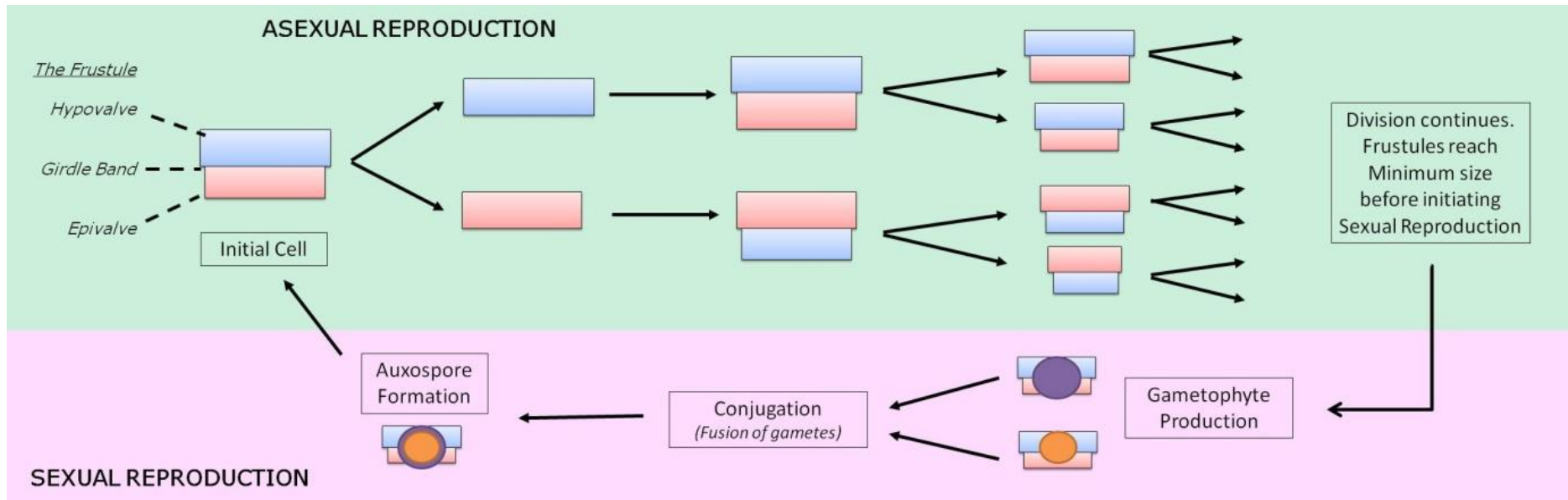


Figure 2. Generalised lifecycle of pennate diatoms. The lifecycle of the pennate diatom has been specifically chosen as a representation of the diatom lifecycle because the two species used in Chapter 5 of this thesis, *Amphora hyalina* and *Cocconeis costata*, are pennate diatoms. **Source:** E. Prime 2016, adapted from Raven *et al.* 2005 and D'Alelio *et al.* 2010.

Microscale Interactions

Variation of microbial abundance and community structure over large spatial scales, from metres to kilometres have been widely studied in numerous environments which sought to compare sites within or between oceans (Mellard *et al.* 2012, Ichinomiya *et al.* 2016, Meyer *et al.* 2016), between different lakes (Kipriyanova *et al.* 2007, Kissman *et al.* 2013) or between coastal and estuarine habitats (Saros and Fritz 2002, Balzano *et al.* 2015, Leterme *et al.* 2015). These large scale comparisons of communities observe variation due to changes in nutrient concentration, temperature, salinity or wind speed (Kipriyanova *et al.* 2007, Balzano *et al.* 2015, Leterme *et al.* 2015). However, microbial organisms are further influenced by abiotic and biotic microscale processes such as turbulence (Stocker *et al.* 2012) and nutrient concentration (Seymour *et al.* 2007). Interactions are very important at the microscale (Azam 1998, Stocker 2012), for example predator and prey interactions such as ciliates and bacteria (Paisie *et al.* 2014), or ciliates and diatoms (Chang *et al.* 2014). Microscale distances are from micrometres to centimetres, up to 1 m (Seymour *et al.* 2005, Azam 1998).

There have been a number of studies which have looked at the microscale distribution of viral and bacterial populations (Mitchell *et al.* 1989, Azam 1998, Seymour *et al.* 2005, 2007). These communities have been identified using High Throughput Sequencing (Dann *et al.* 2014). However, in terms of the eukaryotic community, particularly the photoautotrophic portion, very little work has been done to characterise the microscale spatial variation and few studies have sought to observe microscale variation of microeukaryote populations. As noted in *Microphytobenthos (Microalgae of the Benthos)*, chlorophyll *a* is often used as a measure of biomass for a variety of phototrophic communities. However, previous studies into the distribution of microalgae in the water column (Waters *et al.* 2003, Doubell *et al.*

2006, 2012) and in sediments (Seuront and Spilmont 2002, Franks and Jaffe 2008, Spilmont *et al.* 2011), demonstrating that chlorophyll *a* distribution is indeed heterogeneous in the intertidal environments sampled. Yet only a few studies have taken into account the species presence or abundance of the eukaryotic communities at microscale distances, which may be analysed using methods that are well developed from large scale studies, such as next generation sequencing technology including 18S rRNA and metagenomic profiling (Lie *et al.* 2013, Stanish *et al.* 2013, Balzano *et al.* 2015, Salni *et al.* 2015).

Study Site

All samples were collected from the Coorong, South Australia, is an inverse estuary, composed of two hypersaline coastal lagoons. The Coorong wetlands, associated lakes – Lake Alexandrina and Lake Albert – and the mouth of the River Murray are a diverse ecosystem at the endpoint of the River Murray (Webster 2005, Kämpf 2014). All samples for this thesis were collected from The Coorong. For Chapter 2, five sites were selected over the 140 km distance between the lagoons and the Murray Mouth, whereas for Chapters 3 to 5 one specific location was selected for the microscale studies.

The Coorong is the setting of many recreational activities and provides essential habitat to local and migratory birds, as well as fish species. The River Murray is vital to Australia's freshwater supply, providing essential water supplies to the four states which it flows through, as well as extensive use for human recreational activities (Brookes *et al.* 2009). This Ramsar listed coastal lagoon is greatly affected by lack of freshwater inflows and varying levels of hypersalinity (Brookes *et al.* 2009, Nayar and Loo 2009). The Ramsar Convention is an intergovernmental agreement for the conservation and wise use of wetlands (Ramsar Secretariat 2014). Local hydrology and anthropogenic impacts affect the Coorong wetlands

significantly. Water that flows in and out of the lagoons is controlled by barrages separating the lakes from the lagoon (Webster, 2005, 2010). Salinity in this system was increased by recent drought (2004-2010) (Webster 2010, Jendyk *et al.* 2015). Sampling occurred between March 2009 to February 2010, where salinity in the Coorong ranged from oceanic salinity (38 PSU) at the Murray mouth in the north lagoon to hypersaline (>200 PSU) at Salt Creek in the south lagoon. The lack of water inflow into the lagoons and river mouth due to the presence of locks further up river also contributed to increased salinity during the sampling period (Nayar and Loo, 2009).

Microbial Interaction Networks

Recently, mathematical methods have been developed to make data from time series sampling useful for understanding interactions and making predictions of species to ecosystem responses by using interaction networks (Steele *et al.* 2009, Faust and Raes 2012). Broadly, large amounts of data, often genomic for the case of microbial communities, can be used to present the multiple interactions, or lack of, between groups of microbes (Faust and Raes 2012). Utilising network analysis to analyse these large datasets offers the opportunity to find interactions and identify key species and parameters within microbial communities. It is also a logical path because significant components of microbial communities form tightly connected networks, which respond rapidly to food web changes (Simon *et al.* 2003, Brad *et al.* 2008). In this thesis, interaction network analysis has been used in two different ways. Firstly, to determine the interactions between microbial communities, from data obtained from at the microscale using sequencing data (Chapters 3 and 4). Secondly, network analysis was used to understand which parameters associated with cell size of two benthic diatom species are useful indicators of the ecological function of diatoms (Chapter 5).

Aims and Structure of the Thesis

This thesis seeks to investigate the variation of natural communities of microalgae at large and microscales. Specifically, I aimed to:

- (i) Establish the environmental factors that influence five phytoplankton communities across the north and south lagoons of the Coorong (Large scale study, Chapter 2).
- (ii) Determine key interactions between different classes of microeukaryotes and identify taxonomical groups driving dissimilarity within the microphytobenthos (Microscale study, Chapter 3).
- (iii) Determine the extent to which chlorophyll *a* and *c* concentrations are related to the composition of the microeukaryote community of the microphytobenthos (Microscale study, Chapter 3).
- (iv) Establish which groups of prokaryotes and eukaryotes exhibit crucial interactions within the microbial web in a microphytobenthic community (Microscale study, Chapter 4).
- (v) Measure the microscale distribution of frustules length for two species of diatom, *Amphora hyalina* and *Cocconeis costata*, to identify processes which are contributing to their variation in cell size (Microscale study, Chapter 5).

This thesis is structured in manuscript format. This implies that there are redundancies in the introduction and methods sections, particularly for chapters 3 to 5. Chapter 2 has been submitted to *Estuarine, Coastal and Shelf Science*, while chapters 3 and 5 soon be submitted to *Public Library of Science (PLOS) One* and chapter 4 is prepared and presented in the format required for submission to *Environmental Microbiology Reports*. To reduce further

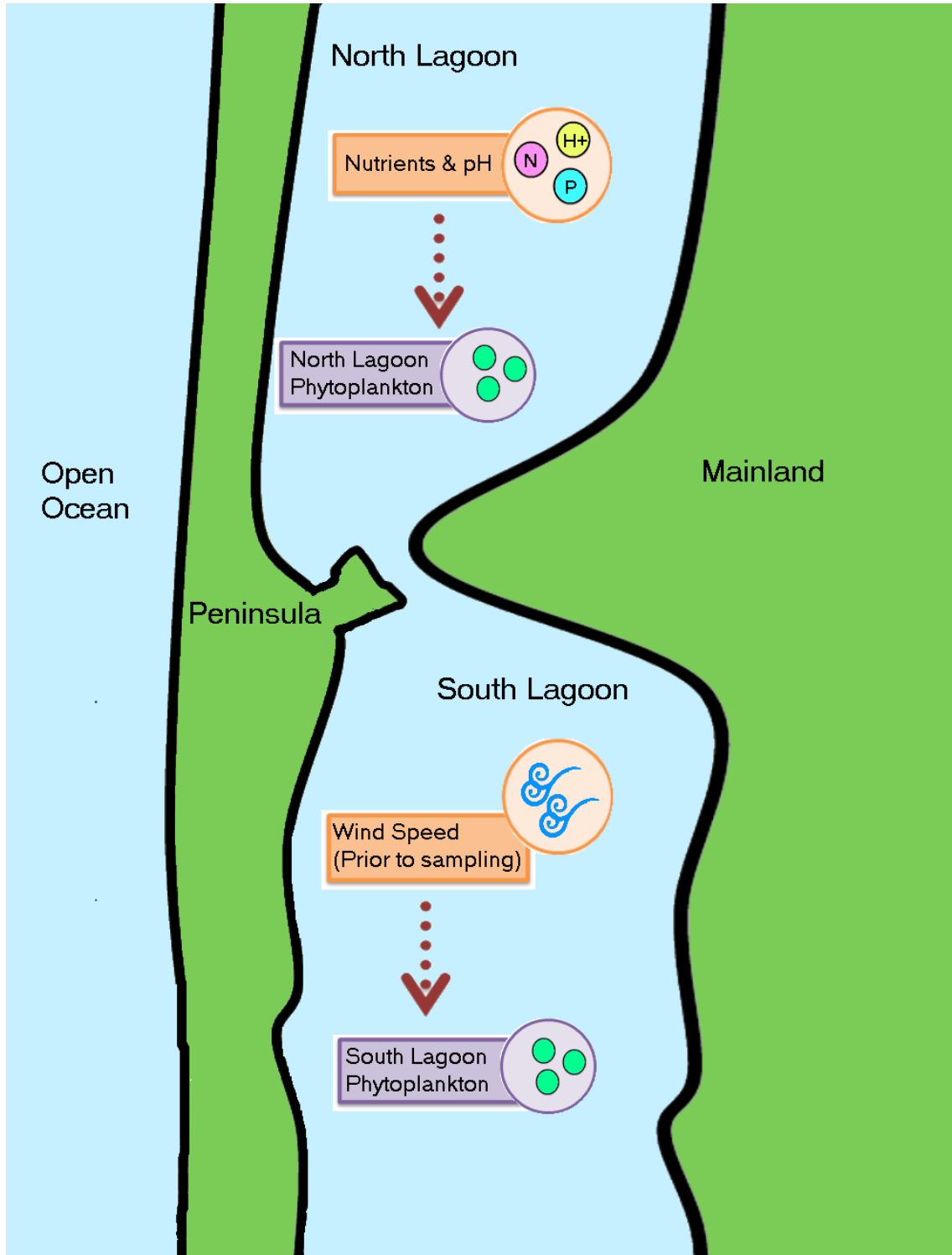
redundancies, one collated bibliography for all literature cited is given at the end of this thesis.

CHAPTER 2

Phytoplankton Dynamics under Drought Conditions in an Inverse Estuary

Graphical Abstract

Used for submission to Estuarine, Coastal and Shelf Science.



Abstract

The Coorong, in South Australia is a hypersaline coastal lagoon approximately 170 km in length, comprised of a south and a north lagoon that joins the Southern Ocean at the mouth of the River Murray. The salinity gradient across these lagoons ranges from 38 PSU at the mouth of the River Murray to over 200 PSU at the end of the south lagoon. In this study, five sites were sampled monthly over a one year period to investigate the temporal and spatial variation of phytoplankton communities. Greatest concentration of dissolved inorganic silica, phosphate and ammonium ranged between 56.94 $\mu\text{mol/L}$ and 30.56 $\mu\text{mol/L}$, 34.38 $\mu\text{mol/L}$ and 6.6 $\mu\text{mol/L}$, 337.01 $\mu\text{mol/L}$ and 23.01 $\mu\text{mol/L}$, respectively along the five study sites of the Coorong throughout the sample period. Meanwhile, assessing the biological conditions of the sites, where highest chlorophyll *a* concentration was 13.21 $\mu\text{g/L}$, and the minimum, 0.05 $\mu\text{g/L}$, at Salt Creek, in August and June respectively. Green algae, dinoflagellate and diatom concentrations as high as 2.1×10^7 cells/L in January at Salt Creek, 7.1×10^4 cells/L in August at Salt Creek and 1.0×10^4 at Long Point in December, respectively. Despite the two lagoons sharing a physical connection which allows for water transfer, PCA analysis indicates that the variation in the south lagoon phytoplankton community taxonomic structure is most strongly controlled by wind speed, while variation in the north lagoon phytoplankton community taxonomic structure is primarily controlled by pH and dissolved nutrient concentration.

Introduction

Estuaries are defined as water bodies which occur at the interface of the open ocean and one or more rivers (Kämpf 2014). In inverse estuaries evaporation exceeds input of freshwater (Kämpf 2014) and they are typically known for exhibiting extreme spatial and temporal variation in temperature and salinity (Gallegos *et al.* 2010, Philps *et al.* 2010, Quinlan and Philps 2007). These are highly diverse and productive environments, which are important as nursery habitats for fish, nesting areas for local and migratory birds (Kämpf 2014, Rodrigues and Pardal 2015) and often exhibit high levels of primary productivity (Gallegos *et al.* 2010, Quinlan and Philps 2007). Phytoplankton, at the base of aquatic food webs, can be used as indicators or predictors of the overall health of those environments (e.g. Buric *et al.* 2007, Cetinić *et al.* 2006).

Temperature and salinity are known to impact on the abundance and diversity of phytoplankton communities in those ecosystems (Kipriyanova *et al.* 2007, Medley and Clements 1998, Pedros-Alio *et al.* 2000, Saros and Fritz 2002, Smith *et al.* 2007, Winder *et al.* 2009). In particular, Pedros-Alio *et al.* (2000) and Kipriyanova *et al.* (2007) observed that diversity and abundance of phytoplankton decreased with increasing salinity. Increases in salinity have also been observed to coincide with increases in temperature and dissolved nutrients such as phosphate and nitrate (Kipriyanova *et al.* 2007, Saros and Fritz 2002, Winder *et al.* 2009) and have been linked to increased metabolism and growth rate in numerous species of phytoplankton (Buric *et al.* 2007, DeMartino *et al.* 2007, Saros and Fritz 2002). Finally, increases in salinity, temperature, heavy metal concentration and limitation of dissolved nutrients impede phytoplankton growth rates and cellular metabolism in various river and oceanic environments (DeMartino *et al.* 2007, Leland *et al.* 2001, Saros and Fritz 2002, Vidussi *et al.* 2011). In the case of inverse estuaries, variability is affected by physical

and biological factors which lead to the formation of environmental gradients and microhabitats, in particular salinity and temperature (Jendyk *et al.* 2014, Kämpf 2014).

The Coorong, South Australia, is an inverse estuary, composed of two hypersaline coastal lagoons (Figure 1). The Coorong lagoons, associated two lakes (Lake Alexandrina and Lake Albert) and the mouth of the River Murray are a diverse ecosystem at the endpoint of the River Murray, one of Australia's most important sources of freshwater. This Ramsar listed coastal lagoon is greatly affected by lack of freshwater inflows and varying levels of hypersalinity (Brookes *et al.* 2009, Nayar and Loo 2009). Local hydrology and anthropogenic impacts affect the Coorong lagoons significantly. Water that flows in and out of the lagoons is generally controlled by barrages separating the lakes from the lagoon, which were not opened during the sampling period (SA Water 2013). However, runoff from farms adjacent to the Coorong probably also affects the lagoons and the phytoplankton communities (Webster, 2005). Salinity in the Coorong ranges from oceanic salinity (38 PSU) at the Murray Mouth in the north lagoon to hypersaline (>200 PSU) at Salt Creek in the south lagoon (Leterme *et al.* 2012, Figure 1). Salinity in this system has been increased by recent drought (2004-2010) and by the lack of water inflow into the lagoons and river mouth due to the construction of locks further up river (Nayar and Loo 2009). Water flows over the locks are impacted by the flow of water allowed into South Australia from further upstream in New South Wales (WaterConnect 2014). Previous work has suggested that seasonal fluctuations in salinity are of important influence on the Coorong. In particular, Nayar and Loo (2009) observed that phytoplankton productivity increased with increasing salinity from 35-115 PSU, although phytoplankton only had a small contribution to overall productivity at two of the three sites studied. However, it has been noted that phytoplankton communities may adapt conditions such as increased salinity (DeMartino *et al.* 2007), so is salinity the major factor driving communities in an environment such as the Coorong lagoons?

Here, we investigated the spatial and temporal variations of phytoplankton communities at 5 sites along the Coorong lagoons to establish the factors that control phytoplankton communities of the north and south lagoons under drought conditions. Finding out how the phytoplankton lagoons change during drought will help reveal the impact of climate change on ecosystems that go through frequent drought events.

Methods

Study sites

Five sites were chosen along the 170 km length of the Coorong, from the mouth of the Murray River to the southern end of the south lagoon, Salt Creek (Figure 1). Sampling was conducted monthly from March 2009 to February 2010 at each of the 5 sites: the mouth of the River Murray (S35° 32.973', E138° 52.965'; Figure 1), Long Point (S35° 69.524', E139° 16.295'), Seven Mile Road (S35° 79.769, E139° 31.780'), Policeman Point (S36° 06.139', E139° 59.436') and Salt Creek (S36° 15.617', E139° 64.630'). The Murray Mouth, Long Point and Seven Mile Road sites are located in the north lagoon, while Policeman Point and Salt Creek are located in the south lagoon.

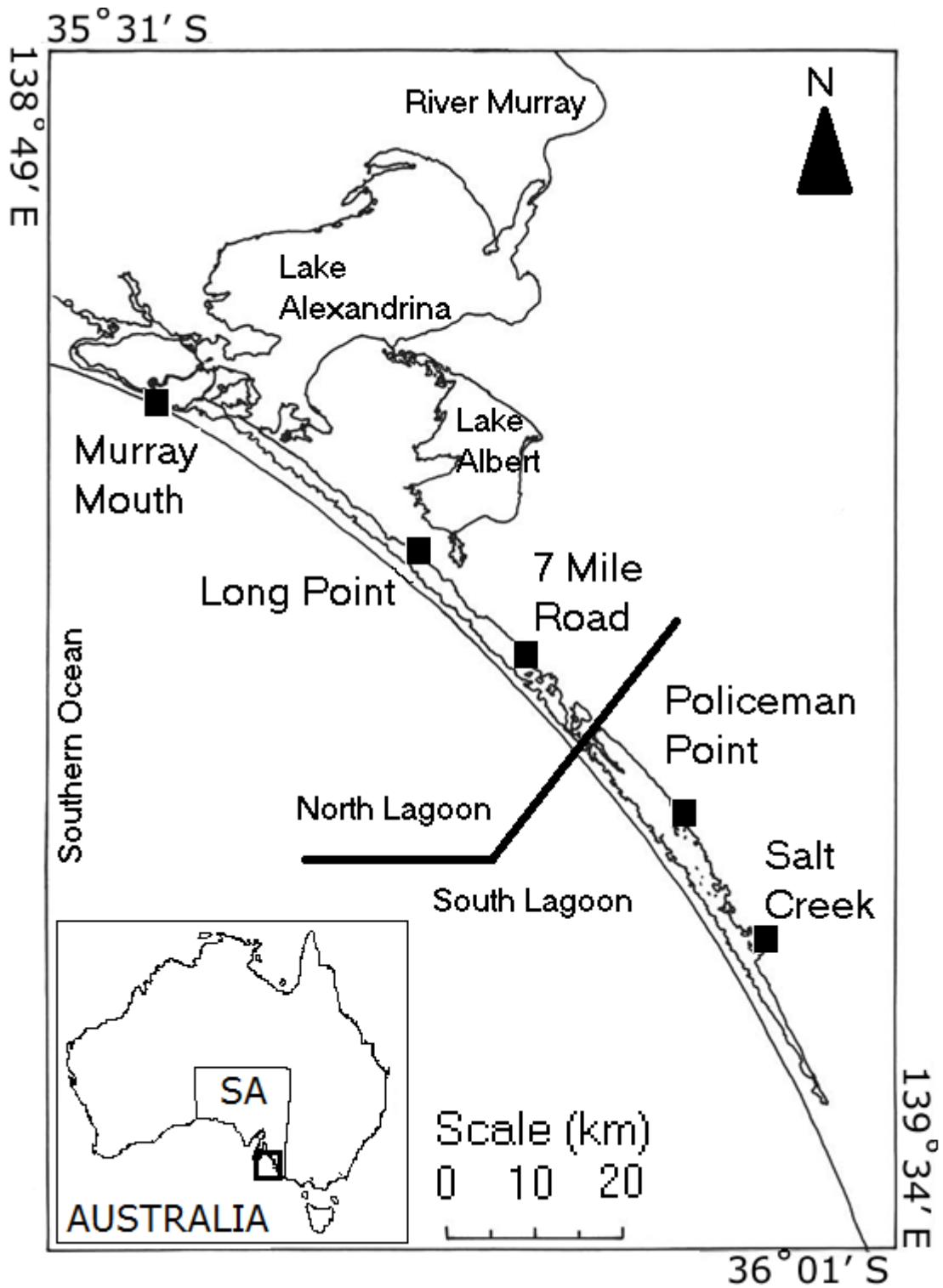


Figure 1. Map of the Coorong lagoons and mouth of the River Murray, South Australia (SA).

Field sites: Salt Creek, Policeman Point, Seven Mile Road, Long Point and Murray Mouth.

All sampling sites are shallow water environments (Wright and Wacey 2005) and are protected from wind blowing directly from the Southern Ocean by the Youngusband Peninsula, except for the Murray Mouth. Water inputs in the Coorong and nearby distal ephemeral lakes consist of rainfall and the seaward movement of groundwater from an open aquifer system (Wright and Wacey 2005). Sediments of these sites were generally sandy, except for Seven Mile Road, where the benthos is dominated by rocks instead of sand. Low water levels in the local area meant that salinity remained consistently high, >100PSU.

Environmental parameters

Subsurface (i.e. 20 cm under the surface of the water) measurements of salinity (PSU, practical salinity units), pH and temperature (°C) were made *in situ* using a multisensory parameter probe (Stennick Scientific). Wind speed (Km.h⁻¹) data were obtained through the Bureau of Meteorology (Meningie and Victor Harbor weather stations, Bureau of Meteorology) and water flow over lock 1 in the River Murray (estimated at lock 1) was obtained from WaterConnect, weekly flow reports for the River Murray.

Dissolved nutrient analysis

Dissolved inorganic nutrients were performed following the protocol described by Schapira *et al.* (2009, 2010). Triplicates 100 mL of water were filtered into sterile sample containers using 0.45 µm syringe filters (Millipore) and stored in the dark at - 20 °C until analysis. The analyses were performed using a portable LF 2400 Photometer (AquaspeX®) using standard colorimetric methods for nitrate (NO₃⁻; Naphtylethylenediamine after zinc reduction), nitrite (NO₂⁻; Naphtylethylenediamine), ammonium (NH₄⁺; Indophenol blue), phosphate (PO₄⁻³; Ascorbic acid reduction) and silica (SiO₂⁻²; Heteropoly blue).

Chlorophyll a Analysis

At each site, glass fibre filters (Whatman GF/C) were used to filter triplicates of 60 mL of sample water for analysis of chlorophyll *a*, from here abbreviated as Chl *a*. The filters were preserved in the dark at -20 °C until analysis. In the laboratory, filters were placed in separate tubes and fixed with 5 mL methanol extraction of the chlorophyllous pigments in the dark at 5 °C for 24 hours. Chl *a* was subsequently measured following Strickland and Parsons (1972) using a Turner 450 Fluorometer previously calibrated with a pure Chl *a* solution (*Anacystis nidulans* extract, Sigma Chemicals, St Louis).

Phytoplankton Sampling and Abundance

Phytoplankton samples were obtained in triplicate by collecting bulk water from each site and preserved in Lugols iodine (5% final concentration). 1 mL of sample was enumerated, in triplicate, under a light microscope using a Sedgewick-Rafter enumeration slide. Phytoplankton was identified to the genus level and, where possible, to the species using identification keys (Gell *et al.* 1999, Loir 2004, Sonneman *et al.* 2000, Tomas, 1997, Wilkinson 2005). For species that could only be identified to genus, these were allocated a species number. Green algae cells were enumerated separately using a further 1 mL of sample with a haemocytometer microscope slide.

Phytoplankton Diversity

To assess the diversity of species at each site, the Shannon-Weaver index (H') was calculated each sample (Holm, 1979) using equation.

$$H' = [n \cdot \log n - \sum(f_i \cdot \log f_i)] / n \quad (1)$$

Where: n is the number of total number of organisms and f_i is the number of individuals of each species identified.

Statistical Analyses

Normality of the dataset was tested using a Kolomogorov-Smirnov test (Zar 1999). Since the data were not normally distributed, significant temporal and spatial differences for biological and physical parameters were tested using Kruskal-Wallis test with Dunn's multiple comparison test (Zar 1999, SPSS v. 20.0). To determine the factors influencing the phytoplankton communities, Spearman's rho was used to find the correlation coefficient (r) and to test the significance of the correlations between biological and physical data for each site (SPSS v. 20.0, Mendenhall *et al.* 1999). These were reduced using sequentially reductive Bonferroni corrections to confirm significance (Holm 1979). This was further used to test the influence of wind speed on all biological and physical parameters. A correlation between wind speed on the day of sampling as well as that on the four consecutive days before sampling was conducted to better elucidate the action of wind on these parameters.

Multivariate analysis was used to explore the importance of the environmental parameters across the site, where the null hypothesis is that there is no difference in the environmental and biological parameters between the lagoons (or sites). All data were square root transformed (best fit of normality, although normality was not obtained), and then further normalised. Principal components analysis (PCA) was used, which seeks to identify parameters with the greatest variance, which means that data was required to be normalised using PRIMER, v. 6. The vectors (principle components) indicate the direction of variance of a parameter. In order to properly identify parameters that are best correlated, BEST analysis (linking of multivariate biotic patterns to environmental variables) was conducted in conjunction with the PCA to determine the environmental parameters to be displayed as

significant vectors using Pearson's correlation coefficient (Pearson's r , PRIMER v.6) (Clarke 1993).

Results

Environmental parameters

A large salinity gradient was observed across the Coorong, from the Murray mouth (oceanic) to Salt Creek (hypersaline), which was present throughout the year (Figure 2A). The annual salinity maximum across the sites was observed during spring, at Salt Creek (201.13 PSU), meanwhile minimum was observed in May at the Murray mouth (37.90 PSU). Salinity at the Murray Mouth shows the least variation of the sites, ranging between 37.9 and 41.62 PSU throughout the year. Salinity levels were significantly different between the five sites throughout the year (Kruskal-Wallis, Dunn's, $p < 0.05$). Water flows over lock 1, which allows water into the Coorong, ranged between 1100 – 1800 ML per day, except in February where it increased to 4000 ML/day due to extremely dry and hot conditions leading to extra water being released.

The water temperature was significantly different at each site and between months (Kruskal-Wallis $p < 0.05$). The highest temperatures were observed from September to December, while lowest temperatures were observed during April and May (Figure 2B). However, there were no spatial or temporal changes in pH between sites (Figure 2C).

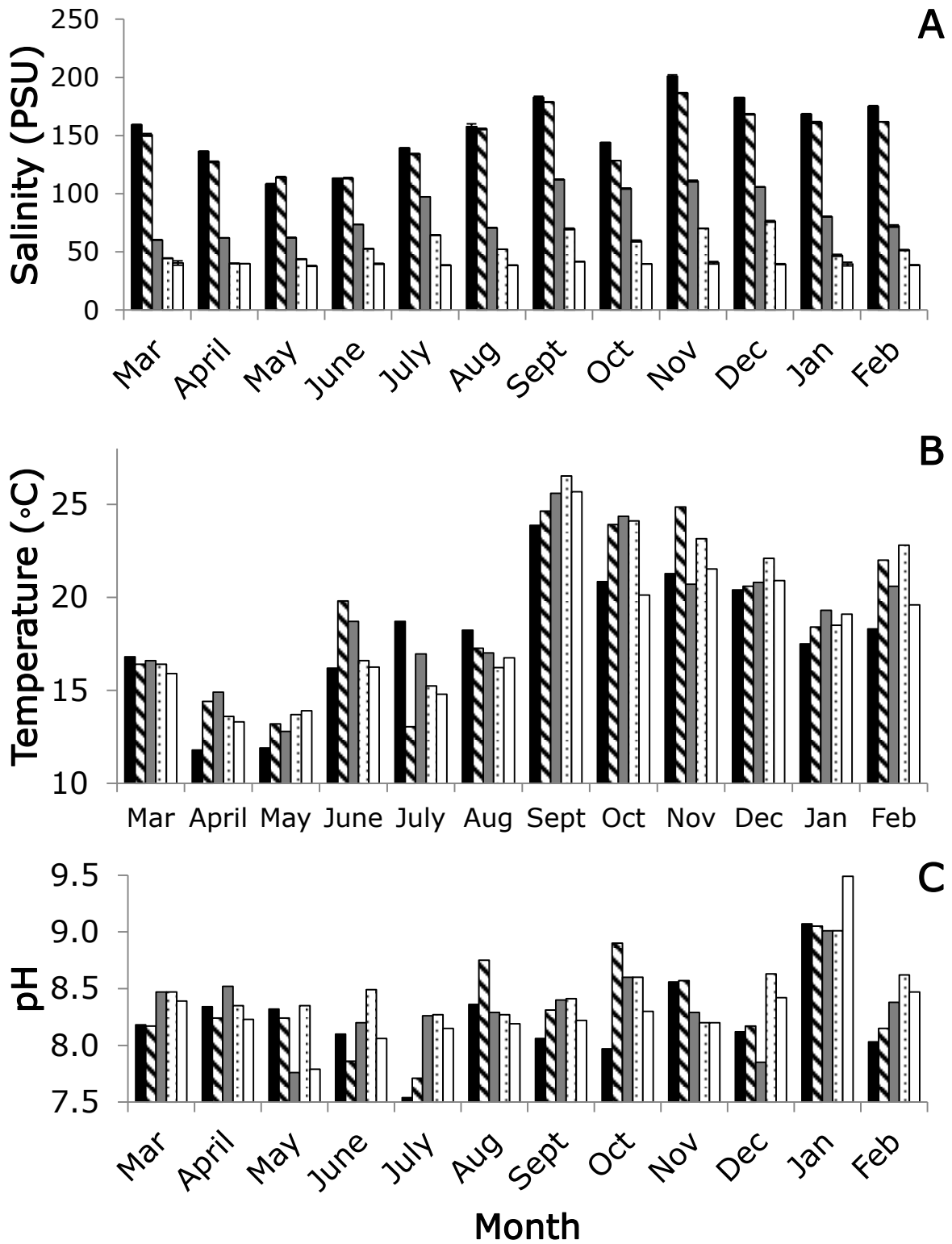


Figure 2. Environmental parameters at five sites of the Coorong and Murray Mouth: (A) Salinity (PSU), (B) Temperature (°C), and, (C) pH. Salt Creek is represented by the black-fill

column, Policeman Point by diagonal stripe, Seven Mile Road by grey-fill column, Long Point by black dots and Murray Mouth by the white-fill column.

The mean daily wind speed on the day of sampling was significantly different between the Victor Harbor weather station which is the reference station for the Murray Mouth and the Meningie weather station which is the reference station for Salt Creek, Policeman Point, Seven Mile Road and Long Point (Kruskal-Wallis $p < 0.05$). Wind speed at the Meningie weather station was lowest during November 4 days before sampling, 3.1 Km/h, October 3 days before sampling, 3.0 Km/h, November 2 days before sampling, 2.4 Km/h, June 1 day before sampling, 1.2 Km/h and September on the day sampling occurred, 0.6 Km/h. Meanwhile, greatest wind speed was observed in July 4 days before sampling, 19.8 Km/h, December 3 days before sampling, 18.5 Km/h, March 2 days before sampling, 20.9 Km/h and during October for the day before and the day of sampling, 25.3 Km/h and 13.6 Km/h, respectively (Figure 3A). Whereas, wind speed at Victor Harbor was lowest during February 4 and 3 days before sampling, 1.8 Km/h and 2.5 Km/h respectively, during May 2 days before sampling, 0.6 Km/h, and during June 1 day and the day of sampling, 3.6 Km/h and 1.8 Km/h respectively. Similarly, greatest mean wind speed at Victor Harbor weather station was observed in August 4 days before sampling, 24.7 Km/h, September 3 days before sampling, 17.4 Km/h, and during October 2 and 1 days before sampling, as well as the day of sampling, 23.4 Km/h, 23.4 Km/h and 14.8 Km/h, respectively (Figure 3B).

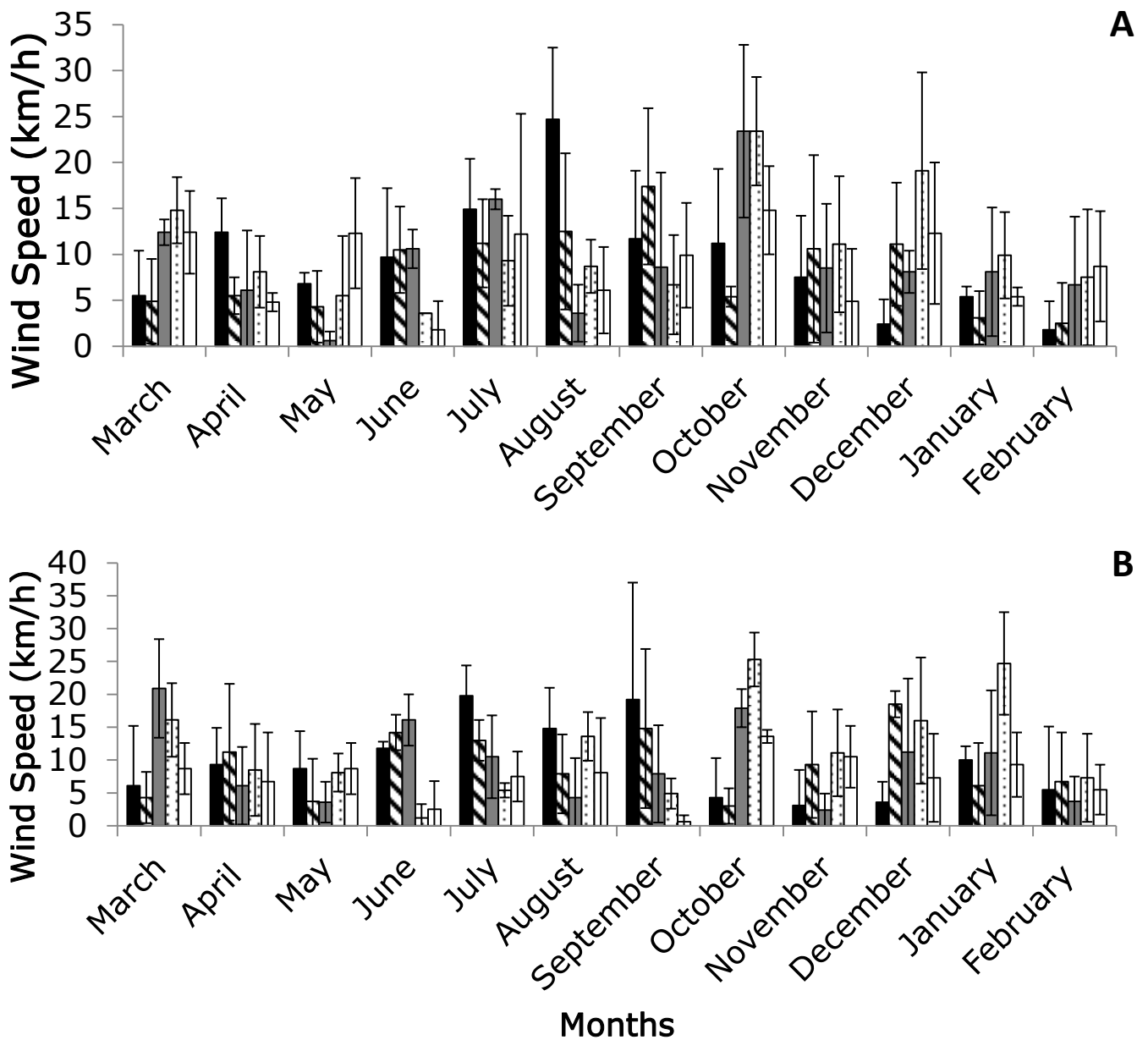


Figure 3. Mean daily wind speed (Km/h) for (A) Meningie and (B) Victor Harbor weather stations with \pm standard deviation for the day of sampling (black fill bars), 1 day before sampling (diagonal stripe), 2 days before sampling (grey fill bars), 3 days before sampling (black dots) and 4 days before sampling (white fill bars). Meningie weather station corresponds to Salt Creek, Policeman Point, Seven Mile Road and Long Point. The Victor Harbor weather station corresponds to the Murray Mouth. Data obtained from Australian Bureau of Meteorology.

Dissolved Nutrients

Concentrations of dissolved nutrients were consistently lower at the Murray Mouth compared to the other four sites, with Salt Creek and Long Point showing the highest concentrations (Table S1). The concentrations of ammonium, phosphate and silica showed particularly clear differences spatially and temporally along the five sites (Figure 4, Kruskal-Wallis $p < 0.05$). Ammonium concentration showed no significant difference temporally or spatially along the sites (Figure 3, Kruskal-Wallis, $p > 0.05$). This is probably caused by a number of readings below detection limits (Figure 4A). Ammonium concentration ranged between $0\mu\text{mol/L}$ (March, June and November) and 337.01 (April) at Salt Creek, $0\mu\text{mol/L}$ (May, August and January) and 204.36 (March) at Policeman Point, $0\mu\text{mol/L}$ (May) and $111.59\mu\text{mol/L}$ (March) at 7 Mile Road, $0\mu\text{mol/L}$ (June) and $35.85\mu\text{mol/L}$ (November) at Long Point, and, $0\mu\text{mol/L}$ (July) and $23.01\mu\text{mol/L}$ (April) at the Murray Mouth (Figure 4A).

Months where the minimum readings were observed varied for phosphate, $0\mu\text{mol/L}$ was observed multiple times throughout March – May and June - October at all sites. However, minimum concentration of silica were observed in June at Salt Creek, $4.16\mu\text{mol/L}$, May at Policeman Point, $2.08\mu\text{mol/L}$, March at 7 Mile Road, $0\mu\text{mol/L}$, and Long Point, $1.04\mu\text{mol/L}$, and during August for the Murray Mouth $0\mu\text{mol/L}$, Figure 4B). Highest phosphate concentration was observed in August at Salt Creek, $34.3856\mu\text{mol/L}$, during May at Long Point, $27.7856\mu\text{mol/L}$, and in February for Policeman Point, $3.8256\mu\text{mol/L}$, and 7 Mile Road, $6.6056\mu\text{mol/L}$, and the Murray Mouth, $23.0156\mu\text{mol/L}$ (Figure 4B). Silica was highest in December at Salt Creek, $56.94\mu\text{mol/L}$, Policeman Point, $40.63\mu\text{mol/L}$, Long Point, $30.56\mu\text{mol/L}$ and the Murray Mouth, $14.71\mu\text{mol/L}$ (Figure 4C).

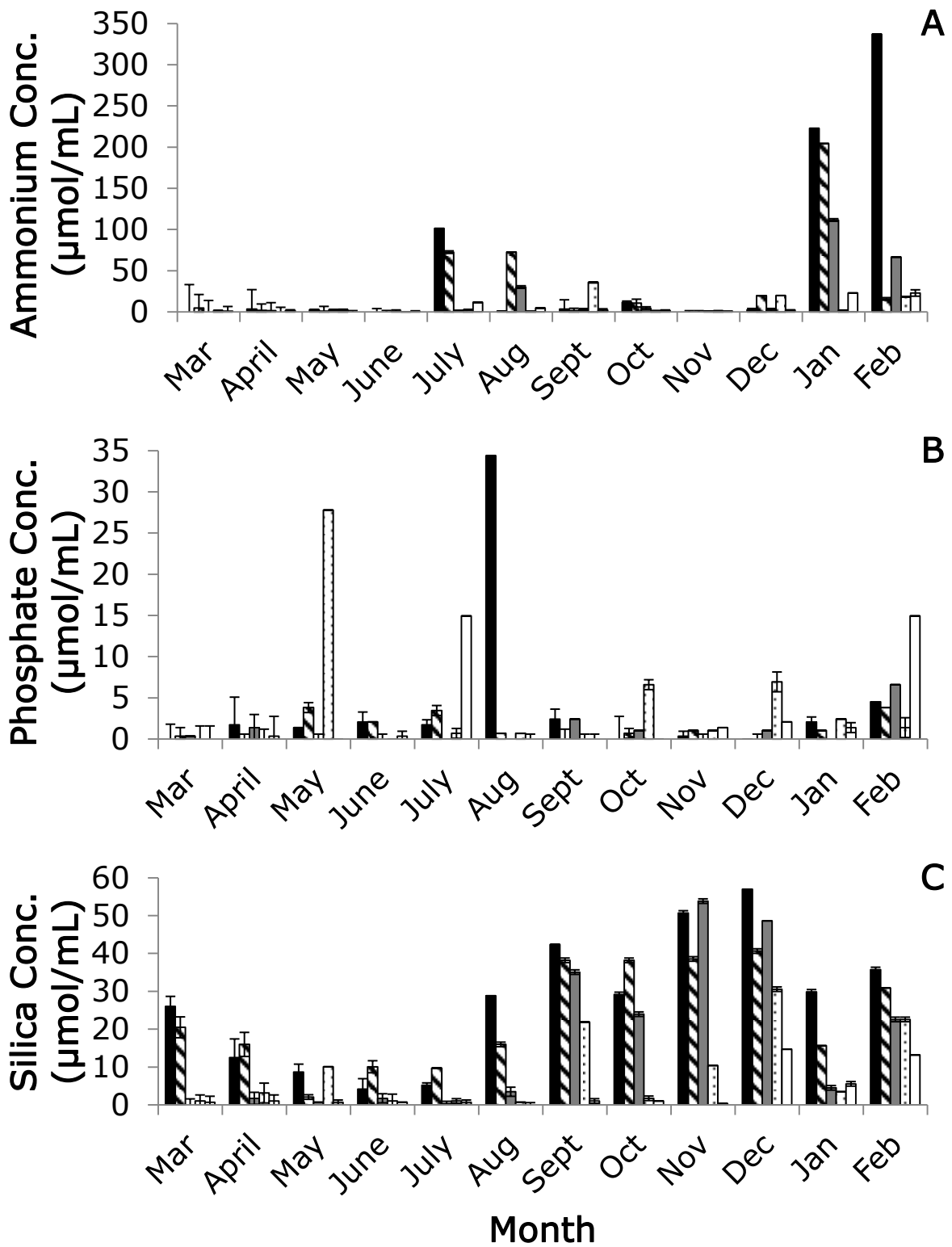


Figure 4. Mean concentration of the dissolved nutrients (A) Ammonium, (B) Phosphate and (C) silica in $\mu\text{mol/L}$ with \pm standard deviation, measured at five sites along the Coorong lagoons from March 2009 to February 2010. Salt Creek is represented by the black-fill column, Policeman Point

by diagonal stripe, Seven Mile Road by grey-fill column, Long Point by black dots and Murray Mouth by the white-fill column.

Chlorophyll a Concentration

Concentration of Chl *a* was significantly varied between stations spatially as well as temporally (Kruskal-Wallis, $p < 0.05$). Lowest observed concentrations of chl *a* varied, where Salt Creek experienced lowest concentration in June, 0.05 $\mu\text{g/L}$, Policeman Point in September, 0.32 $\mu\text{g/L}$, 7 Mile Road in February, 1.56 $\mu\text{g/L}$, and Long Point in April, 0.43 $\mu\text{g/L}$. Highest observed concentration of chl *a* occurred in August at Salt Creek where chl *a* was 13.21 $\mu\text{g/L}$, in October at Policeman Point, 11.34 $\mu\text{g/L}$, and in November at Long Point, 8.58 $\mu\text{g/L}$. 7 Mile Road showed a consistently higher biomass throughout the year, which peaked at 13.12 $\mu\text{g/L}$ in November. Finally, Chl *a* concentration was consistently lower at the Murray mouth compared to the other four stations, where chl concentration ranged between 1.18 $\mu\text{g/L}$ in March and 0.13 $\mu\text{g/L}$ in August (Figure 5).

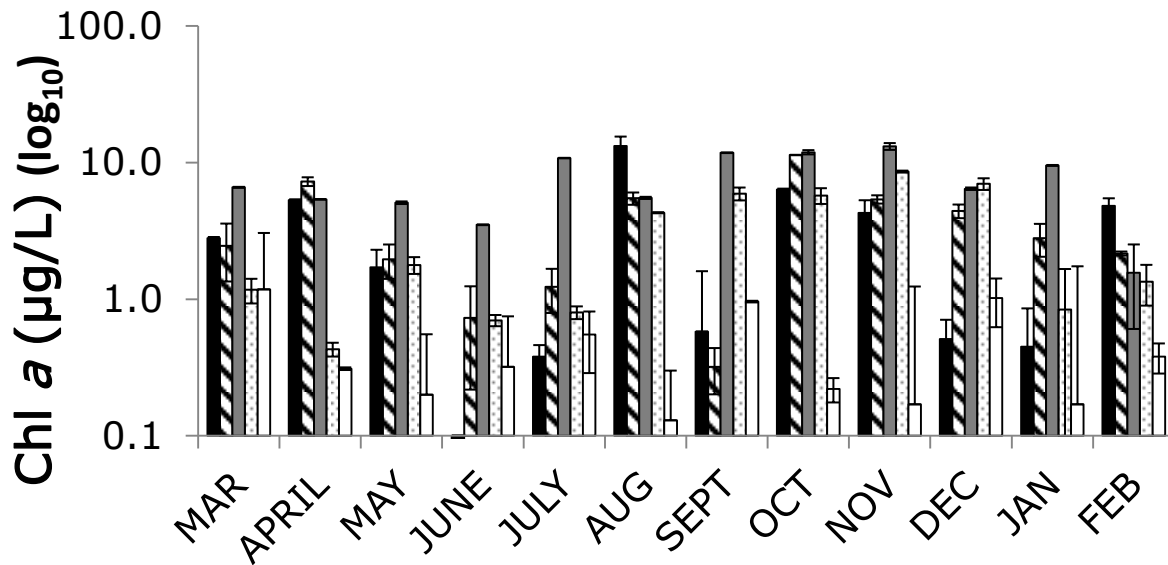


Figure 5. Chl *a* concentration at five sites of the Coorong and Murray Mouth, in µg/L on a log scale. Salt Creek is represented by the black-fill column, Policeman Point by diagonal stripe, Seven Mile Road by grey-fill column, Long Point by black dots and Murray Mouth by the white-fill column.

Phytoplankton Abundance

The phytoplankton communities were mainly composed of green algae, dinoflagellates and diatoms. The analysis of phytoplankton species abundance indicated significantly different communities at each site (Kruskal-Wallis, $p < 0.05$). In addition, the abundance significantly varied monthly (Kruskal-Wallis, $p < 0.05$, Figure 5). Green algae were the most abundant of the groups, making up >90% of the phytoplankton identified throughout the year at all sites. Greatest abundance of green algae was observed in January for Salt Creek (2.1×10^7 cells/L), Policeman Point (1.2×10^7 cells/L) and 7 Mile Road (1.08×10^7 cells/L), in March for Long Point and the Murray mouth, 1.98×10^7 cells/L and 4.4×10^6 cells/L. The lowest green algae abundance was observed in March at Salt Creek (4.2×10^5 cells/L) and in November at

Policeman Point (3.3×10^5 cells/L). On the other hand, lowest green algae abundance was observed in September at 7 Mile Road (1.1×10^6 cells/L), Long Point (4.0×10^5 cells/L) and the Murray Mouth (2.2×10^5 cells/L). Generally, at the Murray Mouth green algae were significantly lower than at the other four stations (Kruskal-Wallis, $p < 0.05$).

Dinoflagellates were the least abundant of the three identified groups of phytoplankton. Overall, 75 species of dinoflagellates were identified in the Coorong over the sampled year, including various species of *Amphidinium*, *Gymnodinium*, *Gyrodinium*, *Katodinium*, *Prorocentrum* and *Protoperidinium*. The composition of the species and abundance of the dinoflagellate population was significantly different between the stations (Kruskal-Wallis, $p < 0.05$, Figure 6B). Dinoflagellate abundances were highest in December at Salt Creek (1.7×10^3 cells/L), Long Point (1.0×10^4 cells/L) and the Murray Mouth (3.7×10^3 cells/L), in May at Policeman Point (3.7×10^3 cells/L) and October at 7 Mile Road (9.6×10^3 cells/L). No particular species was identified to be responsible for these increases in abundance at individual sites.

Diatoms were widely abundant at all sites throughout the year, even if green algae were dominant. In total, 155 species of diatom were identified at the five stations throughout the sampled year, including numerous species of *Achnanthes*, *Amphora*, *Cocconeis*, *Coscinodiscus*, *Navicula*, *Nitzschia* and *Pleurosigma*. The diatom population composition and abundance changed significantly throughout the year at all sites (Kruskal-Wallis, $p < 0.05$, Figure 6C). Furthermore, peaks of diatom abundance occurred between July and August at all sites. Dominating species included *Nitzschia closterium* at Salt Creek and Policeman Point in August. At Seven Mile Road and Long Point the dominant species observed was *Nitzschia sp. 1* also during July (6.0×10^4 cells/L) and August (1.8×10^4 cells/L) (Figure 6C). However, at the Murray Mouth observed greatest total abundance during March (3.7×10^4

cells/L), which coincided with the diatom community being dominated by the pennate diatom *Asterionella glacialis*.

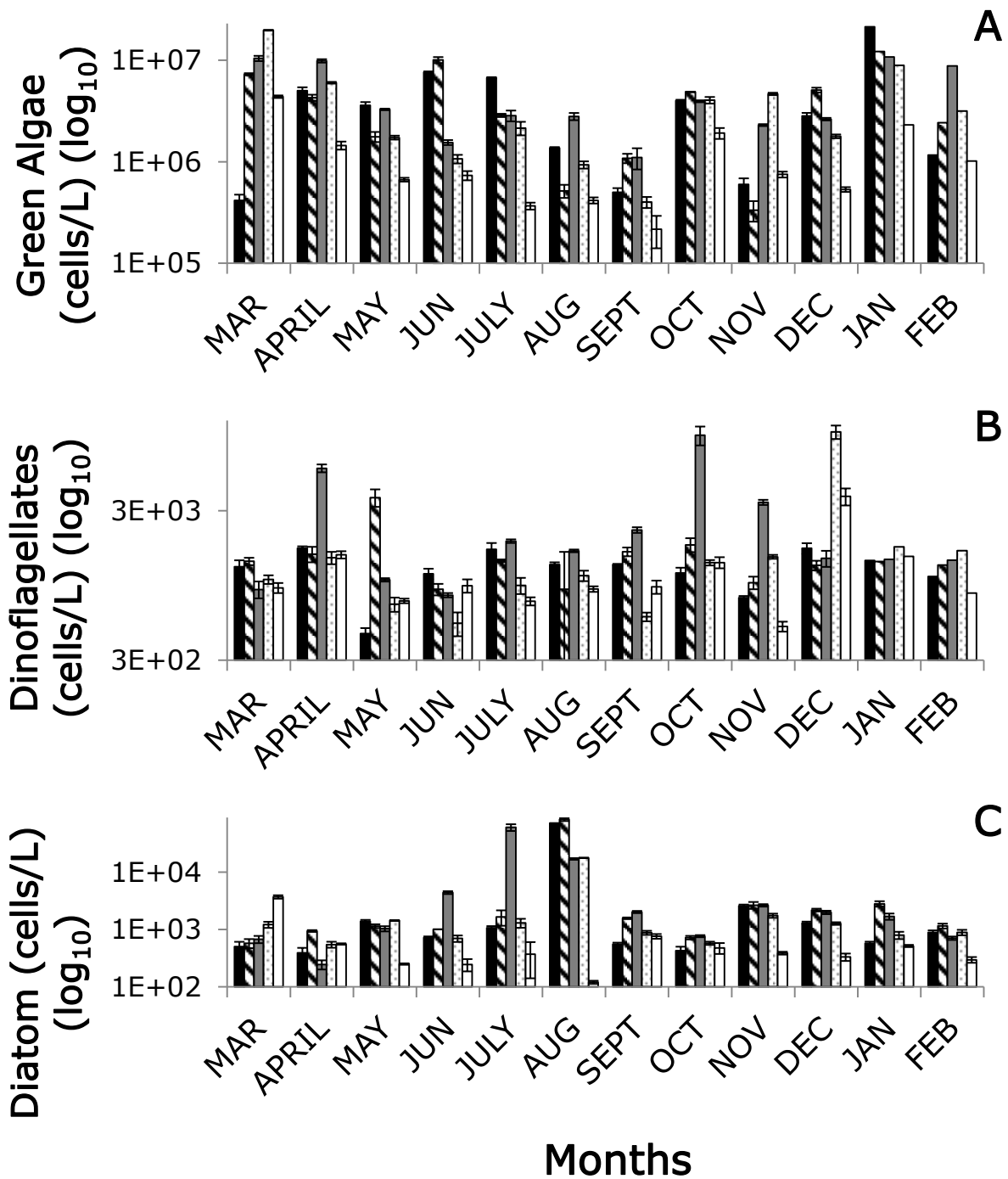


Figure 6. Phytoplankton abundances at five sites of the Coorong and Murray Mouth. (A) Green Algae (cells/L) on a log scale, (B) Total Dinoflagellates (cells/L) on a log scale, and, (C) Total Diatoms (cells/L) on a log scale. Salt Creek is represented by the black-fill column, Policeman Point by diagonal stripe, Seven Mile Road by grey-fill column, Long Point by black dots and Murray Mouth by the white-fill column.

Phytoplankton Diversity

Diversity of the phytoplankton communities varies between sites (Kruskal-Wallis, $p < 0.05$, Figure 7), although there is limited temporal variation (Kruskal-Wallis, $p > 0.05$). Results for the Shannon-Weaver index show that diversity of the phytoplankton communities show lowest diversity in October at Salt Creek (0.29), Policeman Point (0.24) and Long Point (0.58), while lowest diversity was observed during September at 7 Mile Road (0.13) and in May at the Murray Mouth (0.53) (Figure 7). However, greatest diversity was observed in July at Salt Creek (1.48), in April at Policeman Point (1.42) and 7 Mile Road (1.42), in November at Long Point (1.51) and in December at the Murray Mouth (1.39).

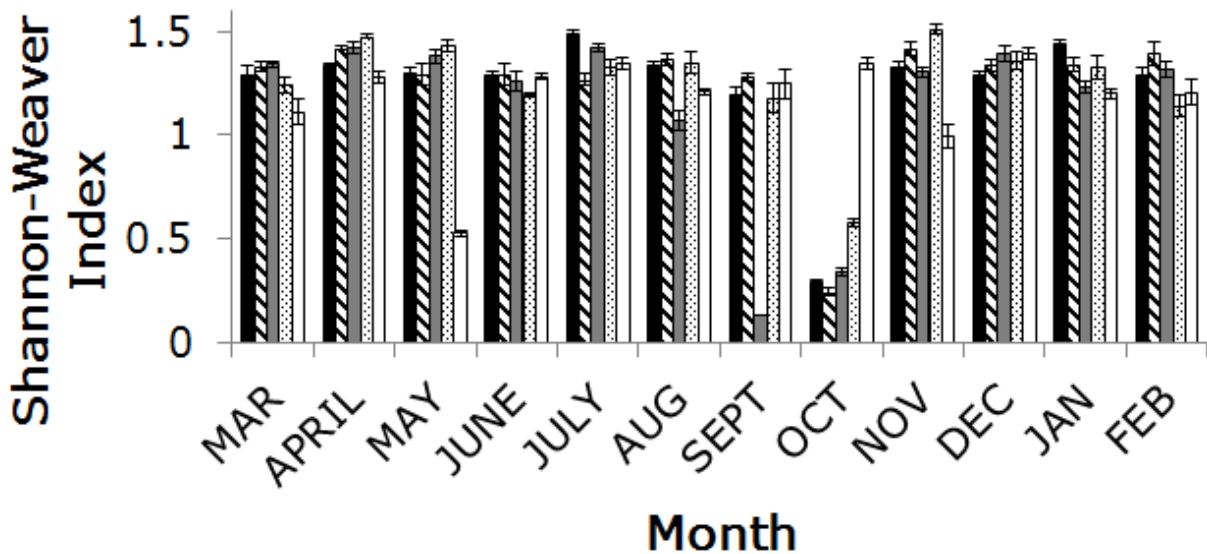


Figure 7. Phytoplankton diversity, using Shannon-Weaver index (H'), at five sites of the Coorong and Murray Mouth. Salt Creek is represented by the black-fill column, Policeman Point by diagonal stripe, Seven Mile Road by grey-fill column, Long Point by black dots and Murray Mouth by the white-fill column.

Correlations Between Communities of the North and South Lagoon

Correlations between the biological and physical parameters reveal that the sites of the hypersaline south lagoon and the saline north lagoon are driven by different environmental factors. In the south lagoon (Salt Creek and Policeman Point), correlations between physical parameters and wind speed four days before sampling, are negative with salinity (Spearman, $r = -0.53$, $p = 0.005$) and silica concentration (Spearman, $r = -0.57$, $p = 0.002$) at Salt Creek four days before sampling. Meanwhile at Policeman Point, the wind speed one day before sampling showed significant positive correlations with diatom abundance (Spearman, $r = 0.54$, $p = 0.02$), chl *a* (Spearman, $r = 0.506$, $p = 0.018$) and pH (Spearman, $r = 0.56$, $p = 0.001$).

In the north lagoon (Seven Mile Road, Long Point and Murray Mouth), no significant correlations were observed between wind speed and any other parameters. However, a number of significant correlations were observed between abundance and diversity with the physical data. At Seven Mile Road the only significant positive correlation observed was between chl *a* and salinity (Spearman, $r = 0.65$, $p = 0.02$). Likewise, at the Murray Mouth, the only significant correlation was between ammonium and dinoflagellate abundance (Spearman, $r = 0.75$, $p = 0.005$). Instead, at Long Point, a number of significant correlations were observed. Firstly, phytoplankton diversity had a negative correlation with nitrite (Spearman, $r = -0.70$, $p = 0.01$) and silica concentrations (Spearman, $r = -0.71$, $p = 0.01$). In addition, Long Point also observed significant correlations between chl *a* and salinity (Spearman, $r = 0.66$, $p = 0.02$), dinoflagellate abundance and pH (Spearman, $r = 0.66$, $p = 0.02$), and, diatom abundance and nitrate concentration (Spearman, $r = -0.80$, $p = 0.002$). These correlations highlight that, unlike in the north lagoon, the biological factors and environmental, excluding wind speed, were all linked.

BEST analysis indicated that significant correlations existed between nitrate, ammonium, phosphate, silica and salinity (BEST, $p > 0.05$, Pearson's $r = 0.81$). Similarly, in the principal components analysis PC1, accounting for 26.1% of the variation, was explained primarily by nitrite and dissolved oxygen, whereas PC2, which accounted for 15.2% of variation was best explained by salinity, ammonium and phosphate. Also, visually from the PCA also shows a clear distinction between the values of the two lagoons (Figure 8).

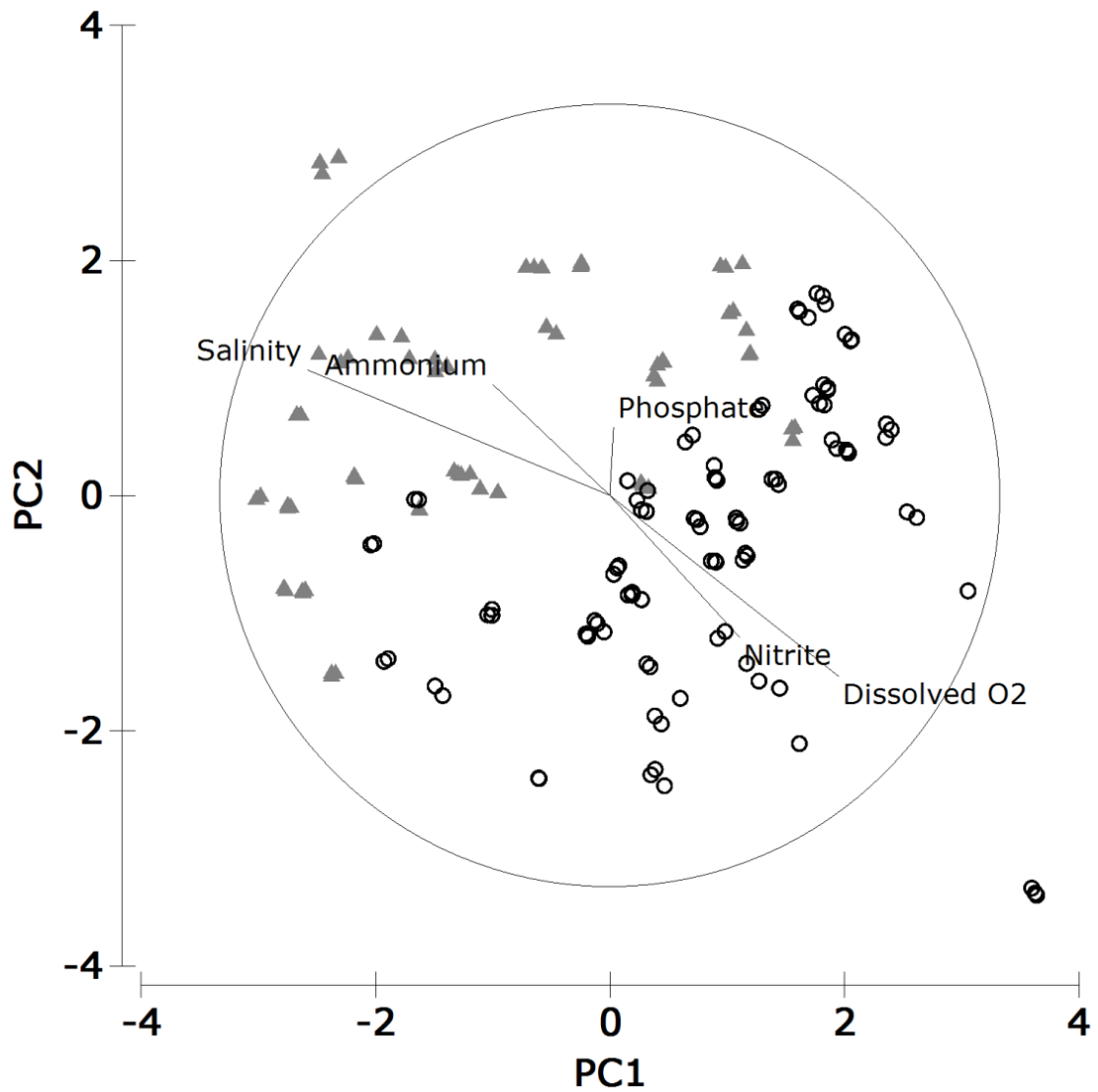


Figure 8. Principal Components Analysis (PCA) of environmental factors measured at the five sites of the Coorong. Grey triangles represent the South Lagoon and white circles represent the north lagoon.

Discussion

Despite pronounced difference in the salinity between the two lagoons of the Coorong, where the south lagoon regularly exceeded 120 PSU and the north lagoon was always below 110 PSU, salinity did not play a key role on the structure and composition of phytoplankton communities as revealed by the PCA analysis. In fact, this showed that there was no one single factor influencing the abundance and diversity of the Coorong communities sampled along the entire hypersalinity gradient. A study conducted during non drought period observed that increasing water levels throughout this inverse estuary, particularly in the south lagoon, were accompanied not only by a decrease in salinity of 1 – 75 PSU along both lagoons, but also by a shift in the phytoplankton species, particularly in the brackish waters of the north lagoon (Jendyk *et al.* 2014). In the current study, which was conducted in drought conditions, we observed that community structure were particularly evident within the individual lagoons rather than the individual sites. In the south lagoon wind speed was a key factor driving other environmental as well as the biological parameters, primarily by means of mixing the water column, as also observed by Kämpf 2014 and Mellard *et al.* 2012. In contrast, phytoplankton communities in the north lagoon were influenced by the physical parameters on the day of sampling, which revealed variation in nutrient availability and water chemistry, in agreement with Kimmerer *et al.* 2012 and Litchman *et al.* 2012.

The South Lagoon

Turbulent mixing of the water column via wind action results in the mixing of phytoplankton cells and dissolved nutrients throughout the water column and the benthos (Clarke 1993, Morgan *et al.* 2014, Rodrigues and Pardal 2015). This in turn affects the abundance and growth rate of phytoplankton communities (Clarke 1993, Mahadevan *et al.* 2012, Rodrigues and Pardal 2015). In the Coorong, positive correlations between wind speed with abiotic and

biotic factors in the south lagoon observed 4 days and 1 day before sampling suggest an offset of the effect of wind speed on the phytoplankton communities.

At Salt Creek salinity was not correlated with phytoplankton community abundance or diversity. It has been previously observed that phytoplankton, in particular diatoms, are able to adapt to changes in salinity over long or seasonal times (DeMartino *et al.* 2007, Jendyk *et al.* 2014, Kipriyanova *et al.* 2007). Instead, in our case we observed a physical response to wind speed linked to the local hydrology, where wind induced increasing fluctuations of water mixing and evaporation in the South Lagoon (Webster 2010). The observed negative correlation with wind speed and salinity seen in the Coorong indicates an increase in salinity with decrease in wind speed may be explained by Webster's (2010) observations (Table 1, Figure 2). Furthermore, the decrease in water depth influenced by the drought also implies that there is significantly less water exchange between the north and south lagoons at Parnka Point, which would add saline water to the south lagoon (Figure 1, Jendyk *et al.* 2014, Leterme *et al.* 2013).

At Salt Creek, silica concentration was negatively correlated with wind speed, where, similar to salinity, silica concentration increased with decreasing in wind speed. The concentration of silica generally decreases in the water column through uptake by diatoms (Brunner *et al.* 2009, Krause *et al.* 2011). Most diatoms extract silica from the water column as monosilicic acid, in turn using this to form the silica frustule that encases the cell (Amo and Brzezinski, 1999). Here, it may be suggested that while wind speed limits diatoms growth due to mixing in a shallow water environment (Pete *et al.* 2010), silica concentration was not a limiting factor and probably fostering their growth (Brunner *et al.* 2009).

Policeman Point diatom abundance, chl *a* and pH were all positively correlated with wind speed. Also, as observed by Ólafsson and Elmgren (1997), Bode *et al.* (2005), and Palmer-Felgate *et al.* (2011), the increase in abundance is here initiated three days after the Salt

Creek. This is also paralleled by chl *a*, which reflects increases in biomass that coincides with the increase in diatom abundance at Policeman Point. There are a number of factors are known to increase water acidity, including riverine input, decomposition of organic matter, respiration and photosynthesis (Feely *et al.* 2010; Range *et al.* 2012). The positive correlation between wind speed and pH may be linked to the increased diatom abundance and chl *a* in the south lagoon. The increase in abundance observed at Policeman Point most likely results from a combination of increased photosynthesis, decreased grazing due to high salinity (George *et al.* 2015) and sedimentation in the shallow water (Ólafsson and Elmgren 1997, Palmer-Felgate *et al.* 2011).

The North Lagoon

In contrast to the south lagoon, no parameter in the north lagoon showed a significant correlation with wind speed. It is well known that dissolved nutrients impact phytoplankton communities, where increase in nutrients leads to increase in biomass, production, community composition and phytoplankton diversity (Hillebrand *et al.* 2002, Litchman *et al.* 2012).

In the case of nitrite and silica, the correlations with diversity suggest that these nutrients play a role in determining community composition and structure (Interlandi and Kilham 2001, Lagaria *et al.* 2011). Therefore, these are likely to be limiting resources in the north lagoon, where the dissolved nutrients decrease due to uptake by phytoplankton (Interlandi and Kilham 2001). At the Murray Mouth, dissolved nutrient concentration was lower than the other four sites throughout the year. Ammonium concentration was the highest measured nutrient. One reason for this could be that increases in pH may result from phytoplankton taking up CO₂ faster than respiration produces it (Paerl 1984, Rost *et al.* 2006) or from the increase in ammonium concentration from uptake of nitrate and nitrite (Paerl 1984, Wall *et al.* 1998).

The pH in the Coorong varied temporally and spatially between 7.5 and 9.5. Previously, it has been shown that where pH approaches between 8.8 and 8.0, allows for dissolution of nutrients into the water (Hansen 2002, Rost *et al.* 2006), and this may be linked to what happened in the north lagoon, where pH was 7.8 and 8.5.

The north lagoon at 38 – 112 PSU was considerably more saline than the South Lagoon, at 108 – 202 PSU. Negative correlation between salinity and chl *a* has been previously linked to an open connection between a coastal lagoon with the ocean (Macedo *et al.* 2001), where the north lagoon does indeed share a connection with the ocean (Webster 2005, 2010). It has further been suggested that a decrease in salinity may cause increased abundance of chlorophytes, after significant tidal flushing (Suikkanen *et al.* 2007), which is a scenario that has been observed in the Coorong during non drought conditions (Jendyk *et al.* 2014). However, human activity has restricted the flow between the Coorong and the ocean, where barrages close to the Murray Mouth are the main input of freshwater into the system (Webster 2005). Moreover, the barrages were not opened during the study period to provide additional inflows into the north lagoon (Murray-Darling Basin Authority 2013). The wide range of salinity levels may allow for growth of species of varying salinity tolerance (Kirkwood and Henley 2006, Nübel *et al.* 1999), and was also observed in the Coorong recently, during non drought conditions (Jendyk *et al.* 2014).

Conclusion

The phytoplankton communities at the Coorong, South Australia show spatial and temporal variability along a salinity gradient, from the oceanic Murray Mouth to the hypersaline Salt Creek. This study, which was conducted during drought conditions, where the Coorong was considered to be in rapid decline, found pronounced differences in salinity between the north and south lagoons. Consistently high salinity in the south lagoon may indicate that the phytoplankton communities have adapted or already selected for to the point where they do not have a significant effect on the community abundance and composition. However, in the north lagoon salinity a significant impact on phytoplankton possibly due to a connection between the lagoon and the open ocean, which induces rapid fluctuations in the north lagoon salinity. Moreover, the reduced water depth in the south lagoon led to the phytoplankton communities being directly affected by the local wind speeds. Due to the shallow water depth, there are limited water exchanges between the lagoons. This in turn leads spatial independence between the north and south lagoons, where each lagoon is impacted differently by different factors.

Chapter 2
Supplementary Material

Table S1. Mean dissolved nutrient (nitrite, nitrate, ammonium, phosphate and silica in $\mu\text{mol/mL}$ with \pm standard deviation) concentration from March 2009 to February 2010 at five sites along the Coorong lagoons: Salt Creek, Policeman Point, 7 Mile Road, Long Point and Murray Mouth.

		Mean Nutrient Concentration ($\mu\text{mol/mL}$) \pm Standard Deviation				
Site	Month	Nitrite	Nitrate	Ammonium	Phosphate	Silica
Salt Creek	March	1.09 \pm 0.00	0.16 \pm 0.00	0.00 \pm 0.00	0.00 \pm 0.00	26.04 \pm 2.08
	April	0.144 \pm 0.13	0.00 \pm 0.00	3.59 \pm 4.11	1.74 \pm 1.21	12.5 \pm 2.76
	May	0.00 \pm 0.00	2.69 \pm 1.86	2.69 \pm 0.00	1.39 \pm 0.60	8.68 \pm 0.61
	June	0.36 \pm 0.25	0.00 \pm 0.00	0.00 \pm 0.00	2.08 \pm 0.00	4.17 \pm 0.00
	July	0.22 \pm 0.21	0.00 \pm 0.00	101.28 \pm 11.19	1.74 \pm 1.20	5.21 \pm 0.00
	August	0.00 \pm 0.00	0.54 \pm 0.93	0.90 \pm 1.55	34.38 \pm 2.76	28.82 \pm 0.60
	September	0.22 \pm 0.00	0.00 \pm 0.00	3.59 \pm 1.55	2.43 \pm 0.60	42.36 \pm 0.62
	October	0.07 \pm 0.12	0.00 \pm 0.00	11.65 \pm 1.55	0.00 \pm 0.00	29.17 \pm 0.00
	November	0.00 \pm 0.00	0.00 \pm 0.00	0.00 \pm 0.00	0.35 \pm 0.60	50.69 \pm 0.60
	December	0.00 \pm 0.00	0.00 \pm 0.00	2.69 \pm 0.00	0.00 \pm 0.00	56.94 \pm 0.60
	January	1.16 \pm 0.25	2.15 \pm 0.93	222.81 \pm 33.21	2.08 \pm 1.80	29.86 \pm 2.62
	February	0.00 \pm 0.00	1.61 \pm 2.7x10 ⁻¹⁶	337.01 \pm 23.49	4.51 \pm 3.35	35.76 \pm 4.92
Policeman Point	March	0.22 \pm 0.00	1.61 \pm 2.7x10 ⁻¹⁶	4.7 \pm 5.9	0.35 \pm 0.60	20.49 \pm 0.60
	April	0.14 \pm 0.25	0.54 \pm 0.93	2.02 \pm 1.78	0.00 \pm 0.00	15.97 \pm 1.59
	May	0.00 \pm 0.00	0.00 \pm 0.00	0.90 \pm 1.55	3.82 \pm 0.61	2.08 \pm 0.00
	June	0.22 \pm 0.22	0.00 \pm 0.00	0.00 \pm 0.00	2.08 \pm 0.00	10.07 \pm 0.60
	July	0.00 \pm 0.00	0.00 \pm 0.00	72.60 \pm 2.69	3.47 \pm 1.20	9.72 \pm 0.61
	August	0.00 \pm 0.00	0.00 \pm 0.00	72.69 \pm 4.74	0.69 \pm 0.60	15.97 \pm 0.60
	September	0.07 \pm 0.13	0.00 \pm 0.00	1.79 \pm 1.55	0.00 \pm 0.00	38.19 \pm 0.60
	October	0.00 \pm 0.00	0.00 \pm 0.00	10.76 \pm 0.00	0.69 \pm 0.60	38.19 \pm 0.61
	November	0.07 \pm 0.13	0.00 \pm 0.00	0.00 \pm 0.00	1.04 \pm 0.00	38.54 \pm 0.00
	December	0.14 \pm 0.12	0.00 \pm 0.00	19.72 \pm 1.55	0.00 \pm 0.00	40.63 \pm 0.00
	January	0.07 \pm 0.13	0.54 \pm 0.93	204.36 \pm 16.48	1.04 \pm 1.04	15.63 \pm 2.76
	February	0.15 \pm 0.13	2.69 \pm 1.86	15.85 \pm 7.6	3.82 \pm 0.60	30.90 \pm 3.18
7 Mile Road	March	0.07 \pm 0.12	1.08 \pm 0.93	0.00 \pm 0.00	0.35 \pm 0.60	0.00 \pm 0.00
	April	2.25 \pm 3.70	1.61 \pm 2.7x10 ⁻¹⁶	1.79 \pm 1.55	1.39 \pm 0.60	1.74 \pm 1.20
	May	0.07 \pm 0.13	2.15 \pm 0.93	2.69 \pm 0.00	0.00 \pm 0.00	0.69 \pm 0.60
	June	0.07 \pm 0.13	0.57 \pm 0.94	0.90 \pm 1.55	0.00 \pm 0.00	1.74 \pm 1.20
	July	0.00 \pm 0.00	0.00 \pm 0.00	1.64 \pm 1.44	0.00 \pm 0.00	0.35 \pm 0.60
	August	0.00 \pm 0.00	0.00 \pm 0.00	30.24 \pm 1.78	0.00 \pm 0.00	3.47 \pm 0.60
	September	0.00 \pm 0.00	0.00 \pm 0.00	2.69 \pm 0.00	2.43 \pm 0.61	35.07 \pm 0.60
	October	0.00 \pm 0.00	0.54 \pm 0.90	4.48 \pm 1.55	1.04 \pm 0.00	23.96 \pm 0.00
	November	0.00 \pm 0.00	0.00 \pm 0.00	0.90 \pm 1.55	0.00 \pm 0.00	53.82 \pm 0.60
	December	0.22 \pm 0.00	0.00 \pm 0.00	2.69 \pm 0.00	1.04 \pm 0.00	48.61 \pm 0.60
	January	0.29 \pm 0.33	1.08 \pm 0.93	111.59 \pm 13.93	0.00 \pm 0.00	4.51 \pm 1.59
	February	0.07 \pm 0.13	1.08 \pm 0.93	66.58 \pm 9.51	6.60 \pm 1.59	22.57 \pm 1.59

Long Point	March	1.16 ± 0.13	0.00 ± 0.00	0.94 ± 1.10	0.00 ± 0.00	1.04 ± 0.00
	April	0.29 ± 0.13	4.84 ± 1.61	0.00 ± 0.00	0.00 ± 0.00	3.13 ± 1.80
	May	0.14 ± 0.25	0.00 ± 0.00	2.24 ± 0.39	27.78 ± 0.60	10.07 ± 0.60
	June	22.97 ± 0.33	0.00 ± 0.00	0.22 ± 0.39	0.00 ± 0.00	1.04 ± 0.00
	July	0.14 ± 0.22	0.00 ± 0.00	2.69 ± 0.67	0.69 ± 0.60	1.04 ± 0.00
	August	0.58 ± 0.45	0.00 ± 0.00	0.67 ± 1.16	0.69 ± 0.60	0.69 ± 0.60
	September	0.00 ± 0.00	0.00 ± 0.00	35.85 ± 0.77	0.00 ± 0.00	21.88 ± 0.00
	October	0.00 ± 0.00	15.59 ± 1.86	0.67 ± 0.00	6.60 ± 1.20	1.74 ± 0.60
	November	0.14 ± 0.12	0.00 ± 0.00	0.9 ± 0.39	1.04 ± 0.00	10.42 ± 0.00
	December	0.00 ± 0.00	0.00 ± 0.00	19.94 ± 0.39	6.94 ± 1.20	30.56 ± 0.60
	January	0.29 ± 0.33	2.69 ± 1.86	1.94 ± 1.21	2.43 ± 1.59	3.47 ± 1.59
	February	3.12 ± 3.00	0.54 ± 0.93	18.43 ± 5.67	1.39 ± 1.20	11.11 ± 2.62
Murray Mouth	March	0.07 ± 0.12	1.08 ± 0.93	0.94 ± 1.63	0.00 ± 0.00	0.69 ± 0.60
	April	0.36 ± 0.12	1.08 ± 0.93	1.69 ± 0.97	0.35 ± 0.60	1.04 ± 0.00
	May	0.14 ± 0.13	0.54 ± 0.93	0.00 ± 0.00	0.00 ± 0.00	0.69 ± 0.60
	June	0.00 ± 0.00	0.54 ± 0.93	0.42 ± 0.39	0.35 ± 0.60	0.69 ± 0.60
	July	0.00 ± 0.00	0.00 ± 0.00	11.59 ± 1.61	14.93 ± 0.60	0.69 ± 0.60
	August	0.14 ± 0.12	0.00 ± 0.00	4.71 ± 0.67	0.00 ± 0.00	0.00 ± 0.00
	September	0.00 ± 0.00	0.54 ± 0.94	2.24 ± 0.38	0.00 ± 0.00	1.04 ± 0.00
	October	0.00 ± 0.00	0.00 ± 0.00	1.79 ± 0.38	0.00 ± 0.00	1.04 ± 0.00
	November	0.00 ± 0.00	0.00 ± 0.00	0.67 ± 0.00	1.39 ± 0.60	0.35 ± 0.60
	December	0.00 ± 0.00	0.54 ± 0.94	2.24 ± 3.88	2.08 ± 0.00	17.71 ± 0.00
	January	0.43 ± 0.58	1.08 ± 1.86	22.99 ± 5.71	1.39 ± 1.59	5.56 ± 1.59
	February	0.58 ± 0.66	0.54 ± 0.93	23.01 ± 0.97	14.93 ± 2.41	13.19 ± 1.59

CHAPTER 3

Microscale Variation of Microbial Eukaryotic Communities Revealed by 18S Sequencing

Abstract

Scale is an important concept in biology. In marine ecosystems the small end of all scales is particularly important because of the predominance of microscopic primary producers. The key processes and distributions for these organisms take place at < 1 m, or what is referred to as the microscale. Variations, gradients and patchiness at the microscale are often much greater than that found at the macroscale. Here we characterise 10 benthic microphytobenthic communities within 70 cm of each other. Our particular focus is on the Chromalveolates, which constituted 23-32% of the total taxa contribution across the microscale locations. PCoA reveals that phyla from the chromalveolata drive the observed differences within the communities, including 3 species of ciliate and an unknown diatom OTU. Diatom and ciliates, like other microbial eukaryotes, strictly interact with each other at microscales and their respective variabilities have ecosystem-wide effects as these organisms form the basis of the aquatic food web. We conclude that while chlorophyll provides an indication of the photosynthetic biomass, diatoms, as revealed by PCoA and network dynamics, are a central and controlling component of benthic microeukaryote community and microscale interactions.

Introduction

Benthic protists include taxa of microeukaryotes such as ciliates, foraminiferans, amoebozoans and diatoms, which form the base of most aquatic food webs. Microbes vary in number and taxa at micro- to large scales (Stocker and Seymour 2012). While a number of studies have investigated the microscale distributions of viral and bacterial populations (Mitchell *et al.* 1989, Azam 1998, Seymour *et al.* 2005, 2006), many more have looked at the large scale distribution of these prokaryotic and eukaryotic single-celled organisms (Waters *et al.* 2003, Seymour *et al.* 2006, Gallegos *et al.* 2010, Jendyk *et al.* 2014, Dann *et al.* 2014).

Large scale studies into microbial eukaryotes show the prevalence of microbial eukaryotic groups such as green algae, diatoms, dinoflagellates, haptophytes and cryptophytes in the water column (Finlay 2002, Xu *et al.* 2014) and the benthos (Bik *et al.* 2012). Previous studies by Balzano *et al.* (2012) and Jendyk *et al.* (2014) assessed diversity and relative abundance of microeukaryotes at the Coorong lagoons, where the site of this study is located, sampling multiple sites over 170 km of the coastal lagoon system. These studies emphasised the influence of the distance along the coastal lagoon system driving the variation of the microeukaryotic communities (Balzano *et al.* 2012, Jendyk *et al.* 2014). Yet there has been very little work characterising spatial variation and identification of microeukaryotes on much smaller spatial scales, i.e. at micrometres and centimetres (Fang *et al.* 2007).

Previous studies have investigated the biological interaction at the microscale between meiofauna and macrofauna (Bik *et al.* 2012, Tan *et al.* 2015). Dispersion patterns of diatoms have been suggested to affect the dispersion of meiofauna (Blanchard 1990). This is a concept that has been more widely explored and observed on scales over tens and hundreds of metres (Bik *et al.* 2012, Jones *et al.* 2013) and is why diatoms may be used as indicators of water quality and aquatic ecosystem health (Tan *et al.* 2015). In addition, Blanchard (1990) also observed heterogeneity in the meiofauna and macrofauna communities associated with

the microphytobenthos. In addition, it has been recently suggested that grazing activity within the microphytobenthos is influenced by factors such as competition for resources between microalgae and grazing by meiofauna and macrofauna on protists and algae (Pratt *et al.* 2015).

The group of microeukaryotic group, the Chromalveolates, are of particular interest here and consists of dinoflagellates, diatoms, green algae and ciliates (Stoecker *et al.* 2009, McManus *et al.* 2012). It has been previously shown that chlorophyll (Spilmont *et al.* 2011, Seuront and Spilmont 2002, Franks and Jaffe 2008), viral and bacterial communities vary on the microscale (Seymour *et al.* 2000, 2005). In order to gain a better understanding of microbial eukaryote distributions in the microphytobenthos at the microscale, we aim to (i) determine the community composition of microeukaryotes in the microphytobenthos, and (ii) relate it to the chlorophyll *a* and *c* biomass. These results aim to demonstrate the relative importance of the identified eukaryotic taxa.

Methods

Study Site

The selected site for this study was Salt Creek, South Australia, located in the south lagoon within the Coorong National Park (S36° 09.936', E139° 39.104'; Figure 1). Salt Creek is typical of the Coorong's shallow water, predominately sandy, high salinity environment (Wright and Wacey, 2005), where the lagoon is also protected from wind blowing directly from the Southern Ocean by the Younghusband Peninsula. Water inputs in the Coorong and nearby distal ephemeral lakes consists of rainfall and seaward movement of groundwater from an open aquifer system (Wright and Wacey 2005, Webster 2010).

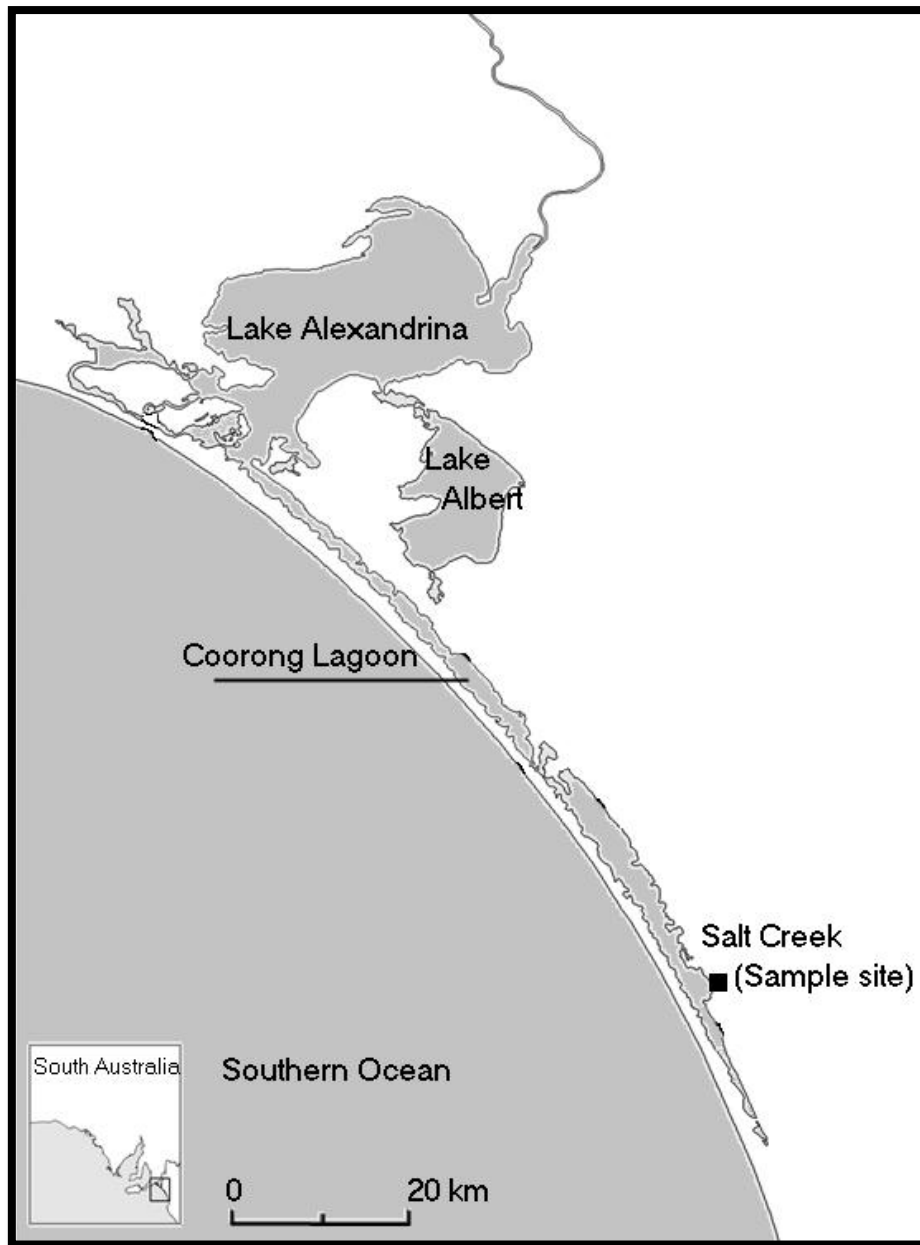


Figure 1. Map of sampling location: Salt Creek, South Australia (Coorong National Park, S36° 09.936', E139° 39.104').

Sample Collection

Sediment samples were taken from an area measuring 100 cm², which was further divided into 100 squares measuring 10 cm². A quadrat was placed in an area where the sediment was made of sand and the water depth was approximately 5 cm. The top 0.5 – 1 cm of surface sediment was removed in each 10 cm² section in triplicate. From the sediment sampled, 1 g sediment, frozen and kept in the dark, for further chlorophyll analyses. Using the methods outlined in Ritchie (2008, 2006) for chlorophyll extraction and calculation of concentration of chlorophyll *a* (chl *a*) and chlorophyll *c* (chl *c*) in g m⁻³, 5 mL 100% ethanol was added to 1 g of sediment and the sample was placed on a vortex for 30 seconds. Pigments were then extracted in the dark for 10 minutes and centrifuged for a further 2 minutes before transferring the resulting supernatant to a cuvette to measure the absorbance of the solution using spectrophotometric analysis (LKB Biochrom 4050 Ultrospec II UV/Vis). Measurements were taken at 632 nm, 649 nm, 665 nm and 696 nm, seen in the equations as A_{632} , A_{649} , A_{665} and A_{696} , respectively and expressed as g m⁻³.

For DNA extraction, 1 g of sediment was frozen and kept in the dark and later extracted using a PowerSoil DNA Isolation Kit (MO BIO Laboratories, Inc.). From the quadrat, 10 samples were selected for sequencing, for the purposes of this paper these are designated as 0 cm, 73 cm, 41 cm, 90 cm, 63 cm, 74 cm, 77 cm, 75 cm, 70 cm and 93 cm (Figure 2). Sequencing for eukaryotic 18S rRNA ribosomal small subunits was done on the Roche 454 GS FLX+ platform using the primer pair Euk7F and Euk570R (MR DNA, Shallowater, Texas).

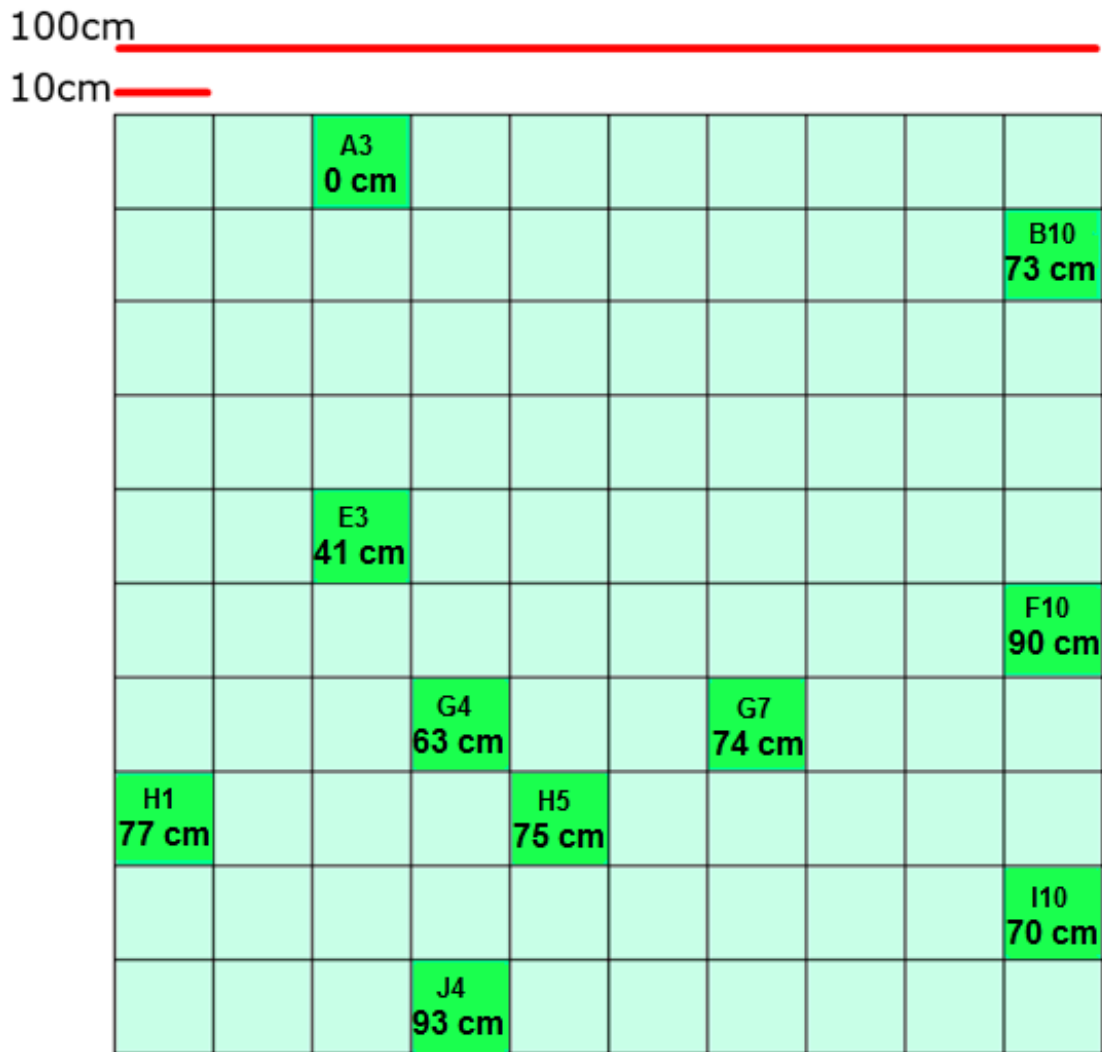


Figure 2. Diagram depicting the sampling strategy from a 1m x 1m quadrant where the 10 microscale locations were selected using a random number generator. For all graphical outputs, distance from A3 (0 cm) was calculated by measuring a straight line between the centre of A3 to the centre of each other square.

Bioinformatics and Data Analysis

To process the sequence data, the quality filtering criteria were a minimum quality score of 25, minimum 200 base pairs in length, no ambiguous bases, no mismatches in the primer sequence and singletons removed using CLC workbench software (CLC Bio, Aarhus, Denmark). Chimeric sequences were removed using UCHIME (Edgar *et al.* 2011). The resulting consensus sequences were compared with sequences in GenBank using the Basic Local Alignment Sequence Tool (BLASTn) and aligned using ClustalW in MEGA5 (Tamura *et al.* 2011). Only the top hits were considered. The resulting data were extracted using Bioinformatics Rapid (Data) Extraction from XML (B-REXml) (Ruthenbeck *et al.* in prep). Statistical analyses were conducted using PRIMER 7 (Version 7.06, Primer-E Ltd. Plymouth, Clarke and Gorley 2015). The Bray-Curtis distance matrix was calculated as a measure of similarity between the samples, with square root transformation, displayed using hierarchical agglomerative clustering (CLUSTER) with SIMPROV to determine significance between samples (Clarke and Gorley 2015). Principal Coordinate Analysis, PCoA, was also conducted where the resemblance matrix is used to project the similarity/dissimilarity between OTUs onto a set of axes and the distance between points is an indication of similarity (Togerson 1958, Gower 1966). To discover what taxa were contributing to the overall dissimilarity between the different microscale locations, SIMPER analysis was conducted. The ratio of the average dissimilarity to the standard deviation (Diss/SD) was used where a ratio greater than 1.9 was used as an indicator of discriminating taxa between sample groups (Clarke and Anderson 2001). In addition, to investigate the relationship between the observed chlorophyll concentrations (chl *a* and chl *c*) and the microeukaryote 18S OTU within the microphytobenthos, Spearman's correlation was calculated using SPSS v. 22.0. Finally, network analysis was conducted using the sequences and the chlorophyll data. The microbial

network was constructed using the CoNet application in Cytoscape 3.2.1. as outlined in Faust and Raes (2012).

Results

Microscale OTUs

In total, 74288 sequences were analysed within the 30 samples (Table S1). Between the 10 microscale locations 639 different 18S OTU hits were identified (Table S2). OTUs identified belonged to the eukaryotic supergroups Excavata (including euglena), Chromalveolata (including heterokonts, haptophytes, dinoflagellates and ciliates), Rhizaria (including radiolarians), Archaeplastidia (including glaucophytes and green algae) and Unikonta (including choanoflagellates).

Between the microscale locations, unknown protozoans, Archaeplastidia and Chromalveolates accounted for more than 96% of the identified microbial eukaryotes. The total percentage contribution of the three groups did not significantly vary between locations (Figure S3).

Looking specifically at the Chromalveolates (Figure 3), eight main clades were identified. By far, the most prominent were the ciliates and the diatoms, which were found at all ten microscale locations. Ciliates contributed to between 2.1% \pm 0.7 (73 cm) and 68% \pm 20 (70 cm) of the chromalveolate OTUs, while diatoms contributed between 22.9% \pm 3.78 (70 cm) and 85.8% \pm 6.49 (73 cm). The Spearman's ρ correlation between ciliates and diatoms was -0.818 ($p = 0.004$).

In addition to diatoms and ciliates, apicomplexa, dinoflagellates and haptophytes were also present. Apicomplexa and cryptophytes are only present at two of the ten microscale

locations and contributed to less than 1% of the total mean contribution of the chromalveolates. Specifically, Apicomplexa were only present at 70 cm, 0.6 % (± 0.2), and 75 cm, 3.6% (± 0.1). In contrast, the haptophytes and dinoflagelates were present at all points sampled, but contributed to less than 30% of the total mean Chromalveolates (Figure 3). Haptophytes ranged between 0.5% ± 0.04 at 93 cm and 20.2% ± 2.2 at 77 cm, while dinoflagellates ranged between 4.7% ± 0.7 at 73 cm, and 20.2% ± 1.4 at 41 cm. Similar to the trend observed been ciliates and diatoms, ciliates also showed a significant positive correlation to the cryptophytes (Spearman's $\rho = 0.730$, $p = 0.025$) and a significant correlation to the dinoflagellates (Spearman's $\rho = -0.811$, $p = 0.004$).

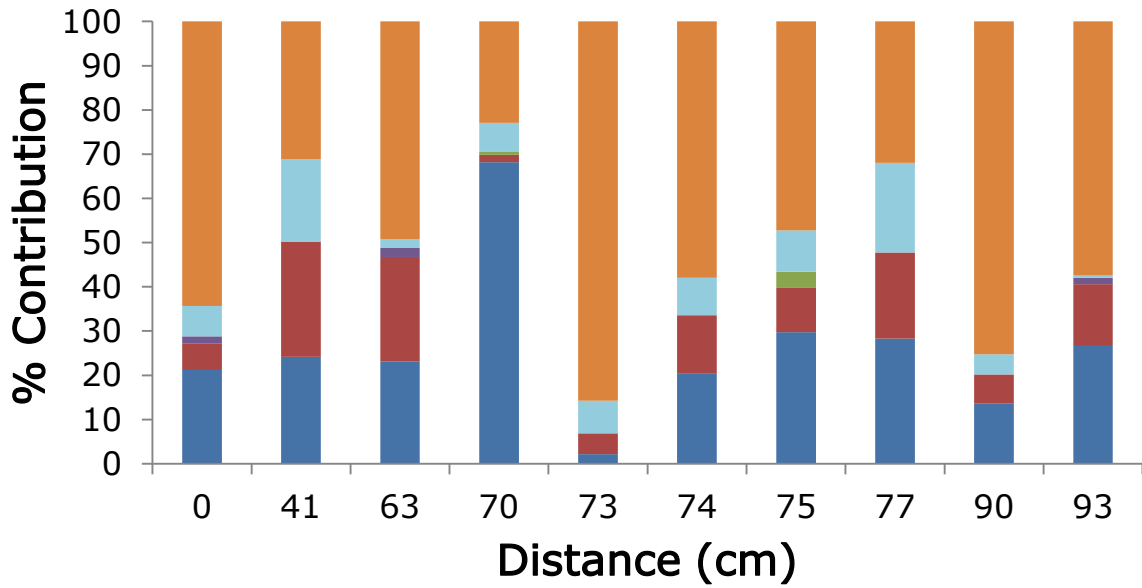


Figure 3. Mean percentage contribution of selected phyla within the Chromalveolates: Haptophyta (Light Blue), unknown Chromalveolates (Purple), Ciliophora (ciliates, Dark Blue), Dinoflagellata (dinoflagellates, Red), Apicomplexa (Green), and, Bacillariophyceae (diatoms, Orange). Sample locations labelled as distance from first sample point, A3 of 0 cm, as shown in Figure 2.

Correlations with Chlorophyll

Pigments chl *a* and chl *c* were observed and measured at the ten microscale locations (Figure S4). Spearman correlation was performed between OTUs and chlorophyll pigments *a* and *c*, however, no significant correlations were observed between microbial eukaryotes and chlorophyll pigment concentration when OTUs were grouped in their respective kingdoms, phyla or classes.

Species Similarity Between Microscale Sites

Using CLUSTER analysis, similarity between microscale location for the 18S OTUs at the class level was between 56% and 68% (Figure S5). For locations 0 cm, 73 cm, 41 cm, 90 cm, 74 cm and 75 cm, these form groups comprising of just the three replicates for each location which form clusters with similarities ranging between 58% and 68%. Using SIMPROF analysis no significant differences were detected for similarity within replicates at all of the locations except for 41 cm (indicated in Figure S5 by the red dotted line). However, for the remaining microscale locations (63 cm, 77 cm, 70 cm and 93 cm) clustered together with similarities between 56% and 65%, including all replicates for each location. SIMPROF analysis also showed no significant difference between the majority of samples.

PCoA analysis was used to visualise the dissimilarity of the 18S OTUs, accounting for a total of 78.2% of variation (Figure 4). From SIMPER, significance of the observed dissimilarity was determined using the Diss/SD ratio. Four groups were distinguished within the PCoA where the dissimilarity is being driven by different species, as indicated by the OTUs. Firstly, the three replicates from location 75 cm form one group where dissimilarity is caused by two OTU. The ciliate *Euplotes dammamensis* where the Diss/SD for 75 cm & 63 cm was 3.83 and that of 75 cm & 77 cm was 4.74. The second OTU responsible for dissimilarly was an unknown diatom OTU, where Diss/SD for 75 cm & 0 cm, 75 cm & 73 cm, 0 cm & 41 cm, 75 cm & 90 cm was 3.28, 7.22, 6.69 and, 6.07, respectively. A second group was formed by the microscale locations 0 cm, 63 cm and 74 cm. In this group an unknown diatom OTU was driving dissimilarity where Diss/SD for 0 cm & 63 cm, 0 cm & 74 cm and 63 cm & 74 cm was 6.62, 6.04 and 5.07, respectively. The third group consists of 93 cm, 77 cm and 41 cm and were affected by two ciliate OTU taxa. The ciliate *Bergeriella ovata* was the cause of dissimilarity at 93 cm & 41 cm, Diss/SD was 2.84, and at 93 cm & 77 cm were the species *B. ovate* (Diss/SD was 2.46) and *Euplotes dammamensis* (Diss/SD was 1.82). However, one

replicate of the three locations 73 cm, 90 cm and 70 cm were also present in this group. 70 cm & 93 cm showed a significant dissimilarity caused by *Euplotes dammamensis* (Diss/SD was 4.44) and the ciliate *Euplotes nobilii* also showed significant dissimilarity for 73 cm & 90 cm (Diss/SD was 16.5) and 73 cm & 70 cm (Diss/SD was 13.93).

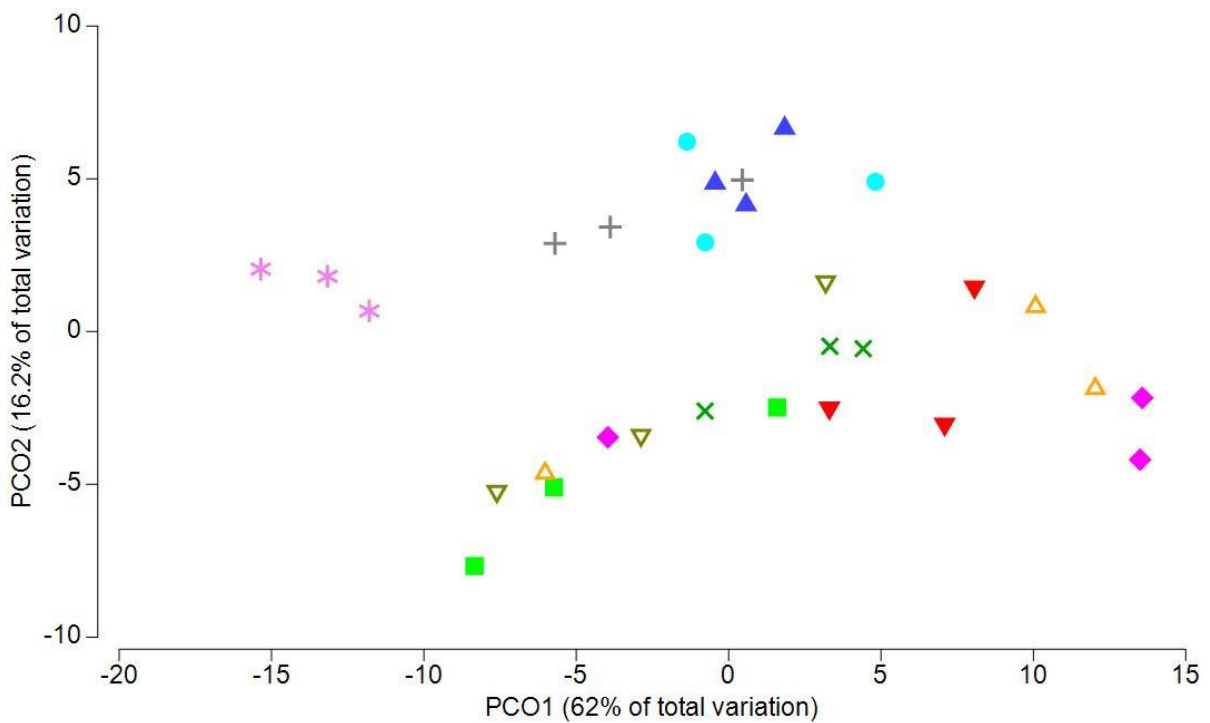


Figure 4. Principle Coordinate (PCoA) Analysis of 18S OTUs samples by Class at 10 microscale locations (in triplicate). The data has been square root transformed and resemblance made using Bray-Curtis similarity. Blue triangles represent location 0 cm, red inverted triangles represent 73 cm, green squares represent 41 cm, pink diamonds represent 90 cm, light blue circles represent 63 cm, grey '+'s represent 74 cm, dark green X's represent 77 cm, pink stars represent 75 cm, orange lined triangles represent 70 cm and green lined triangles represent 90 cm.

Network analysis of the microbial communities including the data from the 10 sampling locations further clarifies the results (Figure 5). In Figure 5, the two largest nodes represent undefined taxa and the diatoms. Yet, the undefined group will include sequences from different taxonomic groups and therefore we will only consider the results from the diatom interactions. The colour of the diatom node, yellow, indicates that there are less efficient interactions with the other taxa represented. Finally, the thicker edges are indicative of greater similarity between the nodes. These show that diatoms, dinoflagellates and chl *c* are highly similar to the undefined group and the haptophytes are similar to chl *a* and dinoflagellates. However, the colour of the edges indicates the importance of the edge. Here, red edges indicate the most important interactions, where the only red edges are shown for the diatoms, connecting to the ciliates and the undefined group.

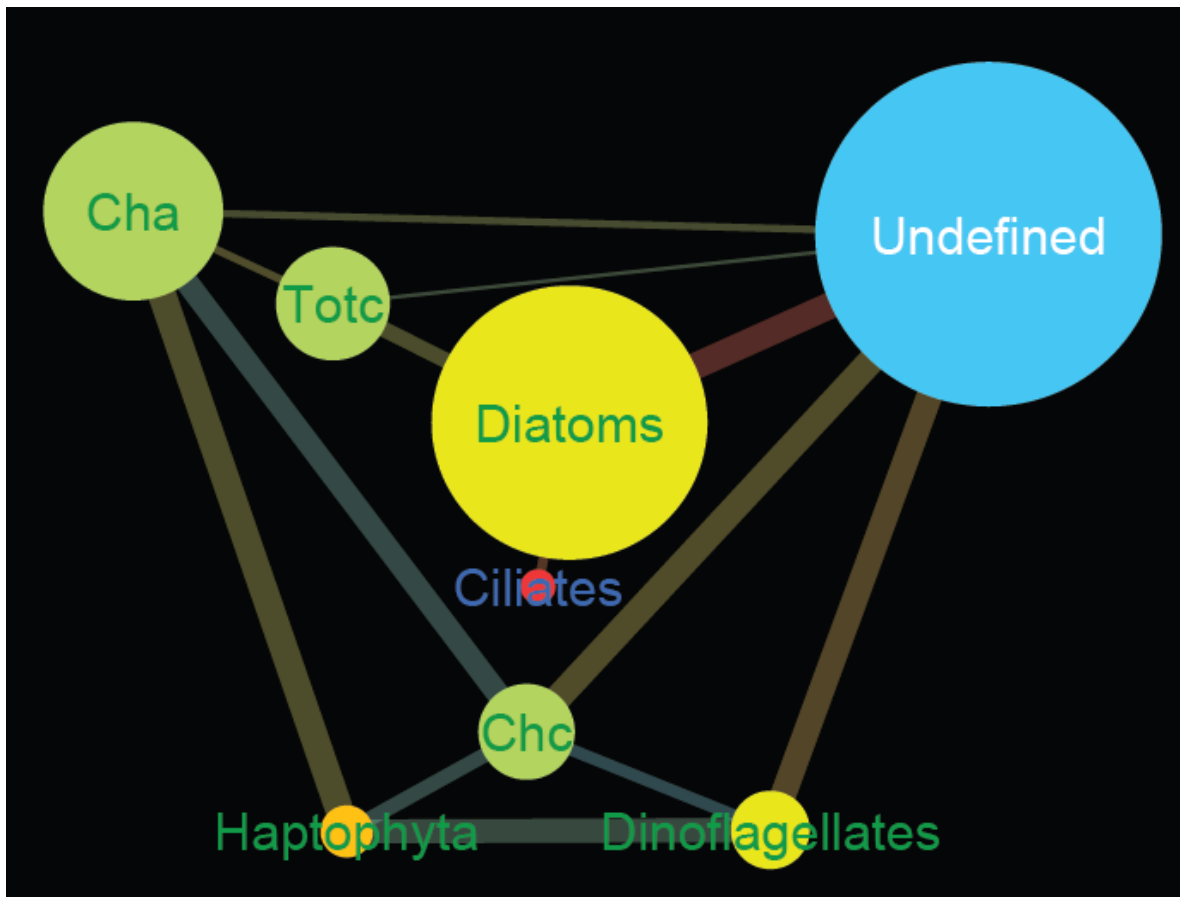


Figure 5. Network analysis for all OTU results at 10 microscale locations where only features significant results. The strength of the interaction, or betweenness centrality, for taxa and chlorophyll parameters is shown at the nodes where the larger nodes indicate the increasing importance of the node to the rest the community. The colour of the node shows average shortest path length, the shortest paths show the greatest efficiency of transfer between network connections where blue is the shortest path followed by green, yellow and red is the longest. Edge creation was via Bray-Curtis dissimilarity and edge selection was by p-value and q-value thresholds (<0.01), thicker edges reflect associations which are more similar than associations with thin edges. The importance of the edges, edge betweenness, is denoted by colour where blue is the least important, followed by green and yellow has greatest importance. On the network, green labels show phototrophs, blue shows ciliates and white

labels show the undefined OTUs. For the chlorophylls, the label “Ch a” represents chlorophyll a, “Ch c” is chlorophyll c and “Totc” is total chlorophyll. All other taxonomic labels are as they appear in the network.

Discussion

Here we show that the species presence, distribution and abundance of microbial eukaryotes are horizontally heterogeneous at the microscale. The microscale environment is dynamic and changing (Stocker *et al.* 2008), and the presence of hotspots and cold spots of microbial abundance has also been shown (Dann *et al.* 2014). Our results are consistent with and expand previous studies showing heterogeneous distributions for viruses and bacteria (Seymour *et al.* 2005, 2007, Dann *et al.* 2014), as well as for chlorophyll *a* (Seuront and Spilmont 2002, Franks and Jaffe 2008, Spilmont *et al.* 2011) and benthic meiofauna/macrofauna (Pratt *et al.* 2014, Sandulli & Pinckney 1999).

Comparison of Taxonomy and Chlorophyll Concentration

The patterns observed in species distribution of the photosynthetic eukaryotes have been linked to the concentration of chl *a* and chl *c* in numerous studies over distances on the order of kilometres (Lie *et al.* 2013, Leterme *et al.* 2015). For example, chlorophyll *a* often correlates positively with green algal abundance and diatom abundance (Lopes *et al.* 2006, Finkel *et al.* 2009, Leterme *et al.* 2015). In addition, chlorophyll *a* is widely used as an estimation of phytoplankton biomass (Kuwahara and Leong 2015, McInnes *et al.* 2015, Pinckney *et al.* 2015). Moreover, microscale heterogeneity of chlorophyll has been well documented in the past at the micro- (Seuront and Spilmont 2002, Spilmont *et al.* 2011) and macroscales (McInnes *et al.* 2015, Pinckney *et al.* 2015). The results from this study show

that the only relationship between chlorophyll *a* and the identified OTUs is made evident in the network analysis (Figure 5), which indicates that the haptophytes, at least in part, are contributing significantly to the chlorophyll *a* biomass. Yet, no other significant relationships were identified between chl *a* or in other groups such as green algae and diatoms, which are known to contribute significantly to aquatic photosynthetic biomass (Franks and Jaffe 2008, Balzano *et al.* 2015, McInnes *et al.* 2015).

Community Taxonomical Variations at the Microscale

Ciliate OTUs, specifically those associated with *Euplotes dammamensis*, *E. nobilii* and *Bergeriella ovata*, contributed to dissimilarity of the community in three of the four groups identified by PCoA in addition to a population of unknown diatoms. One explanation for the negative correlations between ciliates and dinoflagellates (Spearman's $\rho = -0.811$), and ciliates and diatoms (Spearman's $\rho = -0.818$) is the grazing of ciliates on dinoflagellates and diatoms. At the site sampled, the grazers of diatoms are primarily ciliates and zooplankton, including small crustaceans (Nayar and Loo 2009, Jendyk *et al.* 2014). However, for dinoflagellates, the case for grazing by ciliates is more difficult to make, due to the fact that generally ciliates are smaller than dinoflagellates. Although previous studies have shown that larger, heterotrophic dinoflagellates are able to graze smaller bodied dinoflagellates, which may also be the case for ciliates grazing on small dinoflagellates (Kamiyama and Satoshi 2001, Suthe *et al.* 2011, Jeong *et al.* 2013).

Despite contributing to dissimilarity it is evident from the network (Figure 5) that the ciliates are not so relevant contributors to the overall microbial food web interactions. Instead, diatoms appear to be the most important and more abundant. One diatom OTU, which could not be identified beyond the phylum level, drove dissimilarity in the first two groups identified by the PCoA (Table S2, Figure 6). Indeed, it was the diatom OTUs which were

shown to be of greatest importance to the microeukaryote community. The importance of diatoms has been widely demonstrated. Diatoms are ubiquitous to aquatic environments and ecologically important and are a known source of carbon acquisition/storage (Tan *et al.* 2015). They are also a known food source of many species of ciliate (Kobbi-Rebai *et al.* 2013, Larsen *et al.* 2015), although this does depend on the size of the diatom cell compared to the predator (Larsen *et al.* 2015). The network in Figure 5 highlights a significant link between the undefined group and the diatom, chl *c* and dinoflagellates, where chl *c* is an accessory photosynthetic present in diatoms and dinoflagellates (Zhang *et al.* 2014). In the present results, the interaction between the undefined group may be an indication these organisms are grazing on diatoms and dinoflagellates.

Conclusion

Species distributions have been shown to be heterogeneous from micro- to macroscales (Lie et al. 2013, Balzano *et al.* 2015, Leterme *et al.* 2015). Not only have we shown this heterogeneous distribution, but we also show some of the complex interactions between different groups of microeukaryotes and the importance of diatoms within microphytobenthic community. Here, the eukaryotic supergroups Excavata, chromalveolata, Rhizaria and Archaeplastidia contributed to dissimilarity between sampling locations. Yet, we show that microbial eukaryotes were not driving the variation in chlorophyll concentration. Instead, we have demonstrated that there was variability in the species driving the dissimilarity between the microscale locations, specifically diatom and ciliate taxa. SIMPER analysis revealed that the ciliates *B. ovata*, *E. dammamensis* and *E. nobilii* were responsible for dissimilarity. Whereas diatoms tended to dominate the OTUs identified at all sample locations. Additionally, an unknown diatom OTU also was shown to contribute to dissimilarity at 0 cm, 63 cm and 74 cm locations. From network analysis, we show that diatoms are the most important identified taxonomic group within this microbial network with strong interactions with the ciliates and the undefined group. Thus, we conclude that for these communities, diatoms are a keystone group within the microbial community.

Chapter 3
Supplementary Material

Table S1. Sequencing results, including the number of base pairs for the raw sequences and that after going through quality control processes, as well as the total number of sequences analysed.

Site	Raw sequences (<i>n</i> base pairs)	Quality filtered & Chimera removal (<i>n</i> base pairs)	Total Sequences analysed
A3.1	279 450	217 308	2858
A3.2	239 535	195 008	2215
A3.3	273 019	218439	3252
B10.1	359 158	311 631	2802
B10.2	278 747	228 789	2394
B10.3	284 508	226 352	2297
E3.1	267 101	227 432	1692
E3.2	264 306	214 083	2560
E3.3	285 489	242 251	2268
F10.1	145 974	115 386	1910
F10.2	288 664	237 011	2533
F10.3	200 348	151 108	2685
G4.1	304 240	248 864	2824
G4.2	204 428	163 100	1871
G4.3	235 609	195 295	2169
G7.1	309 177	266 598	2155
G7.2	380 875	312 281	4099
G7.3	234 412	199 421	1677
H1.1	330 964	281 773	2774
H1.2	272 361	375 142	2868
H1.3	221 698	218 516	1623
H5.1	265 687	213 259	3277
H5.2	240 142	154 513	2323
H5.3	304 492	252 500	2358
I10.1	323 826	299 501	2623
I10.2	230 209	181 404	2681
I10.3	214 133	180 759	1611
J4.1	285 950	239 185	2202
J4.2	295 237	255 965	2082
J4.3	326 055	270 011	3605

Table S2. 18S OTU hit identification list where “P” indicates the presence of the OTU at the sample locations.

Hit Name	CLASSIFICATION	CLASSIFICATION LEVEL	A3	B10	E3	F10	G4	G7	H1	H5	I10	J4
Acanthocoeopsis unguiculata 16S-like small subunit ribosomal RNA	CHOANOFLAGELLATE	CLASS						P				
Acineta compressa small subunit ribosomal RNA gene, partial sequence	PHYLLOPHARYNGEA	CLASS (CILIAE)	P	P	P	P	P		P	P	P	P
Acineta flava isolate KR-10010701 small subunit ribosomal RNA gene	PHYLLOPHARYNGEA	CLASS (CILIAE)		P	P			P	P	P	P	P
Acineta tuberosa small subunit ribosomal RNA gene, partial sequence	PHYLLOPHARYNGEA	CLASS (CILIAE)	P	P	P	P	P	P	P	P	P	P
Alternaria sp. GE 18S ribosomal RNA gene, partial sequence	DOTHIDEOMYCETES	CLASS (KINGDOM: FUNGI)				P						
Amastigomonas sp. IVY8c 18S ribosomal RNA gene, partial sequence	AMASTIGOMONAS	GENUS (KINGDOM: PROTOZOA)								P		
Amoebosoa sp. amR1 18S ribosomal RNA gene, partial sequence	AMOEBOSOA	PHYLLUM (PROTOZOA)	P									
Amphidinium sp. D2-CMSTAC021 18S ribosomal RNA gene, partial sequence	DINOPHYCEAE	CLASS (DINOFLAGELLATE)		P				P				P
Amphileptus aeschtae small subunit ribosomal RNA gene, complete sequence	LITOSTOMATEA	CLASS (CILIAE)					P					
Amphisiella candida isolate CXM10040703 18S ribosomal RNA gene, partial sequence	HYPOTRICHEA	CLASS (CILIAE)									P	
Amphora cf. capitellata 18S rRNA gene, clone p363	BACILLARIOPHYCEAE	CLASS (HETEROKONTOPHYTA)	P	P	P	P	P	P	P	P	P	P
Amphora coffeaeformis genomic DNA containing 18S rRNA gene, culture collection CCAP 1001/2	BACILLARIOPHYCEAE	CLASS (HETEROKONTOPHYTA)						P				
Amphora coffeaeformis strain CCMP127 18S ribosomal RNA gene, partial sequence	BACILLARIOPHYCEAE	CLASS (HETEROKONTOPHYTA)	P	P	P	P	P	P	P	P	P	P
Amphora sp. CTM 20023 18S ribosomal RNA gene, partial sequence	BACILLARIOPHYCEAE	CLASS (HETEROKONTOPHYTA)									P	
Anteholosticha scutellum small subunit ribosomal RNA gene, partial sequence	SPIROTRICHEA	CLASS (CILIAE)							P			
Anteholosticha sp. SNK-2010 small subunit ribosomal RNA gene, partial sequence	SPIROTRICHEA	CLASS (CILIAE)	P									
Aspergillus fumigatus small subunit ribosomal RNA	EUROTIOMYCETES	CLASS (KINGDOM: FUNGI)									P	
Aspidisca aculeata small subunit ribosomal RNA gene, partial sequence	SPIROTRICHEA	CLASS (CILIAE)							P		P	

Aspidisca fusca voucher JJM08060502 small subunit ribosomal RNA gene, partial sequence	SPIROTRICHEA	CLASS (CILIATE)	P	P	P	P	P	P	P	P	P	P	P	P
Aspidisca hexeris isolate B277 small subunit ribosomal RNA gene, partial sequence	SPIROTRICHEA	CLASS (CILIATE)							P					P
Aspidisca hexeris voucher JJM2010041503 small subunit ribosomal RNA gene, partial sequence	SPIROTRICHEA	CLASS (CILIATE)	P	P	P	P	P	P	P	P	P	P	P	P
Aspidisca leptaspis voucher LLQ-07092802 (OUC) small subunit ribosomal RNA gene, partial sequence	SPIROTRICHEA	CLASS (CILIATE)	P	P	P	P	P	P	P	P	P	P	P	P
Aspidisca steini small subunit ribosomal RNA gene, partial sequence	SPIROTRICHEA	CLASS (CILIATE)	P	P	P	P	P	P	P	P	P	P	P	P
Asteroplanus karianus 18S rRNA gene	BACILLARIOPHYCEAE	CLASS (HETEROKONTOPHYTA)									P			
Athalamea environmental sample clone Elev_18S_508 18S ribosomal RNA gene, partial sequence	ATHALAMEA	CLASS (PHYLUM FORAMINIFERA)	P	P		P								
Bacillaria paxillifer 16S-like ribosomal RNA, complete	BACILLARIOPHYCEAE	CLASS (HETEROKONTOPHYTA)	P	P	P		P	P		P				P
Bacillaria paxillifer strain UTEX FD468 18S small subunit ribosomal RNA gene, partial sequence	BACILLARIOPHYCEAE	CLASS (HETEROKONTOPHYTA)					P	P		P				
Bacillariophyta sp. MBIC10102 gene for 18S rRNA, partial sequence, strain: MBIC10102	BACILLARIOPHYCEAE	CLASS (HETEROKONTOPHYTA)	P	P	P	P	P	P	P	P	P	P	P	P
Bacillariophyta sp. Z211 clone A1 18S ribosomal RNA gene, partial sequence	BACILLARIOPHYCEAE	CLASS (HETEROKONTOPHYTA)	P	P		P	P	P	P	P	P	P		P
Berkeleya rutilans strain ECT3616 18S small subunit ribosomal RNA gene, partial sequence	BACILLARIOPHYCEAE	CLASS (HETEROKONTOPHYTA)					P	P		P				
Bicosoeca petiolata strain ATCC 50639 18S ribosomal RNA gene, partial sequence	BICOSECA	CLASS (HETEROKONTOPHYTA)	P	P		P	P				P			P
Bicosoeca vacillans strain ATCC 50063 18S ribosomal RNA gene, partial sequence	BICOSECA	CLASS (HETEROKONTOPHYTA)			P						P			
Blepharisma americanum small subunit ribosomal RNA gene sequence	HETEROTICHEA	CLASS (CILIATE)	P											
Bodo saltans 18S ribosomal RNA gene, partial sequence	KINETOPLASTEAE	CLASS (PHYLUM EUGLENOZOA)			P	P	P							P
Bodo saltans JC02 18S ribosomal RNA gene, partial sequence	KINETOPLASTEAE	CLASS (PHYLUM EUGLENOZOA)												P
Bodo saltans strain HFCC12 18S ribosomal RNA gene, partial sequence	KINETOPLASTEAE	CLASS (PHYLUM EUGLENOZOA)				P								
Bodonidae sp. Dev1 18S ribosomal RNA gene, partial sequence	KINETOPLASTEAE	CLASS (PHYLUM EUGLENOZOA)												P
Bodonidae sp. RS407A2 clone #4 18S ribosomal RNA gene, partial	KINETOPLASTEAE	CLASS (PHYLUM EUGLENOZOA)			P	P				P	P	P		

sequence		EUGLENOZOA)												
Boveria subcylindrica strain FXP2009030301 small subunit ribosomal RNA gene, partial sequence	OLIGOHYMENOPHERA	CLASS (CILIAE)					P							
C.guilliermondii small subunit ribosomal RNA	SACCHAROMYCETES	CLASS (KINGDOM: FUNGI)												P
Camelina sativa 18S rRNA gene, ITS1, 5.8S rRNA gene, ITS2 and partial 25S rRNA gene, cultivar Calena	PLANTAE	-		P										P
Candida rhagii gene for 18S rRNA, partial sequence	SACCHAROMYCETES	CLASS (KINGDOM: FUNGI)					P							P
Ceratopora sp. NVS-2013 isolate UH109.3 18S ribosomal RNA gene, partial sequence	ANIMALIA	(PLATYHELMINTHE)	P											
Cercomonadidae environmental sample clone Amb_18S_1443 18S ribosomal RNA gene, partial sequence	CERCOMONADIDAE	CLASS (PHYLUM CERCOZOA)	P								P			
Cercomonas plasmodialis 18S ribosomal RNA gene, complete sequence	CERCOMONADIDAE	CLASS (PHYLUM CERCOZOA)		P							P			
Cercozoa environmental sample clone Elev_18S_933 18S ribosomal RNA gene, partial sequence	CERCOMONADIDAE	CLASS (PHYLUM CERCOZOA)					P							
Cf. Polychytrium sp. JEL606 18S small subunit ribosomal RNA gene, partial sequence	CHYTRIDIOMYCOTA	CLASS (KINGDOM: FUNGI)	P	P	P	P	P					P		P
Chlamydomonas reinhardtii 18S ribosomal RNA gene, partial sequence	CENTROHELEA	CLASS (PROTIST, HELIOZOA)		P	P				P				P	P
Chlamydomonas reinhardtii clone 2 small subunit ribosomal RNA gene, partial sequence	PHYLLOPHARYNGEA	CLASS (CILIAE)									P			
Chlorarachnion reptans CCMP 238 clones pF55 and pF56 18S rRNA small subunit	CHLORARACHNIOPHYCEAE	CLASS (PHYLUM CERCOZOA)							P					
Chlorella ellipsoidea 18S rRNA gene, strain SAG 211-1a	TREBEAUXIOPHYCEAE	CLASS (CHLOROPHYTA)												P
Chlorella kessleri 18S rRNA gene, strain SAG 211-11g	TREBEAUXIOPHYCEAE	CLASS (CHLOROPHYTA)												P
Chlorella minutissima gene for 18S rRNA, partial sequence	TREBEAUXIOPHYCEAE	CLASS (CHLOROPHYTA)	P	P	P	P	P	P	P	P	P	P	P	
Chlorella mirabilis 18S rRNA gene, strain Andreyeva 748-I	TREBEAUXIOPHYCEAE	CLASS (CHLOROPHYTA)		P	P									
Chlorella sorokiniana 18S rRNA gene, strain SAG 211-8k	TREBEAUXIOPHYCEAE	CLASS (CHLOROPHYTA)	P											
Chlorella sp. 18S rRNA gene, isolate Yanaqocha RA1	TREBEAUXIOPHYCEAE	CLASS (CHLOROPHYTA)	P	P	P	P	P	P	P	P	P	P	P	P

Chlorella sp. MDL5-18 18S ribosomal RNA gene, partial sequence	TREBEAUXIOPHYCEAE	CLASS (CHLOROPHYTA)						P					
Chlorokybus atmophyticus 18S ribosomal RNA (18S rDNA) gene, partial	PLANTAE	-			P		P				P		
Choricystis sp. Pic8/18P-11w 18S ribosomal RNA gene, partial sequence	ULVOPHYCEAE	CLASS (CHLOROPHYTA)							P				
Cinetochilum ovale isolate PHB08111304 small subunit ribosomal RNA gene, complete sequence	OLIGOHYMENOPHERA	CLASS (CILIATE)										P	
Cladonia corsicana isolate COR3 28S-18S ribosomal RNA intergenic spacer, partial sequence	LECANOROMYCETES	CLASS (KINGDOM: FUNGI)					P						
Clathrina luteoculcitella 18S rRNA gene, specimen voucher G313684 (Queensland Museum)	CALCAREA	CLASS (PHYLUM PORIFERA)	P		P	P							
Clytia sp. AGC-2001 small subunit ribosomal RNA gene, partial sequence	CNIDARAIA	PHYLUM (ANIMALIA)					P						
Coccidiodes immitis small subunit ribosomal RNA	EUROTIOMYCETES	CLASS (KINGDOM: FUNGI)	P										
Coccomyxa sp. KN-2011-C14 genomic DNA containing 18S rRNA gene, ITS1, 5.8S rRNA gene and ITS2, strain C14	CHLOROPHYCEAE	CLASS (CHLOROPHYTA)										P	
Cocconeis cf. molesta 18S rRNA gene, clone p800	BACILLARIOPHYCEAE	CLASS (HETEROKONTOPHYTA)										P	
Cocconeis placentula 18S rRNA gene, strain AT-212Gel11	BACILLARIOPHYCEAE	CLASS (HETEROKONTOPHYTA)	P	P	P	P	P	P	P	P	P	P	P
Colpodidiidae sp. HWB-2007 small subunit ribosomal RNA gene, partial sequence; macronuclear	NASSOPHOREA	CLASS (CILIATE)	P	P	P			P	P	P	P	P	P
Colponema sp. Vietnam strain Colp-7a 18S ribosomal RNA gene, partial sequence	KINETOPLASTEIA	CLASS (PHYLUM EUGLENOZOA)					P						
Condyllostoma sp. CXM08110901 small subunit ribosomal RNA gene, partial sequence	POLYHYMENOPHORA	CLASS (CILIATE)								P			
Craticula cuspidata strain UTEX FD35 18S small subunit ribosomal RNA gene, partial sequence	BACILLARIOPHYCEAE	CLASS (HETEROKONTOPHYTA)	P	P	P	P	P	P	P	P	P	P	P
Cruciplaccolithus neohelis 18S rRNA gene, strain ccmp298	COCCOLITHOPHYCEAE	CLASS (PHYLUM HAPTOPHYA)									P		
Cryptocaryon irritans small subunit ribosomal RNA, partial sequence	PROSTOMATEA	CLASS (CILIATE)	P										
Cryptococcus carnescens gene for 18S rRNA, partial sequence, strain: CBS 973	TREMELLOPHYCEAE	CLASS (KINGDOM: FUNGI)							P				
Cryptoperidiniopsis sp. PLO21 small subunit ribosomal RNA gene, internal transcribed spacer 1	OLIGOHYMENOPHERA	CLASS (CILIATE)			P								

Cyclidium marinum strain KL 2 small subunit ribosomal RNA gene, partial sequence	OLIGOHYMENOPHERA	CLASS (CILIATE)	P	P	P	P	P	P	P	P			P
Cyclidium plouneouri small subunit ribosomal RNA gene, partial sequence	OLIGOHYMENOPHERA	CLASS (CILIATE)	P		P								P
Cylindrotheca closteriva 16S-like ribosomal RNA, complete	BACILLARIOPHYCEAE	CLASS (HETEROKONTOPHYTA)		P		P		P					
Cylindrotheca fusiformis strain CCMP339 18S ribosomal RNA gene, partial sequence	BACILLARIOPHYCEAE	CLASS (HETEROKONTOPHYTA)	P	P	P		P	P	P	P	P		
Cymbella cistuliformis clone 1120 18S ribosomal RNA gene, partial sequence	BACILLARIOPHYCEAE	CLASS (HETEROKONTOPHYTA)											P
Diacronema sp. AC54 18S ribosomal RNA gene, partial sequence	PAVLOVOPHYCEAE	PHYLUM (HAPTOPHYTA)				P		P				P	P
Diacronema vlkianum 18S ribosomal RNA gene, partial sequence	PAVLOVOPHYCEAE	PHYLUM (HAPTOPHYTA)	P					P					
Dictyosphaerium sp. CCAP 222/41 18S ribosomal RNA gene, partial sequence	CHLOROPHYCEAE	CLASS (CHLOROPHYTA)			P			P					
Dimorpha-like sp. ATCC 50522 18S ribosomal RNA gene, complete sequence	SARCOMONADEA	CLASS (PHYLUM CERCOZOA)					P						
Dinophyceae sp. Shepherd's Crook small subunit ribosomal RNA gene, partial sequence	DINOPHYCEAE	CLASS (DINOFLAGELLATE)	P			P				P	P	P	P
Diophrys cf. oligothrix small subunit ribosomal RNA gene, partial sequence	SPIROTRICHEA	CLASS (CILIATE)		P				P		P			
Diophrys japonica isolate FYB2010111002 small subunit ribosomal RNA gene, partial sequence	SPIROTRICHEA	CLASS (CILIATE)							P				
Discocephalus pararotatorius isolate JJM09050101 small subunit ribosomal RNA gene, partial sequence	SPIROTRICHEA	CLASS (CILIATE)											P
Dunaliella parva 18S rDNA gene	CHLOROPHYCEAE	CLASS (CHLOROPHYTA)	P	P	P	P	P	P	P	P	P	P	P
Dunaliella salina strain CCAP 19/30 18S ribosomal RNA gene, partial sequence	CHLOROPHYCEAE	CLASS (CHLOROPHYTA)	P	P	P	P	P	P	P	P	P	P	P
Eimeriidae environmental sample clone Amb_18S_1017 18S ribosomal RNA gene, partial sequence	CANOIDASIDA	CLASS (PHYTLUM APICOMPLEXA)							P				
Eimeriidae environmental sample clone Amb_18S_1171 18S ribosomal RNA gene, partial sequence	CANOIDASIDA	CLASS (PHYTLUM APICOMPLEXA)											P
Eimeriidae environmental sample clone Elev_18S_1191 18S ribosomal RNA gene, partial sequence	CANOIDASIDA	CLASS (PHYTLUM APICOMPLEXA)										P	
Enchelys polynucleata small subunit ribosomal RNA gene, partial sequence	GYMNOSTOMATEA	CLASS (CILIATE)				P							

Encyonema triangulatum 18S rRNA gene, strain L1313	BACILLARIOPHYCEAE	CLASS (HETEROKONTOPHYTA)		P		P			P		P	
Entomoneis sp. CS782 18S small subunit ribosomal RNA gene, partial sequence	BACILLARIOPHYCEAE	CLASS (HETEROKONTOPHYTA)										P
Ephydatia fluviatilis clone EfG03 18S ribosomal RNA gene, partial sequence	DEMOSPONGIAE	CLASS (PHYLLUM PORIFERA)	P			P			P			
Epiphyllum shenzhenense isolate PHB09040106 small subunit ribosomal RNA gene, complete sequence	CILIOPHORA	PHYLUM: CILIATE	P	P	P	P	P	P	P	P	P	P
Epithemia argus strain CH211 18S small subunit ribosomal RNA gene, partial sequence	BACILLARIOPHYCEAE	CLASS (HETEROKONTOPHYTA)										P
Eufolliculina uhligi nuclear small subunit ribosomal RNA gene	HETEROTICHEA	CLASS (CILIATE)		P							P	
Euplotes dammamensis small subunit ribosomal RNA gene, partial sequence	SPIROTRICHEA	CLASS (CILIATE)	P	P	P	P	P	P	P	P	P	P
Euplotes minuta 18S rRNA gene	SPIROTRICHEA	CLASS (CILIATE)							P			
Euplotes nobilii strain 1QN1 18S ribosomal RNA gene, partial sequence; macronuclear	SPIROTRICHEA	CLASS (CILIATE)		P								
Euplotes orientalis 18S ribosomal RNA gene, partial sequence	SPIROTRICHEA	CLASS (CILIATE)	P	P	P	P	P	P	P	P	P	P
Euplotes rariseta isolate QD-2 18S ribosomal RNA gene, partial sequence	SPIROTRICHEA	CLASS (CILIATE)	P	P	P	P	P	P	P	P	P	P
Euplotes rariseta isolate QDS435 small subunit ribosomal RNA gene, complete sequence	SPIROTRICHEA	CLASS (CILIATE)	P	P	P	P	P	P	P		P	P
Euplotes sp. SNK-2011 isolate KR-08111001 small subunit ribosomal RNA gene, partial sequence; macronuclear	SPIROTRICHEA	CLASS (CILIATE)	P	P	P	P	P	P	P	P	P	P
Euplotes vannus small subunit ribosomal RNA gene, partial sequence	SPIROTRICHEA	CLASS (CILIATE)		P			P		P	P	P	
Eurotium amstelodami gene for 18S rRNA, partial sequence, strain:FRR2792	EUROTIOMYCETES	CLASS (KINGDOM: FUNGI)	P		P							
Eurystomatella sinica small subunit ribosomal RNA gene, partial sequence	OLIGOHYMENOPHERA	CLASS (CILIATE)		P								
Fabrea salina small subunit ribosomal RNA gene, partial sequence	SPIROTRICHEA	CLASS (CILIATE)	P	P		P	P	P	P	P	P	P
Flabellulidae sp. SEDF/I small subunit ribosomal RNA gene, partial sequence	FLABELLULIDAE	CLASS (AMOEOBOZOA)		P								
Fragilaria capucina strain D-149 18S ribosomal RNA gene, partial sequence	BACILLARIOPHYCEAE	CLASS (HETEROKONTOPHYTA)						P		P		
Fragilaria famelica strain UTEX FD255 18S small subunit ribosomal RNA gene, partial sequence	BACILLARIOPHYCEAE	CLASS (HETEROKONTOPHYTA)									P	P
Frustulia cassieae partial 18S rRNA gene, strain NZ190	BACILLARIOPHYCEAE	CLASS			P	P	P	P	P	P	P	P

		(HETEROKONTOPHYTA)												
Frustulia cf. magaliesmontana PU-2012 partial 18S rRNA gene, strain NZ162	BACILLARIOPHYCEAE	CLASS (HETEROKONTOPHYTA)				P		P						P
Fusarium fujikuroi IMI 58289 draft genome, chromosome FFUJ_chr02	SARDIOMYCETES	CLASS (KINGDOM: FUNGI)										P		
G.nostochinearum gene for 16S-like ribosomal RNA	GLAUCOPHYCEAE	CLASS (PHYLUM GLAUCOPHYTA)									P			
Geleia sinica strain A440 small subunit ribosomal RNA gene, partial sequence	KARYORELICTEA	CLASS (CILIAE)	P	P	P	P	P	P	P	P			P	P
Gymnophrys sp. ATCC 50923 18S ribosomal RNA gene, partial sequence	PROTEOMYXIDEA	CLASS (PHYLUM CERCOZOA)												P
Gyrodinium instriatum strain GIXM01 18S ribosomal RNA gene, partial sequence	DINOPHYCEAE	CLASS (DINOFLAGELLATE)				P				P				
Gyrosigma acuminatum strain UTEX FD317 18S small subunit ribosomal RNA gene, partial sequence	DINOPHYCEAE	CLASS (DINOFLAGELLATE)								P				
H.catenoides gene for 18S ribosomal RNA	HYPOCHYTRIDIOMYCETES	CLASS (KINGDOM: FUNGI)						P						
Halamphora coffeaeformis isolate 7977-AMPH101 18S small subunit ribosomal RNA gene, partial sequence	BACILLARIOPHYCEAE	CLASS (HETEROKONTOPHYTA)		P	P			P						P
Halamphora oligotraphenta isolate 9561-AMPH009 18S small subunit ribosomal RNA gene, partial sequence	BACILLARIOPHYCEAE	CLASS (HETEROKONTOPHYTA)	P	P	P			P			P		P	P
Haliclona oculata clone HocII05 18S ribosomal RNA gene, partial sequence	DEMOSPONGIAE	CLASS (PHYLUM PORIFERA)	P	P	P	P	P	P	P	P	P	P	P	P
Halocafeteria seosinensis 18S ribosomal RNA gene, partial sequence	BICOSECA	CLASS (HETEROKONTOPHYTA)	P											
Haslea ostrearia 18S ribosomal RNA gene, partial sequence	BACILLARIOPHYCEAE	CLASS (HETEROKONTOPHYTA)	P	P	P	P	P	P	P	P	P	P	P	P
Hemiophrys procera small subunit ribosomal RNA gene, complete sequence	CILIOPHORA	PHYLUM: CILIAE	P	P	P	P	P	P	P	P			P	P
Herpetomonas sp. TCB-2012d isolate TCC247 18S ribosomal RNA gene, partial sequence	KINETOPLASTEAE	CLASS (PHYLUM EUGLENOZOA)										P		
Heteramoeba clara small subunit ribosomal RNA gene, complete sequence	HETEROLOBOSEA	CLASS (PROTIST, PERCOLOZOA)											P	
Holosticha diademata small subunit ribosomal RNA gene, complete sequence	SPIROTRICHEA	CLASS (CILIAE)	P	P	P	P	P	P	P	P	P	P	P	P
Hyalosynedra cf. laevigata strain WK52 small subunit ribosomal RNA gene, partial sequence	BACILLARIOPHYCEAE	CLASS (HETEROKONTOPHYTA)											P	

Hydnocchaete duportii isolate AFTOL-ID 666 18S ribosomal RNA gene, partial sequence	AGARICOMYCETES	CLASS (KINGDOM: FUNGI)			P								
Hypotruchia sp. I-99 18S ribosomal RNA gene, partial sequence	SPIROTRICHEA	CLASS (CILIATE)	P	P	P	P	P	P				P	P
Ichthyophonus sp. A3 18S ribosomal RNA gene, partial sequence	MESOMYCETAZOEA	CLASS (CHOANAZOEA)					P						
Isochrysis galbana strain SAG 13.92 18S ribosomal RNA gene, partial sequence	PRYMESIOPHYCEAE	CLASS (PHYLUM HAPTOPHYTA)	P	P	P	P	P	P	P	P	P	P	P
Kentrophoros gracilis isolate QD061131 small subunit ribosomal RNA gene, partial sequence	KARYORELICTEA	CLASS (CILIATE)	P			P						P	P
Koliella spiculiformis 18S small subunit ribosomal RNA gene, partial sequence	TREBEAUXIOPHYCEAE	CLASS (CHLOROPHYTA)	P				P		P			P	P
Lacrymaria marina 16S ribosomal RNA gene, complete sequence	LACRYMARIDAE	CLASS (CILIATE)	P			P	P						
Laurus nobilis 18S ribosomal RNA gene, partial sequence	PLANTAE	-						P					
Licmophora flabellata strain WK47 small subunit ribosomal RNA gene, partial sequence	BACILLARIOPHYCEAE	CLASS (HETEROKONTOPHYTA)						P					
Litonotus pictus clone 3 small subunit ribosomal RNA gene, partial sequence	LITOSTOMATEA	CLASS (CILIATE)				P							
Lodderomyces sp. Y-1 18S ribosomal RNA gene, partial sequence	SACCHAROMYCETES	CLASS (KINGDOM: FUNGI)										P	
Lotharella globosa strain LEX01 small subunit ribosomal RNA gene, partial sequence	CHLORARACHNIOOHYCEAE	CLASS (PHYLUM CERCOZOA)	P	P	P	P	P	P	P	P	P	P	P
Lotharella sp. CCMP622 chromosome 3 nucleomorph, complete sequence	CHLORARACHNIOOHYCEAE	CLASS (PHYLUM CERCOZOA)		P		P	P		P	P	P		
Loxophyllum caudatum voucher PHB2009121501 small subunit ribosomal RNA gene, partial sequence	PLEUROSOMATIDA	CLASS (CILIATE)		P	P		P	P				P	P
Loxophyllum jini small subunit ribosomal RNA gene, partial sequence	PLEUROSOMATIDA	CLASS (CILIATE)		P	P	P	P	P	P	P	P	P	P
Loxophyllum meridionale small subunit ribosomal RNA gene, partial sequence	PLEUROSOMATIDA	CLASS (CILIATE)						P			P		
Loxophyllum perihoplophorum strain wl20120407-02 small subunit ribosomal RNA gene, partial sequence	PLEUROSOMATIDA	CLASS (CILIATE)	P	P	P		P	P	P	P	P	P	P
Loxophyllum rugosum voucher PHB2009102001 small subunit ribosomal RNA gene, partial sequence	PLEUROSOMATIDA	CLASS (CILIATE)		P			P		P	P	P	P	P
M.squamata gene for 18S small subunit rRNA	CHLOROPHYCEAE	CLASS (CHLOROPHYTA)	P	P		P							
Massisteria sp. diva strain HFCC385 18S ribosomal RNA gene, partial sequence	CERCOMONADIDAE	CLASS (PHYLUM CERCOZOA)	P							P		P	P
Massisteria sp. diva strain HFCC391 18S ribosomal RNA gene, partial	CERCOMONADIDAE	CLASS (PHYLUM	P										

sequence		CERCOZOA)																
Mastocarpus stellatus 18S ribosomal RNA gene, partial sequence	CERCOMONADIDAE	CLASS (PHYLUM CERCOZOA)				P												
Mastogloia sp. 29x07-6B 18S small subunit ribosomal RNA gene, partial sequence	BACILLARIOPHYCEAE	CLASS (HETEROKONTOPHYTA)		P														
Metanophrys sinensis isolate FXP2009052901 18S small subunit ribosomal RNA gene, complete sequence	SPIROTRICHEA	CLASS (CILIAE)							P									
Meyerella planktonica isolate Itas 2/24 S-9d 18S ribosomal RNA gene, partial sequence	TREBEAUXIOPHYCEAE	CLASS (CHLOROPHYTA)	P					P	P									P
Miamiensis avidus isolate JM2 small subunit ribosomal RNA gene, partial sequence	SPIROTRICHEA	CLASS (CILIAE)			P													
Modicella malleola 18S ribosomal RNA gene, partial sequence	MORTIERELLALES	ORDER (KINGDOM: FUNGI)							P									
Moneuplotes vannus voucher KR-09101902 small subunit ribosomal RNA gene, partial sequence; macronuclear	SPIROTRICHEA	CLASS (CILIAE)		P														P
Monosiga brevicollis 18S small subunit ribosomal RNA gene, partial sequence	CHOANOFLLAGELLATE	CLASS (CHOANOZOA)							P									
Mytilophilus pacificae strain DL 4 small subunit ribosomal RNA gene, partial sequence	SPIROTRICHEA	CLASS (CILIAE)	P															
Nannochloris bacillaris gene for 18S rRNA, partial sequence	CHLOROPHYCEAE	CLASS (CHLOROPHYTA)	P	P	P	P	P	P	P			P	P		P	P	P	
Nannochloris sp. ANR-9 18S ribosomal RNA gene, partial sequence	CHLOROPHYCEAE	CLASS (CHLOROPHYTA)	P	P	P				P									P
Nannochloris sp. MBIC10596 gene for 18S rRNA, partial sequence, strain: MBIC10596	CHLOROPHYCEAE	CLASS (CHLOROPHYTA)			P													
Nannochloropsis gaditana 18S ribosomal RNA gene, complete sequence	EUSTIGMATACEAE	CLASS (HETEROKONTOPHYTA)			P													
Nannochloropsis gaditana strain CCAP 849/6 18S ribosomal RNA gene, partial sequence	EUSTIGMATACEAE	CLASS (HETEROKONTOPHYTA)		P					P									P
Nannochloropsis gaditana strain CCMP526 18S ribosomal RNA gene, complete sequence	EUSTIGMATACEAE	CLASS (HETEROKONTOPHYTA)																P
Nannochloropsis salina 16S-like ribosomal RNA, complete	EUSTIGMATACEAE	CLASS (HETEROKONTOPHYTA)				P												
Nannochloropsis salina CCAP849/2 18S ribosomal RNA gene, complete sequence	EUSTIGMATACEAE	CLASS (HETEROKONTOPHYTA)	P	P	P	P	P	P	P	P	P	P	P	P	P	P	P	P
Nanochlorum eucaryotum 18S rDNA	CHLOROPHYCEAE	CLASS (CHLOROPHYTA)		P		P	P			P	P			P	P			P

Navicula diserta 18S rRNA gene, clone p750	BACILLARIOPHYCEAE	CLASS (CHLOROPHYTA)	P	P	P	P	P	P	P	P	P	P	P
Navicula pelliculosa strain CCMP543 18S ribosomal RNA gene, partial sequence	BACILLARIOPHYCEAE	CLASS (CHLOROPHYTA)			P	P						P	
Navicula sp. ArM0003 small subunit ribosomal RNA gene, partial sequence	BACILLARIOPHYCEAE	CLASS (CHLOROPHYTA)	P	P	P	P	P	P	P	P	P	P	P
Neobodo designis isolate Raglan3 18S ribosomal RNA gene, partial sequence	KINETOPLASTEAE	CLASS (PHYLUM EUGLENOZOA)		P	P				P	P	P	P	P
Neoparamoeba aestuarina small subunit ribosomal RNA gene, partial sequence	FLABELLULIDAE	CLASS (AMOEBOZOA)										P	P
Nitzschia amphibia partial 18S rRNA gene, strain FDCC L602	BACILLARIOPHYCEAE	CLASS (HETEROKONTOPHYTA)			P								
Nitzschia longissima 18S ribosomal RNA gene, partial sequence	BACILLARIOPHYCEAE	CLASS (HETEROKONTOPHYTA)		P									
Nitzschia vitrea partial 18S rRNA gene, strain FDCC L1276	BACILLARIOPHYCEAE	CLASS (HETEROKONTOPHYTA)	P	P	P	P	P	P	P	P	P	P	P
Nuclearia pattersoni 18S ribosomal RNA gene, complete sequence	NUCLEARIIDAE	CLASS (OPISTHOKONTA)									P		
Nucleariidae environmental sample clone Elev_18S_563 18S ribosomal RNA gene, partial sequence	NUCLEARIIDAE	CLASS (OPISTHOKONTA)										P	P
Oocystaceae sp. MDL6-7 18S ribosomal RNA gene, partial sequence	TREBEAUXIOPHYCEAE	CLASS (CHLOROPHYTA)	P										
Opephora guenter-grassii gene for small subunit ribosomal RNA, partial sequence	BACILLARIOPHYCEAE	CLASS (HETEROKONTOPHYTA)	P	P	P	P	P	P	P	P	P	P	P
Opephora sp. s0357 gene for 18S rRNA, partial sequence, strain: s0357	BACILLARIOPHYCEAE	CLASS (HETEROKONTOPHYTA)	P								P	P	P
Oxnerella micra 18S ribosomal RNA gene, partial sequence	CENTROHELIDA	CLASS (HACROBIA)	P						P	P			
Oxytricha saltans small subunit ribosomal RNA gene, complete sequence	SPIROTRICHEA	CLASS (CILIAE)	P	P									
Oxytricha sp. JS-2012 voucher LS 38 18S ribosomal RNA gene, complete sequence	SPIROTRICHEA	CLASS (CILIAE)		P									
Parvamoeba rugata strain CCAP 1556/1 clone 12212 18S ribosomal RNA gene, partial sequence	DISCOSEA	CLASS (AMOEBOZOA)		P	P			P	P			P	
Pavlova noctivaga strain ACOI449 18S ribosomal RNA gene, partial sequence	PAVLOVOPHYCEAE	CLASS (PHYLUM HAPTOPHYA)		P									
Pavlova pinguis strain CCAP940/3 18S ribosomal RNA gene, partial sequence	PAVLOVOPHYCEAE	CLASS (PHYLUM HAPTOPHYA)											P

Pavlova sp. AC248 18S ribosomal RNA gene, partial sequence	PAVLOVOPHYCEAE	CLASS (PHYLUM HAPTOPHYA)	P		P	P	P		P				
Pentapharsodinium tyrrhenicum strain GeoB*230 small subunit ribosomal RNA gene, partial sequence	DINOPHYCEAE	CLASS (DINOFLAGELLATE)										P	
Peridinium foliaceum endosymbiont partial 18S rRNA gene	DINOPHYCEAE	CLASS (DINOFLAGELLATE)		P	P	P	P	P	P	P	P	P	P
Pessonella sp. PRA-29 18S ribosomal RNA gene, partial sequence	DISCOSEA	CLASS (AMOEBOZOA)						P					
Pfiesteria-like sp. CCMP1828 small subunit ribosomal RNA gene, partial sequence	DINOPHYCEAE	CLASS (DINOFLAGELLATE)	P		P						P		P
Pfiesteria-like sp. F525Jul02 small subunit ribosomal RNA gene, partial sequence	DINOPHYCEAE	CLASS (DINOFLAGELLATE)							P				
Phaeodactylum tricorutum 18S ribosomal RNA gene, partial sequence	BACILLARIOPHYCEAE	CLASS (CILIAE)	P	P	P	P	P	P	P	P	P	P	P
Phaeothamnion confervicola partial 18S rRNA gene, strain SAG 119.79	PHAEOTHAMNIOPHYCEAE	CLASS (HETEROKONTOPHYTA)				P							
Phytophthora megasperma glycinea ribosomal RNA small subunit (16S-like) gene	OOMYCETES	CLASS (HETEROKONTOPHYTA)							P	P			
Picochlorum maculatum 18S ribosomal RNA gene, partial sequence	TREBEAUXIOPHYCEAE	CLASS (CHLOROPHYTA)	P	P	P	P	P	P	P	P	P	P	P
Picochlorum sp. SENEW3 18S ribosomal RNA gene, partial sequence	TREBEAUXIOPHYCEAE	CLASS (CHLOROPHYTA)							P				
Pirsonia guinardiae partial 18S rRNA gene, isolate P844	PIRSONIA	GENUS (PROTOZOA)			P								
Plagiopyliella pacifica small subunit ribosomal RNA gene, partial sequence	OLIGOHYMENOPHERA	CLASS (CILIAE)					P						
Pleuronema coronatum 16S-like small subunit ribosomal RNA gene, partial sequence	OLIGOHYMENOPHERA	CLASS (CILIAE)	P										
Pleuronema coronatum voucher WYG2007050701 small subunit ribosomal RNA gene, partial sequence	OLIGOHYMENOPHERA	CLASS (CILIAE)		P								P	
Pleuronema sp. CFL08110901 small subunit ribosomal RNA gene, partial sequence	OLIGOHYMENOPHERA	CLASS (CILIAE)											P
Prestauroneis integra 18S rRNA gene, strain AT-177.13	BACILLARIOPHYCEAE	CLASS (HETEROKONTOPHYTA)	P	P	P		P	P	P	P	P	P	P
Proterospongia choanojuncta 18S small subunit ribosomal RNA gene, complete sequence	CHOANOFLAGELLATE	CLASS (CHOANOZOA)						P					
Proterospongia sp. ATCC 50818 18S ribosomal RNA gene, partial sequence	CHOANOFLAGELLATE	CLASS (CHOANOZOA)						P					
Proterospongia sp. ATCC 50818 18S ribosomal RNA gene, partial sequence	CHOANOFLAGELLATE	CLASS (CHOANOZOA)											P

Pseudocollinia beringensis isolate 07 18S ribosomal RNA gene, partial sequence	OLIGOHYMENOPHERA	CLASS (CILIAE)	P		P									
Pseudokeronopsis cf. flava isolate GZ-CXR08040808 small subunit ribosomal RNA gene, partial sequence	MESOMYCETAZOA	CLASS (CHOANAZOA)										P		P
Pseudo-nitzschia cf. cuspidata 18S ribosomal RNA gene, partial sequence	BACILLARIOPHYCEAE	CLASS (HETEROKONTOPHYTA)	P						P					
Pseudo-nitzschia pseudodelicatissima 18S ribosomal RNA gene, partial sequence	BACILLARIOPHYCEAE	CLASS (HETEROKONTOPHYTA)	P											
Pseudoparamoeba pagei small subunit ribosomal RNA gene, partial sequence	DISCOSEA	CLASS (AMOEBOZOA)						P	P	P				P
Pseudoperkinsus tapetis small subunit ribosomal RNA gene, complete sequence	MESOMYCETAZOA	CLASS (CHOANAZOA)		P	P	P	P	P				P	P	P
Pyramimonas sp. Mae3P12 gene for 18S rRNA, partial sequence	PRASINOPHYCEAE	CLASS (CHLOROPHYTA)										P		
R.mucilaginosus 18S rRNA gene	UREDINIOMYCETES	CLASS (KINGDOM: FUNGI)					P							
Racomitrium elongatum 18S rRNA gene	BRYOPSIDA	CLASS (PLANTAE, BRYOPHYTA)	P											
Rhabdonema adriaticum isolate Coz3Rhabdo 18S ribosomal RNA gene, partial sequence	BACILLARIOPHYCEAE	CLASS (HETEROKONTOPHYTA)	P	P	P				P	P	P	P		
Rhaphoneis amphicerus gene for small subunit ribosomal RNA, partial sequence, strain: s0296	BACILLARIOPHYCEAE	CLASS (HETEROKONTOPHYTA)			P									
Rhizidiomyces apophysatus small subunit ribosomal RNA gene, partial sequence	HYPHOCHYTRIOMYCETES	CLASS (KINGDOM: FUNGI)						P					P	
Rhizochromulina cf marina 18S small-subunit rRNA gene	ACTINOPHYCEAE	CLASS (HETEROKONTOPHYTA)		P	P	P	P	P	P	P	P	P	P	P
Rhynchomonas nasuta strain HFCC17 18S ribosomal RNA gene, partial sequence	KINETOPLASTEA	CLASS (EUGLENOZOA)		P										
Rhynchomonas nasuta strain HFCC322 18S ribosomal RNA gene, partial sequence	KINETOPLASTEA	CLASS (EUGLENOZOA)					P							
Rhynchopus sp. ATCC 50229 18S ribosomal RNA gene, partial sequence	DIPLOMOMYXIDA	CLASS (PHYLUM EUGLENOZOA)						P				P	P	
S.thamesis 18S rRNA gene	BACILLARIOPHYCEAE	CLASS (HETEROKONTOPHYTA)	P											P
Salpingoeca sp. ATCC 50929 18S ribosomal RNA gene, partial sequence	CHOANOPHYLAGELLATE	CLASS (CHOANAZOA)			P			P						
Salpingoeca urceolata 18S ribosomal RNA gene, partial sequence	CHOANOPHYLAGELLATE	CLASS (CHOANAZOA)	P	P	P				P	P				P

Schmidingerothrix sp. 1 TS-2013 18S ribosomal RNA gene, partial sequence; macronuclear	HYPOTRICHA	CLASS (CILIATE)		P	P				P			P	
Scrucopcellaria maderensis 18S ribosomal RNA gene, partial sequence	GYMNOLAEMATA	CLASS (PLANTAE, BRYOPHYTA)										P	
Sellaphora cf. minima clone BM42 18S ribosomal RNA gene, partial sequence	BACILLARIOPHYCEAE	CLASS (HETEROKONTOPHYTA)										P	
Sellaphora pupula clone RBG1 18S ribosomal RNA gene, partial sequence	BACILLARIOPHYCEAE	CLASS (HETEROKONTOPHYTA)						P					
Spirotrachelostyla tani isolate JJM08112402 small subunit ribosomal RNA gene, complete sequence	SPIROTRICHEA	CLASS (CILIATE)		P									
Stauroneis acuta strain UTEX FD51 18S small subunit ribosomal RNA gene, partial sequence	BACILLARIOPHYCEAE	CLASS (HETEROKONTOPHYTA)	P	P	P	P	P	P	P	P	P	P	P
Stauroneis anceps 18S rRNA gene, strain AT-160Gel11	BACILLARIOPHYCEAE	CLASS (HETEROKONTOPHYTA)		P				P	P				
Stauroneis gracilior 18S rRNA gene, strain AT-117Gel17	BACILLARIOPHYCEAE	CLASS (HETEROKONTOPHYTA)		P		P	P	P	P	P	P	P	P
Stauroneis phoenicenteron 18S rRNA gene, strain AT-182.07	BACILLARIOPHYCEAE	CLASS (HETEROKONTOPHYTA)		P									
Steinia sphagnicola voucher KHP23 18S ribosomal RNA gene, complete sequence	HYPOTRICHA	CLASS (CILIATE)										P	
Sterkiella sp. CH55 18S ribosomal RNA gene, complete sequence; macronuclear	SPIROTRICHEA	CLASS (CILIATE)				P		P					
Sterkiella sp. CH55 18S ribosomal RNA gene, complete sequence; macronuclear	SPIROTRICHEA	CLASS (CILIATE)											P
Sterkiella sp. JS-2012a voucher PL 43 18S ribosomal RNA gene, complete sequence	SPIROTRICHEA	CLASS (CILIATE)											P
Sterkiella sp. JS-2012b voucher BOR14 18S ribosomal RNA gene, complete sequence	SPIROTRICHEA	CLASS (CILIATE)		P									
Stichococcus bacillaris gene for 18S rRNA, partial sequence, strain:D10-1	TREBEAUXIOPHYCEAE	CLASS (CHLOROPHYTA)						P					P
Stichococcus bacillaris gene for 18S rRNA, partial sequence, strain:K4-4	TREBEAUXIOPHYCEAE	CLASS (CHLOROPHYTA)	P										
Stichococcus chodati gene for 18S rRNA, partial sequence	TREBEAUXIOPHYCEAE	CLASS (CHLOROPHYTA)											P
Stoeckeria algicida genomic DNA containing 18S rRNA gene	DINOPHYCEAE	CLASS (DINOFLAGELLATE)	P	P									P
Stramenopile sp. ME13100 18S ribosomal RNA gene, partial sequence	STRAMENOPILE/HETEROKONT	PHYLUM: HETEROKONTA	P										

Striatella unipunctata gene for 18S rRNA, partial sequence, strain: s0208	BACILLARIOPHYCEAE	CLASS (HETEROKONTOPHYTA)						P					
Strongyloidium orientale isolate CXM09120301 small subunit ribosomal RNA gene, partial sequence	SPIROTRICHEA	CLASS (CILIATE)	P		P						P	P	P
Stygamoeba regulata strain ATCC 50892 small subunit ribosomal RNA gene, partial sequence	HETEROLOBOSEA	CLASS (PROTIST, PERCOLOZOA)										P	
Stylonychia lemnae macronuclear small-subunit ribosomal RNA gene, complete sequence	SPIROTRICHEA	CLASS (CILIATE)				P		P					
Stylonychia mytilus 17S ribosomal RNA gene, internal transcribed spacer 1	SPIROTRICHEA	CLASS (CILIATE)		P						P			
Surirella sp. DA1 18S small subunit ribosomal RNA gene, partial sequence	BACILLARIOPHYCEAE	CLASS (HETEROKONTOPHYTA)	P			P		P				P	
Symbiotaphrina kochii voucher CBS 589.63 16S small subunit ribosomal RNA gene	ASCOMYCETE	PHYLUM (KINGDOM: FUNGI)								P			
Synedra toxoneides strain WK57 small subunit ribosomal RNA gene, partial sequence	BACILLARIOPHYCEAE	CLASS (HETEROKONTOPHYTA)	P		P			P		P			
Synedra ulna strain UTEX FD404 18S small subunit ribosomal RNA gene, partial sequence	BACILLARIOPHYCEAE	CLASS (HETEROKONTOPHYTA)							P			P	
Tabularia cf. tabulata strain CCMP846 18S small subunit ribosomal RNA gene, partial sequence	BACILLARIOPHYCEAE	CLASS (HETEROKONTOPHYTA)											P
Talaroneis posidoniae 18S ribosomal RNA gene, partial sequence	BACILLARIOPHYCEAE	CLASS (HETEROKONTOPHYTA)										P	
Thalassionema frauenfeldii isolate ECT3929ThalXL 18S ribosomal RNA gene, partial sequence	BACILLARIOPHYCEAE	CLASS (HETEROKONTOPHYTA)											P
Thalassiosira concavuscula clone 1124 18S ribosomal RNA gene, partial sequence	BACILLARIOPHYCEAE	CLASS (HETEROKONTOPHYTA)		P		P	P	P	P	P	P	P	P
Thigmokeronopsis stoecki small subunit ribosomal RNA gene, partial sequence	SPIROTRICHEA	CLASS (CILIATE)	P										P
Thraustochytrium multirudimentale gene for 18S rRNA	THAUSTROCHYTRIACEAE	CLASS (HETEROKONTOPHYTA)					P						
Trachelocerca ditis small subunit ribosomal RNA gene, partial sequence	KARYORELICTEA	CLASS (CILIATE)									P		
Trachelocerca sagitta small subunit ribosomal RNA gene, partial sequence	KARYORELICTEA	CLASS (CILIATE)			P							P	P
Trachelocerca sp. FG-2014 isolate XY2009121601 small subunit ribosomal RNA gene, partial sequence	KARYORELICTEA	CLASS (CILIATE)	P	P	P	P	P	P	P	P	P	P	P
Tracheloraphis sp. ribosomal RNA small-subunit	KINETOPLASTEAE	CLASS (CILIATE)	P		P	P	P	P	P	P	P	P	P

Trachelostyla pediculiformis small subunit ribosomal RNA gene, partial sequence	POLYHYMENOPHORA	CLASS (CILIAE)	P	P	P	P	P	P	P	P	P	P	P
Trypanosoma simiae 18S srRNA1, complete sequence	KINETOPLASTEAE	CLASS (CILIAE)	P										
Tulamoeba peronaphora strain A1 18S ribosomal RNA gene, partial sequence	HETEROLOBOSEA	CLASS (PROTIST, PERCOLOZOA)											P
Ulkenia visurgensis gene for 18S rRNA	THRAUSTROCHYTRIACEAE	CLASS (HETEROKONTOPHYTA)	P		P								
Uncultured alveolate clone CCA46 18S small subunit ribosomal RNA gene, partial sequence	ALVEOLATE	KINGOM				P							
Uncultured alveolate clone CCI16 18S small subunit ribosomal RNA gene, partial sequence	ALVEOLATE	KINGOM	P	P	P	P	P	P	P	P	P	P	P
Uncultured alveolate clone CCI74 18S small subunit ribosomal RNA gene, partial sequence	ALVEOLATE	KINGOM	P	P	P			P	P	P	P	P	P
Uncultured alveolate clone WD0-44 18S ribosomal RNA gene, partial sequence	ALVEOLATE	KINGOM	P	P	P	P	P	P	P	P	P	P	P
Uncultured ascomycete clone 11-K17 18S ribosomal RNA gene, partial sequence	ASCOMYCETE	PHYLUM (KINGDOM: FUNGI)		P			P						
Uncultured Banisveld eukaryote clone P1-3m5 18S ribosomal RNA gene, partial sequence	UNKNOWN	UNKNOWN			P		P						
Uncultured bicosoecid clone env_Pavin_epi_T_NS83E 18S ribosomal RNA gene, partial sequence	BICOSECA	CLASS (HETEROKONTOPHYTA)	P	P	P	P	P	P	P	P	P	P	P
Uncultured Boletaceae clone Amb_18S_1320 18S ribosomal RNA gene, partial sequence	AGARICOMYCETES	CLASS (KINGDOM: FUNGI)	P							P			
Uncultured Boletaceae clone Elev_18S_1032 18S ribosomal RNA gene, partial sequence	AGARICOMYCETES	CLASS (KINGDOM: FUNGI)					P	P	P	P			
Uncultured Cafeteriaceae partial 18S rRNA gene, clone GM1_A5	BACILLARIOPHYCEAE	CLASS (HETEROKONTOPHYTA)											P
Uncultured centroheliozoan clone EB17.116 18S ribosomal RNA gene, partial sequence	HETEROLOBOSEA	CLASS (PROTIST, PERCOLOZOA)				P						P	
Uncultured cercomonad partial 18S rRNA gene, clone BS19_A3	CERCOMONADIDAE	CLASS (PHYLUM CERCOZOA)	P	P					P	P			
Uncultured cercozoan clone D8 small subunit ribosomal RNA gene, partial sequence	CERCOMONADIDAE	CLASS (PHYLUM CERCOZOA)	P				P						
Uncultured cercozoan clone G0Esp_2_8 18S ribosomal RNA gene, partial sequence	CERCOMONADIDAE	CLASS (PHYLUM CERCOZOA)											P
Uncultured cercozoan isolate 12-1.5 18S ribosomal RNA gene, partial sequence	CERCOMONADIDAE	CLASS (PHYLUM CERCOZOA)		P									

Uncultured cercozoan isolate DB-B13 18S ribosomal RNA gene, partial sequence	CERCOMONADIDAE	CLASS (PHYLUM CERCOZOA)		P	P	P	P			P	P	P
Uncultured chlorarachniophyte clone BLENRinf2 6 18S ribosomal RNA gene, partial sequence	CHLORARACHNIOOHYCEAE	CLASS (PHYLUM CERCOZOA)										P
Uncultured Chlorophyta gene for 18S rRNA, partial sequence, clone: DA-14	CHLORARACHNIOOHYCEAE	CLASS (PHYLUM CERCOZOA)	P				P	P	P			
Uncultured chlorophyte clone GHB17.5 18S ribosomal RNA gene, partial sequence	CHLORARACHNIOOHYCEAE	CLASS (PHYLUM CERCOZOA)	P	P	P	P	P	P	P	P	P	P
Uncultured chlorophyte clone GHB33.10 18S ribosomal RNA gene, partial sequence	CHLORARACHNIOOHYCEAE	CLASS (PHYLUM CERCOZOA)		P		P						
Uncultured chlorophyte clone LC32.32 18S ribosomal RNA gene, partial sequence	CHLORARACHNIOOHYCEAE	CLASS (PHYLUM CERCOZOA)								P		
Uncultured chlorophyte clone MLB32.155 18S ribosomal RNA gene, partial sequence	CHLORARACHNIOOHYCEAE	CLASS (PHYLUM CERCOZOA)	P	P							P	
Uncultured chlorophyte clone MLBA11.21 18S ribosomal RNA gene, partial sequence	CHLORARACHNIOOHYCEAE	CLASS (PHYLUM CERCOZOA)	P									
Uncultured choanoflagellate clone 0-7 18S ribosomal RNA gene, partial sequence	CHOANOFLAGELLATE	CLASS (CHOANOZOA)	P	P	P	P	P	P	P	P	P	P
Uncultured choanoflagellate partial 18S rRNA gene, clone DGGE band 18	CHOANOFLAGELLATE	CLASS (CHOANOZOA)			P		P	P		P		
Uncultured Chytridiomycota clone PFH9SP2005 18S ribosomal RNA gene, partial sequence	CHYTRIDIOMYCOTA	CLASS (KINGDOM: FUNGI)	P		P					P	P	P
Uncultured Chytridiomycota clone T3P1AeB07 18S ribosomal RNA gene, partial sequence	CHYTRIDIOMYCOTA	CLASS (KINGDOM: FUNGI)		P							P	
Uncultured Chytridiomycota clone T4P1AeE08 18S ribosomal RNA gene, partial sequence	CHYTRIDIOMYCOTA	CLASS (KINGDOM: FUNGI)										P
Uncultured ciliate clone 0-28 18S ribosomal RNA gene, partial sequence	CILIOPHORA	PHYLUM					P					
Uncultured ciliate clone 0-5 18S ribosomal RNA gene, partial sequence	CILIOPHORA	PHYLUM										P
Uncultured ciliate clone CCI60 18S small subunit ribosomal RNA gene, partial sequence	CILIOPHORA	PHYLUM			P	P	P			P		P
Uncultured ciliate clone EB67.133 18S ribosomal RNA gene, partial sequence	CILIOPHORA	PHYLUM				P						
Uncultured ciliate clone EB84.135 18S ribosomal RNA gene, partial sequence	CILIOPHORA	PHYLUM		P								
Uncultured ciliate clone MLB48.159 18S ribosomal RNA gene, partial sequence	CILIOPHORA	PHYLUM						P				

Uncultured ciliate clone SEO81101_24 18S ribosomal RNA gene, partial sequence	CILIOPHORA	PHYLUM			P								
Uncultured ciliate clone SEO81101_8 18S ribosomal RNA gene, partial sequence	CILIOPHORA	PHYLUM							P				
Uncultured cryptophyte clone EB29.120 18S ribosomal RNA gene, partial sequence	CRYPTOPHYCEAE	CLASS (CRYPTOPHYTA)				P							
Uncultured diatom clone Es109 18S ribosomal RNA gene, partial sequence	BACILLARIOPHYCEAE	CLASS (HETEROKONTOPHYTA)									P		
Uncultured diatom clone Es123 18S ribosomal RNA gene, partial sequence	BACILLARIOPHYCEAE	CLASS (HETEROKONTOPHYTA)		P									
Uncultured dinoflagellate clone CCA32 18S small subunit ribosomal RNA gene, partial sequence	DINOPHYCEAE	CLASS (DINOFLAGELLATE)			P								
Uncultured dinoflagellate clone HYB0012 18S ribosomal RNA gene, partial sequence	DINOPHYCEAE	CLASS (DINOFLAGELLATE)								P			P
Uncultured Dunaliellaceae clone Amb_18S_715 18S ribosomal RNA gene, partial sequence	CHLOROPHYCEAE	CLASS (CHLOROPHYTA)						P					
Uncultured eukaryote 18S rRNA gene, clone RA010412.17	DINOPHYCEAE	CLASS (DINOFLAGELLATE)		P	P	P	P			P	P	P	P
Uncultured eukaryote 18S rRNA, partial sequence, clone: RM1-SGM20	UNKNOWN MICRO-EUKARYOTE									P			P
Uncultured eukaryote clone 0-9 18S ribosomal RNA gene, partial sequence	CILIOPHORA	PHYLUM		P									
Uncultured eukaryote clone A 18S ribosomal RNA gene, partial sequence	UNKNOWN MICRO-EUKARYOTE										P		P
Uncultured eukaryote clone Amb_18S_1305 18S ribosomal RNA gene, partial sequence	CHOANOFLAGELLATE	CLASS									P		
Uncultured eukaryote clone Amb_18S_6891 18S ribosomal RNA gene, partial sequence	RESTIONACEAE	FAMILY											P
Uncultured eukaryote clone AMT15_15_10m_113 18S ribosomal RNA gene, partial sequence	DINOPHYCEAE	CLASS (DINOFLAGELLATE)						P					
Uncultured eukaryote clone B0Esp_3_16 18S ribosomal RNA gene, partial sequence	UNKNOWN MICRO-EUKARYOTE												P
Uncultured eukaryote clone B19bA51 18S ribosomal RNA gene, partial sequence	BACILLARIOPHYCEAE	CLASS (HETEROKONTOPHYTA)	P	P	P	P	P	P	P	P	P	P	P
Uncultured eukaryote clone BB01_19 18S ribosomal RNA gene, partial sequence	UNKNOWN	UNKNOWN				P	P	P			P		
Uncultured eukaryote clone BB01_76 18S ribosomal RNA gene, partial sequence	UNKNOWN	UNKNOWN				P						P	P

Uncultured eukaryote clone c9d2t4 18S small subunit ribosomal RNA gene, partial sequence	BACILLARIOPHYCEAE	CLASS (HETEROKONTOPHYTA)								P			
Uncultured eukaryote clone CC02A175.008 18S ribosomal RNA gene, partial sequence	CILIOPHORA	PHYLUM						P					
Uncultured eukaryote clone CC02SE05.095 18S ribosomal RNA gene, partial sequence	FUNGI	KINGOM	P										
Uncultured eukaryote clone CCA61 18S small subunit ribosomal RNA gene, partial sequence	FUNGI	KINGOM		P		P	P			P		P	P
Uncultured eukaryote clone CL-F6 18S ribosomal RNA gene, partial sequence	UNKNOWN	UNKNOWN	P	P	P	P	P	P	P	P	P	P	P
Uncultured eukaryote clone cs618-52 18S ribosomal RNA gene, partial sequence	UNKNOWN	UNKNOWN							P	P			P
Uncultured eukaryote clone cs618-68 18S ribosomal RNA gene, partial sequence	UNKNOWN	UNKNOWN	P	P	P	P	P			P	P		
Uncultured eukaryote clone cs618-89 18S ribosomal RNA gene, partial sequence	UNKNOWN	UNKNOWN						P					
Uncultured eukaryote clone D 18S ribosomal RNA gene, partial sequence	HAPTOPHYTE	PHYLUM	P	P	P							P	
Uncultured eukaryote clone D3P05E08 18S ribosomal RNA gene, partial sequence	SYNDINIALES	ORDER (CLASS: DINOPHYCEAE)	P	P		P	P	P	P	P	P	P	P
Uncultured eukaryote clone D3P06E05 18S ribosomal RNA gene, partial sequence	BACILLARIOPHYCEAE	CLASS (HETEROKONTOPHYTA)	P	P	P	P	P	P	P	P	P	P	P
Uncultured eukaryote clone D4P08B02 18S ribosomal RNA gene, partial sequence	CHLOROPHYCEAE	CLASS (CHLOROPHYTA)	P	P		P	P					P	P
Uncultured eukaryote clone Elev_18S_5331 18S ribosomal RNA gene, partial sequence	UNKNOWN MICRO-EUKARYOTE				P								
Uncultured eukaryote clone EUK1A A1 18S ribosomal RNA gene, partial sequence	DINOPHYCEAE	CLASS (DINOFLAGELLATE)											P
Uncultured eukaryote clone EUK1A F10 18S ribosomal RNA gene, partial sequence	DINOPHYCEAE	CLASS (DINOFLAGELLATE)			P								
Uncultured eukaryote clone EUK3-1A H2 18S ribosomal RNA gene, partial sequence	DINOPHYCEAE	CLASS (DINOFLAGELLATE)											P
Uncultured eukaryote clone EUK50_D10 18S ribosomal RNA gene, partial sequence	DINOPHYCEAE	CLASS (DINOFLAGELLATE)	P	P				P		P			
Uncultured eukaryote clone F3-112 18S ribosomal RNA gene, partial sequence	PELAGOPHYCEAE	CLASS (HETEROKONTOPHYTA)							P				P
Uncultured eukaryote clone F5K2Q4C04IIPHV 18S ribosomal RNA gene, partial sequence	UNKNOWN	UNKNOWN											P

Uncultured eukaryote clone N4aD65 18S ribosomal RNA gene, partial sequence	LABYRINTHULEA	CLASS		P	P				P				
Uncultured eukaryote clone P-11_E2 18S ribosomal RNA gene, partial sequence	UNKNOWN	UNKNOWN		P						P			
Uncultured eukaryote clone P-13_E6 18S ribosomal RNA gene, partial sequence	UNKNOWN	UNKNOWN	P	P							P	P	P
Uncultured eukaryote clone PF1E4F12 18S ribosomal RNA gene, partial sequence	UNKNOWN	UNKNOWN										P	P
Uncultured eukaryote clone RF1E3G11 18S ribosomal RNA gene, partial sequence	UNKNOWN	UNKNOWN	P	P	P	P	P	P			P	P	P
Uncultured eukaryote clone RS1E4B06 18S ribosomal RNA gene, partial sequence	UNKNOWN	UNKNOWN		P		P	P	P				P	P
Uncultured eukaryote clone rt18Bms 18S ribosomal RNA gene, partial sequence	ZYGNEMATALES	DIVISION (KINGDOM: PLANTAE)	P										
Uncultured eukaryote clone RT5iin4 18S ribosomal RNA gene, complete sequence	TREBEAUXIOPHYCEAE	CLASS (CHLOROPHYTA)	P		P			P	P			P	P
Uncultured eukaryote clone RT5iin8 18S ribosomal RNA gene, complete sequence	ZYGNEMATALES	DIVISION (KINGDOM: PLANTAE)	P	P						P			
Uncultured eukaryote clone s14_13 18S ribosomal RNA gene, partial sequence	UNKNOWN	UNKNOWN	P										
Uncultured eukaryote clone S2-65 18S ribosomal RNA gene, partial sequence	UNKNOWN	UNKNOWN		P					P				
Uncultured eukaryote clone S2-79 18S ribosomal RNA gene, partial sequence	UNKNOWN	UNKNOWN										P	
Uncultured eukaryote clone S6-022 18S ribosomal RNA gene, partial sequence	UNKNOWN	UNKNOWN										P	
Uncultured eukaryote clone S6-046 18S ribosomal RNA gene, partial sequence	UNKNOWN	UNKNOWN		P	P				P	P			P
Uncultured eukaryote clone S6-089 18S ribosomal RNA gene, partial sequence	UNKNOWN	UNKNOWN											P
Uncultured eukaryote clone S6-09 18S ribosomal RNA gene, partial sequence	UNKNOWN	UNKNOWN	P	P		P	P	P			P	P	P
Uncultured eukaryote clone SGUH1059 18S ribosomal RNA gene, partial sequence	UNKNOWN	UNKNOWN		P									
Uncultured eukaryote clone SGUH1063 18S ribosomal RNA gene, partial sequence	DINOPHYCEAE	CLASS (DINOFLAGELLATE)			P								
Uncultured eukaryote clone SGUH1070 18S ribosomal RNA gene, partial sequence	DINOPHYCEAE	CLASS (DINOFLAGELLATE)	P	P	P	P	P	P	P	P	P	P	P

Uncultured eukaryote clone SGUH1164 18S ribosomal RNA gene, partial sequence	UNKNOWN	UNKNOWN			P	P	P	P	P		P	P
Uncultured eukaryote clone SGUH1344 18S ribosomal RNA gene, partial sequence	UNKNOWN	UNKNOWN	P	P				P		P		P
Uncultured eukaryote clone SGUH1349 18S ribosomal RNA gene, partial sequence	UNKNOWN	UNKNOWN		P								
Uncultured eukaryote clone SGUH1367 18S ribosomal RNA gene, partial sequence	UNKNOWN	UNKNOWN	P	P	P	P	P	P	P	P	P	P
Uncultured eukaryote clone SGUH1448 18S ribosomal RNA gene, partial sequence	CILIOPHORA	PHYLUM	P		P	P			P		P	
Uncultured eukaryote clone SGUH1454 18S ribosomal RNA gene, partial sequence	CILIOPHORA	PHYLUM		P								
Uncultured eukaryote clone SGUH427 18S ribosomal RNA gene, partial sequence	UNKNOWN	UNKNOWN		P								
Uncultured eukaryote clone SGUH476 18S ribosomal RNA gene, partial sequence	UNKNOWN	UNKNOWN			P			P				
Uncultured eukaryote clone SGUH501 18S ribosomal RNA gene, partial sequence	UNKNOWN	UNKNOWN			P		P	P	P	P		
Uncultured eukaryote clone SGUH532 18S ribosomal RNA gene, partial sequence	UNKNOWN	UNKNOWN						P				
Uncultured eukaryote clone SGUH621 18S ribosomal RNA gene, partial sequence	DINOPHYCEAE	CLASS (DINOFLAGELLATE)	P	P	P		P	P	P	P	P	P
Uncultured eukaryote clone SGUH865 18S ribosomal RNA gene, partial sequence	UNKNOWN	UNKNOWN		P				P				
Uncultured eukaryote clone SGUH873 18S ribosomal RNA gene, partial sequence	UNKNOWN	UNKNOWN				P						
Uncultured eukaryote clone SGUH919 18S ribosomal RNA gene, partial sequence	UNKNOWN	UNKNOWN		P								
Uncultured eukaryote clone SGYH405 18S ribosomal RNA gene, partial sequence	UNKNOWN	UNKNOWN										P
Uncultured eukaryote clone SGYH782 18S ribosomal RNA gene, partial sequence	UNKNOWN	UNKNOWN					P					P
Uncultured eukaryote clone SGYH794 18S ribosomal RNA gene, partial sequence	UNKNOWN	UNKNOWN										P
Uncultured eukaryote clone SGYI1070 18S ribosomal RNA gene, partial sequence	UNKNOWN	UNKNOWN	P	P	P	P	P	P	P	P	P	P
Uncultured eukaryote clone SGYI1130 18S ribosomal RNA gene, partial sequence	UNKNOWN	UNKNOWN	P	P				P			P	P

Uncultured eukaryote clone SGYI1150 18S ribosomal RNA gene, partial sequence	UNKNOWN	UNKNOWN	P											
Uncultured eukaryote clone SGYI1169 18S ribosomal RNA gene, partial sequence	UNKNOWN	UNKNOWN	P	P	P	P	P	P	P	P	P	P	P	P
Uncultured eukaryote clone SGYI1176 18S ribosomal RNA gene, partial sequence	UNKNOWN	UNKNOWN	P	P	P	P	P	P	P	P	P	P	P	P
Uncultured eukaryote clone SGYI1395 18S ribosomal RNA gene, partial sequence	UNKNOWN	UNKNOWN		P	P					P	P			
Uncultured eukaryote clone SGYI433 18S ribosomal RNA gene, partial sequence	UNKNOWN	UNKNOWN							P					
Uncultured eukaryote clone SGYI529 18S ribosomal RNA gene, partial sequence	UNKNOWN	UNKNOWN	P		P				P	P				
Uncultured eukaryote clone SGYI544 18S ribosomal RNA gene, partial sequence	UNKNOWN	UNKNOWN						P						
Uncultured eukaryote clone SGYI628 18S ribosomal RNA gene, partial sequence	UNKNOWN	UNKNOWN							P	P				
Uncultured eukaryote clone SGYI769 18S ribosomal RNA gene, partial sequence	UNKNOWN	UNKNOWN												P
Uncultured eukaryote clone SGYI801 18S ribosomal RNA gene, partial sequence	UNKNOWN	UNKNOWN											P	
Uncultured eukaryote clone SGYI950 18S ribosomal RNA gene, partial sequence	UNKNOWN	UNKNOWN											P	P
Uncultured eukaryote clone SGYI998 18S ribosomal RNA gene, partial sequence	UNKNOWN	UNKNOWN							P					
Uncultured eukaryote clone SGYO1533 18S ribosomal RNA gene, partial sequence	UNKNOWN	UNKNOWN			P									
Uncultured eukaryote clone SGYP1235 18S ribosomal RNA gene, partial sequence	UNKNOWN	UNKNOWN							P					
Uncultured eukaryote clone SGYP1486 18S ribosomal RNA gene, partial sequence	UNKNOWN	UNKNOWN												P
Uncultured eukaryote clone SGYP647 18S ribosomal RNA gene, partial sequence	UNKNOWN	UNKNOWN		P	P				P					P
Uncultured eukaryote clone SGYP678 18S ribosomal RNA gene, partial sequence	UNKNOWN	UNKNOWN		P										
Uncultured eukaryote clone SGYP684 18S ribosomal RNA gene, partial sequence	UNKNOWN	UNKNOWN	P					P	P	P				
Uncultured eukaryote clone SGYP754 18S ribosomal RNA gene, partial sequence	UNKNOWN	UNKNOWN	P					P	P	P				P

Uncultured eukaryote clone SGYS1392 18S ribosomal RNA gene, partial sequence	UNKNOWN	UNKNOWN	P	P	P	P	P	P	P	P	P	P	P
Uncultured eukaryote clone SGYS698 18S ribosomal RNA gene, partial sequence	UNKNOWN	UNKNOWN	P										P
Uncultured eukaryote clone SGYT1182 18S ribosomal RNA gene, partial sequence	UNKNOWN	UNKNOWN	P			P							
Uncultured eukaryote clone SGYT1301 18S ribosomal RNA gene, partial sequence	UNKNOWN	UNKNOWN								P			
Uncultured eukaryote clone SGYT529 18S ribosomal RNA gene, partial sequence	UNKNOWN	UNKNOWN				P	P						P
Uncultured eukaryote clone SGYU1139 18S ribosomal RNA gene, partial sequence	UNKNOWN	UNKNOWN	P				P	P					
Uncultured eukaryote clone SGYU1318 18S ribosomal RNA gene, partial sequence	UNKNOWN	UNKNOWN									P		
Uncultured eukaryote clone SGYU668 18S ribosomal RNA gene, partial sequence	UNKNOWN	UNKNOWN		P									
Uncultured eukaryote clone SGYU819 18S ribosomal RNA gene, partial sequence	UNKNOWN	UNKNOWN									P		
Uncultured eukaryote clone SGYU902 18S ribosomal RNA gene, partial sequence	UNKNOWN	UNKNOWN								P			
Uncultured eukaryote clone SGYW525 18S ribosomal RNA gene, partial sequence	UNKNOWN	UNKNOWN						P					
Uncultured eukaryote clone SGYW569 18S ribosomal RNA gene, partial sequence	UNKNOWN	UNKNOWN	P	P	P		P	P	P	P	P	P	P
Uncultured eukaryote clone SGYW699 18S ribosomal RNA gene, partial sequence	UNKNOWN	UNKNOWN									P		
Uncultured eukaryote clone SGYW769 18S ribosomal RNA gene, partial sequence	UNKNOWN	UNKNOWN	P	P	P		P	P	P	P	P	P	P
Uncultured eukaryote clone SGYY1250 18S ribosomal RNA gene, partial sequence	UNKNOWN	UNKNOWN		P									
Uncultured eukaryote clone SGYY1340 18S ribosomal RNA gene, partial sequence	UNKNOWN	UNKNOWN									P		
Uncultured eukaryote clone SGYY1386 18S ribosomal RNA gene, partial sequence	UNKNOWN	UNKNOWN		P									
Uncultured eukaryote clone SGYY741 18S ribosomal RNA gene, partial sequence	UNKNOWN	UNKNOWN											P
Uncultured eukaryote clone SGYY760 18S ribosomal RNA gene, partial sequence	UNKNOWN	UNKNOWN						P				P	

Uncultured eukaryote clone SGYY984 18S ribosomal RNA gene, partial sequence	UNKNOWN	UNKNOWN		P									
Uncultured eukaryote clone SHAU635 16S ribosomal RNA gene, partial sequence	UNKNOWN	UNKNOWN	P							P			
Uncultured eukaryote clone SHBB552 16S ribosomal RNA gene, partial sequence	UNKNOWN	UNKNOWN						P					
Uncultured eukaryote clone T2S302D04 18S ribosomal RNA gene, partial sequence	UNKNOWN	UNKNOWN			P								
Uncultured eukaryote clone T4A4_12 18S ribosomal RNA gene, partial sequence	CRYPTOPHYCEAE	CLASS (CRYPTOPHYTA)		P									
Uncultured eukaryote clone ThJAR3-48 18S ribosomal RNA gene, partial sequence	UNKNOWN	UNKNOWN			P	P							
Uncultured eukaryote clone TKR07E.14 18S ribosomal RNA gene, partial sequence	CHRYSOPHYCEAE	CLASS					P						
Uncultured eukaryote clone TKR07M.19 18S ribosomal RNA gene, partial sequence	CHYTRIDIOMYCOTA	CLASS	P	P	P	P	P	P	P	P	P	P	P
Uncultured eukaryote clone TKR07M.83 18S ribosomal RNA gene, partial sequence	CHRYSOPHYCEAE	CLASS		P				P	P				
Uncultured eukaryote clone TKR07M.92 18S ribosomal RNA gene, partial sequence	CHRYSOPHYCEAE	CLASS										P	
Uncultured eukaryote clone TW-A1-2-8d 18S ribosomal RNA gene, partial sequence	PROTOZOA	KINGDOM	P									P	
Uncultured eukaryote clone TWII-3h 18S ribosomal RNA gene, partial sequence	PROTOZOA	KINGDOM		P	P	P	P			P	P	P	P
Uncultured eukaryote clone Winter_19 18S ribosomal RNA gene, partial sequence	ALVEOLATE	KINGDOM		P									
Uncultured eukaryote clone WLB10.148 18S ribosomal RNA gene, partial sequence	CRYPTOPHYCEAE	CLASS (CRYPTOPHYTA)		P			P						
Uncultured eukaryote clone X2-097 18S ribosomal RNA gene, partial sequence	UNKNOWN	UNKNOWN										P	P
Uncultured eukaryote clone X6-014 18S ribosomal RNA gene, partial sequence	UNKNOWN	UNKNOWN		P									
Uncultured eukaryote gene for 18S ribosomal RNA, complete sequence, clone: MPE2-27	CERCOZOA	KINGDOM				P							
Uncultured eukaryote gene for 18S ribosomal RNA, partial sequence, clone: Rwe-1	UNKNOWN	UNKNOWN								P			P P
Uncultured eukaryote gene for 18S rRNA, partial sequence, clone: 18S-AK-W-40	UNKNOWN	UNKNOWN											P P

Uncultured eukaryote gene for 18S rRNA, partial sequence, clone: CF_DNA_52	UNKNOWN	UNKNOWN								P			
Uncultured eukaryote gene for 18S rRNA, partial sequence, clone: CompH_DNA_04	UNKNOWN	UNKNOWN			P								
Uncultured eukaryote gene for 18S rRNA, partial sequence, clone: CompH_DNA_32	UNKNOWN	UNKNOWN					P						
Uncultured eukaryote gene for 18S rRNA, partial sequence, clone: CompL_DNA_45	UNKNOWN	UNKNOWN		P					P				
Uncultured eukaryote gene for SSU rRNA, partial sequence, clone: DSGM-36	CILIOPHORA	PHYLUM											P
Uncultured eukaryote isolate BS_DGGE_Euk-4 18S ribosomal RNA gene, partial sequence	HAPTOPHYTA	PHYLUM			P								
Uncultured eukaryote isolate DGGE band R 18S ribosomal RNA gene, partial sequence	UNKNOWN	UNKNOWN						P					P
Uncultured eukaryote isolate DGGE gel band JLJ-1-10 18S ribosomal RNA gene, partial sequence	UNKNOWN	UNKNOWN	P		P			P	P			P	P
Uncultured eukaryote isolate DGGE gel band JLJ-8-41 18S ribosomal RNA gene, partial sequence	UNKNOWN	UNKNOWN	P										
Uncultured eukaryote isolate DGGE gel band JLR2S-E40 18S ribosomal RNA gene, partial sequence	UNKNOWN	UNKNOWN	P					P	P	P			P
Uncultured eukaryote isolate DGGE gel band KSLS_Dino_DGGE3 18S ribosomal RNA gene, partial sequence	DINOPHYCEAE	CLASS (DINOFLAGELLATE)	P	P			P	P			P	P	P
Uncultured eukaryote isolate DGGE gel band KSLS_Dino_DGGE4 18S ribosomal RNA gene, partial sequence	DINOPHYCEAE	CLASS (DINOFLAGELLATE)	P										P
Uncultured eukaryote isolate P6X1b-2 18S ribosomal RNA gene, partial sequence	CHOANOFLAGELLATE	CLASS	P		P	P	P			P	P		
Uncultured eukaryote partial 18S rRNA gene, clone 01DPZ110600021	UNKNOWN	UNKNOWN	P						P				P
Uncultured eukaryote partial 18S rRNA gene, clone DGGE band 46	UNKNOWN	UNKNOWN			P	P			P				P
Uncultured eukaryote partial 18S rRNA gene, DGGE band Gahai2-05-7	STRAMENOPILE/HETEROKONT	PHYLUM: HETEROKONTA								P			P
Uncultured eukaryote rRNA for 18S rRNA, partial sequence, clone: CF_RNA_24	UNKNOWN	UNKNOWN	P	P	P			P	P			P	P
Uncultured eukaryote rRNA for 18S rRNA, partial sequence, clone: CompH_RNA_36	UNKNOWN	UNKNOWN										P	
Uncultured eukaryote rRNA for 18S rRNA, partial sequence, clone: NoF_RNA_05	UNKNOWN	UNKNOWN											P
Uncultured eukaryote rRNA for 18S rRNA, partial sequence, clone:	UNKNOWN	UNKNOWN	P	P	P	P	P	P	P	P	P	P	P

NoF_RNA_12														
Uncultured eukaryote rRNA for 18S rRNA, partial sequence, clone: NoF_RNA_21	UNKNOWN	UNKNOWN												P
Uncultured eukaryote rRNA for 18S rRNA, partial sequence, clone: NoF_RNA_28	UNKNOWN	UNKNOWN				P								
Uncultured eukaryote rRNA for 18S rRNA, partial sequence, clone: NoF_RNA_50	UNKNOWN	UNKNOWN			P									P
Uncultured eukaryotic partial 18S rDNA gene, isolate DGGE band JCF1	UNKNOWN	UNKNOWN			P									P
Uncultured Euplotida partial 18S rRNA gene, clone BS14_B11	SPIROTRICHEA	CLASS (CILIAE)		P				P					P	P
Uncultured freshwater cercozoan clone PCG6AU2004 18S ribosomal RNA gene, partial sequence	CERCOMONADIDAE	CLASS (PHYLUM CERCOZOA)				P								
Uncultured freshwater cercozoan clone PCH11AU2004 18S ribosomal RNA gene, partial sequence	CERCOMONADIDAE	CLASS (PHYLUM CERCOZOA)	P		P									
Uncultured freshwater eukaryote gene for 18S rRNA, partial sequence, clone: K9MAY2010	UNKNOWN	UNKNOWN		P	P			P			P	P		
Uncultured freshwater eukaryote gene for 18S rRNA, partial sequence, clone: SB21_2010	UNKNOWN	UNKNOWN							P					
Uncultured fungus clone ESS220206.038 18S ribosomal RNA gene, partial sequence	FUNGI	KINGOM										P		P P
Uncultured fungus clone ESS270706.065 18S ribosomal RNA gene, partial sequence	FUNGI	KINGOM	P	P	P	P	P	P	P				P	P P
Uncultured fungus clone FAS_57 18S small subunit ribosomal RNA gene, partial sequence	FUNGI	KINGOM				P								
Uncultured fungus clone FAS_91 18S small subunit ribosomal RNA gene, partial sequence	FUNGI	KINGOM	P						P					P P
Uncultured fungus clone G0Esp_1_17 18S ribosomal RNA gene, partial sequence	FUNGI	KINGOM		P		P								
Uncultured fungus clone nco40a04c1 18S ribosomal RNA gene, partial sequence	FUNGI	KINGOM												P
Uncultured fungus clone nco64h05c1 18S ribosomal RNA gene, partial sequence	FUNGI	KINGOM		P								P	P	
Uncultured fungus clone PFB1AU2004 18S ribosomal RNA gene, partial sequence	FUNGI	KINGOM	P	P					P				P	
Uncultured fungus clone PFF6AU2004 18S ribosomal RNA gene, partial sequence	FUNGI	KINGOM	P											
Uncultured fungus clone WD4-32 18S ribosomal RNA gene	FUNGI	KINGOM		P										

Uncultured fungus isolate DGGE gel band f10 18S ribosomal RNA gene, partial sequence	FUNGI	KINGOM	P	P			P		P			
Uncultured fungus partial 18S rRNA gene, clone BIO9_E9	FUNGI	KINGOM				P						
Uncultured fungus partial 18S rRNA gene, clone WIM48	FUNGI	KINGOM	P	P	P	P	P	P	P	P	P	P
Uncultured fungus partial 18S rRNA gene, DGGE band 3DB16	FUNGI	KINGOM	P	P	P	P	P	P	P	P	P	P
Uncultured Galactomyces clone CEobese305 5.8S ribosomal RNA gene and internal transcribed spacer 2	SACCHAROMYCETES	CLASS (KINGDOM: FUNGI)			P							
Uncultured haptophyte clone BrayaSo_water_18S 18S ribosomal RNA gene, partial sequence	PAVLOVOPHYCEAE	PHYLUM (HAPTOPHYTA)		P								
Uncultured marine cercozoan partial 18S rRNA gene, clone BS15_B5	CERCOMONADIDAE	CLASS (PHYLUM CERCOZOA)	P		P	P	P					
Uncultured marine diatom clone RA070411N.099 18S ribosomal RNA gene, partial sequence	BACILLARIOPHYCEAE	CLASS (HETEROKONTOPHYTA)							P			
Uncultured marine diatom partial 18S rRNA gene, clone BS18_B5	BACILLARIOPHYCEAE	CLASS (HETEROKONTOPHYTA)	P									
Uncultured marine dinoflagellate clone B60 18S ribosomal RNA gene, partial sequence	DINOPHYCEAE	CLASS (DINOFLAGELLATE)						P				
Uncultured marine eukaryote clone AD851 18S ribosomal RNA gene, partial sequence	CODONOSIGIDAE	FAMILY	P		P	P	P	P		P	P	P
Uncultured marine eukaryote clone BLACKSEA_cl_32 18S ribosomal RNA, partial sequence	BICOSECA	CLASS (HETEROKONTOPHYTA)						P				
Uncultured marine eukaryote clone BTPL20040617.0092 18S ribosomal RNA gene, partial sequence	UNKNOWN	UNKNOWN	P	P	P	P	P	P	P	P	P	P
Uncultured marine eukaryote clone BTPL20040617.0111 18S ribosomal RNA gene, partial sequence	UNKNOWN	UNKNOWN	P	P	P	P	P	P	P	P	P	P
Uncultured marine eukaryote clone BTPL20040617.0114 18S ribosomal RNA gene, partial sequence	UNKNOWN	UNKNOWN							P			
Uncultured marine eukaryote clone BTPL20040617.0116 18S ribosomal RNA gene, partial sequence	UNKNOWN	UNKNOWN	P	P		P	P	P	P	P		P
Uncultured marine eukaryote clone BTPL20040617.0127 18S ribosomal RNA gene, partial sequence	UNKNOWN	UNKNOWN	P	P								P
Uncultured marine eukaryote clone BTPL20040617.0140 18S ribosomal RNA gene, partial sequence	UNKNOWN	UNKNOWN	P	P	P	P	P	P	P	P	P	P
Uncultured marine eukaryote clone BTPL20040617.0148 18S ribosomal RNA gene, partial sequence	UNKNOWN	UNKNOWN		P	P	P	P	P	P	P	P	
Uncultured marine eukaryote clone BTPL20040617.0153 18S ribosomal RNA gene, partial sequence	UNKNOWN	UNKNOWN	P	P	P	P	P	P	P	P	P	P

Uncultured marine eukaryote clone BTPL20040617.0162 18S ribosomal RNA gene, partial sequence	UNKNOWN	UNKNOWN						P					P	P
Uncultured marine eukaryote clone BTPL20040713.0070 18S ribosomal RNA gene, partial sequence	UNKNOWN	UNKNOWN					P							
Uncultured marine eukaryote clone BTPL20040713.0180 18S ribosomal RNA gene, partial sequence	UNKNOWN	UNKNOWN		P										
Uncultured marine eukaryote clone BTPL20040713.0181 18S ribosomal RNA gene, partial sequence	UNKNOWN	UNKNOWN		P										
Uncultured marine eukaryote clone BTPL20040810.0041 18S ribosomal RNA gene, partial sequence	UNKNOWN	UNKNOWN									P			
Uncultured marine eukaryote clone BTPL20040810.0061 18S ribosomal RNA gene, partial sequence	UNKNOWN	UNKNOWN				P								
Uncultured marine eukaryote clone BTPL20040810.0070 18S ribosomal RNA gene, partial sequence	UNKNOWN	UNKNOWN	P	P	P	P	P	P	P	P	P	P	P	P
Uncultured marine eukaryote clone BTPL20040810.0082 18S ribosomal RNA gene, partial sequence	UNKNOWN	UNKNOWN	P	P	P	P	P	P	P	P	P	P	P	P
Uncultured marine eukaryote clone BTPL20040810.0083 18S ribosomal RNA gene, partial sequence	UNKNOWN	UNKNOWN	P	P										
Uncultured marine eukaryote clone BTPL20040810.0088 18S ribosomal RNA gene, partial sequence	UNKNOWN	UNKNOWN	P											
Uncultured marine eukaryote clone BTPL20040810.0128 18S ribosomal RNA gene, partial sequence	UNKNOWN	UNKNOWN	P	P	P	P	P	P	P			P	P	P
Uncultured marine eukaryote clone BTPL20040810.0133 18S ribosomal RNA gene, partial sequence	UNKNOWN	UNKNOWN									P			
Uncultured marine eukaryote clone BTPL20040810.0141 18S ribosomal RNA gene, partial sequence	UNKNOWN	UNKNOWN	P	P			P	P	P					
Uncultured marine eukaryote clone BTPL20040810.0142 18S ribosomal RNA gene, partial sequence	UNKNOWN	UNKNOWN		P										P
Uncultured marine eukaryote clone BTPL20040810.0161 18S ribosomal RNA gene, partial sequence	UNKNOWN	UNKNOWN								P				
Uncultured marine eukaryote clone BTPL20040810.0173 18S ribosomal RNA gene, partial sequence	UNKNOWN	UNKNOWN										P		
Uncultured marine eukaryote clone BTPL20040810.0176 18S ribosomal RNA gene, partial sequence	UNKNOWN	UNKNOWN				P								
Uncultured marine eukaryote clone BTQB20030503.0038 18S ribosomal RNA gene, partial sequence	UNKNOWN	UNKNOWN	P	P				P	P	P				P
Uncultured marine eukaryote clone BTQB20030806.0017 18S ribosomal RNA gene, partial sequence	UNKNOWN	UNKNOWN				P	P							

Uncultured marine eukaryote clone BTQB20030806.0027 18S ribosomal RNA gene, partial sequence	UNKNOWN	UNKNOWN	P	P	P	P	P	P	P	P	P	P	P
Uncultured marine eukaryote clone BTQB20030806.0062 18S ribosomal RNA gene, partial sequence	UNKNOWN	UNKNOWN		P		P	P		P				
Uncultured marine eukaryote clone BTQB20040501.0087 18S ribosomal RNA gene, partial sequence	UNKNOWN	UNKNOWN	P	P	P		P	P		P	P		
Uncultured marine eukaryote clone BTQB20040501.0118 18S ribosomal RNA gene, partial sequence	UNKNOWN	UNKNOWN	P	P	P	P	P	P	P	P	P	P	P
Uncultured marine eukaryote clone BTQB20040501.0120 18S ribosomal RNA gene, partial sequence	UNKNOWN	UNKNOWN			P	P	P			P	P		
Uncultured marine eukaryote clone BTQB20040501.0165 18S ribosomal RNA gene, partial sequence	UNKNOWN	UNKNOWN	P	P		P	P	P	P	P	P	P	
Uncultured marine eukaryote clone BTQB20040603.0104 18S ribosomal RNA gene, partial sequence	UNKNOWN	UNKNOWN	P	P	P	P	P	P	P	P	P	P	P
Uncultured marine eukaryote clone BTQB20040603.0116 18S ribosomal RNA gene, partial sequence	UNKNOWN	UNKNOWN					P		P	P	P	P	
Uncultured marine eukaryote clone BTQB20040603.0136 18S ribosomal RNA gene, partial sequence	UNKNOWN	UNKNOWN		P	P		P	P		P	P		
Uncultured marine eukaryote clone BTQB20040603.0150 18S ribosomal RNA gene, partial sequence	UNKNOWN	UNKNOWN										P	
Uncultured marine eukaryote clone BTQB20040603.0151 18S ribosomal RNA gene, partial sequence	UNKNOWN	UNKNOWN	P	P	P	P	P	P	P	P	P	P	P
Uncultured marine eukaryote clone BTQB20040603.0156 18S ribosomal RNA gene, partial sequence	UNKNOWN	UNKNOWN	P		P	P				P	P		
Uncultured marine eukaryote clone BTQB20040603.0164 18S ribosomal RNA gene, partial sequence	UNKNOWN	UNKNOWN	P	P	P	P	P	P	P	P	P	P	P
Uncultured marine eukaryote clone BTQB20040603.0186 18S ribosomal RNA gene, partial sequence	UNKNOWN	UNKNOWN			P		P	P	P				
Uncultured marine eukaryote clone BTQB20040719.0133 18S ribosomal RNA gene, partial sequence	UNKNOWN	UNKNOWN	P										
Uncultured marine eukaryote clone cLA13C09 small subunit ribosomal RNA gene, partial sequence	UNKNOWN	UNKNOWN										P	P
Uncultured marine eukaryote clone DP-041 18S ribosomal RNA gene, partial sequence	CHLOROPHYCEAE	CHLOROPHYCEAE	P	P	P	P	P	P	P	P	P	P	P
Uncultured marine eukaryote clone DP-051 18S ribosomal RNA gene, partial sequence	CHLOROPHYCEAE	CHLOROPHYCEAE			P	P		P		P	P		
Uncultured marine eukaryote clone EukaV4-106 18S ribosomal RNA gene, partial sequence	BACILLARIOPHYCEAE	CLASS				P							

Uncultured marine eukaryote clone FV23_2D3 small subunit ribosomal RNA gene, partial sequence	PLAGIOPYLEA	CLASS (CILIATE)	P	P			P	P	P		P	P
Uncultured marine eukaryote clone FV23_2H12G4 small subunit ribosomal RNA gene, partial sequence	PLAGIOPYLEA	CLASS (CILIATE)						P				
Uncultured marine eukaryote clone FV36_CilC9 small subunit ribosomal RNA gene, partial sequence	SPIROTRICHEA	CLASS (CILIATE)						P			P	
Uncultured marine eukaryote clone G1404-1096 18S ribosomal RNA gene, partial sequence	UNKNOWN	UNKNOWN								P	P	
Uncultured marine eukaryote clone HA/BE3 18S ribosomal RNA gene, partial sequence	UNKNOWN	UNKNOWN	P	P								P
Uncultured marine eukaryote clone I-6-MC195-OTU-67 18S ribosomal RNA gene, partial sequence	UNKNOWN	UNKNOWN	P	P	P	P	P	P	P	P	P	P
Uncultured marine eukaryote clone I-6-MC205-OTU-19 18S ribosomal RNA gene, partial sequence	UNKNOWN	UNKNOWN	P	P	P	P	P	P	P	P	P	P
Uncultured marine eukaryote clone I-6-MC217-OTU-61 18S ribosomal RNA gene, partial sequence	UNKNOWN	UNKNOWN		P								
Uncultured marine eukaryote clone I-6-MC233-OTU-69 18S ribosomal RNA gene, partial sequence	UNKNOWN	UNKNOWN	P	P	P	P	P	P	P	P	P	P
Uncultured marine eukaryote clone I-7-MC508-OTU-21 18S ribosomal RNA gene, partial sequence	UNKNOWN	UNKNOWN	P	P		P	P	P		P	P	P
Uncultured marine eukaryote clone I-7-MC534-OTU-52 18S ribosomal RNA gene, partial sequence	UNKNOWN	UNKNOWN					P	P	P			
Uncultured marine eukaryote clone I-7-MC550-OTU-68 18S ribosomal RNA gene, partial sequence	UNKNOWN	UNKNOWN	P	P	P	P	P	P	P	P	P	P
Uncultured marine eukaryote clone I-7-MC660-OTU-28 18S ribosomal RNA gene, partial sequence	UNKNOWN	UNKNOWN	P	P	P	P	P	P	P	P		P
Uncultured marine eukaryote clone I--7-MC690-OTU-66 18S ribosomal RNA gene, partial sequence	UNKNOWN	UNKNOWN	P	P	P							P
Uncultured marine eukaryote clone I-8-MC722-OTU-25 18S ribosomal RNA gene, partial sequence	UNKNOWN	UNKNOWN									P	
Uncultured marine eukaryote clone I-8-MC728-OTU-57 18S ribosomal RNA gene, partial sequence	UNKNOWN	UNKNOWN			P	P		P	P	P		P
Uncultured marine eukaryote clone I-8-MC738-OTU-58 18S ribosomal RNA gene, partial sequence	UNKNOWN	UNKNOWN								P		
Uncultured marine eukaryote clone I-8-MC744-OTU-35 18S ribosomal RNA gene, partial sequence	UNKNOWN	UNKNOWN				P				P		
Uncultured marine eukaryote clone I-8-MC812-OTU-59 18S ribosomal RNA gene, partial sequence	UNKNOWN	UNKNOWN	P	P			P			P	P	P

Uncultured marine eukaryote clone I-9-MC866-OTU-37 18S ribosomal RNA gene, partial sequence	UNKNOWN	UNKNOWN							P	P			
Uncultured marine eukaryote clone M2_18B03 small subunit ribosomal RNA gene, partial sequence	UNKNOWN	UNKNOWN			P		P	P	P	P	P	P	P
Uncultured marine eukaryote clone M2_18C01 small subunit ribosomal RNA gene, partial sequence	UNKNOWN	UNKNOWN		P	P	P	P		P	P			P
Uncultured marine eukaryote clone M2_18C05 small subunit ribosomal RNA gene, partial sequence	UNKNOWN	UNKNOWN		P	P	P		P	P	P			P
Uncultured marine eukaryote clone M2_18D10 small subunit ribosomal RNA gene, partial sequence	UNKNOWN	UNKNOWN		P	P	P	P	P	P			P	P
Uncultured marine eukaryote clone M2_18E09 small subunit ribosomal RNA gene, partial sequence	UNKNOWN	UNKNOWN										P	
Uncultured marine eukaryote clone M2_18F12 small subunit ribosomal RNA gene, partial sequence	UNKNOWN	UNKNOWN											P
Uncultured marine eukaryote clone M3_18F06 small subunit ribosomal RNA gene, partial sequence	KINETOPLASTEA	CLASS (PHYLUM EUGLENOZOA)	P	P									P
Uncultured marine eukaryote clone ME_Euk_FW74 18S small subunit ribosomal RNA gene, partial sequence	UNKNOWN	UNKNOWN				P							P
Uncultured marine eukaryote clone ME_Euk_FW99 18S small subunit ribosomal RNA gene, partial sequence	UNKNOWN	UNKNOWN						P					
Uncultured marine eukaryote clone NA1_1A8 18S ribosomal RNA gene, partial sequence	UNKNOWN	UNKNOWN											P
Uncultured marine eukaryote clone NA1_1B8 18S ribosomal RNA gene, partial sequence	UNKNOWN	UNKNOWN											P
Uncultured marine eukaryote clone NA1_1G5 18S ribosomal RNA gene, partial sequence	UNKNOWN	UNKNOWN	P	P	P	P	P	P	P	P	P	P	P
Uncultured marine eukaryote clone NIF_1E11 18S ribosomal RNA gene, partial sequence	UNKNOWN	UNKNOWN										P	
Uncultured marine eukaryote clone NIF_1F2 18S ribosomal RNA gene, partial sequence	UNKNOWN	UNKNOWN											P
Uncultured marine eukaryote clone NIF_4C10 18S ribosomal RNA gene, partial sequence	UNKNOWN	UNKNOWN	P	P	P	P	P	P	P	P	P	P	P
Uncultured marine eukaryote clone p15SBG2 18S small subunit ribosomal RNA gene, partial sequence	Non-stramenopile flagellate						P	P					
Uncultured marine eukaryote clone SA1_3C06 18S ribosomal RNA gene, partial sequence	UNKNOWN	UNKNOWN			P								
Uncultured marine eukaryote clone SA2_1A12 18S ribosomal RNA gene, partial sequence	UNKNOWN	UNKNOWN											P

Uncultured marine eukaryote clone SA2_1D2 18S ribosomal RNA gene, partial sequence	UNKNOWN	UNKNOWN		P		P		P			P	
Uncultured marine eukaryote clone SA2_1F5 18S ribosomal RNA gene, partial sequence	UNKNOWN	UNKNOWN					P					
Uncultured marine eukaryote clone SA2_1F8 18S ribosomal RNA gene, partial sequence	UNKNOWN	UNKNOWN	P	P		P	P		P		P	P
Uncultured marine eukaryote clone SA2_4F7 18S ribosomal RNA gene, partial sequence	UNKNOWN	UNKNOWN	P						P		P	
Uncultured marine eukaryote clone SGUH1121.FRAG.MO.5m 18S ribosomal RNA gene, partial sequence	UNKNOWN	UNKNOWN	P	P		P	P	P		P		P
Uncultured marine eukaryote clone SIF_1F12 18S ribosomal RNA gene, partial sequence	UNKNOWN	UNKNOWN					P					
Uncultured marine eukaryote clone SIF_4A2 18S ribosomal RNA gene, partial sequence	UNKNOWN	UNKNOWN		P	P				P		P	
Uncultured marine eukaryote clone UEPAC30Cp2 18S small subunit ribosomal RNA gene, partial sequence	PRASINOPHYCEAE	CLASS (CHLOROPHYTA)							P			
Uncultured marine eukaryote clone WC-12-MC361-OTU-12 18S ribosomal RNA gene, partial sequence	UNKNOWN	UNKNOWN	P	P	P	P	P	P	P	P	P	P
uncultured marine picoeukaryote partial 18S rRNA gene, isolate ws_101, clone 1807E06	STRAMENOPILE/HETEROKONT	PHYLUM: HETEROKONTA		P	P	P	P		P	P	P	P
uncultured marine picoeukaryote partial 18S rRNA gene, isolate ws_159, clone 1815C04	STRAMENOPILE/HETEROKONT	PHYLUM: HETEROKONTA			P			P				
uncultured marine picoeukaryote partial 18S rRNA gene, isolate ws_164, clone 1816G03	STRAMENOPILE/HETEROKONT	PHYLUM: HETEROKONTA		P	P	P	P	P	P	P	P	P
uncultured marine picoeukaryote partial 18S rRNA gene, isolate ws_59, clone 1806H01	STRAMENOPILE/HETEROKONT	PHYLUM: HETEROKONTA	P	P	P	P	P	P	P	P	P	P
Uncultured microeukaryote clone E-28 18S ribosomal RNA gene, partial sequence	STRAMENOPILE/HETEROKONT	PHYLUM: HETEROKONTA				P						
Uncultured microeukaryote clone E-31 18S ribosomal RNA gene, partial sequence	STRAMENOPILE/HETEROKONT	PHYLUM: HETEROKONTA						P				
Uncultured microeukaryote clone E-33 18S ribosomal RNA gene, partial sequence	STRAMENOPILE/HETEROKONT	PHYLUM: HETEROKONTA		P								
Uncultured microeukaryote clone M23E1C06 18S ribosomal RNA gene, partial sequence	STRAMENOPILE/HETEROKONT	PHYLUM: HETEROKONTA	P						P		P	
Uncultured microeukaryote clone M23E1C10 18S ribosomal RNA gene, partial sequence	STRAMENOPILE/HETEROKONT	PHYLUM: HETEROKONTA										P
Uncultured microeukaryote clone M60E1C07 18S ribosomal RNA gene, partial sequence	STRAMENOPILE/HETEROKONT	PHYLUM: HETEROKONTA			P							

Uncultured stramenopile clone TB0-26 18S ribosomal RNA gene, partial sequence	STRAMENOPILE/HETEROKONT	PHYLUM: HETEROKONTA							P	P			
Uncultured Strombidium sp. clone XM14b 18S ribosomal RNA gene, partial sequence	SPIROTRICHEA	CLASS (CILIATE)		P									
Uncultured Suctorina partial 18S rRNA gene, clone GM1_B1	PHYLLOPHARYNGEA	CLASS (CILIATE)	P	P	P	P	P	P	P	P	P	P	P
Uncultured Vannellidae partial 18S rRNA gene, clone BS15_B2	FLABELLULIDAE	CLASS (AMOEBOZOA)		P								P	
Uronema elegans 16S-like small subunit ribosomal RNA gene, partial sequence	OLIGOHYMENOPHERA	CLASS (CILIATE)					P						
Vahlkampfia damariscottae SSU rRNA gene, strain CCAP 1588/7	HETEROLOBOSEA	CLASS (PROTIST, PERCOLOZOA)									P		
Vannella sp. COHH 61 18S ribosomal RNA gene, partial sequence	FLABELLULIDAE	CLASS (AMOEBOZOA)	P	P						P	P	P	P

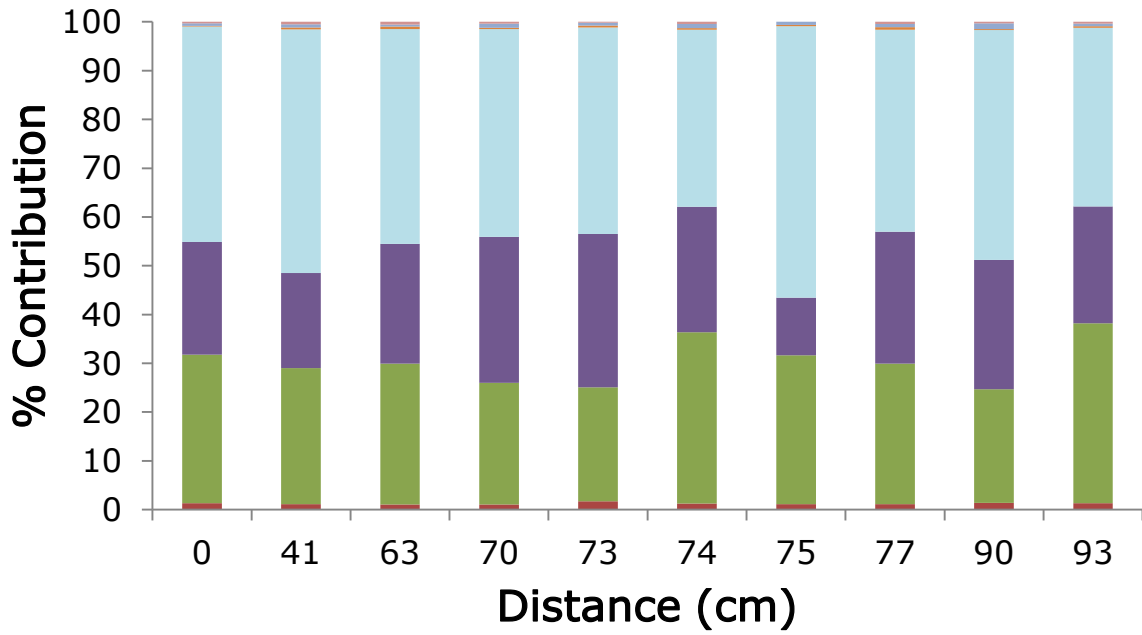


Figure S3. Mean percentage contribution of OTUs from the kingdoms plant (Dark Blue) and fungi (Dark Red), as well as the protistan supergroups Excavata (Light Purple), Chromalveolata (Dark Purple), Rhizaria (Light Red), Archaeplastidia (green algae, Light Blue), Unikonta (Orange), and unknown OTUs (Green). Sample locations labelled as distance from first sample point, A3 of 0 cm, as shown in Figure 2.

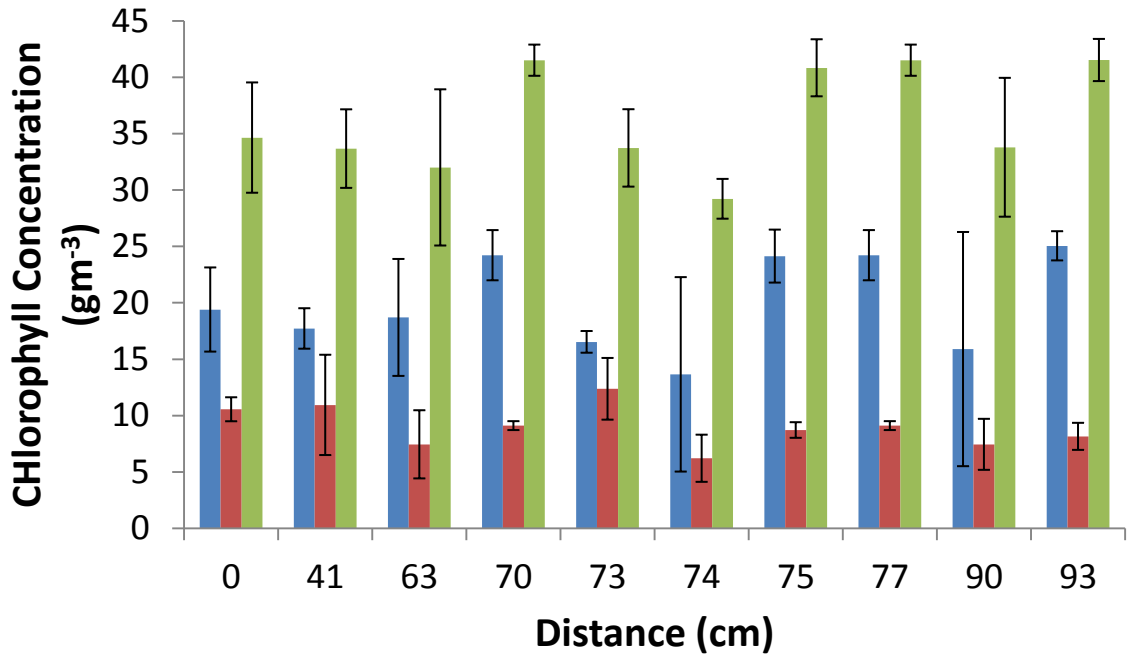


Figure S4. Mean concentration of chlorophyll *a*, blue bars; chlorophyll *c*, red bars; and total chlorophyll, green bars, measured in gm^{-3} . Error bars indicate standard deviation of triplicate samples. Sample locations labelled as distance from first sample point, A3 of 0 cm, as shown in Figure 2.

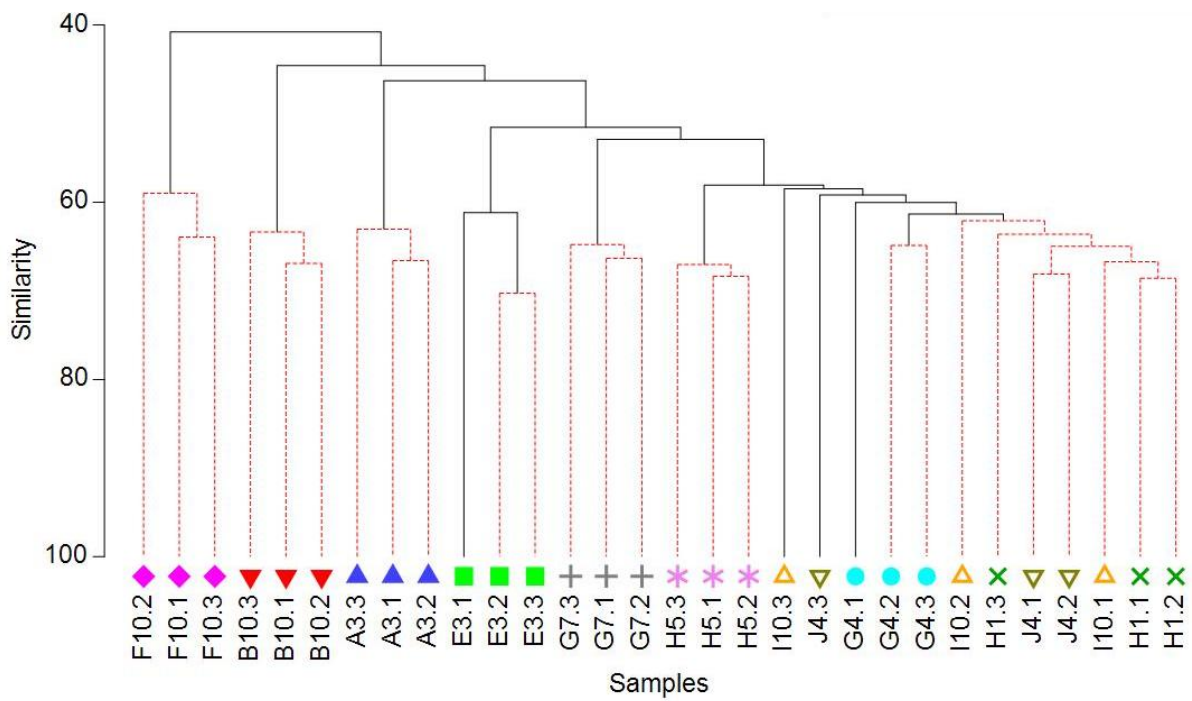


Figure S5. CLUSTER analysis of 18S OTUs samples by Class at 10 microscale locations (in triplicate) which displays similarity between samples as a percentage. Red dotted lines indicate where there is no significant difference at the 0.05 level between samples derived from SIMPROF test. The data has been square root transformed and resemblance made using Bray-Curtis similarity.

CHAPTER 4

Marine microbial benthic community interactions along a hypersaline microscale transect

Summary

We assessed the microscale presence and variation of phototrophic bacterial and eukaryotic organisms along a 1m horizontal transect from Salt Creek in the north lagoon of the Coorong, South Australia. This builds upon previous horizontal microscale studies, which have examined biomass micovariations of phytoplankton within coastal waters. Total chlorophyll concentration varied between $26.3 \pm 0.79\text{gm}^{-2}$ and $54.2 \pm 5.24\text{gm}^{-2}$ over a 1 m^2 quadrat. Cyanobacteria were the most abundant bacteria, contributing between 50% and 58% of total autotrophic abundance. The remaining bacteria, contributing 31% and 44% relative abundance, included Chloroflexi and Chlorobi representatives. The dominant eukaryotes were diatoms, contributing up to 11% of the total abundance. Using network analysis, we show that diatoms form vital links in the microbial network, where the anaerobic bacteria are negatively correlated with other groups of photosynthetic eukaryotes such as green algae, euglenids, dinoflagellates and cryptophytes. The revealed interactions may be explained by environmental processes and species-specific interactions between the various nodes within the community network. This study adds to current understanding of taxonomic composition at the microscale by highlighting the key role of a minor member, in this case diatoms, of a marine benthic microbial community and the sometimes inverse relationship between abundance and functionality.

Introduction

Photosynthetic microbes, including eukaryotes and cyanobacteria, form the base of aquatic food webs, being the primary source of organic matter for the growth and metabolic demands of all higher organisms (Halsey and Jones 2015). It is the cyanobacteria that allowed for the oxygenation of the oceans and atmosphere on earth 2.45 billion years ago (Holland 2006). It is predicted that photosynthetic microorganisms contribute approximately 48% to global primary production (Carr *et al.* 2006). Frequent, widespread measurement of primary production is difficult and so chlorophyll is often used as a proxy of phytoplankton biomass, assuming also a direct correlation between biomass and productivity (Spilmont *et al.* 2011, Hill *et al.* 2013).

The measurement of chlorophyll is commonly used as a predictor of primary production and algal biomass, particularly in the ocean over scales greater than 1km (Hill *et al.* 2013, van de Poll *et al.* 2013). Chlorophyll *a*, in particular, provides a good predictor of biomass because it is present in most photosynthetic organisms including cyanobacteria, green and red algae (Cloern *et al.* 2014), although other pigments are also present and used, such as chlorophyll *c* (Donald *et al.* 2013).

The most well-known contributors to aquatic chlorophyll are the phytoplankton, also known as microalgae and microeukaryotes. In particular, variations of abundance in groups such as the diatoms, from the phylum Bacillariophyceae, reflect the local environmental variation at the metre and kilometre scales (Donald *et al.* 2013, Thompson *et al.* 2015). Due to the prominent differences of frustule features between species, such as pores and ridges, and species-specific habitat adaptations, diatom population structures are widely used as indicators of water quality and ecosystem health (Finkel *et al.* 2005, Kireta *et al.* 2012).

To gain a further understanding of the interactions within these microbial communities, genomic sequencing has become a very useful tool by which to identify the organisms

present. Recent advances in the accuracy of sequencing technologies to identify microbial communities on varying temporal and spatial scales has resulted in large volumes of data (Fuhrman 2009, Xia *et al.* 2011) and has presented obstacles in our ability to analyse communities (Faust and Raes 2012). Interaction networks provide one solution for the analysis of these vast datasets, where full data series can be used to describe the interaction, or lack of, between microbes (Faust and Raes 2012). These will also help identify significant components of microbial communities within these tight networks which may have been overlooked in the past and respond rapidly to changes within the food web (Simon *et al.* 2003, Xia *et al.* 2011).

Here, we first assess the horizontal microscale variation of the total chlorophyll concentration using spatial autocorrelation, using Moran's *I* and Geary's *C* statistic. Moran's *I* is a method for quantifying spatial autocorrelation which can be applied in multi-dimensions and multidirections, i.e. horizontal, vertical and diagonal (Sokal 1978, Moran 1950). It is a global test which seeks to determine whether a data set has a random or non-random distribution whereas Geary's *C* is a local test which is used to determine the significance of clustering patterns (Sokal 1978). Additionally, we demonstrate the microscale variability of the concentration of total chlorophyll over 1m^2 and over a transect across the 30 cm row, and identify the photosynthetic eukaryotes and bacteria present. Using interaction network analysis, we show that diatoms provide an important connection between the heterotrophic bacteria and the other photosynthetic microeukaryotes.

Results & Discussion

Chlorophyll concentration is widely used as an estimation of community biomass (Kuwahara and Leong 2015, McInnes *et al.* 2015, Pinckney *et al.* 2015) and few studies have assessed microscale heterogeneity of chlorophyll in the microphytobenthos (Seuront and Spilmont 2002, Spilmont *et al.* 2011). Within a 1m² area, divided in 10cm sections (Figures S1, S2), the concentration of total chlorophyll varied between $26.3 \pm 0.8 \text{ gm}^{-2}$ and $48.4 \pm 5.2 \text{ gm}^{-2}$ (Figure 1). Moran's *I* statistic for total chlorophyll was 0.08 and as the *z*-value for the test was greater than 1.96, where $z = 6.4$, confirming that the result is statistically significant ($p = 0.0001$). This indicates that the horizontal microscale variation of total chlorophyll is spatially independent and suggests clustering of extreme values (Sokal 1978, Moran 1950, Dann *et al.* 2014, Moustakas 2014). Geary's *C* statistic is additionally used in conjunction with the Moran's *I* to determine the significance of extreme local patterns (Sokal 1978, Dann *et al.* 2014). For total chlorophyll, Geary's *C* results confirm that spatial autocorrelation is positive and significant (Geary's *C* = 0.85, $p = 0.0001$), thus suggesting significant clustering within the sample area. However, this merely shows that there is variability of total chlorophyll within the sample area, something that already has been shown at the micro- (Spilmont *et al.* 2011) and macro- scales (Anfuso *et al.* 2013). However, this does not give any indication of composition or diversity of the community, which may be impacted by species interactions.

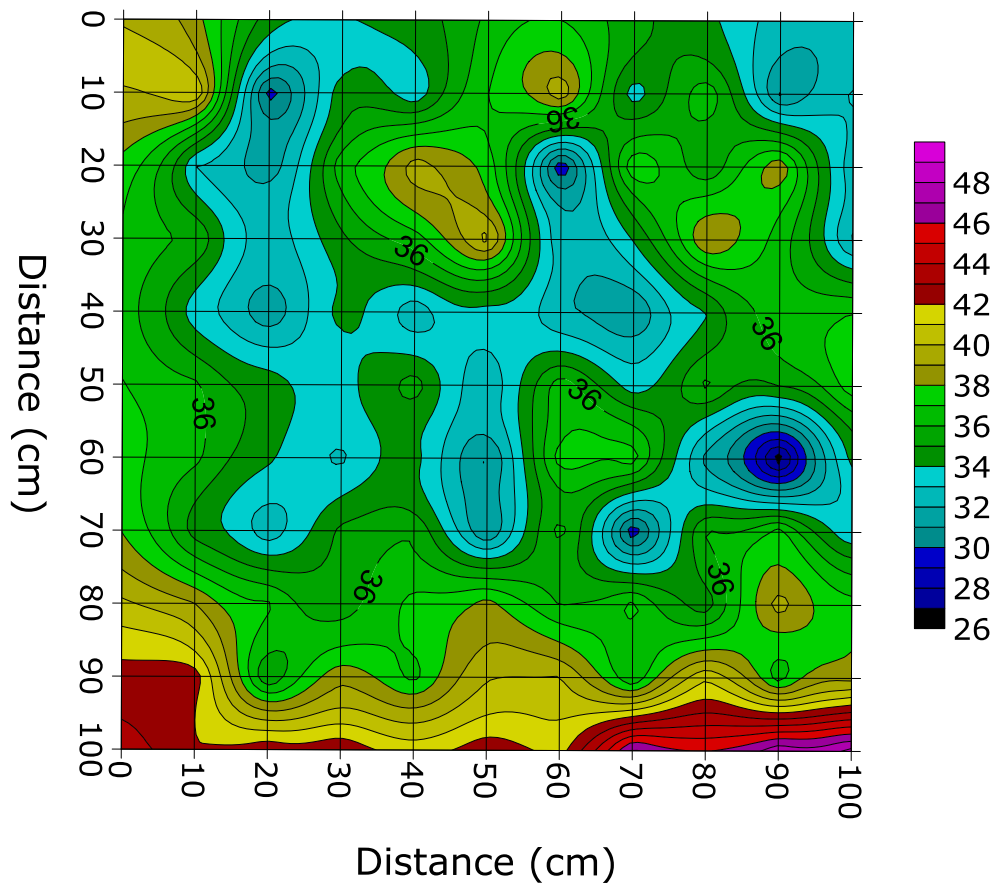


Figure 1. Concentration of Total Chlorophyll in gm^{-3} over a 1m^2 area, where the top 0.5cm of sediment were taken within 10cm sections for analysis. Using the methods and quadratic equations outlined in Ritchie (2008, 2006) for chlorophyll extraction, 5 mL 100% ethanol was added to 1 g of sediment and the sample was placed on a vortex for 30 seconds. Pigments were then extracted in the dark for 10 minutes and centrifuged for a further 2 minutes before transferring the resulting supernatant to a cuvette to measure the absorbance of the solution using spectrophotometric analysis (LKB Biochrom 4050 Ultrospec II UV/Vis). Measurements were taken at 632 nm, 649 nm, 665 nm and 696 nm. For statistical analysis, spatial autocorrelation (Moran's I and Geary's C) was used to determine randomness, clustering or dispersal within the area in multi-directions (CrimeStat 3.3, courtesy of Ned, Levine Software; Dann *et al.* 2014, Waters *et al.* 2003).

Previous studies have characterised and identified microscale variations of the microbial community in the water column for chlorophyll *a* (Waters *et al.* 2003), viruses (Seymour *et al.* 2006) and viruses and bacteria (Dann *et al.* 2014). As for the eukaryotic microbes, previous studies have only shown heterogeneity of chlorophyll *a* distributions at the microscale, without linking this to the identification of the organisms present and contributing to the community biomass (Seuront and Spilmont 2002, Spilmont *et al.* 2011). Metagenomic analysis across the 30cm row of the quadrat (Figure S2, see Table S3 for sequence summary data) revealed 9 classes of prokaryotes capable of oxygenic photosynthesis present along the microscale transect, which were affiliated with the phyla Chlorobi, Chloroflexi and Cyanobacteria. In total, bacteria accounted for at least 80% of the total abundance of phototrophic organisms at all ten distances (Table S4). The most abundant of these were the Cyanobacteria, where there was one order of magnitude difference between the unclassified Cyanobacteria and classes of Chlorobia and Chloroflexi along the transect (Figure 2, Table S4). Eukaryotic microalgae contributed up to 20% of the total organisms identified (Table S5). The two most abundant phyla were the Chlorophyta (green algae) and Bacillariophyta (diatoms). The diatoms, with 4 classes identified, showed the greatest relative abundance, up to 2% of the total population, of microalgae across the transect (Table S5).

Rank abundance plots with trendlines of best fit were used to investigate the community distributions within prokaryotic and eukaryotic groups. The abundance distributions of diatoms and bacteria followed a power law distribution ($R^2 = 0.97$), while all other microalgae displayed an exponential distribution ($R^2 = 0.99$, Figure 2a). A power law fit is indicative of a highly ordered community (Dann *et al.* 2014). Further comparisons revealed exponential fits between bacteria and green algae ($R^2 = 0.96$, Figure 2b), diatoms and green algae ($R^2 = 0.97$, Figure 2c), diatoms and dinoflagellates ($R^2 = 0.90$, Figure 2d), and, green algae and ciliates ($R^2 = 0.97$, Figure 2e). In rank abundance plots, communities that display exponential decay

are considered randomly distributed (Sæther et. al. 2013). Our results indicate diatoms and bacteria heavily influence the structure of this particular community. Supporting, previous studies showing that eukaryotic microalgal community composition is dependent on cyanobacteria (Grossart *et al.* 2005). Furthermore, the interactions between bacteria and a number of diatoms species such as, *Pseudo-nitzschia sp.*, *Stephanodiscus minutulus*, *Thalassiosira rotula*, *Skeletonema costatum*, show that there is a positive relationship between the diatom and the surrounding bacteria. These studies showed that the presence of species-specific bacterial populations surrounding the diatoms allowed for increased productivity and photosynthesis by the diatom species. (Grossart *et al.* 2005, Eigemann *et al.* 2013, Sison-Mangus *et al.* 2014).

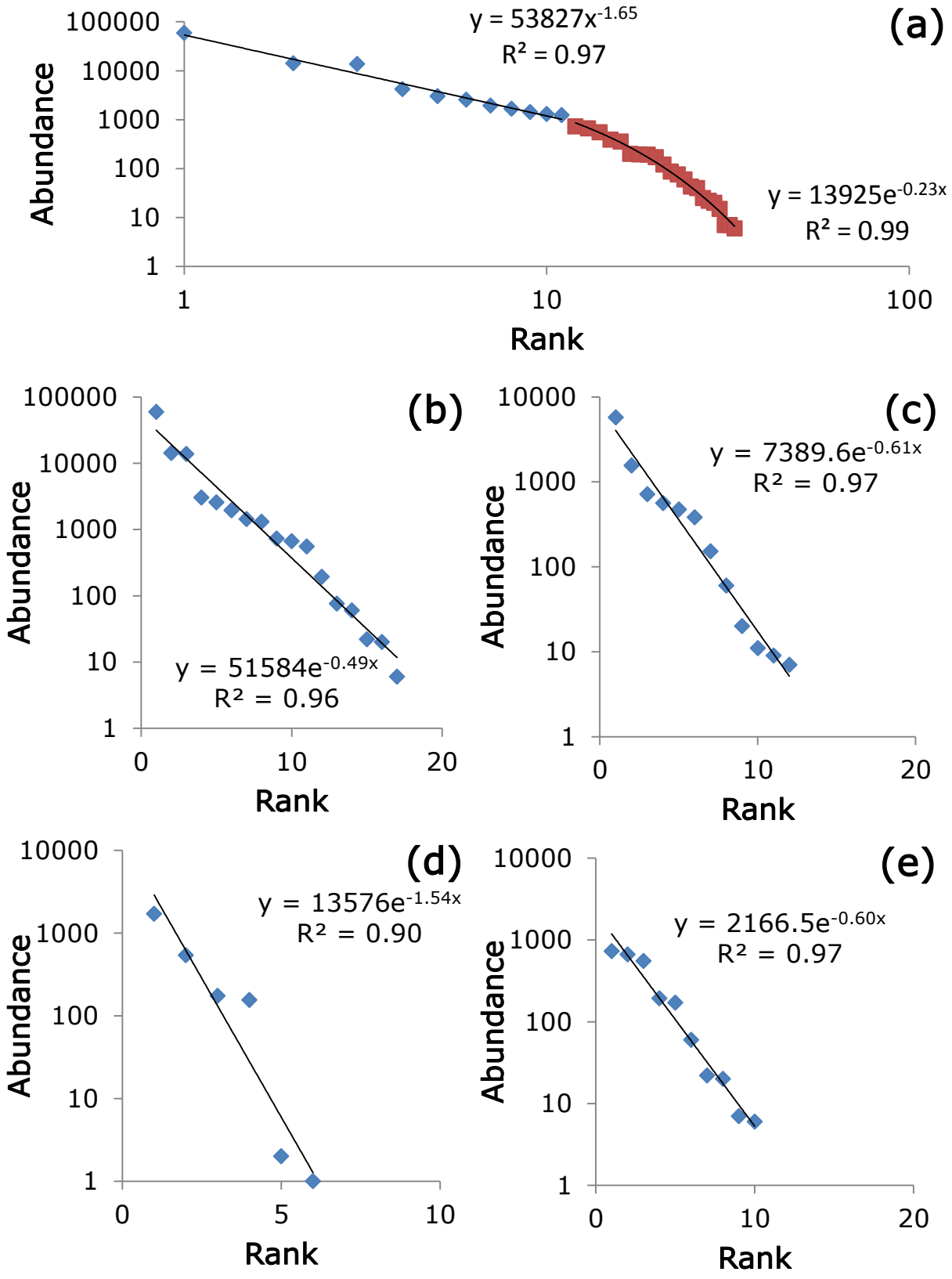


Figure 2. Log Rank-Abundance graphs for selected samples determined as the best representation of the relationships along the 1m transect. (a) Diatoms and bacteria (power

curve) in addition to all other eukaryotes (exponential curve) at 10cm. (b) Bacteria and green algae (exponential curve) at 10cm. (c) Diatoms and green algae (exponential curve) at 40cm. (d) Diatoms and dinoflagellates (exponential curve) at 50cm. (e) Green algae and ciliates (exponential curve) at 10cm. Rank abundance data was obtained from metagenomic sequences along the 30cm row in the quadrat, with a total of 10 samples sequenced. Sediment was extracted using a PowerSoil DNA Isolation Kit (MO BIO Laboratories, Inc.) for sequencing on the MiSeq platform (Illumina, Inc.; Flinders Genomic Facility, South Australia). PrinSeq (v0.20.4) was used in order to filter sequence copies, short or long sequences, low quality and low complexity sequences (Schmieder and Edwards, 2011a). DeconSeq was then used to remove human sequences that may be contaminating the sample (Schmieder and Edwards 2011b). The file was uploaded to MG-RAST, joining paired ends of the forward and reverse sequence, further filtered for low quality reads so that sequences with phred scores lower than 20 were removed (Cox *et al.* 2010, Wilke *et al.* 2015). The M5NR database was used to assign taxonomy to the sequences. The MG-RAST default annotation parameters such as maximum E-value $<1 \times 10^{-5}$, minimum length of alignment of 15 base pairs, and minimum sequence identity of 60%, were used to identify the best database matches (Tables S3, S4).

Positive interactions between bacteria and phytoplankton in microbial time series have confirmed that seasonal changes in phytoplankton assemblages influence the bacterial community due to increased growth and primary production of microalgae (Paver *et al.* 2013, Needham and Fuhrman 2016). Here, network analysis was used to quantitatively describe the interactions between the taxonomic groups identified within the samples, where only significant results from the correlation matrix are depicted in the network (Faust *et al.* 2015). The resulting network suggests the presence of two taxonomic clusters connected by three major nodes, represented by the diatoms classes, Mediophyceae, Coscinodiscophyceae and Bacillariophyceae (Figure 3). The edges of the network are indicative of the correlation between the nodes where green edges represent positive association and red edges a negative relationship.

Here, it is shown that the bacteria and the unclassified eukaryotes are grouped together, suggesting a positive association between nodes, including bacterial classes Dehalococcoidetes, Gleobacteria and Chlorobia (Figure 3). This is, perhaps, not a surprising result considering that the classes of bacteria observed are highly abundant in aquatic mats and sediments (Lau *et al.* 2009, Faust *et al.* 2015). These positive associations are likely explained by the fact that a majority of the bacterial classes represented in the network share a similar environmental niche (Bryant *et al.* 2007, Liu *et al.* 2011, 2014).

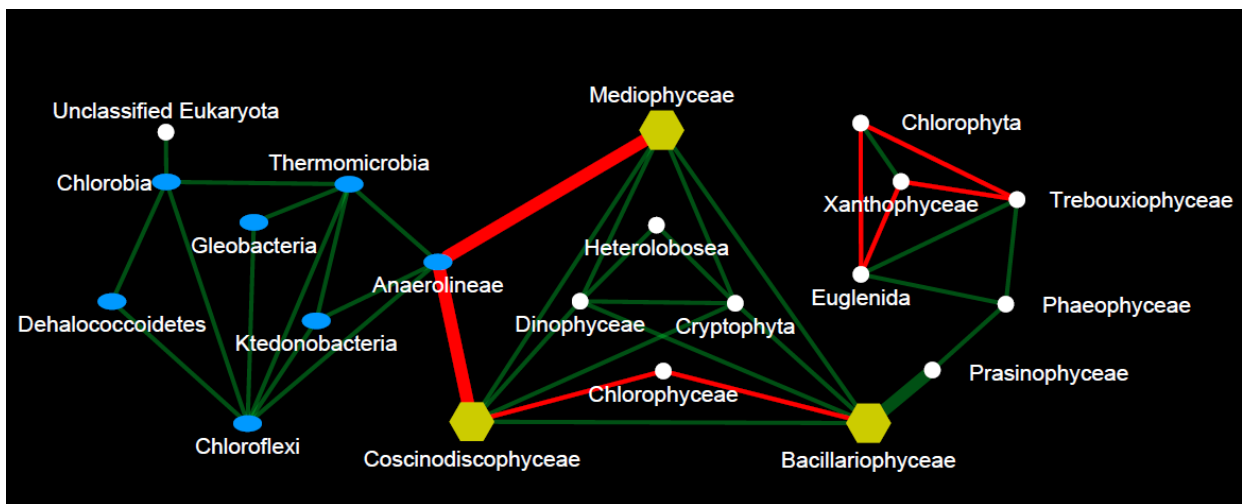


Figure 3. Correlation network depicting only significant results using data obtained from metagenomic analysis of 10 samples along the 1m transect sampled from the 30cm row. The microbial network was constructed using the CoNet application in Cytoscape 3.2.1. with methods as outlined in Faust and Raes (2012). Edge creation was via Bray-Curtis dissimilarity, Mutual Information, Kullback Liebler dissimilarity, Pearson and Spearman correlation; edge selection was by p-value and q-value thresholds (<0.01). Node appearance is given by taxon, with blue ovals for bacteria, white circles representing eukaryotes, and yellow hexagons representing diatoms. Green edges denote a positive correlation; red edges a negative correlation. Wider edge width is assigned to correlations linking different taxonomic domains.

From the results presented, the diatom classes Mediophyceae and Coscinodiscophyceae connect to the cluster of bacteria, while there is a negative correlation between these classes and the bacteria Anaerolineae. Previous research has revealed the complex species-specific interactions and host specificity between diatoms and bacteria (Grossart *et al.* 2005, Amin *et al.* 2012, Eigemann *et al.* 2013, Sison-Mangus *et al.* 2014). In particular, Grossart *et al.* (2005) showed a link between abundance and composition of bacteria and the species composition of the algal community. For example Bacteroidetes and α -Proteobacteria have been found to thrive with the diatom *Thalassiosira rotula* (Grossart *et al.* 2005). In another study by Sison-Mangus *et al.* (2014) experiments with 3 strains of the diatom *Pseudo-nitzschia* with varying degrees of toxicity demonstrated phylogenetically distinct bacterial associations where bacterial diversity was lower in the more toxic strain of *Pseudo-nitzschia*. Furthermore, species-specific interactions may also account for, in this study, the small cluster of negative correlations observed between eukaryotic flagellates, Euglenida, yellow-green algae, Xanthophyceae, and Chlorophyta (Figure 3). One possible explanation for this is that the flagellated Euglenids are predated particularly on the green and yellow-green algal species present within the community as in Ma *et al.* 2016.

In conclusion, from the present study, while rank abundance graphs suggested a link between diatoms and bacteria, it was the interactions network which highlighted the importance of diatoms and provided specific connections among taxonomic groups. The strength of the interactions between the diatoms and other microbial taxa observed along the transect highlights ecological importance of diatoms within aquatic food webs. Historically, studies have shown that diatoms provide nutrients to saprophytic bacteria, in addition to species-specific predator-prey or mutualistic interactions (Sison-Mangus *et al.* 2014). The results presented add further to our understanding of taxonomic composition at the microscale and

highlight the importance of investigating the interactions between the prokaryotic and eukaryotic portion of the microbial community.

Chapter 4
Supplementary Data

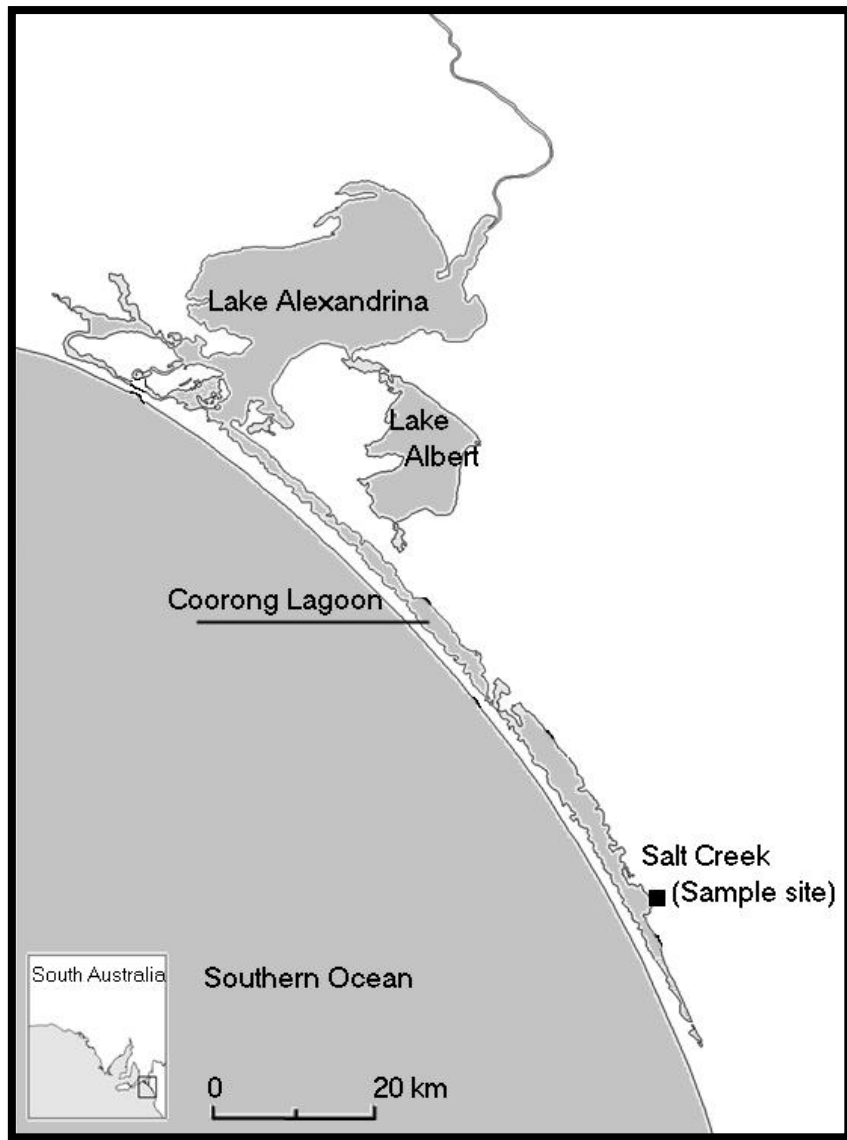


Figure S1. Map of sampling location, Salt Creek, South Australia (Coorong National Park, S36° 09.936', E139° 39.104').

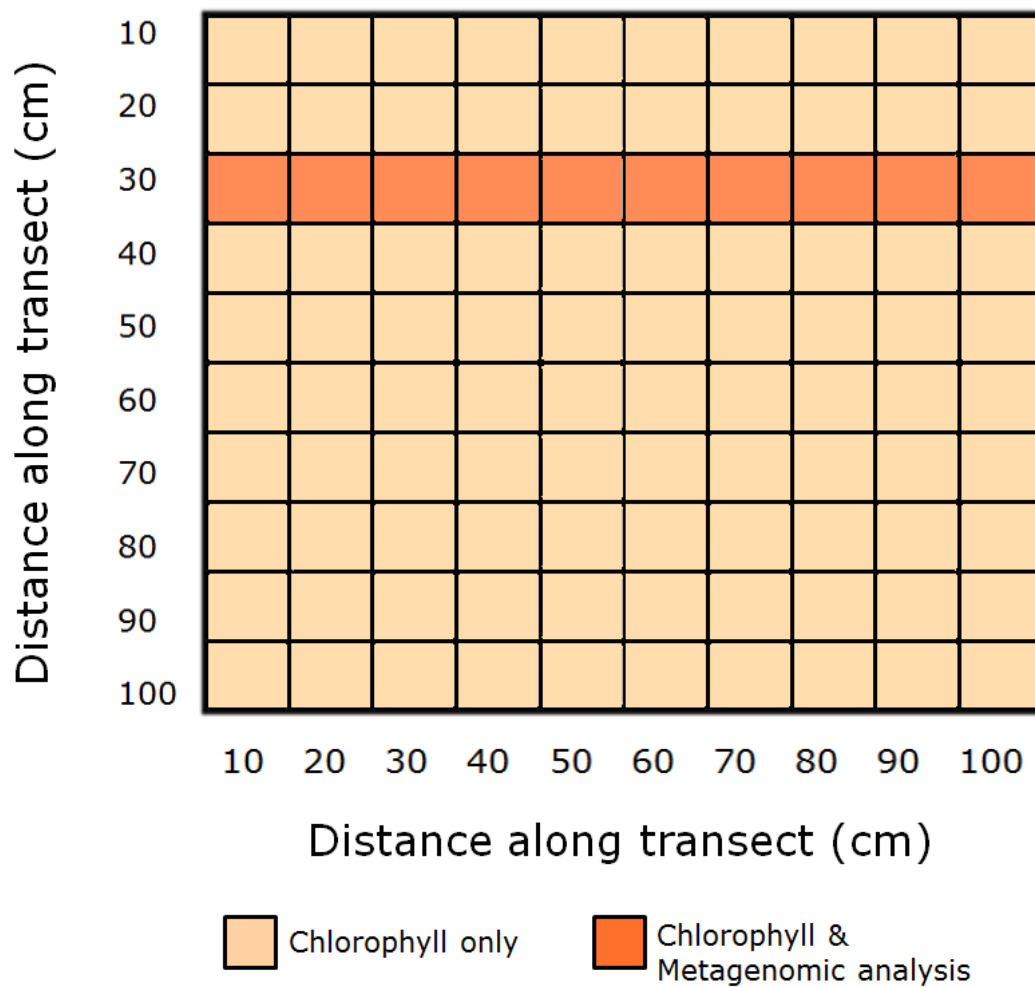


Figure S2. Diagram depicting the sampling strategy from a 1m² where the top 0.5cm of sediment was scraped off the surface in 10cm sections. Water depth was approximately 5cm and the sand formed a flat, even surface. The 30cm row was used for metagenomic analysis, as signalled by the dark orange in the figure. Sediment was frozen and stored at - 4°C prior to analysis.

Table S3. Summary of sequences and MG-RAST ID

Sequence Summary							MG-RAST information	
Distance along transect (cm)	Initial # bp	Initial # sequences	# Duplicate sequences	Post-QC # bp	Post-QC # sequences	Mean sequence length (bp)	Sample Name	ID #
10	651, 203, 148	2, 739, 498	21, 764	496, 680, 165	2, 520, 328	197 ± 93	Microscale_Hypersaline_C1	4665059.3
20	429, 245, 436	2, 091, 288	15, 608	394, 471, 499	2, 011, 829	196 ± 80	Microscale_Hypersaline_C2	4676357.3
30	527, 119, 595	2, 761, 131	22, 154	484, 444, 443	2, 598, 936	186 ± 81	Microscale_Hypersaline_C3	4676359.3
40	475, 727, 520	2, 297, 441	18, 696	433, 965, 043	2, 187, 535	198 ± 80	Microscale_Hypersaline_C4	4676360.3
50	416, 412, 435	1, 536, 475	9, 871	378, 204, 925	1, 520, 553	248 ± 57	Microscale_Hypersaline_C5	4676363.3
60	583, 210, 462	1, 955, 017	15, 246	464, 581, 765	1, 916, 695	242 ± 89	Microscale_Hypersaline_C6	4683986.3
70	769, 907, 810	3, 236, 756	30, 290	616, 408, 390	3, 061, 808	201 ± 93	Microscale_Hypersaline_C7	4684112.3
80	556, 669, 507	1, 953, 355	14, 242	443, 558, 518	1, 908, 600	232 ± 86	Microscale_Hypersaline_C8	4684113.3
90	594, 203, 990	2, 118, 938	16, 626	472, 317, 894	2, 067, 893	228 ± 86	Microscale_Hypersaline_C9	4684114.3
100	467, 453, 604	1, 637, 700	12, 810	353, 803, 006	1, 572, 542	224 ± 93	Microscale_Hypersaline_C10	4684116.3

Table S4. Bacteria table of relative abundances expressed as a percentage.

Class	Distance along transect (cm)									
	10	20	30	40	50	60	70	80	90	100
Anaerolineae	12.66	12.07	12.83	12.71	12.70	16.15	15.82	15.37	15.23	15.60
Dehalococcoidetes	1.79	1.62	1.65	1.96	2.23	2.63	2.44	2.78	2.76	2.84
Ktedonobacteria	13.09	12.31	12.58	13.35	13.83	17.80	16.67	17.24	17.44	17.96
Unclassified Chloroflexi	1.20	1.08	1.09	1.11	1.18	1.47	1.44	1.33	1.35	1.44
Chlorobia	1.32	1.27	1.26	1.35	1.43	1.63	1.64	1.69	1.71	1.79
Chloroflexi	2.79	2.55	2.54	2.91	2.92	3.72	3.75	3.80	3.89	3.86
Thermomicrobia	0.07	0.08	0.06	0.08	0.11	0.10	0.09	0.10	0.09	0.10
Gloeobacteria	2.36	2.23	2.23	2.35	2.35	2.87	2.65	2.81	2.85	2.75
Unclassified Cyanobacteria	54.58	56.04	54.23	51.43	55.95	47.56	48.01	48.41	47.83	46.76

Table S5. Eukaryote table of relative abundances expressed as a percentage.

Class	Distance along transect (cm)									
	10	20	30	40	50	60	70	80	90	100
Bacillariophyceae	3.871	4.574	4.945	5.827	1.947	0.756	1.458	0.820	0.801	1.225
Coccinodiscophyceae	1.142	1.263	1.418	1.579	0.615	0.377	0.603	0.366	0.355	0.442
Fragilariophyceae	0.006	0.006	0.006	0.009	0.001	0.004	0.007	0.001	0.002	0.000
Mediophyceae	0.359	0.346	0.386	0.480	0.199	0.135	0.205	0.139	0.109	0.167
Unclassified Bacillariophyta	0.000	0.000	0.000	0.000	0.002	0.000	0.000	0.000	0.001	0.000
Chlorophyceae	0.611	0.581	0.595	0.570	0.680	0.743	0.746	0.770	0.879	0.712
Mamiellophyceae	0.670	0.663	0.682	0.726	0.689	0.643	0.719	0.712	0.782	0.635
Prasinophyceae	0.020	0.009	0.015	0.020	0.016	0.008	0.001	0.004	0.005	0.008
Trebouxiophyceae	0.508	0.413	0.416	0.388	0.685	0.578	0.015	0.014	0.012	0.549
Ulvophyceae	0.055	0.052	0.050	0.061	0.056	0.077	0.587	0.642	0.862	0.084
Unclassified Chlorophyta	0.006	0.000	0.000	0.007	0.000	0.003	0.088	0.075	0.076	0.003
Unclassified Euglenida	0.023	0.026	0.023	0.024	0.033	0.034	0.003	0.001	0.002	0.028
Unclassified Phaeophyceae	0.179	0.186	0.217	0.205	0.156	0.187	0.021	0.044	0.050	0.213
Unclassified Xanthophyceae	0.000	0.000	0.000	0.009	0.000	0.000	0.209	0.194	0.184	0.003
Armophorea	0.000	0.000	0.000	0.000	0.000	0.000	0.000	0.000	0.001	0.003
Bangiophyceae	0.177	0.181	0.176	0.154	0.140	0.181	0.183	0.173	0.178	0.175
Chrysophyceae	0.000	0.000	0.000	0.000	0.000	0.000	0.003	0.003	0.000	0.000
Cryptophyta	0.037	0.038	0.036	0.030	0.021	0.003	0.032	0.004	0.021	0.023
Dinophyceae	0.328	0.339	0.407	0.414	0.177	0.011	0.214	0.025	0.136	0.175
Florideophyceae	0.040	0.028	0.036	0.031	0.040	0.137	0.041	0.133	0.034	0.036
Glaucocystophyceae	0.018	0.032	0.023	0.011	0.021	0.030	0.017	0.032	0.016	0.013
Heterolobosea	0.111	0.114	0.112	0.110	0.108	0.012	0.123	0.001	0.120	0.144
Heterotrichea	0.000	0.000	0.000	0.000	0.000	0.001	0.000	0.013	0.000	0.002
Ichthyospora	0.080	0.093	0.092	0.088	0.081	0.102	0.091	0.114	0.117	0.128

Karyorelictea	0.000	0.000	0.000	0.000	0.000	0.000	0.000	0.000	0.001	0.000
Litostomatea	0.000	0.000	0.000	0.000	0.000	0.000	0.002	0.108	0.000	0.002
Oligohymenophorea	0.157	0.160	0.162	0.242	0.119	0.148	0.162	0.001	0.134	0.172
Pelagophyceae	0.184	0.187	0.178	0.191	0.145	0.170	0.152	0.147	0.169	0.182
Raphidophyceae	0.014	0.019	0.019	0.018	0.013	0.011	0.011	0.204	0.007	0.013
Spirotrichea	0.006	0.006	0.010	0.013	0.000	0.011	0.005	0.014	0.008	0.003
Synurophyceae	0.000	0.000	0.000	0.000	0.000	0.000	0.000	0.000	0.001	0.002
Rhodellophyceae	0.000	0.000	0.000	0.000	0.000	0.000	0.003	0.005	0.000	0.003
Unclassified Eukaryota	1.540	1.430	1.525	1.540	1.364	1.711	1.798	1.699	1.795	1.756

CHAPTER 5

Microscale Variation of Diatom Frustule Length in the Microphytobenthos

Abstract

Spatial microscale heterogeneity in aquatic environments occurs over millimetres to centimetres. This is represented by patchiness in microbial productivity, abundance and diversity. However, previous studies that aimed to characterise microscale heterogeneity have focused on the abundance and composition of bacterial and viral populations, in addition to assessing chlorophyll as an indicator of the algal biomass. Cell size is usually not a consideration. However, diatom size contains not only biomass information but also corresponds to time since last sexual reproduction. Here, variation of diatom frustule length was examined for two diatom species, *Amphora hyalina* (Kützing) and *Cocconeis costata* (Gregory) and compared to chlorophyll concentration over 1 m² at 100 cm² increments. Frustules of *A. hyalina* ranged from 19 µm to 47 µm, and those of *C. costata* ranged between 9 µm to 29 µm over the 1 m² area, with particular lengths occurring in patches. Variation in skewness of frustule lengths shows areas that favour longer frustules lengths than shorter frustules, where skewness ranged from -2.5 to 2.1 for the two species. The frustule length variation indicates local variation in the reproduction rate. Network analysis shows that the size range of a diatom is more informative about interactions within the community than the mean size, total chlorophyll or other commonly measured parameters.

Introduction

Microbial communities vary from micrometres to kilometres, which can be attributed to environmental and biological parameters and processes (Stocker and Seymour 2012). Microscale specifically refers to processes and variation that occur over millimetres to centimetres (Seymour *et al.* 2005, Mitchell *et al.* 1989, Azam 1998). Many studies have focused on bacterial and viral community abundance, in the water column or in the sediment, as well as bulk chlorophyll (Dann *et al.* 2014, Seymour *et al.* 2007, 2006, 2005, Waters *et al.* 2003). However, there are only a handful of studies that assess the ecology of the horizontal microscale of the microphytobenthos and these only assess the presence of chl *a* (Spilmont *et al.* 2011, Seuront and Spilmont 2002, Franks and Jaffe 2008). Microphytobenthos refers to micro-organisms, in particular unicellular algae, which are present within surface sediments of aquatic environments (Kireta *et al.* 2012). On the large scale, community heterogeneity of marine planktonic communities affects the structure of the food web in terms of predator-prey interactions (Hansen *et al.* 1994), reproductive rates (Sjöqvist *et al.* 2015, Mann and Vanormelingen 2013) and physical processes such as carbon transport cycles (Finkel *et al.* 2005). Yet these studies do not take into account species diversity and abundance variation within samples, thus missing the key specific microbial interactions between species which are driving these communities. The present study focuses on the microscale variation of two diatom species, *Amphora hyalina* (Kützing) and *Cocconeis costata* (Gregory), specifically examining the frustule size.

Diatoms (Bacillariophyceae) are essential to their environments and are important globally, responsible for 40% of oceanic primary productivity (Tréguer and De La Rocha 2013). These ubiquitous unicellular photoautotrophs are characterised by a siliceous shell-like exoskeleton called a frustule (Armbrust *et al.* 2009). Additionally, the frustule surfaces have fine architectural features, such as spines, channels and pores (Jones 2007), which are species

specific (Mitchell *et al.* 2013). Diatom size and population structures are widely used as indicators of water quality due to species-specific habitat preferences (Kireta *et al.* 2012, Finkel *et al.* 2005). However, descriptions of their interactions with other components in any ecosystem has had limited to no success, despite extensive effort (Fuhrman 2009, Steele *et al.* 2011, Faust and Raes 2012). This has been particularly difficult in the search for key species. Methods for deciphering the role of a single taxa or group amongst a microbial community remains unclear and even how to define microbial niches and the extent to which a taxonomic group remains in that niche is unclear (Cibils *et al.* 2015, Zimmerman and Cardinale 2014). Classical indicators of biomass and numerical abundance alone are inadequate and metagenomics only shows metabolic potential (Bates *et al.* 2013, Raven 2012).

The frustules are unique to the diatoms and the group give a characteristic appearance and shape to the cells. Frustules are made of two halves, the epivalve, which originates from the parent cell, and the hypovalve, which is formed after cell division (Kennington 2002). As a result of the constraints on cell size imposed by the silica frustules, diatoms undergo a series of divisions followed by sexual reproduction (D'Alelio *et al.* 2010). Starting at the maximum size, the diatom will asexually divide until reaching a critical minimum size where the cell then undergoes sexual reproduction. This life cycle of diatoms, where there are progressive decreases in size, occurs over years (D'Alelio *et al.* 2010) and therefore there is the potential to track diatom populations based on these size variations (Montresor and Lewis 2006). One method by which this may be achieved is by using interaction networks.

Recently, methods have been developed to make time series useful for understanding interactions and making predictions of species to ecosystem responses by using interaction networks (Steele *et al.* 2009, Faust and Raes 2012). The basic concept of an interaction network is that using large amounts of data a description is obtained of which microbes do and do not maintain functional relationships (Faust and Raes 2012). This is appealing because

it offers the opportunity to find interactions and identify key species and parameters. It is also a logical path to represent communities as mathematical networks because significant components of microbial communities form tightly connected natural networks, which respond rapidly to environmental changes (Simon *et al.* 2003, Brad *et al.* 2008). This is particularly true for benthic communities. Here we have applied network interaction analysis to 2 benthic diatom species as a spatial analysis to better understand which parameters are the best indicators of variation of diatom length within the populations.

The aims of this paper are to (i) determine the variation of pigments chl *a* and *c* over microscale distances, (ii) determine the microscale distributions of frustule lengths for *A. hyalina* and *C. costata*, and, (iii) determine the extent of any correlation between the distributions of chl biomass and frustule length. Therefore, the hypotheses for this study are that, (i) microscale distribution of chlorophyll concentrations and frustule lengths are homogenous, and, (ii) there is no positive correlation between high concentration chl and the maximum frustule length.

Methods

Study Site

The selected site for this study was Salt Creek, South Australia, located in the south lagoon within the Coorong National Park (S36° 09.936', E139° 39.104'; Figure 1). Salt Creek is typical of the Coorong's shallow water, predominately sandy, high salinity environment (Wright and Wacey, 2005), where the lagoon is also protected from wind blowing directly from the Southern Ocean by the Youngusband Peninsula. Local hydrology indicates water inputs in the Coorong and nearby distal ephemeral lakes consists of rainfall and seaward

movement of groundwater from an open aquifer system (Wright and Wacey, 2005, Webster 2010).

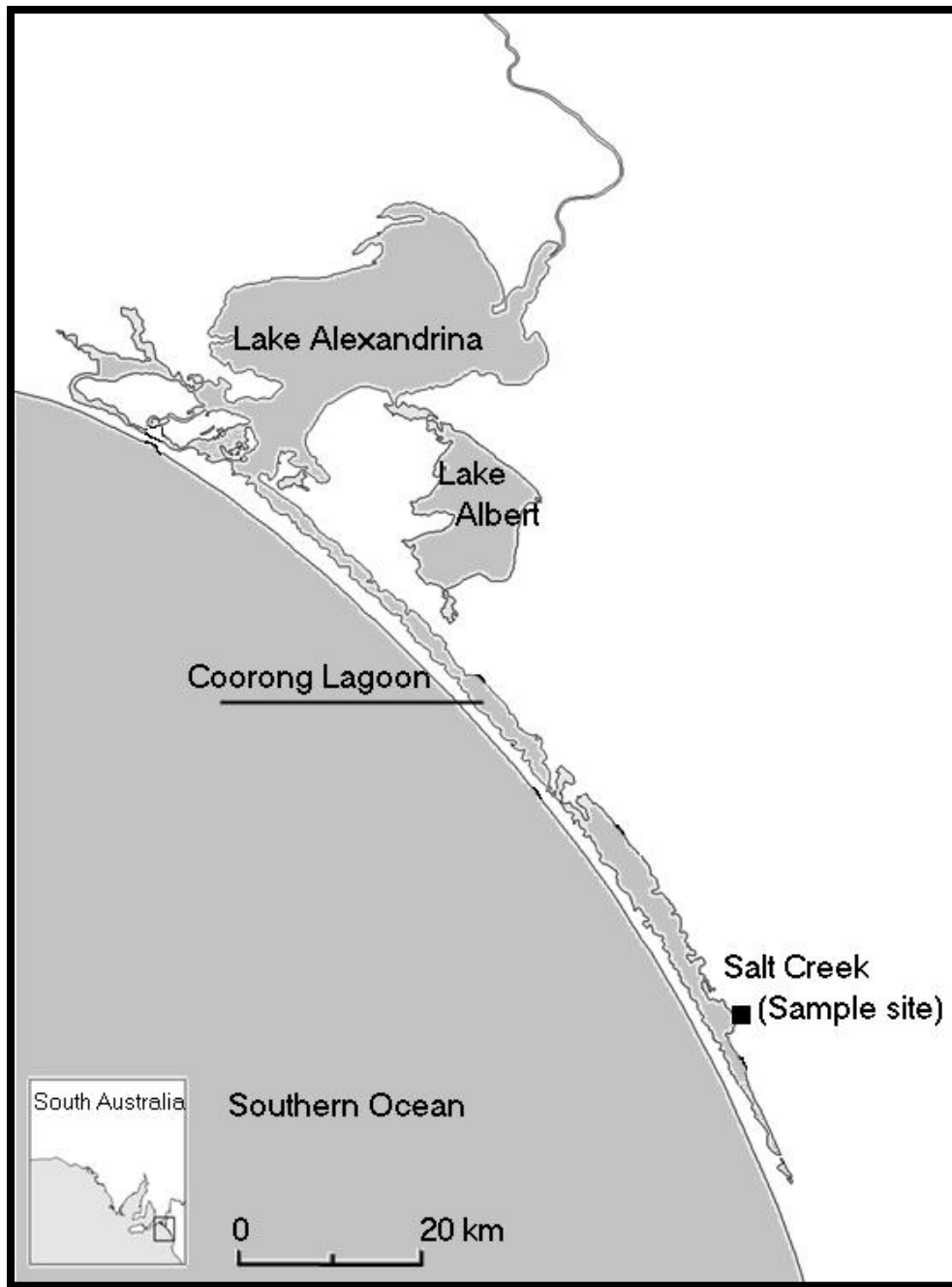


Figure 1. Map of sampling location, Salt Creek, South Australia (Coorong National Park, S36° 09.936', E139° 39.104').

Sample Collection

Sediment samples were taken from an area measuring 10, 00 cm², which was further divided into 100 squares measuring 100 cm². A quadrat was placed in an area where the sediment was made of sand and the water depth was approximately 5 cm. The top 0.5 – 1 cm of surface sediment was removed in 100 cm² sections. From the sediment sampled, 1 g sediment was frozen and kept in the dark, for chlorophyll analysis. This process was replicated three times for each of the 100 squares within the quadrat. The remaining sediment was preserved with formaldehyde, to make a final concentration of 2%, in order to measure the length of diatom frustules in the lab.

Chlorophyll Analysis

The photosynthetic pigments chlorophyll *a* and *c* (chl *a* and *c*) were assessed for each square in the sample grid, using the methods outlined in Ritchie (2008, 2006), 5 mL 100% ethanol was added to 1 g of sediment and the sample was placed on a vortex for 30 seconds. Pigments were then extracted in the dark for 10 minutes and centrifuged for a further 2 minutes before transferring the resulting supernatant to a cuvette to measure the absorbance of the solution using spectrophotometric analysis (LKB Biochrom 4050 Ultrospec II UV/Vis). Measurements were taken at 632 nm, 649 nm, 665 nm and 696 nm, seen in the equations as A_{632} , A_{649} , A_{665} and A_{696} , respectively. Using Ritchie's (2008) equations (equation 1 and equation 2), chlorophyll concentration was calculated as g m⁻³ as follows:

$$\text{Chl } a = 0.0604 \cdot A_{632} - 4.5224 \cdot A_{649} + 13.2969 \cdot A_{665} - 1.7453 \cdot A_{696} \quad (1)$$

$$\text{Chl } c = 28.4593 \cdot A_{632} - 9.9944 \cdot A_{649} + 1.9344 \cdot A_{665} - 1.8093 \cdot A_{696} \quad (2)$$

Microscopy

Amphora hyalina and *Cocconeis costata* were the two diatoms species selected for observation of frustule length over the 1 m² area, where the length of random frustules was measured for each 100 cm² section where n for *A. hyalina* was 78 and n for *C. costata* was 30. Therefore, in the 1 m² quadrat, n for *A. hyalina* was 7800 and n for *C. costata* was 3000. For *A. hyalina*, a pennate diatom, measurements were only recorded for individuals found in the valve view, this was also the case for *C. costata*, a centric diatom to maintain consistent measurement between individuals. To measure the frustule length for the two diatom species, light microscopy (Olympus BX50) with a camera (Prosilica GE1660 camera with Streampix III software) was used to visualise the diatoms and lengths were measured using Motic Images Plus 2.0 (Motic China Group Co. Ltd.).

Statistical Analysis

Descriptive Statistics

Descriptive statistics of the frustule length and chlorophyll data were obtained to initially determine the best method in which to see the spatial differences among the data (SPSS v. 20.0). Surfer 10 (Golden Software, Inc.) was used to create two dimensional contour plots of the minimum length, maximum length, skewness and kurtosis for frustule length of the 1 m² area. Contour intervals were set at 0.5 µm for maximum and minimum length, according to the resolution of the measurement. However, for skewness the contour interval was set using the coefficient of variation. In addition, contour maps were also constructed for mean chl *a* and mean chl *c*, with contour intervals were set at 0.2 g.m⁻³. Furthermore, contour maps constructed to visualise Spearman's rho correlation (SPSS v. 20) between frustule length of the two species and chl *a* and *c* concentration.

Spatial Autocorrelation, Moran's I

To complement the descriptive statistics, in particular the results from skewness and kurtosis, spatial autocorrelation was also determined. Spatial autocorrelation can be used to determine randomness, clustering and dispersal within an area in multi-directions, where the most common tests are the Moran's I and Geary's C statistics (CrimeStat 3.3, courtesy of Ned, Levine Software; Dann *et al.* 2014, Waters *et al.* 2003).

Moran's I is a method for quantifying spatial autocorrelation which can be applied in multi-dimensions and multidirections, i.e. horizontal, vertical and diagonal (Sokal 1978, Moran 1950). It is a global test which seeks to determine if a data set has a random or non-random distribution. The equation for Moran's I is:

$$I = \frac{N \sum_i \sum_j W_{ij} (X_i - \bar{X})(X_j - \bar{X})}{(\sum_i \sum_j W_{ij}) \sum_i (X_i - \bar{X})^2} \quad (3)$$

Moran's I is calculated by the cross-product of deviations from the mean within a dataset, where N is the sample number, X_i and X_j are the variable value at specific locations i and j and \bar{X} is the mean of the variable in question. Here we use the weighted form of the test to take into account spatial proximity, where W_{ij} is the weight applied to the i and j comparison. This means that sample points that were adjacent to each other were assigned a weight value of 1 and sample points that were not adjacent were assigned a weight value of 0. Moran's I ranges between +1 and -1. Significant Moran's I value, positive and negative, is suggestive of the distribution showing spatial structure, where a positive value is indicative of clustering and a negative value is indicative of dispersal. However, if Moran's I is 0, then this suggests a random distribution. Moran's I z-values values that are $> +1.96$ and < -1.96 , spatial autocorrelation is significant, at least, at the 0.05 level (Sokal 1978).

To further investigate the spatial relationship between sample values, Moran correlograms were constructed by applying the Moran's I statistic to pairs of samples and separated by a

specified lag distance. Here, the lag distance was set at 10 cm, which is the length and width of each grid section sampled. For reliable results, each lag distance requires having at least 30 pairs of sample point (Waters *et al.* 2003, Rossi *et al.* 1992). Significance of the lag distances were determined using the standard error calculated in the Moran's I analysis.

Spatial Autocorrelation, Geary's C

The Geary's C statistic is used in conjunction with the Moran's I to determine the significance of extreme local patterns. While Moran's I is a global spatial autocorrelation test, Geary's C is more sensitive to local clustering. Therefore using Geary's C we are able to identify the significance, if any, of patterns between extreme values and patterns that are not related to spatial differences, which cannot be determined using only Moran's I. Geary's C is calculated using the following equation:

$$C = \frac{(N-1) [\sum_i \sum_j W_{ij} (x_i - x_j)^2]}{2(\sum_i \sum_j W_{ij}) \sum_i (x_i - \bar{x})^2} \quad (4)$$

Geary's C is calculated by deviation in intensity of each sample value's location compared to one another and the equation uses the same terms as the Moran's I statistic. The Geary's C statistic starts from 0 and has no definitive limit; a value of 1 indicates that a parameter is spatially independent. Meanwhile, positive spatial autocorrelation is indicated by values <1 and negative when the value is >1 and furthermore, z-values which are positive are indicative of negative spatial autocorrelation and negative z-values indicate positive spatial autocorrelation (Sokal 1978).

Network Analysis:

Network interaction analysis was carried out using extended local similarity analysis (eLSA) to produce the correlation matrices. Using eLSA, it is possible to identify complex association between species, and between species and the environment (Ruan *et al.* 2006).

Cytoscape 3.2.1 was used to visualise and analyse the networks. Pearson, Spearman and local similarity correlation coefficients was used to quantify and show relative strengths of relationships.

Results

Frustule Length

The pennate diatom *A. hyalina* and the centric diatom *C. costata* exhibit distinct sizes over microscale distances. This will be presented here by observing variation in the minimum and maximum frustule length to show the range of variation in lengths within the 1 m² quadrat. Firstly, the minimum length of *A. hyalina* frustules varied between 10 and 28 µm was observed in 33 frustules within the sampled area (Figures 2a, c). However, there were a further 8 outliers of smaller frustules of approximately 7 µm which occurred at x, y coordinates (50, 60), (50, 70), (60, 40) and (80, 90) (Figure 2a). *C. costata* was a much smaller species, where the minimum length ranged throughout the grid area between 8 and 13 µm, observed in a total of 689 of 3000 frustules (Figures 3a, c). Additionally, no outliers were observed for *C. costata* (Figure 3c). Observations of the maximum frustule length of these species further reflect the difference in size between *A. hyalina* and *C. costata*. Maximum length of *A. hyalina* frustules were between 40 and 47 µm for 713 of the sampled frustules (Figures 2b, c). Whereas, *C. costata* length has a much smaller maximum range, between 15 and 28 µm for 809 frustules within the sampled area (Figures 3b, c).

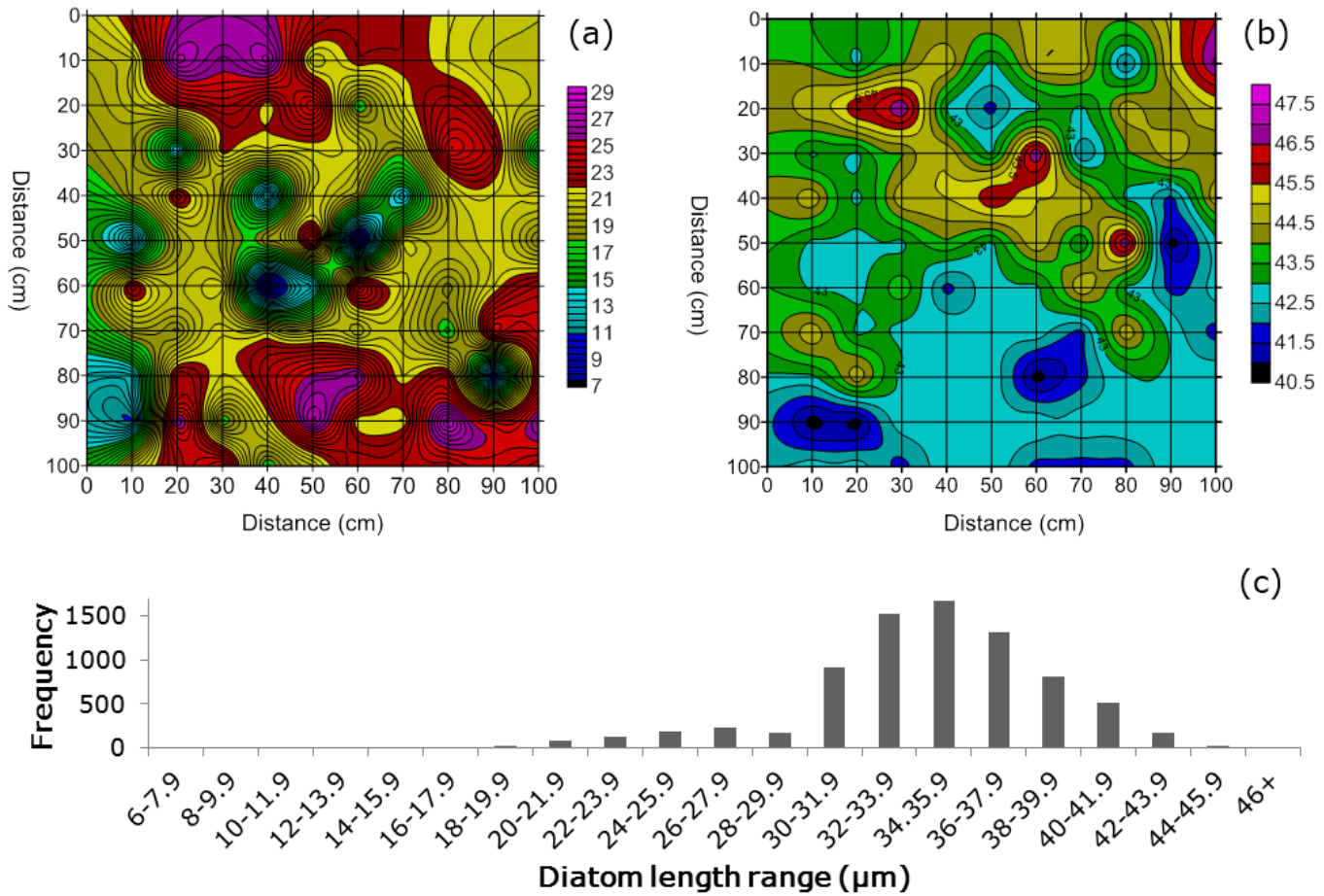


Figure 2. Contour maps of frustule length (μm) for *A. hyalina*, (a) minimum length (μm) with contour interval set at 0.5 μm , (b) maximum length (μm), (c) frequency distribution of frustules lengths over 1 m² quadrat, with contour interval set at 0.5 μm and $n = 7800$.

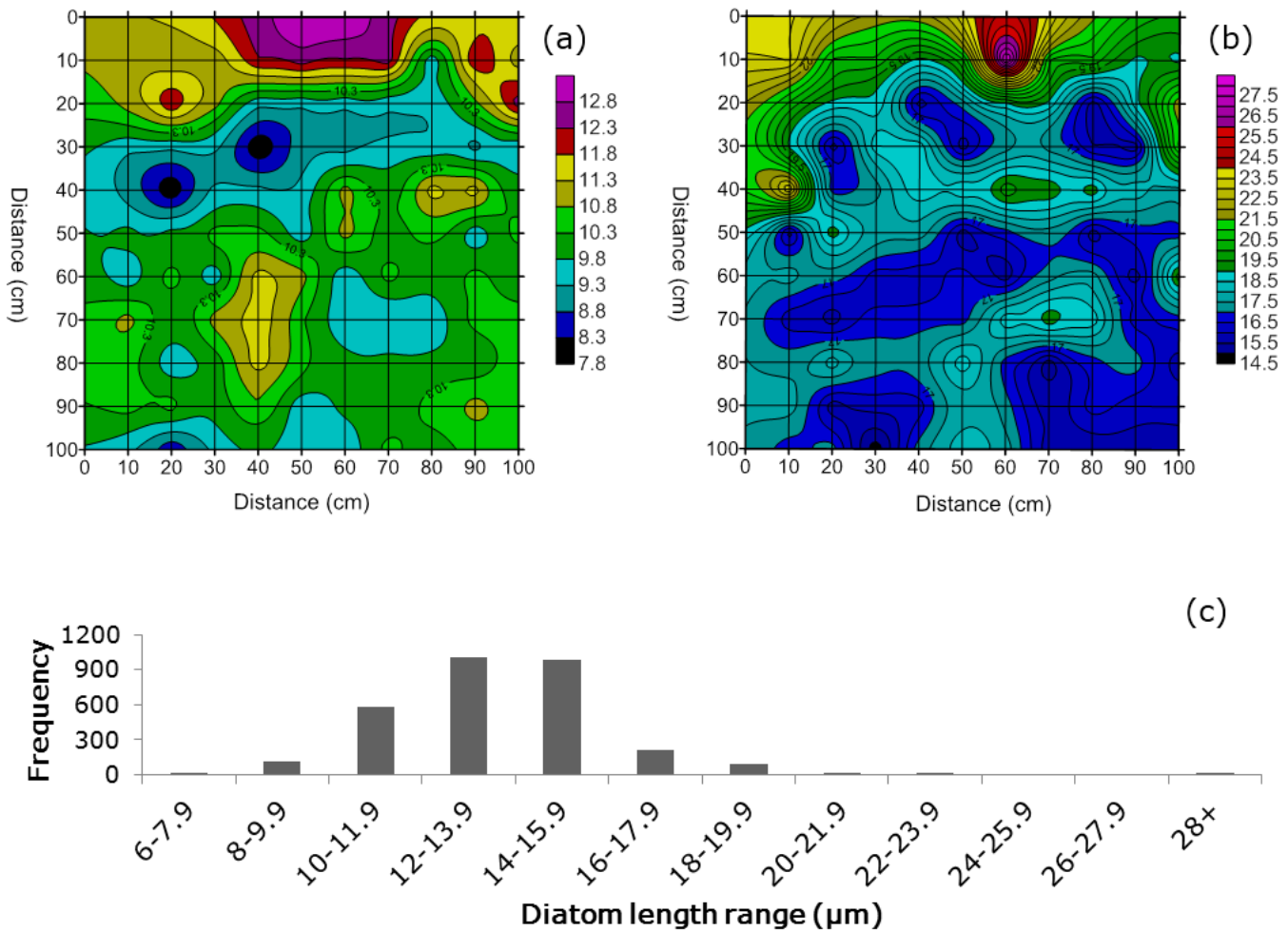


Figure 3. Contour maps of frustule length (μm) for *C. costata*, (a) minimum length (μm) with contour interval set at 0.5 μm , (b) maximum length (μm), (c) frequency distribution of frustules lengths over 1 m² quadrat, with contour interval set at 0.5 μm and $n = 3000$.

To gain an understanding of the divisional dynamics of *A. hyalina* we calculated the skewness of all frustules within each square, the results of which show that the skewness of 78% of the 100 sampled square > -0.8 (Figure 4a), although positive skewness was only observed in 19% of total samples. Still, there are a number of noticeable points where the skewness is > -2 , at x, y coordinates (60, 40), (70, 30) and (90, 10), which indicates that

longer frustules of *A. hyalina* are present. Additionally, we also considered the kurtosis to gain further understanding of the spread of data, where a kurtosis of zero indicates a Gaussian distribution. For *A. hyalina*, kurtosis was positive and is indicative of a peaked distribution (Figure 4b), which is seen in the frequency distribution of frustule length at x, y coordinates (60, 60) (skewness = 0.334, kurtosis = 0.075; Figure 4c) and (10, 90) (skewness = -0.065, kurtosis = 0.688; Figure 4d). In contrast, skewness of *C. costata* for 72% of the total area was > 0 (Figure 5a). In particular, there are a number of points of maximum positive skew, favouring smaller individuals (x, y coordinates (60, 10), (50, 80) and (80, 70)), and points of maximum negative skew, favouring longer individuals (x, y coordinates (30, 40), (30, 70) and (80, 40)). In considering the kurtosis, 78% of the area displayed negative values (Figure 5b). For example, positive skewness for *C. costata* of x, y coordinate (60, 10) is indicative of greater number of individuals smaller in the population, where the frequency distribution shows a majority of frustules ranging between 13-16 μm and frustule length distribution ranged from 12-28 μm (Figure 5c). Likewise, at x, y coordinates (50, 80) skewness and kurtosis was positive indicating that smaller individuals between 12-14 μm (Figure 5d). However, the range of *C. costata* length was much smaller than seen in Figure 5c, where frustules ranged between 10.5-19 μm .

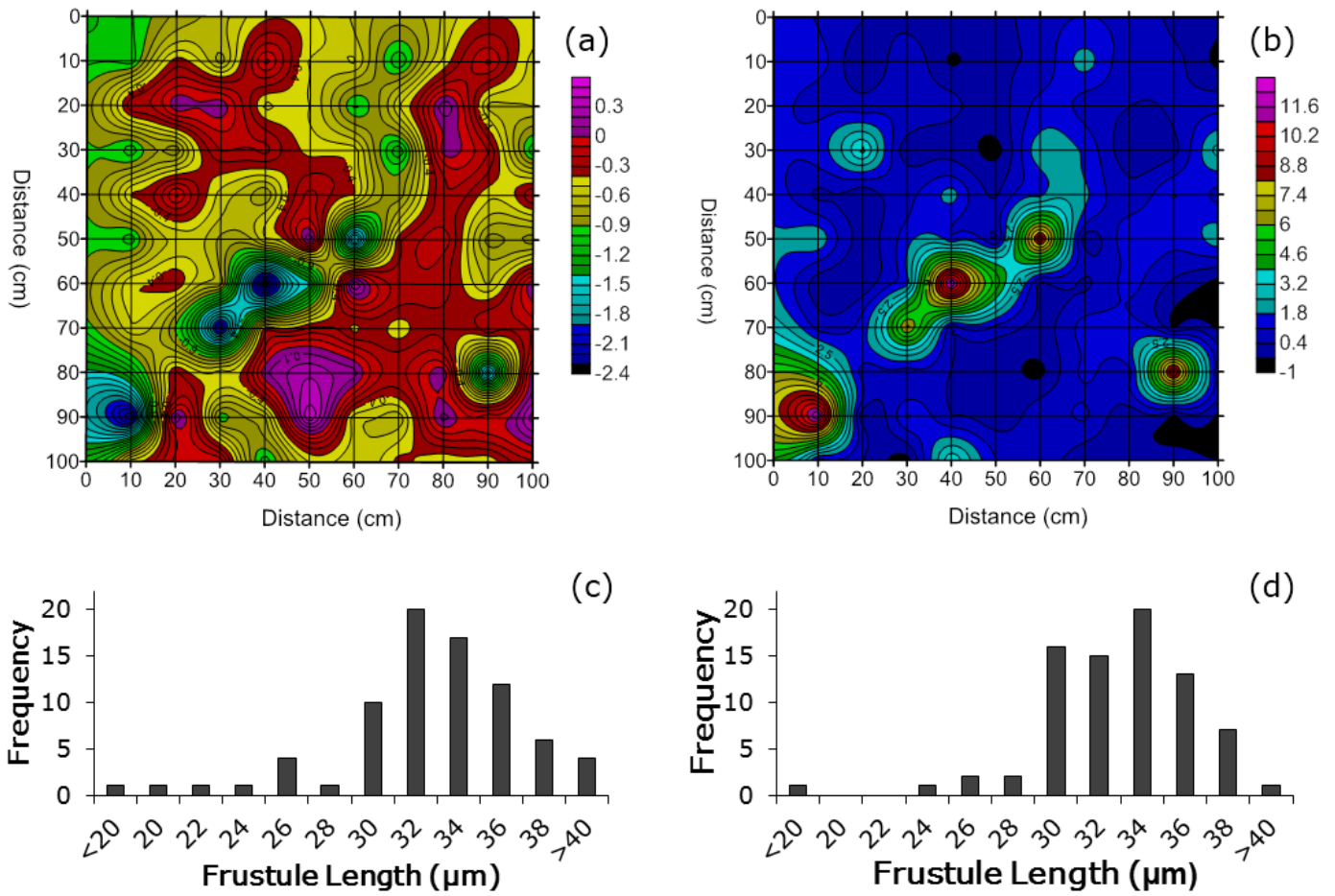


Figure 4. (a) Skewness and (b) kurtosis of frustule length for *A. hyalina* over 1 m² area. Contour interval for skewness set at 0.1 where interval is based on the mean coefficient of variation for 1 m² of diatom length measurements, where mean CoV = 0.12. Contour interval for kurtosis set at 0.5. Frequency distribution of *A. hyalina* length (μm) for two sampled squares (c) x, y coordinates (60, 60) (positively skewed, positive kurtosis) and (d) x, y coordinates (10, 90) (negatively skewed, positive kurtosis) where n = 78.

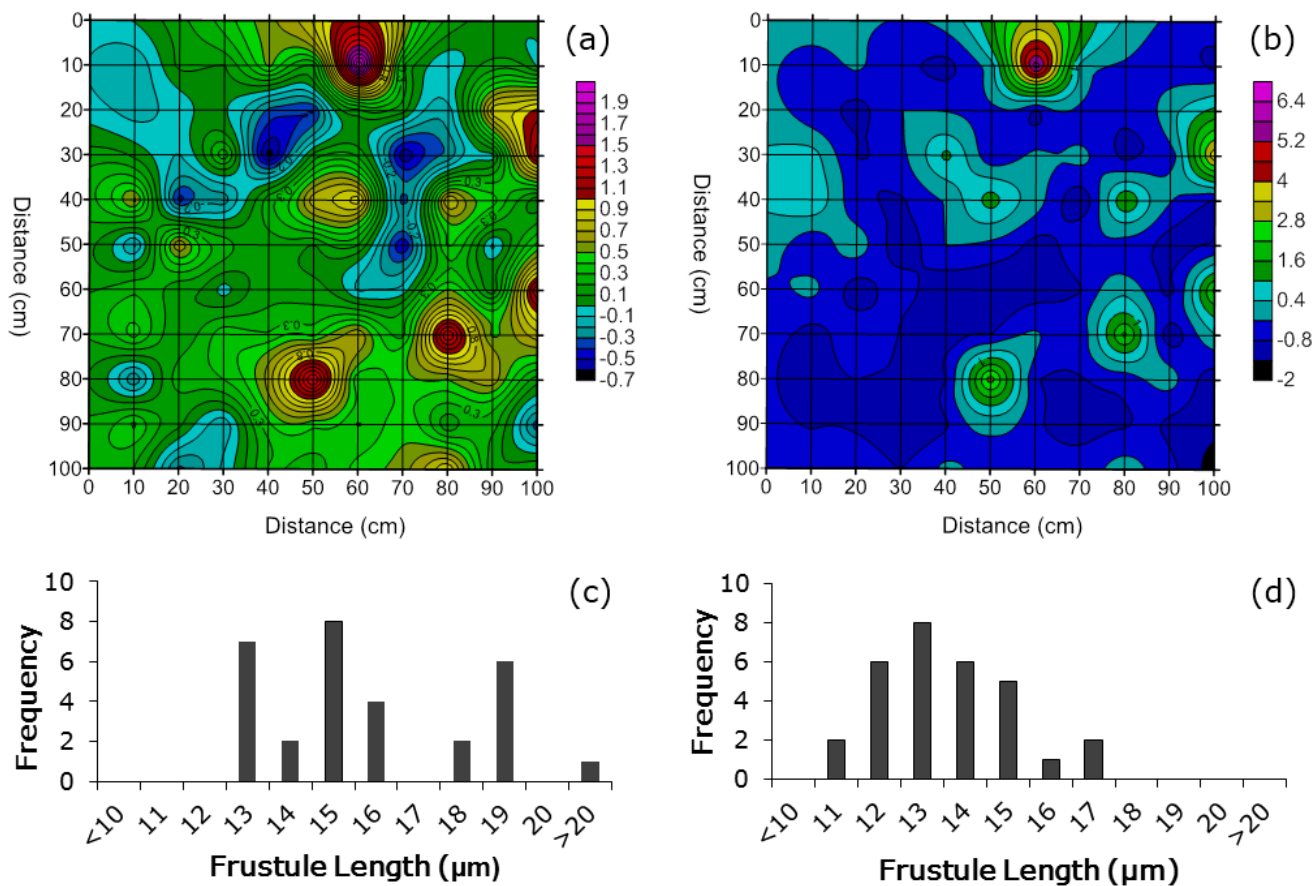


Figure 5. (a) Skewness and (b) kurtosis of frustule length for *C. costata* over 1 m² area. Contour interval for skewness set at 0.1 where interval is based on the mean coefficient of variation for 1 m² of diatom length measurements, where mean CoV = 0.12. Contour interval for kurtosis set at 0.5. Frequency distribution of *C. costata* frustule length (μm) for two sampled squares (c) x, y coordinates (60, 10) (positively skewed) and (d) x, y coordinates (50, 80) (positively skewed) where n = 30.

Chlorophyll concentrations

The photosynthetic pigments chl *a* and chl *c* were detected throughout the 1 m² sample grid. The maximum chl *a* mean concentration at x,y coordinates (100, 90) was 32.73 g m⁻³ ± 5.93 g m⁻³. However, chl *a* minimum mean, 13.65 g m⁻³ ± 8.62 g m⁻³, was observed at x,y coordinates (70, 70) (Figure 6a). Meanwhile, the minimum mean chl *c* concentration was 4.36 g m⁻³ ± 1.38 g m⁻³ at x, y coordinates (10, 70) and maximum was 14.40 g m⁻³ ± 3.92 g m⁻³ was at x, y coordinates (50, 50) (Figure 6b).

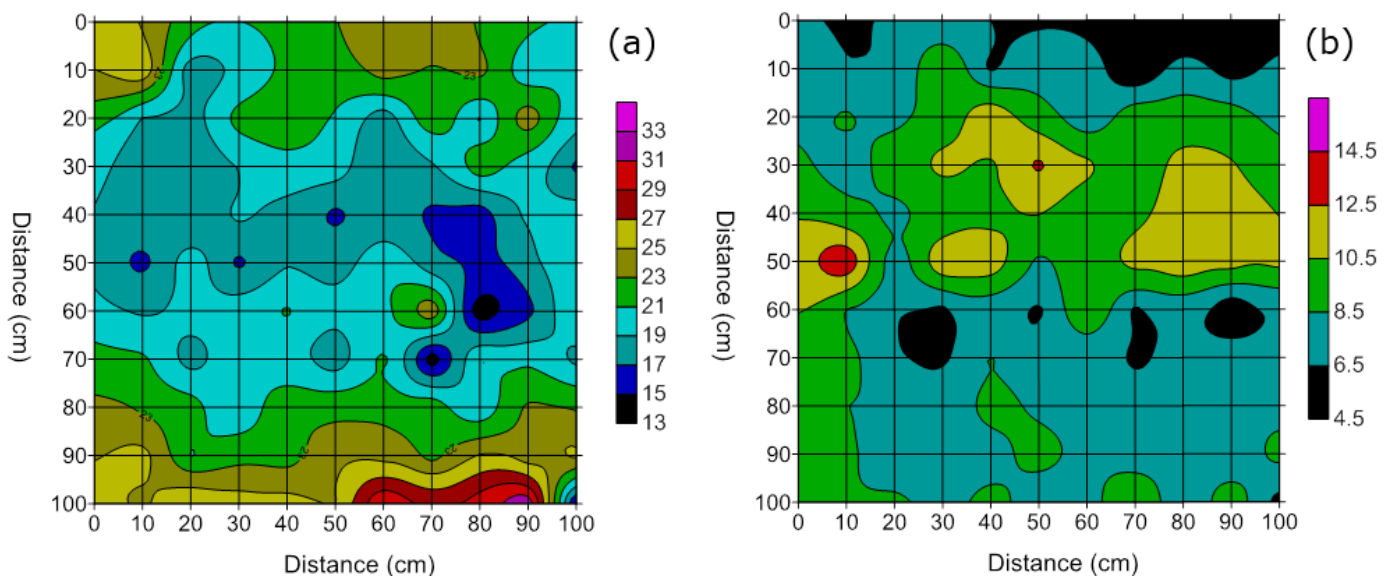


Figure 6. Mean concentration of photosynthetic pigments (a) chlorophyll *a* (gm⁻³) and (b) chlorophyll *c* (gm⁻³) over 1 m² area; contour intervals set at 0.2 g.m⁻³.

Spatial Autocorrelation

The diatom frustule length of *A. hyalina* had a Moran's *I* value of -0.015. However, since the *z*-value, where *z*-value = -0.449, was less than -1.96, there was no significant spatial autocorrelation. This was further confirmed by the Geary's *C* statistic, which is more

sensitive to localised variation, and yielded a non-significant result (Geary's $C = 1.108$). Conversely, frustule length of *C. costata* showed very different spatial autocorrelation results. Moran's I value for *C. costata* was 0.115, while the z -value was 8.714, where a positive z -value is greater than +1.96 the result is significant ($p = 0.0001$). Geary's C results confirms that the observed spatial autocorrelation is positive and locally significant (Geary's $C = 0.770$). Thus, positive spatial autocorrelation for *C. costata* suggests that there is significant clustering of frustule length in favour of longer frustule length.

Chl a revealed a similar spatial autocorrelation trend to that of the frustule length of *C. costata*, where Moran's I for chl a was positive and significant (Moran's $I = 0.097$). Moran's I for chl c , however, was positive but was not significant (Moran's $I = 0.004$, z -value = 0.96). In addition, Geary's C results confirm these findings for chl a of spatial dependence (Geary's $C = 0.8362$). Yet, for chl c no significant spatial autocorrelation was observed (Geary's $C = 1.001$). Therefore, positive spatial autocorrelation indicates that there is significant clustering of chl a in favour of increased concentrations, whereas there was no significant spatial autocorrelation that would indicate either clustering or dispersal of chl c concentration.

Chlorophyll and Frustule Length Correlations

Spearman's correlation coefficient was calculated between diatom frustules length and chl pigment concentration, for chl a and chl c . Significant correlations were only observed where Spearman's correlation coefficient was between 0.8 and 0.95 for significant positive correlations and -0.6 and -0.85 for significant negative correlations (Figure 7a-d). Results for *A. hyalina* and chl a show that negative correlation coincided with frustules length range $> 25 \mu\text{m}$ and for positive correlations this coincided with frustules lengths $< 25 \mu\text{m}$ (Figure 7a). Whereas negative correlations between *C. costata* and chl a coincided frustule length $< 8 \mu\text{m}$ (Figure 7b). Additionally, correlations with frustule length and chl c suggest a similar trend

where correlations with *A. hyalina* corresponded to where the range of the frustule length was $> 20 \mu\text{m}$ (Figure 7c), and that of *C. costata* was observed where frustules range was $> 5 \mu\text{m}$ (Figure 7d).

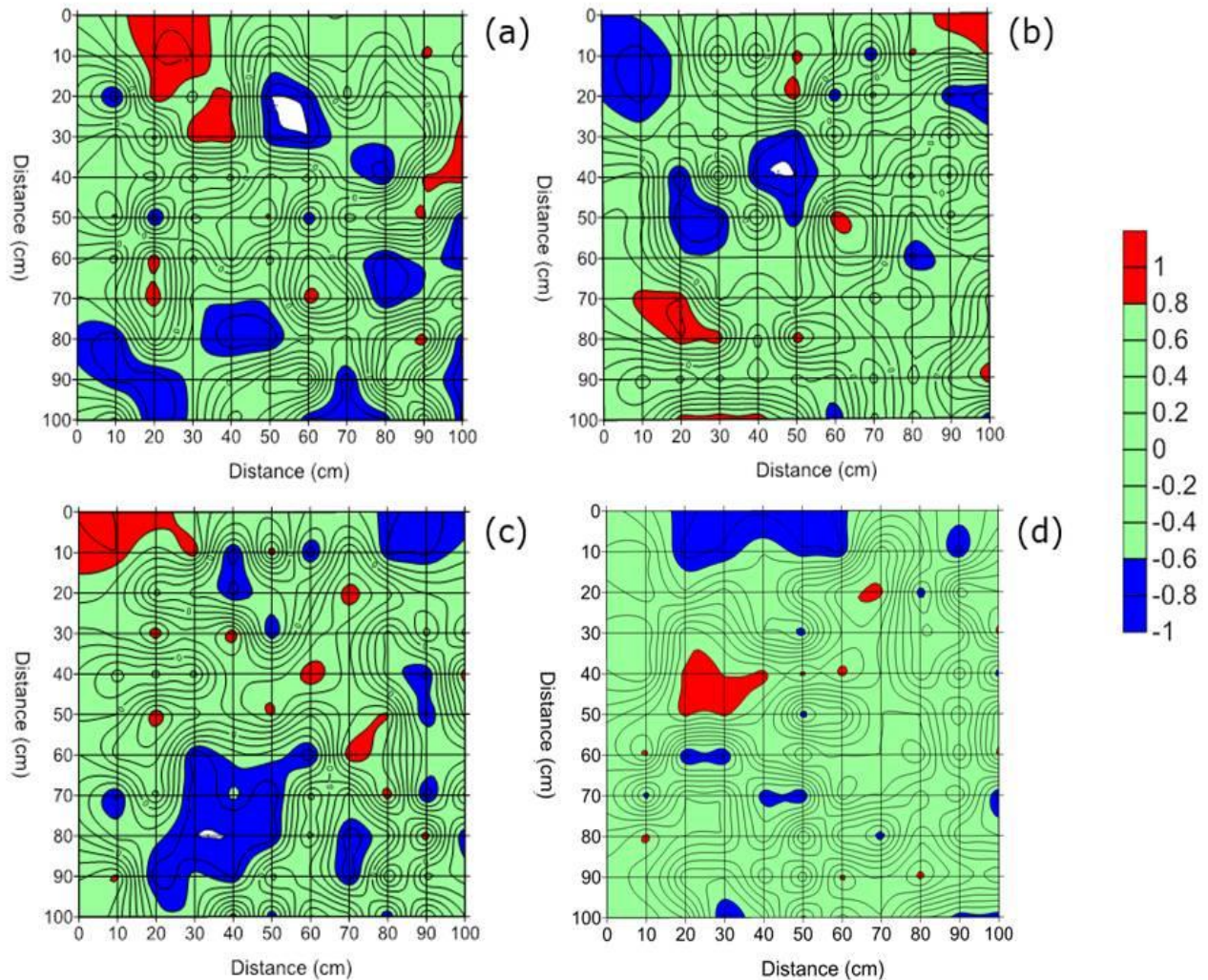


Figure 7. Contour map of Spearman's correlation for (a) Chlorophyll *a* and *A. hyalina*, (b) Chlorophyll *a* and *C. costata*, (c) Chlorophyll *c* and *A. hyalina*, (d) Chlorophyll *c* and *C. costata*. On the colour key, dark blue indicates a significant negative correlation and red indicates significant positive correlation; contour intervals set at 0.2.

Network Analysis

The correlation network developed for *A. hyalina* and *C. costata* frustule length and chl parameters, shown in Figure 8a, show only positive Pearson correlation coefficients greater than 0.99. The size and colour of the nodes are proportional to the connectedness of the parameter within the network. Here, the range of frustule length and the maximum length of *A. hyalina* are represented by the largest, red and orange nodes, respectively, which are indicative of the greatest connectedness. However, nodes for *C. costata* are yellow in colour, denoting that the *C. costata* parameters are less important. The edges connecting these nodes show strong polytonic correlations between Amph-Range and Amph-Kurtosis, Amph-Min and Amph-Skew, Cocc-Max and Cocc-Range and mean-chla and mean-totalchl. Weaker relationships include correlations between Amph-Mean and Amph-Range, Amph-Min and Amph-Range, and, Cocc-Max and Cocc-Min. Additionally, developing a network using an eLSA matrix for the same parameters confirms the importance of the range and maximum statistics for diatom frustule length (Figure 8b). Here all connections have a local similarity score > 0.99 . However, this network reveals the equal and high importance of Amph-Range, length range of *A. hyalina*, and Cocc-Max, maximum length of *C. costata* (Figure 8b). Furthermore, thick red edges indicate strong linear and non-linear components in the polytonic eLSA, observed for Amph-Range and Amph-Kurtosis, Amph-Min and Amph-Skew, mean-chla and mean-totalchl and Cocc-Max and Cocc-Range. Overall, from Figures 9a and 9b, the edges of these networks show that *C. costata* has fewer stronger interdependent connections, while *A. hyalina* has more, but weaker connections.

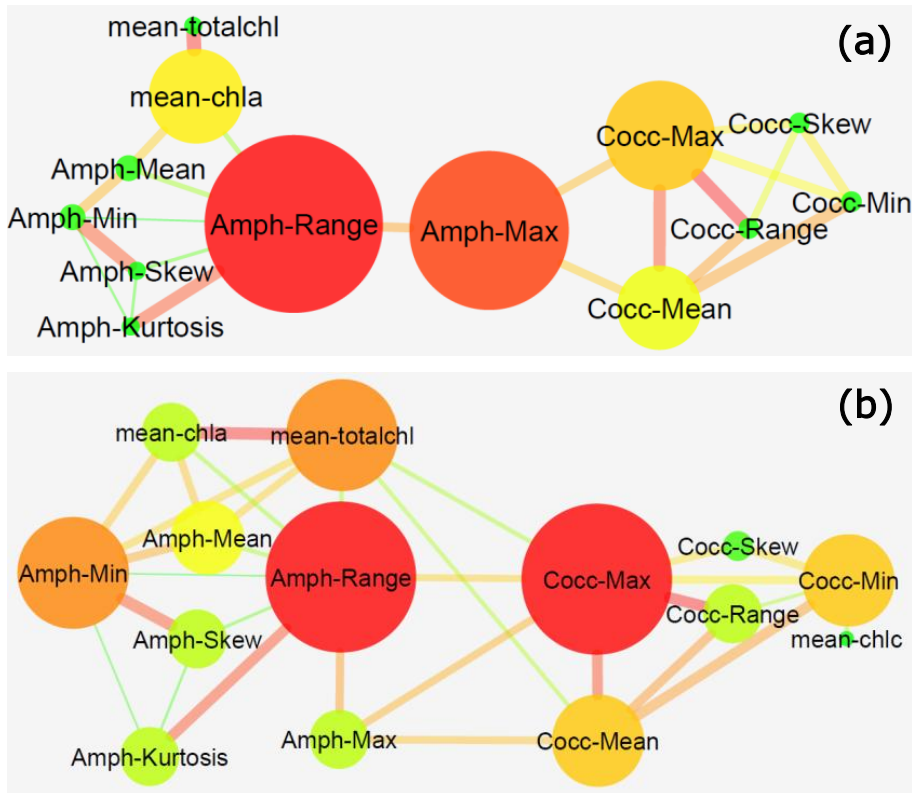


Figure 8: Correlation network for parameters of *A. hyalina* and *C. costata* based on measurements from all samples. (a) All edge connections have a Pearson correlation coefficient of greater than 0.99. Thick edges indicate strong, relative to other edges in the network, polytonic correlations as measured by extended Local Similarity Analysis (eLSA, Xia *et al.* 2011). Red edges indicate strong non-linear correlations as measured by Spearman correlations. Node size and colour indicate betweenness centrality, an indication of how important each node is to the overall network structure. Large, red nodes denote high importance, and small green nodes indicate low importance. (b) All edge connections have an eLSA score of greater than 0.99. Thick edges indicate strong Pearson correlations. Red edges indicate strong Spearman correlations. Thick, red edges have strong linear and non-linear components in their polytonic eLSA. *A. hyalina* is on the left and *C. costata* is on the right in each network. Amph is for *A. hyalina* and Cocc is for *C. costata*. Skew indicates the skewness, Kurtosis indicates kurtosis, Max indicates maximum frustules length, Min

indicates minimum frustules length, Mean indicates the mean, Range indicates the range. The networks were made with Cytoscape 3.2.1.

Discussion

Understanding the reasons for patchiness in community properties at any spatial scale may enable us to understand the processes that are controlling population dynamics (Doubell *et al.* 2006). Furthermore, insights into the patchiness will also increase the understanding of the role played by microbial communities in ecosystem functioning (McInnes *et al.* 2015). Here microscale heterogeneity in the microphytobenthos was measured using the frustule lengths of *A. hyalina* and *C. costata*, in addition to the concentration of chlorophyll pigments, chlorophyll *a* and chlorophyll *c*.

Chlorophyll Concentration Variation

Chlorophyll *a* is widely used as an estimation of community biomass (Kuwahara and Leong 2015, McInnes *et al.* 2015, Pinckney *et al.* 2015). However, few studies have assessed microscale heterogeneity of chlorophyll *a* concentration (Seuront and Spilmont 2002, Spilmont *et al.* 2011). The results from spatial autocorrelation analysis here show that for chlorophyll *a* there is significant clustering of higher concentrations of chlorophyll, as indicated by the positive and significant result from the Moran's *I* test (Waters *et al.* 2003). Conversely, chlorophyll *c* did not display any significant spatial autocorrelation and therefore no significant clustering or dispersal of chlorophyll *c*. In large scale studies, it has been previously noted that chlorophyll concentration and diatom size are correlated in environments where diatoms are the dominant class of phytoplankton, it is generally assumed that the larger cells have greater chlorophyll content than smaller cells (Lopes *et al.* 2006). As such, previous results have shown either positive (Finkel *et al.* 2009, Lopes *et al.* 2006), negative (Shukla *et al.* 2013) and no significant correlations between chlorophyll biomass and diatom size (Adams *et al.* 2013).

Spatial Autocorrelation, Skewness and Kurtosis of Frustule Length

Nutrient limitation (Leterme *et al.* 2010, 2013), reproduction (Vanormelingen *et al.* 2013, Vanstechelma *et al.* 2013) and grazing (Barton *et al.* 2013, Suzuki *et al.* 2013, Wasserman *et al.* 2015) contribute to diatom length patchiness. Patchiness of dissolved nutrients is known to lead to changes in the abundance of viruses and bacteria at the micrometre scale (Seymour *et al.* 2000, 2007, Stocker and Seymour 2012). Taking into account the results from spatial autocorrelation, it has been suggested that where skewness or kurtosis are high spatial autocorrelation is also high and significant, which leads to extremes in body size (Moustakas 2014). The results for skewness of *C. costata* frustule length (Figure 5), which was the only diatom species that showed significant clustering from spatial autocorrelation, also show high skewness. The maximum skewness for *C. costata* was 2.1, compared to the maximum skewness of *A. hyalina*, 0.6. Using skewness and kurtosis of the length of *A. hyalina* and *C. costata* it can be suggested which biotic and abiotic act on the diatom populations, such as predation and reproductive pressures, are thus responsible for the patchiness of the frustule length. Meanwhile, negative skew, indicative of larger body sizes, is apparently linked to predation and local environmental factors (Rossi *et al.* 2012, Kotwicki *et al.* 2013). Specifically, for *A. hyalina*, 19% of the quadrat area showed positive skewness, meaning that in 19% of the sampled area the smaller frustule length was favoured. In contrast, for *C. costata* 72% of the sampled area showed positive skewness. Previous studies have shown that positive skew, indicative of smaller body sizes, is linked to reproduction and abiotic parameters (Rossi *et al.* 2012, Chon *et al.* 2013).

Therefore, we suggest that the variation of the frustule length of *A. hyalina* and *C. costata* may be explained by differences in growth or reproduction rates of the diatom populations (Montresor and Lewis 2006). Characteristic of diatom reproduction is an asexual phase where

cell size is constrained by the size and production of the silica frustule (Chepurnov *et al.* 2004, Mann and Vanormelingen 2013). This may impact on the microscale distribution of frustule length, as well as the biomass of the diatoms within discrete patches caused by the position within the life cycle of individuals within a population (Godhe *et al.* 2013, Chepurnov *et al.* 2008). Yet, preferential predation of diatoms may also account for skewness in the population (Lie *et al.* 2013). At the site sampled, the predators of diatoms present are primarily ciliates (Jendyk *et al.* 2014, Nayar and Loo 2009). We suggest that smaller predators, i.e. ciliates, will preferentially graze on smaller diatoms than comparatively larger diatoms (Hansen *et al.* 1994, Larson *et al.* 2015). Thus, it is suggested that positive skew of diatom frustule length is indicative of microscale predation by ciliates, and likewise negative skew towards larger frustule may indicate the absence of predation as the frustule are too large for the predators to ingest.

The negative skewness in Figure 5a and 5b, indicates the larger frustule sizes are favoured, from 30 μm to $>40 \mu\text{m}$. The observed *A. hyalina* transition from larger frustule size, greater than 45 μm , to smaller frustule size, less than 23 μm , may be accounted by its lifecycle or environmental constraints on the population. In contrast, the significant spatial autocorrelation and positive skewness for *C. costata* suggests that this population favours the smaller, less than 11 μm , cell sizes. This may be accounted for by variation in the reproduction rates of both species, which are further affected by external environmental factors, including large- and microscale effects (Sjöqvist *et al.* 2015, Rossi *et al.* 2012, Godhe *et al.* 2013).

Network Analysis of Frustule Length

The Pearson and eLSA networks in Figure 8 show the robustness of the network analyses conducted from the separation of *A. hyalina* and *C. costata* parameters in the two networks

(Faust and Raes 2012, Ruan *et al.* 2006). Networks made with local similarity coefficients greater than 0.99 are unusual compared to studies where the similarity coefficient is 0.5 (Steele *et al.* 2009). However, the high values in the present study are likely explained by the diatom parameters being closely interdependent, where samples were taken at the same time within a one metre quadrat. In comparison, other studies have used identification of microbial communities and relative abundance using identification of genomic and transcriptomic data which have monthly (Chow *et al.* 2014, Steele *et al.* 2009) and seasonal (Gilbert *et al.* 2012) sampling intervals or span over ocean basin scales (Aylward *et al.* 2014). Yet, the networks presented in here suggest that the size range of an individual species can be more informative of interactions than the mean size, total chlorophyll or other commonly measured statistics. It is evident from Figures 8a and 8b, where the network is built on linear correlations, that the frustule length range and the maximum frustule length of *A. hyalina* are the most important nodes for the network.

Conclusion

In this study we show for the first time that spatial heterogeneity is observed for the frustule length of two diatom species. Spatial autocorrelation revealed that frustule length of *C. costata* and chlorophyll *a* showed significant clustering. Furthermore, the results show distinct patches of large *A. hyalina* frustules, greater than 45 μm , and smaller *C. costata* frustules, less than 12 μm . We suggest that the variation observed may be attributed to the rate of reproduction and the unique life cycle of diatoms (Montresor and Lewis 2006) or predation by ciliates (Lie *et al.* 2013, Larson *et al.* 2015). Finally, using network analysis, we show that individual species parameters to identify the best component to assess variation within the populations. Specifically, *C. costata* maximum frustule length, *A. hyalina* frustules length range and maximum frustules length are the strongest nodes for the Pearson and eLSA networks. These results, for the first time, show the importance of understanding variation of cell size within microscale populations can reveal more about community interactions than only relying on chlorophyll biomass measurements.

CHAPTER 6

Discussion

Overview

The research conducted in this thesis provides new insights to the spatial variation of benthic microeukaryotes on large- and microscales. The large scale study presented shows the variability of community composition in the shallow waters of the Coorong lagoons during drought conditions. Previous research into the north lagoon of the Coorong has shown that, during non drought conditions, salinity is the primary factor influencing phytoplankton communities (Jendyk *et al.* 2014). In a number of coastal and estuarine locations worldwide, species diversity and abundance have been shown to decrease with increasing salinity (Cloern and Dufford 2005, Kipriyanova *et al.* 2007, Carstensen *et al.* 2015). Yet, in contrast, my data shows that salinity does not have a direct influence on the phytoplankton communities, in particular diatoms and green algae populations, sampled over 140 km distance. This is possibly due to the communities changing and adapting to the changes in the environment over time.

The microscale studies also showed that diatoms are key organisms to the ecosystems studied. In general, diatoms are ecologically important as a known carbon storage and significant contribution to global oceanic primary production (Kamp *et al.* 2013, Tan *et al.* 2015). The importance of the diatoms in the study site, Chapter 3, and three diatom classes identified, Chapter 4, is specifically shown in this thesis from the results from network analyses. These show the specific interactions between diatoms and other groups of prokaryotes and eukaryotes in the microphytobenthos. The variation in diatom frustule distributions over the microscale area, Chapter 5, may also be linked to these interactions, whereas ciliates and other protists are present in greater numbers of larger individuals than smaller (Rossi *et al.* 2012, Larson *et al.* 2013).

Large Scale Phytoplankton

The large scale study conducted, Chapter 2, observed phytoplankton variation along the Coorong lagoons and Murray Mouth over a 12 month period during drought conditions. The lagoons are connected by a channel which allows water to flow from the north lagoon into the south lagoon (Webster 2005, 2010). However, summer evaporation causes less water to flow into the south lagoon and thus resulting in higher salinities (Webster 2010).

Interestingly, despite the salinity of the south lagoon regularly exceeding 120 PSU and in the north lagoon being below 110 PSU, salinity did not play a key role influencing the Coorong phytoplankton communities. Instead, in the south lagoon, the wind speed four days before sampling was the primary factor influencing the phytoplankton communities. The shallow water depth combined with wind speed means that water is mixed and unable to maintain periods of sustained stratification (Webster 2010, Kämpf 2014).

In contrast, the benthic communities sampled in the north lagoon were influenced by the physical parameters measured on the day of sampling, specifically pH, salinity, ammonium, nitrite and silica concentrations. These parameters have been shown widely to affect phytoplankton species composition, abundance and diversity in coastal phytoplankton communities. In particular, increases in nitrogen based nutrients have been shown to promote an increase in phytoplankton abundance (Domingues *et al.* 2015, Burson *et al.* 2016). Likewise increase in silica availability has been shown to increase diatom abundance due the requirement of diatoms for silica in order to form silica frustules during reproduction (Ryves *et al.* 2013, Burson *et al.* 2016).

Microscale Microphytobenthos

Two microscale studies were undertaken to characterise and account for the photosynthetic portion of the community. Previous studies use different spectrometry and fluorescence methods to measure chlorophyll concentration, which is used as a measurement of the photosynthetic biomass in the microphytobenthos (MacIntyre *et al.* 1996, Spilmont *et al.* 2011). However, by collecting chlorophyll measurements, these studies fail to observe variation of the taxonomic composition of the microeukaryotic communities. Here, from chlorophyll data and 18S sequencing, heterogeneous distribution of the microphytobenthos is indeed confirmed. Although, this is not surprising considering previous studies showing that chlorophyll biomass is heterogeneously distributed in the microphytobenthos (Kelly *et al.* 2001, Seuront and Spilmont 2002, Franks and Jaffe 2008, Spilmont *et al.* 2011).

In Chapter 3 further statistical analysis indicated the importance of a number of taxa which are contributing to the dissimilarity observed. Three ciliate OTUs, *Euplotes dammamensis*, *E. nobili* and *Bergeriella ovata*, in addition to an unidentified diatom OTU, were identified as taxa driving dissimilarity in the community. Ciliates and diatoms, in addition to the green algae were found to be the most abundant OTUs identified by 18S sequencing using a universal eukaryotic primer. These three groups have been previously identified as ecologically abundant and functionally important groups by large scale studies in coastal and intertidal zones (Buric *et al.* 2007, Tekwani *et al.* 2013, Jendyk *et al.* 2014). Ciliates provide an important connection within aquatic food webs between the bacterioplankton and phytoplankton (Sherr and Sherr 2002). Meanwhile diatoms, which are grazed upon by ciliates (Straile 1997, Larson *et al.* 2013), are the most abundant and diverse groups in aquatic microbial communities (Armbrust *et al.* 2009).

These concepts are supported by the interaction network constructed for Chapter 3, where interaction between diatoms and ciliates indicates that the diatoms are indeed being grazed

upon by ciliates and strong interaction with the unknown group may also suggest grazing from these taxa. The fact that the diatoms are the largest node in this network after the unknown group indicates that diatoms are the keystone group of this community. Yet it is not clear from these results how the specific identity of group of organisms is influencing the variation in chlorophyll concentration, which may in fact be due to phototrophic bacteria such as cyanobacteria.

The importance of diatoms to the microphytobenthic community is further demonstrated in Chapters 4 and 5. Specifically, in Chapter 4, a 1 m transect sampled in 10 cm sections was selected for metagenomic analysis. Using metagenomic sequencing means that the prokaryotes and eukaryotes in microbial communities may be accounted for. Previous research has shown, on large scales in the ocean, that changes in phytoplankton communities does indeed influence bacterial communities (Paver *et al.* 2013, Needham and Fuhrman 2015). Rank-abundance analysis showed random distributions when comparing taxonomic groups, except for the diatoms and bacteria, which have a power law distribution and is indicative of a highly ordered community (Dann *et al.* 2014).

The strength of the interactions between the diatoms to other microbial taxa within the transect highlights the ecological importance of diatoms. In this particular network, diatoms are the largest nodes, indicating a high degree of betweenness centrality and therefore suggest that diatoms are the most important organisms identified in this particular microbial community. The resulting network analysis indicated the high importance of the classes of diatom, Bacillariophyceae, Coscinodiscophyceae and Mediophyceae. The integral connections observed show the Mediophyceae and Coscinodiscophyceae diatoms showing high similarity to the class of Chloroflexi bacteria, Anaerolineae, and Coscinodiscophyceae and Bacillariophyceae show high similarity with Chlorophyceae, green algae.

This theme of the importance of diatoms within microbial communities over microscale distances is further developed in Chapter 5 where the length of diatom frustules, of *A. hyalina* and *C. costata*. Frustule length varied between 19 μm and 47 μm for *A. hyalina* and 9 μm and 29 μm for *C. costata*. Variation in skewness of frustules length shows areas which favour larger frustules lengths than smaller, where for the two species skewness ranging between -2.5 and 2.1.

Previous use of skewness in an ecological context have shown that positive skew is indicative of smaller body sizes and linked to cell division and abiotic parameters (Rossi *et al.* 2012, Chon *et al.* 2013), whereas negative skew is indicative of larger body sizes, has been linked to predation and local environmental factors (Rossi *et al.* 2012, Kotwicki *et al.* 2013). Additionally, this confirms observations from a previous study which suggested that where skewness is high, either positively or negatively, spatial autocorrelation is high and significant, leading to extremes in body size (Moustakas 2014). Diatom reproductive strategy, including asexual and sexual reproduction as outlined in the Chapter 1, is an important factor to consider for this variation in frustules length. This is because the full diatom life cycle, which is species specific, can occur on time scales over six and ten years (D'Alelio *et al.* 2010), which may indicate that populations within the same community are at different stages of the lifecycle (Montresor and Lewis 2006). However, from Chapter 3, the importance of ciliates with the microeukaryote community was shown. This is significant to the findings of Chapter 5 because diatoms are grazed upon by ciliates (Wasserman *et al.* 2015, Straile 1997), where ciliates generally tend to favour smaller size diatoms over larger individuals (Larsen *et al.* 2015).

Insights to the Microbial Community using Network Analysis

Network correlation analysis was utilised in the microscale studies of Chapters 3 to 5 in order to investigate the intricate connections between the species and relative abundances of species identified using 18S and metagenomic identification, in addition to relating the summary data and chlorophyll biomass parameters sampled for the length of the diatom species *A. hyalina* and *C. costata*. Ultimately, in this thesis the networks presented have been used to show the importance of diatoms within microbial communities.

The network presented in Chapter 3 was used to show that within the microeukaryotic community sampled diatom OTUs form a keystone group. The interactions indicated between the unknown group and the ciliates suggest that diatoms are being grazed upon, at least by the ciliates and possibly by some of the unknown taxa. Similarly, Chapter 4, the network presented strongly indicates the importance of diatom within the sampled microbial community using metagenomic sequencing. The network presented suggests that diatoms provide an important link between the bacteria and other groups of eukaryotic microalgae, where the removal of the diatoms could cause a complete disconnection between prokaryotes and eukaryotes of the sampled microbial community.

In contrast, Chapter 5 uses network analysis for a very different function. Here, networks were used to help give an indication of the best ways in which to describe and characterise a community. For *A. hyalina* size range and maximum size and for *C. costata* maximum size are indicated as the strongest nodes. Further exploration into this use of network analysis for ecological data may help to provide more insight when trying to characterise key species and components within microbial communities.

Future Directions

While it is not possible to make direct comparisons between large scale to microscale variation, the outcomes of this thesis do provide insights to phytoplankton and microphytobenthic communities at these scales individually. The primary limitation allowing this analysis is the fact that the large scale study of Chapter 2 sampled phytoplankton, the microscale studies of Chapters 3 to 5 sampled the microphytobenthos.

Previous research has previously predicted the intensive effort that is required to make comparisons over varying temporal scales (Spilmont *et al.* 2011). This same paper also describes the need to for unified methods of sampling the biomass of the microphytobenthos, using field spectrometry. However, these methods may also be integrated with the use of sequencing or microscopy to determine taxa which exist in aquatic sediment and further expanded to include water column studies on phytoplankton. This may be important ecologically to improve field sampling strategies, particularly in intertidal and shallow water regions where variability of biotic and abiotic is known but not always accounted for in sampling (Kelly *et al.* 2001, Jesus *et al.* 2006, Spilmont *et al.* 2011).

Conclusion

The results of this thesis provides insights on the large scale phytoplankton variation of abundance and species composition and species composition and cell length distributions of microalgae in the microphytobenthos on the microscale. The featured studies sampled from a shallow-water, coastal lagoons and estuary system, the Coorong in South Australia, which was sampled during drought conditions and was characterised by an increasing hypersalinity gradient from the mouth of the Murray River. While Chapter 2 employed traditional microscopy methods in order to identify and enumerate phytoplankton communities, 18S and

metagenomic analysis was utilised in order to characterise the microeukaryotes in the microscale studies of Chapters 3 and 4.

This thesis adds to the current understanding of large scale processes on phytoplankton communities. Specifically, the spatial disconnect between the sampling locations of the north lagoon and the south lagoon in the Coorong, suggested from the physical parameters which influenced the phytoplankton communities of the two lagoons. This thesis presents results from the first studies to identify interaction between species microeukaryotes present at microscale distances, where high and varied abundances of diatoms, ciliates and green algae were observed in Chapters 3 and 4. The microbial networks produced here show the usefulness of network analysis to represent relationships between microeukaryotes, where in Chapter 4 the importance of the diatoms within the microbial food web was demonstrated. Secondly, network analysis was used to determine parameters which are suitable for community indicators, in chapter 5 results demonstrated that the range of diatom length was the best indication of variation of population cell length. Ecologically, this understanding of microscale variation of diatom length, in addition to chlorophyll concentration and community sequencing provides insight to the interactions between microeukaryotes at the centimetre level.

BIBLIOGRAPHY

Adams GL, Pichler DE, Seeney A, Woodward G, Reuman DC. (2013). Diatoms can be an important exception to temperature-size rules at species and community levels of organisation. *Global Change Biology*. **19**(11): 3540-3552.

Amin SA, Parker MS, Armbrust EV. (2012) Interactions between Diatoms and Bacteria. *Microbiology and Molecular Biology Reviews*. **76**(3): 667-684.

Amo YD, Brzezinski MA (1999) The chemical form of dissolved Si taken up by marine diatoms. *Journal of Phycology*. **35**: 1162-1170.

Anfuso E, Debelius B, Castro CG, Ponce R, Forja JM, Lubian LM. (2013) Seasonal evolution of chlorophyll-a and cyanobacteria (*Prochlorococcus* and *Synechococcus*) on the northeast continental shelf of the gulf of Cádiz: relation to thermohaline and nutrients field. *Scientia Marina*. **77S1**: 025-036.

Araújo CVM, Romero-Romero S, Lourençat LF, Moreno-Garrido I, Blasco J, Gretz MR, Moreira-Santos M, Ribeiro R. (2013) Going with the Flow: Detection of Drift in Response to Hypo-Saline Stress by the Estuarine Benthic Diatom *Cylindrotheca closterium*. *PLoS One*. **8**(11): e81073.

Armbrust EV. (2009) The life of diatoms in the world's oceans. *Nature*. **459**: 185-192.

Aylward FO, Eppley JM, Smith JM, Chavez FP, Scholin CA, DeLong EF. (2015) Microbial Community transcriptional networks are conserved in three domains at ocean basin scales. *Proceedings of the National Academy of Sciences of the United States of America*. **112**(17): 5443-5448.

Azam F (1998) Microbial control of oceanic carbon flux: the plot thickens. *Science*. **280**: 694–696.

Balzano S, Abs E, Leterme SC. (2015) Protist diversity along a salinity gradient in a coastal lagoon. *Aquatic Microbial Ecology*. **74**: 263-277.

Bates ST, Clemente JC, Flores GE, Walters WA, Parfrey LW, Knight R, Fierer N. (2013) Global biogeography of highly diverse protistan communities in soil. *The ISME Journal*. **7**:652-659.

Barton AD, Finkel ZV, Ward BA, Johns DG, Follows MJ. (2013) On the roles of cell size and trophic strategy in North Atlantic diatom and dinoflagellate communities. *Limnology and Oceanography*. **58**(1): 254-266.

Bik HM, Sung, W, De Ley P, Baldwin JG, Sharma J, Rocha-Olivares A, Thomas WK (2012) Metagenetic community analysis of microbial eukaryotes illuminates biogeographic patterns in deep-sea and shallow water sediments. *Molecular Ecology*. **21**(5): 1048-1059.

Blanchard GF (1990) Overlapping microscale dispersion patterns of meiofauna and microphytobenthos. *Marine Ecology Progress Series*. **68**: 101-111.

Bode A, Álvarez-Ossorio MT, González N, Lorenzo J, Rodríguez C, Varela M, Varela MM (2005) Seasonal variability of plankton blooms in the Ria de Ferrol (NW Spain): II. Plankton abundance, composition and biomass. *Estuarine Coastal and Shelf Science*. **63**: 285-300.

Boyd PW, Strzepek R, Fu F, Hutchins DA (2010) Environmental control of open-ocean phytoplankton groups: now and in the future. *Limnology and Oceanography*. **55**: 1353-1376.

Brad T, Braster M, van Breukelen BM, van Straalen NM, Röling WF. (2008) Eukaryotic Diversity in an Anaerobic Aquifer Polluted with Landfill Leachate. *Applied and Environmental Microbiology*. **71**(13): 3959-3958.

Brookes JD, Lamontagne S, Alridge KT, Bengler S, Bissett A, Bucater L, Cheshire AC, Cook PLM, Deegan BM, Dittmann S, Fairweather PG, Fernandes MB, Ford PW, Geddes MC, Gillanders BM, Grig NJ, Haese RR, Krull E, Langley RA, Lester RE, Loo M, Munro AR, Noell CJ, Nayar S, Paton DC, Revill AT, Rogers DJ, Rolston A, Sharma SK, Short DA, Tanner JE, Webster IT, Wellman NR, Ye Q (2009) An Ecosystem Assessment Framework to Guide Management of the Coorong: Final Report of the CLLAMMecology Research Cluster C.W.f.a.H.C.N.R. Flagship, ed. (Canberra). 61 pp.

Brunner E, Gröger C, Lutz K, Richthammer P, Spinde K, Sumper M (2009) Analytical studies of silica biomineralization: towards an understanding of silica processing by diatoms. *Applied Microbiology and Biotechnology*. **84**: 607-616.

Bryant DA, Garcia Costas AM, Maresca JA, Gomez A, Chew M, Klatt CG, Bateson MM, Tallon LJ, Hostetler J, Nelson WC, Heidelberg JF, Ward DM. (2007) *Candidatus Chloracidobacterium thermophilum*: An Aerobic Phototrophic Acidobacterium. *Science*. **317** (5837): 523-526.

Bureau of Meteorology (2013). Meningie and Encounter Bay Weather Station data 2009-2010.

Buric Z, Cetinić I, Viličić D, Mihalić KC, Carić M, Olujić G (2007) Spatial and temporal distribution of phytoplankton in a highly stratified estuary (Zrmanja, Adriatic Sea). *Marine Ecology*. **28**: 169-177.

Burson A, Stomp M, Akil L, Brussaard CPD, Huisman J. (2016) Unbalanced reuction of nutrient loads has created an offshore gradient from phosphorus to nitrogen limitation in the North Sea. *Limnology and Oceanography*. 61: 869-888.

Canion A, McIntyre HL, Phipps S. (2013) Short-term to seasonal variability in factors driving primary productivity in a shallow estuary: Implications for modelling production. *Estuarine, Coastal and Shelf Science*. **131**: 224-234.

Carr M-E, Friedrichs MAM, Schmeltz M, Aita MN, Antoine D, Arrigo KR, Asanuma I, Aumont O, Barber R, Behrenfeld M, Bidigare R, Buitenhuis ET, Campbell K, Ciotti A, Dierssen H, Dowell M, Dunne J, Esaias W, Gentili B, Gregg W, Groom S, Hoepffner N, Ishizaka J, Kameda T, Le Quéré C, Lohrenz S, Marra J, Mélin F, Moore K, Morel A, Reddy TE, Ryan J, Scardi M, Smyth T, Turpie K, Tilstone G, Waters K, Yamanaka Y. (2006) A comparison of global estimates of marine primary production from ocean color. *Deep-Sea Research Part II*. **53**: 741-770.

Carstensen J, Klais R, Cloern JE. (2015) Phytoplankton blooms in estuarine and coastal waters: Seasonal patterns and key species. *Estuarine, Coastal and Shelf Science*. **162**: 98-109.

Cetinić I, Viličić D, Buric Z, Olujić G (2006). Phytoplankton seasonality in a highly stratified karstic estuary (Krka, Adriatic Sea). *Hydrobiologia*. **555**: 31-40.

Chang K-H, Doi H, Nishibe Y, Nam G-S, Nakano S-I. (2014) Feeding behaviour of the copepod *Temora turbinata*: clearance rate and prey preference on the diatom and microbial food web components in coastal area. *Journal of Ecology and Environment*. **37**(4): 225-229.

Chepurnov VA, Mann DG, von Dassow P, Vanormelingen P, Gillard J, Inzé D, Sabbe K, Vyverman W. (2008). In search of new tractable diatoms for experimental biology. *BioEssays*. **30**(7): 692-702.

Chon T-S, Qu X, Cho W-S, Hwang H-J, Tang H, Liu Y, Choi J-H, Jung M, Chung BS, Lee HY, Chung YR, Koh S-C (2013) Evaluation of stream ecosystem health and species

association based on multi-taxa (benthic macroinvertebrates, algae, and microorganisms) patterning with different levels of population. *Ecological Informatics*. **17**: 58-72.

Chow C-ET, Kim DY, Sachdeva R, Caron DA, Fuhrman JA. (2014) Top-down controls on bacterial community structure: microbial network analysis of bacteria, T4-like viruses and protists. *The ISME Journal*. **8**: 816-829.

Cibils L, Principe R, Márques J, Gari N, Albariño. (2015) Functional diversity of algal communities from headwater grassland streams: How does it change following afforestation? *Aquatic Ecology*. **49**: 453-466.

Clarke K. (1993). Non-Parametric multivariate analyses of changes in community structure. *Australian Journal of Ecology*. **18**: 117-143.

Clarke KR, Gorley RN. (2015). PRIMER v7: User Manual/Tutorial. PRIMER-E Ltd., Plymouth, 296pp

Clarke KR, Warwick RM (2001) Change in Marine Communities: An Approach to Statistical Analysis and Interpretation, 2nd Edition PRIMER-E Ltd., Plymouth.

Cloern JE, Dufford R. (2005) Phytoplankton community ecology: principles applied in San Francisco Bay. *Marine Ecology Progress Series*. **285**: 11-28

Cloern JE, Foster SQ, Kleckner AE. (2014) Phytoplankton primary production in the world's estuarine-coastal ecosystems. *Biogeosciences*. **11**: 2477-2501.

Cox MP, Peterson DA, Biggs PJ (2010) Solexaqa: At-a-glance quality assessment of Illumina second-generation sequencing data. *BMC Bioinformatics*. **11**: 485.

D'Alelio D, d'Alcalá MR, Dubroca L, Sarno D, Zingone A, Montresor M (2010) The time for sex: A biennial life cycle in a marine planktonic diatom. *Limnology and Oceanography*. **55**(1): 106-114.

Dann LM, Mitchell JG, Speck PG, Newton K, Jeffries T, Paterson J. (2014). Virio- and Bacterioplankton Microscale Distributions at the Sediment-Water Interface. *PLoS One*. **9** (7): e102805.

DeMartino A, Meichenin A, Shi J, Pan K, Bowler C. (2007). Genetic and phenotypic characterisation of *Phaeidactylum tricornutum* (Bacillariophyceae) accessions. *Journal of Phycology*. **43**: 992-1009.

Domingues RB, Guerra CC, Barbosa AB, Galvão HM. (2015) Are nutrients and light limiting summer phytoplankton in a temperate coastal lagoon. *Aquatic Ecology*. **49**(2): 127-146.

Donald DB, Bogard MJ, Finlay K, Bunting L, Leavitt PR. (2013) Phytoplankton-Specific Response to Enrichment of Phosphorus-Rich Surface Waters with Ammonium, Nitrate, and Urea. *PLoS One*. **8**(1): e53277.

Doubell MJ, Seuront L, Seymour JR, Patten NL, Mitchell JG. (2006) High-Resolution Fluorometer for Mapping Microscale Phytoplankton Distributions. *Applied and Environmental Microbiology*. **72**(6): 4475-4478.

Doubell MJ, Prairie JC, Yamazaki H. (2012) Millimeter scale profiles of chlorophyll fluorescence: Deciphering the microscale spatial structure of phytoplankton. *Deep-Sea Research II*. **101**: 207-215.

Dugdale, R. C. and Wilkerson, F. P. (1998). Silicate regulation of new production in the equatorial Pacific upwelling. *Nature*. **391**(6664): 270–273.

Edgar RC, Haas BJ, Clemente JC, Quince C, Knight R. (2011) UCHIME improves sensitivity and speed of chimera detection. *Bioinformatics*. **27**(16): 2194-2200.

Eigemann F, Hilt S, Salka I, Grossart H-P. (2013) Bacterial community composition associated with freshwater algae: species specificity vs. dependency on environmental conditions and source community. *FEMS Microbiology Ecology*. **83**: 650-663.

Fang J, Hasiotis ST, Gupta SD, Brake SS, Bazylinski DA. (2007) Microbial biomass and community structure of a stromatolite from an acid mine drainage system as determined by lipid analysis. *Chemical Geology*. **243**: 191-204.

Faust K, Raes J. (2012) Microbial interactions: from networks to models. *Nature Reviews Microbiology*. **10**: 538-550.

Faust K, Lahti L, Gonze D, de Vos WM, Raes J. (2015) Metagenics meets time series analysis: unravelling microbial community dynamics. *Current Opinion in Microbiology*. **25**: 56-66.

Feely RA, Alin SR, Newton J, Sabine CL, Wamer M, Devol A, Krembs C, Maloy C. (2010). The combined effects of ocean acidification, mixing and respiration on pH and carbonate saturation in an urbanized estuary. *Estuarine, Coastal and Shelf Science*. **88**: 442-449.

Finkel ZV, Katz ME, Wright JD, Schofield OME, Falkowski PG. (2005). Climatically driven macroevolutionary patterns in the size of marine diatoms over the Cenozoic. *Proceedings of the National Academy of Science*. **102**(25): 8927-8932.

Finlay BJ. (2002) Global Dispersal of Free-Living Microbial Eukaryote Species. *Science*. **296**: 1061-1063.

Franks PJS, Jaffe JS. (2008). Microscale variability in the distributions of large fluorescent particles observed in situ with a planar laser imaging fluorometer. *Journal of Marine Systems*. **69**: 254-270.

Fuhrman JA (2009) Microbial community structure and its functional implications. *Nature*. **459**: 193-199.

Gallegos, C.L., Jordan, T.E., and Hedrick, S.S. (2010). Long-term dynamics of phytoplankton in the Rhode River, Maryland (USA). *Estuaries and Coasts*. **33**: 471-484.

Garrido M, Cecchi P, Collos Y, Agostini S, Pasqualini V. (2016) Water flux management and phytoplankton communities in a Mediterranean coastal lagoon. Part I: How to promote dinoflagellate dominance? *Marine Pollution Bulletin*. **104**: 139-152.

Gell, P. A., Bulpin, S., Wallbrink, P., Hancock, G., Bickford, S. (2005). Tareena Billabong - a palaeolimnological history of an ever-changing wetland, Chowilla Floodplain, lower Murray-Darling Basin, Australia. *Marine and Freshwater Research*. **56**: 441-456.

George J, Lonsdale D, Merlo L, Gobler C. (2015). The interactive roles of temperature, nutrients, and zooplankton grazing in controlling the winter-spring phytoplankton bloom in a temperate, coastal ecosystem, Long Island Sound. *Limnology and Oceanography*. **60**: 110-126.

Gilbert JA, Steele JA, Caporaso G, Steinbrück L, Reeder J, Temperton B, Huse S, McHardy AC, Knight R, Joint I, Somerfield P, Fuhrman JA, Field D. (2012) Defining seasonal marine microbial community dynamics. *The ISME Journal*. **6**: 298-308.

Godhe A, Egardt J, Kleinhans D, Sundqvist L, Hordoir R, Jonsson PR (2013) Seascape analysis reveals regional gene flow patterns among populations of a marine planktonic diatom. *Proceedings of the Royal Society B*. **280**: 20131599

Gower JC (1966) Some distance properties of latent root and vector methods used in multivariate analysis. *Biometrika*. **53**(3-4): 325-338.

Grossart H-P, Levold F, Allgaier M, Simon M, Brinkhoff T. (2005) Marine diatom species harbour distinct bacterial communities. *7*(6): 860-873.

Halsey KH, Jones BM (2015) Phytoplankton Strategies for Photosynthetic Energy Allocation. *Annual Review of Marine Science*. **7**: 265-297.

Hansen B, Bjornsen PK, Hansen PJ (1994) The size ratio between planktonic predators and their prey. *Limnology and Oceanography*. **39**(2): 395-403.

Hansen P. (2002). Effect of high pH on the growth and survival of marine phytoplankton. *Aquatic Microbial Ecology*. **28**: 279-288.

Hill VJ, Matrai PA, Olson E, Suttles S, Steele M, Codispoti LA, Zimmerman RC. (2013) Synthesis of integrated primary production in the Arctic Ocean: II. In situ and remotely sensed estimates. *Progress in Oceanography*. **110**: 107-125.

Hillebrand H, Kahlert M, Haglund AL, Berninger UG, Nagel S, Wickham S. (2002). Control of microbenthic communities by grazing and nutrient supply. *Ecology*. **83**: 2205-2219.

Holland HD. (2006) The oxygenation of the atmosphere and oceans. *Philosophical Transactions of the Royal Society B*. **361**: 903-915.

Holm S. (1979). A Simple Sequentially Rejective Multiple Test Procedure. *Board of the Foundation of the Scandinavian Journal of Statistics*. **6**: 65-70.

Ichinomiya M, Lopes dos Santos A, Gourvil P, Yoshikawa S, Kamiya M, Ohki K, Audic S, de Vargas C, Noël M-H, Vaultot D, Kuwata A. (2016) Diversity and oceanic distribution of

the Parmales (Bolidophyceae), a picoplanktonic group closely related to diatoms. *The ISME Journal*. doi: 10.1038/ismej.2016.38.

Interlandi SJ, Kilham SS. (2001). Limiting resources and the regulation of diversity in phytoplankton communities. *Ecology*. **82**: 1270-1282.

Jendyk, J., Hemraj, D., Brown, M., Ellis, A., and Leterme, S. (2014). Environmental variability and phytoplankton dynamics in a South Australian inverse estuary. *Continental Shelf Research*. **91**: 134-144.

Jeong HJ, Lim AS, Yoo YD, Lee MJ, Lee KH, Jang TY (2013) Feeding by Heterotrophic Dinoflagellates and Ciliates on the Free-living Dinoflagellate *Symbiodinium* sp. (Clade E). *Journal of Eukaryotic Microbiology*. **0**: 1-15

Jesus B, Mendes CR, Brotas V, Paterson DM (2006) Effect of sediment type on microphytobenthos vertical distribution: Modelling the productive biomass and improving ground truth measurements. *Journal of Experimental Marine Biology and Ecology*. **332**: 60-74.

Jin J, Liu SM, Ren JL, Lue CG, Zhang J, Zhang GL, Huang DJ (2013) Nutrient dynamics and coupling with phytoplankton species composition during the spring blooms in the Yellow Sea. *Deep Sea Research Part II: Topical Studies in Oceanography*. **97**: 16-32.

Jones AC, Liao TSV, Najjar FZ, Roe BA, Hambright KD, Caron DA (2013) Seasonality and disturbance: annual pattern and response of the bacterial and microbial eukaryotic assemblages in a freshwater ecosystem. *Environmental Microbiology*. **15**(9): 2557-2572.

Jones, V. (2007) Diatom Introduction. *Encyclopedia of Quaternary Science*. Ed: Elias SA. (Elsevier Science) pp. 523-529

- Kamiyama T, Satoshi A (2001) Feeding characteristics of two tintinnid ciliate species on phytoplankton including harmful species: effects of prey size on ingestion rates and selectivity. *Journal of Experimental Marine Biology and Ecology*. **257**(2): 281-296.
- Kamp A, Stief P, Knappe K, de Beer D. (2013) Response of the Ubiquitous Pelagic Diatom *Thalassiosira weissflogii* to Darkness and Anoxia. *PLoS One*. **8**(12): e82605.
- Kämpf J. (2014). South Australia's Large Inverse Estuaries: On the Road to Ruin. In *Estuaries of Australia in 2050 and beyond*. Ed: E. Wolanski (Springer Netherlands) pp. 153-166.
- Keeling PJ, Burki F, Wilcox HM, Allam B, Allen EE, Amaral-Zettler LA, et al. (2014) The Marine Microbial Eukaryote Transcriptome Sequencing Project (MMETSP): Illuminating the Functional Diversity of Eukaryotic Life in the Oceans through Transcriptome Sequencing. *PLoS Biology*. **12**(6): e1001889.
- Kelly JA, Honeywill C, Paterson DM (2001) Microscale analysis of chlorophyll-a in cohesive, intertidal sediments: the implications of microphytobenthos distribution. *Journal of the Marine Biological Association of the UK*. **81**: 151-162.
- Kennington K. (2002) Chapter 8: the Environmental Applications of Diatoms. In *Quaternary Environmental Micropaleontology*. Ed: Haslett SK. (Hodder Headline Group, London) pp. 167-184
- Kimmerer WJ, Parker AE, Lidström UE, Carpenter EJ. (2012). Short-term and interannual variability in primary production in the low-salinity zone of the San Francisco Estuary. *Estuaries and Coasts*. **35**: 913-929.

Kipriyanova LM, Yermolaeva NI, Bezmaternykh DM, Dvurechenskaya SY, Mitrofanova EY. (2007). Changes in the biota of Chany Lake along a salinity gradient. *Hydrobiologia*. **576**: 83-93.

Kireta AR, Reavie ED, Sgro GV, Angradi TR, Bolgrien DW, Hill BH, Jicha TM (2012) Planktonic and periphytic diatoms as indicators of stress on great rivers of the United States: Testing water quality and disturbance models. *Ecological Indicators*. **13**: 222-231.

Kirkwood AE, Henley WJ. (2006). Algal community dynamics and halotolerance in a terrestrial hypersaline environment. *Journal of Phycology*. **42**: 537-547.

Kissman CEH, Williamson CE, Rose KC, Saros JE. (2013) Response of phytoplankton in an alpine lake to inputs of dissolved organic matter through nutrient enrichment and trophic forcing. *Limnology and Oceanography*. **58**(3): 867-880.

Kobbi-Rebai R, Annabi-Trabelsi N, Khemakhem H, Ayadi H, Aleya L. (2013) Impacts of restoration of an uncontrolled phosphogypsum dumpsite on the seasonal distribution of abiotic variables, phytoplankton, copepods, and ciliates in a man-made solar saltern. *Environmental Monitoring and Assessment*. **185**: 2139-2155.

Kotwicki L, Grzelak K, Czub M, Dellwig O, Gentz T, Szymczycha B, Böttcher MÉ (2013). Submarine groundwater discharge to the Baltic coastal zone: Impacts on the meiofaunal community. *Journal of Marine Systems*. doi: 10.1016/j.jmarsys.2013.06.009

Krause JW, Nelson DM, Brzezinski MA. (2011). Biogenic silica production and the diatom contribution to primary production and nitrate uptake in the eastern equatorial Pacific Ocean. *Deep Sea Research II*. **58**: 434-448.

Kroger N (2001) The sweetness of diatom molecular engineering. *Journal of Phycology*. **37**: 657-658.

- Kuwahara VS, Leong SCY. (2015) Spectral fluorometric characterisation of phytoplankton types in the tropical coastal waters of Singapore. *Journal of Experimental Marine Biology and Ecology*. **466**: 1-8.kobbi
- Lagaria A, Psarra S, Lefèvre D, Wambeke FV, Courties C, Pujon-Pay M, Oriol L, Tanaka T, Christaki U. (2011). The effects of nutrient additions on particulate and dissolved primary production and metabolic state in surface waters of three Mediterranean eddies. *Biogeosciences*. **8**: 2595-2607.
- Larsen A, Egge JK, Nejstgaard JC, Di Capua I, Thyrraug R. (2015) Contrasting response to nutrient manipulation of Arctic mesocosms are reproduced by a minimum microbial food web model. *Limnology and Oceanography*. **60**: 360-374.
- Larson CA, Belovsky GE. (2013) Salinity and nutrients influence species richness and evenness of phytoplankton communities in microcosm experiments from Great Salt Lake, Utah, USA. *Journal of Plankton Research*. doi: 10.1093/plankt/fbt053.
- Lau MCY, Aitchison JC, Pointing SB. (2009) Bacterial community composition in thermophilic microbial mats from five hot springs in central Tibet. *Extremophiles*. **13**(1): 139-149.
- Leland HV, Brown LR, Mueller DK. (2001). Distribution of algae in the San Joaquin River, California, in relation to nutrient supply, salinity and other environmental factors. *Freshwater Biology*. **46**: 1139-1167.
- Leterme SC, Allais L, Jendyk J, Hemraj DA, Newton K, Mitchell J, Shanafield M. (2015) Drought Conditions and recovery in the Coorong wetland, South Australia in 1997-2013. *Estuarine, Coastal and Shelf Science*. **163**: 175-184.

- Leterme SC, Ellis AV, Mitchell J, Buscot M.J, Pollet T, Schapira M, Seuront L. (2010) Morphological flexibility of *Cocconeis placentula* (Bacillariophyceae) nanostructure to changing salinity levels. *Journal of Phycology*. **46**: 715-719.
- Leterme SC, Prime E, Mitchell J, Brown, MH, and Ellis AV (2013). Diatom adaptability to environmental change: a case study of two *Cocconeis* species from high-salinity areas. *Diatom Research*. **28**: 29-35.
- Lie AAY, Kim DY, Schnetzer A, Caron DA (2013) Small-scale temporal and spatial variations in protistan community composition at the San Pedro Ocean Time-series station off the coast of southern California. *Aquatic Microbial Ecology*. **70**: 93-110.
- Light BR, Beardall J. (2001) Photosynthetic characteristics of sub-tidal benthic microalgal populations from a temperate, shallow water marine ecosystem. *Aquatic Botany*. **70**: 9–27.
- Litchman E, Edwards KF, Klausmeier CA, Thomas MK. (2012). Phytoplankton niches, traits and eco-evolutionary responses to global environmental change. *Marine Ecology Progress Series*. **470**: 235-248.
- Liu D, Morrison RJ, West RJ. (2013) Phytoplankton assemblages of two intermittently open and closed coastal lakes in SE Australia. *Estuarine, Coastal and Shelf Science*. **132**: 45-55.
- Liu Y, Zhang J, Zhao L, Zhang X, Xie, S. (2014) Spatial distribution of bacterial communities in high-altitude freshwater wetland sediment. *Limnology*. **15**(3): 249-256.
- Loir M. (2004). Guide des diatomées (France: Delachaux et Nèstlé).
- Lopes C, Mix AC, Abrantes F. (2006). Diatom in northeast Pacific surface sediments as paleoceanographic proxies. *Marine Micropaleontology*. **60**: 45-65.

- Ly J, Phillipart CJM, Kromkamp JC. (2014) Phosphorus limitation during a phytoplankton spring bloom in the western Dutch Wadden Sea. *Journal of Sea Research*. **88**: 109-120.
- Ma AT, Daniels EF, Gulizia N, Brahamsha B. (2016) Isolation of diverse amoebal grazers of freshwater cyanobacteria for the development of systems to study predator-prey interactions. *Algal Research*. **13**: 85-93.
- Macedo MF, Duarte P, Mendes P, Ferreira JG. (2001). Annual variation of environmental variables, phytoplankton species composition and photosynthetic parameters in a coastal lagoon. *Journal of Plankton Research*. **23**: 719-732.
- MacIntyre HL, Geider RJ, Miller DC. (1996) Microphytobenthos: The ecological role of the “secret garden” of unvegetated shallow-water marine habitats. I. Distribution, abundance and primary production. *Estuaries*. **19**(2): 186-201.
- Mahadevan A, D'Asaro E, Lee C, Perry MJ (2012). Eddy-driven stratification initiates North Atlantic spring phytoplankton blooms. *Science*. **337**: 54-58.
- Mann DG, Vanormelingen P. (2013) An Inordinate Fondness? The Number, Distributions, and Origins of Diatom Species. *Journal of Eukaryotic Microbiology*. **60**: 414-420
- McInnes AS, Nunnally CC, Rowe GT, Davis RW, Quigg A. (2015) Undetected Blooms in Prince William Sound: Using Multiple Techniques to Elucidate the Base of the Summer Food Web. *Estuaries and Coasts*. **doi**: 10.1007/s12237-014-9924-0.
- McManus GB, Schoener DM, Haberlandt K. (2012) Chloroplast symbiosis in a marine ciliate: ecophysiology and the risks and rewards of hosting foreign organelles. *Frontiers in Microbiology*. **3**: 321-329.

Medley CN, Clements WH. (1998). Responses of diatom communities to heavy metals in streams: the influence of longitudinal variation. *Ecological Applications*. **8**: 631-644.

Mellard JP, Yoshiyama K, Klausmeier CA, Litchman E. (2012). Experimental test of phytoplankton competition for nutrients and light in poorly mixed water columns. *Ecological Monographs*. **82**: 239-256.

Mendenhall W, Beaver RJ, Beaver BM. (1999). Introduction to Probability and Statistics, 10th Edition edn (Boston, MA: Duxbury Press).

Meyer J, Löscher CR, Neulinger SC, Reichel AF, Loginova A, Borchard C, Schmitz RA, Hauss H, Kiko R, Rebesell U. (2016) Changing nutrient stoichiometry affects phytoplankton production, DOP accumulation and dinitrogen fixation – a mesocosm experiment in the eastern tropical North Atlantic. *Biogeosciences*. **13**: 892-794.

Mitchell JG, Fuhrman JA (1989) Centimeter scale vertical heterogeneity in bacteria and chlorophyll a. *Marine Ecology Progress Series*. **54**: 141-148.

Mitchell JG, Seuront L, Doubell MJ, Losic D, Voelcker NH, Seymour J, Lal R. (2013) Role of Diatom Nanostructures in Biasing Diffusion to Improve Uptake in a Patchy Nutrient Environment. *PLoS One*. **8**(5): e59548.

Montresor M, Lewis J. 2006. Phases, stages, and shifts in the life cycles of marine phytoplankton. In Algal cultures, analogues of blooms and applications. Ed: D. V. Subba Rao, *Science*. pp 91–129.

Moran MA. (2015) The global ocean microbiome. *Science*. **DOI**: 10.1126/science.aac8455.

Moran PAP (1950) Notes on continuous stochastic phenomena. *Biometrika*. **37**: 17–23.

- Morgan S, Fisher J, McAfee S, Largier J, Miller S, Sheridan M, Neigel J. (2014). Transport of Crustacean Larvae Between a Low-Inflow Estuary and Coastal Waters. *Estuaries and Coasts*. **37**: 1269-1283.
- Moustakas A (2015). Fire acting as an increasing spatial autocorrelation force: Implications for pattern formation and ecological facilitation. *Ecological Complexity*. **21**: 142-149.
- Murray-Darling Basin Authority (2013). Lower Lakes Barrage Open/Close Days 2008-2010 (Canberra, Australia).
- Nayar S, Loo MGK (2009) Phytoplankton and Phytobenthic Productivity along a Salinity Gradient in the Coorong and Murray Mouth. CSIRO: Water for a healthy country, National Research Flagship and South Australian Research and Development Institute (Aquatic Sciences, Adelaide), pp. 19.
- Needham M, Fuhrman JA. (2016) Pronounced daily succession of phytoplankton, archaea and bacteria following a spring bloom. *Nature Microbiology*. doi:10.1038/nmicrobiol.2016.5.
- Nübel U, Garcia-Pichel F, Kühl M, Muyzer G. (1999). Spatial scale and the diversity of benthic cyanobacteria and diatoms in a salina. *Hydrobiologia*. **401**: 199-206.
- Ólafsson E, Elmgren R. (1997). Seasonal Dynamics of Sublittoral meiobenthos in Relation to Phytoplankton Sedimentation in the Baltic Sea. *Estuarine Coastal and Shelf Science*. **45**: 149-164.
- Paerl H. (1984). Transfer of N₂ and CO₂ fixation products from *Anabaena oscillarioides* to associated bacteria during inorganic carbon sufficiency and deficiency. *Journal of Phycology*. **20**: 600-608.

- Palmer-Felgate E, Mortimer R, Krom M, Jarvie H, Williams R, Spraggs R, Stratford C. (2011). Internal loading of phosphorus in a sedimentation pond of a treatment wetland: Effect of a phytoplankton crash. *Science of the Total Environment*. **409**: 2222-2232.
- Pan J, Bournod CN, Cuadrado DG, Vitale A, Piccolo MC. (2013) Interaction between Estuarine Microphytobenthos and Physical Forcings: The Role of Atmospheric and Sedimentary Factors. *International Journal of Geosciences*. **4**:352-361.
- Paver SF, Hayek KR, Gano KA, Fagen JR, Brown CT, Davis-Richardson AG, Crabb DB, Rosario-Passapera R, Giongo A, Triplett EW, Kent AD. (2013) Interactions between specific phytoplankton and bacteria affect lake bacterial community succession. *Environmental Microbiology*. **DOI**: 10.1111/1462-2920.12131.
- Pedros-Alio C, Calderon-Paz JI, MacLean MH, Medina G, Marrase C, Gasol JM, Guixa-Boixereu N. (2000) The microbial food web along salinity gradients. *FEMS Microbiology Ecology*. **32**: 143-155.
- Pennisi E (2004). DNA Reveals Diatom's Complexity. *Science*. **306**: 31.
- Pete R, Davidson K, Hart MC, Gutierrez T, Miller AEJ. (2010). Diatom derived dissolved organic matter as a driver of bacterial productivity: the role of nutrient limitation. *Journal of Experimental Marine Biology and Ecology*. **391**: 20-26.
- Philps E, Badylak S, Christmas MC, Lasi MA. (2010). Climatic trends and patterns of phytoplankton composition, abundance and succession in the Indian River Lagoon, Florida, USA. *Estuaries and Coasts*. **33**: 498-512.
- Pinckney JL, Benitez-Nelson CR, Thunell RC, Muller-Karger F, Lorenzoni L, Troccoli L, Varela R (2015) Phytoplankton community structure and depth distribution changes in the Cariaco Basin between 1996 and 2010. *Deep-Sea Research I*. **101**:27-37.

Pniewski F, Biskup P, Bubak I, Richard P, Latala A, Blanchard G. (2015) Photo-regulation in microphytobenthos from intertidal mudflats and non-tidal coastal shallows. *Estuarine, Coastal and Shelf Science*. **152**: 153-161.

Pratt DR, Pilditch CA, Lohrer AM, Thrush SF, Kraan C. (2014) Spatial Distributions of Grazing Activity and Microphytobenthos Reveal Scale-Dependent Relationships Across a Sedimentary Gradient. *Estuaries and Coasts*. **38**: 722-724.

Quigg A, Nunnally CC, McInnes AS, Gay S, Rowe GT, Dellapenna TM, Davis RW. (2013) Hydrographic and biological controls in two subarctic fjords: an environmental case study of how climate change could impact phytoplankton communities. *Marine Ecology Progress Series*. **480**: 21-37.

Quinlan EL, Philips EJ. (2007). Phytoplankton assemblages across the marine to low-salinity transition zone in a blackwater dominated estuary. *Journal of Plankton Research*. **29**: 401-416.

Ramsar Secretariat. (2014) Introducing the Convention on Wetlands. Ramsar Convention Secretariat, Switzerland.

Range P, Piló D, Ben-Hamadou R, Chícharo MA, Matias D, Joaquim S, Oliveira AP, Chícharo L. (2012). Seawater acidification by CO₂ in a coastal lagoon environment: effects on life history traits of juvenile mussels *Mytilus galloprovincialis*. *Journal of Experimental Marine Biology and Ecology*. **424-425**: 89-98.

Raven PH, Evert RF, Eichhorn SE. (2005) Biology of Plants. 7th Edition. W.H. Freeman and Company, New York. p 314.

Raven JA (2012) Dispatch: Algal Biogeographic: Metagenomics Shows Distribution of a Picoplanktonic Pelagophyte. *Current Biology*. **22** (17): R682-R683.

Ritchie RJ (2006). Consistent sets of spectrophotometric chlorophyll equations for acetone methanol and ethanol solvents. *Photosynthesis Research*. **89**: 27-41.

Ritchie RJ (2008). Universal chlorophyll equations for estimating chlorophylls a, b, c and d and total chlorophylls in natural assemblages of photosynthetic organisms using acetone, methanol, or ethanol solvents. *Photosynthetica*. **46**(1): 115-126.

Rodrigues E, Pardal M. (2015). Primary Productivity Temporal Fluctuations in a Nutrient-Rich Estuary due to Climate-Driven Events. *Estuaries and Coasts*. **38**: 1-12.

Rossi S, Bramanti L, Broglio E, Gili JM (2012). Trophic impact of long-lived species indicated by population dynamics in the short-lived hydrozoans *Eudendrium racemosum*. *Marine Ecology Progress Series*. **467**: 97-111.

Rost B, Richter KU, Riebesell U, Hansen PJ. (2006). Inorganic carbon acquisition in red tide dinoflagellates. *Plant, Cell & Environment*. **29**: 810-822.

Round FE, Crawford RM, Mann DG. (1990) The Diatoms: Biology & Morphology of the Genera. Cambridge University Press, United Kingdom. 751 pp.

Ruan Q, Dutta D, Schwalbach MS, Steele JA, Fuhrman JA, Sun F. (2006) Local similarity analysis reveals unique associations among marine bacterioplankton species and environmental factors. *Bioinformatics*. **22**(20): 2532-2538.

Ruthenbeck G, Smith R, Tobe S (in prep.) B-REXml - Rapid analysis of BLAST results.

Ryves DB, Anderson NJ, Flower RJ, Rippey B. (2013) Diatom taphonomy and silica cycling in two freshwater lakes and their implications for inferring past lake productivity. *Journal of Paleolimnology*. **49**(3): 411-430.

SA Water (2013). Pipelines.

Sæther B-E, Engen S, Grøtan V. (2013) Species Diversity and community similarity in fluctuating environments: parametric approaches to using species abundance distributions. *Journal of Animal Ecology*. **82**(4): 721-728.

Salni K, Bengtsson-Palme J, Nilsson RH, Kristiansson E, Rosenblad MA, Blanck H, Ericksson KM. (2015) Metagenomic sequencing of marine periphyton: taxonomic and functional insights into biofilm communities. *Frontiers in Microbiology*. **6**: 1192

Sandulli R, Pinckney J. (1999) Patch sizes and spatial patterns of meiobenthic copepods and benthic microalgae in sandy sediments: a microscale approach. *Journal of Sea Research*. **41**: 179-187.

Saros JE, Fritz SC. (2002). Resource competition among saline-lake diatoms under varying N/P ratio, salinity and anion composition. *Freshwater Biology*. **47**: 87-95.

Schapira, M., Buscot, M.J., Leterme, S.C., Pollet, T., Chapperon, C. and Seuront, L. (2009) Distribution of heterotrophic bacteria and virus-like particles along a salinity gradient in a hypersaline coastal lagoon. *Aquatic Microbial Ecology*. **54**: 171-183.

Schapira, M., Buscot, M.-J., Pollet, T., Leterme, S. and Seuront, L. (2010) Distribution of picophytoplankton communities from brackish to hypersaline waters in a south australian coastal lagoon. *Saline Systems*. **6**: 2.

Schmieder R, Edwards R. (2011a) Quality control and preprocessing of metagenomic datasets. *Bioinformatics*. **27**: 863-864.

Schmieder R, Edwards R. (2011b) Fast Identification and Removal of Sequence Contamination from Genomic and Metagenomic Datasets. *PLoS One*. **6**(3): e17288.

Seuront L, Spilmont N (2002) Self-organised criticality in intertidal microphytobenthos patch patterns. *Physica A*. **313**: 513-539.

Seymour JR, Mitchell JG, Pearson L, Waters R (2000) Heterogeneity in bacterioplankton abundance from 4.5 millimetre resolution sampling. *Aquatic Microbial Ecology*. **22**: 143–153.

Seymour JR, Seuront L, Mitchell JG (2005) Microscale and small-scale temporal dynamics of a coastal planktonic microbial community. *Marine Ecology Progress Series*. **300**: 21-37.

Seymour JR, Seuront L, Doubell M, Waters RL, Mitchell JG. (2006) Microscale patchiness of virioplankton. *Journal of the Marine Biology Association of the United Kingdom*. **86**: 551-561.

Seymour JR, Seuront L, Mitchell JG (2007) Microscale gradients of planktonic microbial communities above the sediment surface in a mangrove estuary. *Estuarine, Coastal and Shelf Science*. **73**: 651-666.

Sherr EB, Sherr BF. (2002) Significance of predation of protists in aquatic microbial food webs. *Antonie van Leeuwenhoek*. **81**: 293-308.

Simon KS, Pipan T, Culver DC. (2003) Spatial and temporal heterogeneity in the flux of organic carbon in caves. Eds: Riberio L, Stigter TY, Chambel A, Condesso de Melo MT, Monteiro JP, Medeiros A. In: *Groundwater and Ecosystems, IAH Selected Papers on Hydrogeology*, CRC Press/Balkema, Leiden, the Netherlands.

Sison-Mangus MP, Jiang S, Tran KN, Kudela R. (2014) Host-specific adaptation governs the interaction of the marine diatom, *Pseudo-nitzschia* and their microbiota. *The ISME Journal*. **8**: 63-76.

Sjöqvist C, Godhe A, Jonsson PR, Sundqvist L, Kremp A (2015). Local adaptation and oceanographic connectivity patterns explain genetic differentiation of a marine diatom across the North Sea-Baltic Sea salinity gradient. *Molecular Ecology*. doi: 10.1111/mec.13208

Smith MJ, Schreiber ESG, Kohout M, Ough K, Lennie R, Turnbull D, Jin C, Clancy T. (2007). Wetlands as landscape units: spatial patterns in salinity and water chemistry. *Wetlands Ecology and Management*. **15**: 95-103.

Sokal RR (1978) Spatial autocorrelation in biology: 1. Methodology. *Biological Journal of the Linnean Society*. **10**: 199–228.

Sonneman JA, Sincock J, Fluin J, Reid M, Newall P, Tibby J, Gell P. (2000). An Illustrated Guide to Common stream Diatom Species from Temperate Australia, Vol Identification Guide No 33 (Cooperative Research Centre for Freshwater Ecology).

Spilmont N, Davoult D, Migné A. (2006) Benthic primary production during emersion: In situ measurements and potential primary production in the Seine Estuary (English Channel, France). *Marine Pollution Bulletin*. **53**: 49-55.

Spilmont N, Seuront L, Meziane T, Welsh DT (2011) There's more to the picture than meets the eye: Sampling microphytobenthos in a heterogeneous environment. *Estuarine, Coastal and Shelf Science*. **95**: 470-476.

Stanish LF, O'Neill SP, Gonzalez A, Legg TM, Knelman J, McKnight DM, Spaulding S, Nemergut DR. (2013) Bacteria and diatom co-occurrence patterns in microbial mats from polar desert streams. *Environmental Microbiology*. **15**(4): 1115-1131.

Steele JA, Countway PD, Xia L, Vigil PD, Beman JM, Kim DY, Chow C-ET, Sachdeva R, Jones AC, Schwalbach MS, Rose JM, Hewson I, Patel A, Sun F, Caron DA, Fuhrman JA.

(2011) Marine bacterial, archeal and protistan association networks reveal ecological linkages. *The ISME Journal*. **5**(9): 1414-1425.

Stocker R, Seymour JR (2012) Ecology and Physics of Bacterial Chemotaxis in the Ocean. *Microbiology and Molecular Biology Reviews*. **76**(4): 792 – 812.

Stocker R, Seymour JR, Samadani A, Hunt DE, Polz MF (2008) Rapid chemotactic response enables marine bacteria to exploit ephemeral microscale nutrient patches. *Proceedings of the National Academy of Science*. **105**(11): 4209-4214.

Stocker R. (2012) Marine Microbes See a Sea of Gradients. *Science*. **338**: 628-633.

Stoecker DK, Johnson MD, De Vargas C, Not F. (2009) Acquired phototrophy in aquatic protists. *Aquatic Microbial Ecology*. **57**: 279-310.

Straile D. (1997) Gross growth efficiencies of protozoan and metazoan zooplankton and their dependence on food concentration, predator-prey weight ratio, and taxonomic group. *Limnology and Oceanography*. **42**(6): 1375-1385.

Strickland JH, Parsons TR. (1972). A Practical Handbook of Sea Water Analysis, 2nd Edition. Bulletin Fisheries Research Board of Canada. 310pp.

Suikkanen S, Laamanen M, Huttunen M. (2007). Long-term changes in summer phytoplankton communities of the open northern Baltic Sea. *Estuarine Coastal and Shelf Science*. **71**: 580-592.

Tréguer PJ, De La Rocha CL (2013). The World Ocean Silica Cycle. *Annual Review of Marine Science*. DOI: 10.1146/annurev-marine-121211-172346.

Tamura K, Peterson D, Peterson N, Stecher G, Nei M, Kumar S. MEGA5: molecular evolutionary genetics analysis using maximum likelihood, evolutionary distance and maximum parsimony methods. *Molecular Biology and Evolution*. **28**(10): 2731-2739.

Tan X, Ma P, Bunn SE, Zhang Q (2015) Development of a benthic diatom index of biotic integrity (BD-IBI) for ecosystem health assessment of human dominant subtropical rivers, China. *Journal of Environmental Management*. **151**: 286-294.

Tekwani N, Majdi N, Mialet B, Tornés E, Urrea-Clos G, Buffan-Dubau E, Sabater S, Tackx M. (2013) Contribution of epilithic diatoms to benthic-pelagic coupling in a temperate river. *Aquatic Microbial Ecology*. **69**: 47-57.

Thomas MK, Kremer CT, Klausmeier CA, Litchman E. (2012) A Global Pattern of Thermal Adaptation in Marine Phytoplankton. *Science*. **388**(6110): 1085-1088.

Thompson PA, O'Brien TD, Paerl HW, Peierls BL, Harrison PJ, Robb M. (2015) Precipitation as a driver of phytoplankton ecology in coastal waters: A climatic perspective. *Estuarine, Coastal and Shelf Science*. **165**(5): 119-129.

Togerson WS (1958) Theory and methods of scaling. New York: Wiley. 460pp.

Tomas CR. (1997). Identifying Marine Phytoplankton. (Academic Press, San Diego USA).

Van de Poll WH, Kulk G, Timmermans KR, Brussaard CPD, van der Woerd HJ, Kehoe MJ, Mojica KDA, Visser RJW, Rozema PD, Buma AGJ. (2013) Phytoplankton chlorophyll a biomass, composition, and production along a temperature and stratification gradient in the northeast Atlantic Ocean. *Biogeosciences*. **10**: 4227- 4240.

Vanormelingen P, Vanellander B, Shinya S, Gillard J, Trobajo R, Sabbe K, Vyverman W. (2013) Heterthallic sexual reproduction in the model diatom *Cylindrotheca*. *European Journal of Phycology*. **48**(1): 93-105.

Vidussi F, Mostajir B, Fouilland E, Floc'h EL, Nouguyier J, Roques C, Got P, Thibault-Botha D, Bouvier T, Troussellier M. (2011). Effects of experimental warming and increased ultraviolet B radiation on the Mediterranean plankton food web. *Limnology and Oceanography*. **56**: 206-218.

Vieira S, Ribeiro L, da Silva JM, Cartaxana P. (2013) Effects of short-term changes in sediment temperature on the photosynthesis of two intertidal microphytobenthos communities. *Estuarine, Coastal and Shelf Science*. **119**: 112-118.

Wall GR, Phillips PJ, Riva-Murray K. (1998). Seasonal and spatial patterns of nitrate and silica concentrations in Canajoharie Creek, New York. *Journal of Environmental Quality*. **27**: 381-389.

Wasserman RJ, Vink TJF, Dalu T, Froneman PW (2015) Fish predation regimes modify benthic diatom community structures: Experimental evidence from an in situ mesocosm study. *Austral Ecology*. DOI:10.1111/aec.12255.

WaterConnect (2014). River Murray Flow Reports.

Waters RL, Mitchell JG, Seymour J (2003) Geostatistical characterisation of centimetre-scale spatial structure of in vivo fluorescence. *Marine Ecology Progress Series*. **251**: 49-58.

Webster IT. (2005). An overview of the hydrodynamics of the Coorong and Murray Mouth: Water levels and salinity – key ecological drivers C.W.f.a.H.C.N.R. Flagship. (Canberra), 23 pp.

- Webster IT. (2010). The hydrodynamics and salinity regime of a coastal lagoon – The Coorong, Australia – Seasonal to multi-decadal timescales. *Estuarine, Coastal and Shelf Science*. **90**: 264-274.
- Wilke A, Bischof J, Gerlach W, Glass E, Harrison T, Keegan KP, Paccizian T, Trimble WL, Bagchi S, Grama A, Chaterji S, Meyer F. (2015) The MG-RAST metagenomics database and portal in 2015. *Nucleic Acids Research*. doi: 10.1093/nar/gkv1322
- Wilkinson C. (2005). Common Macroalgae of South Australia South A.S.Q.A. Program.
- Winder M, Reuter JE, Schladow SG. (2009). Lake warming favours small-sized planktonic diatom species. *Proceedings of the Royal Society B*. **276**: 427-435.
- Wright DT, Wacey D. (2005). Precipitation of dolomite using sulphate-reducing bacteria from the Coorong Region, South Australia: significance and implications. *Sedimentology*. **52**: 987-1008.
- Wyatt T. (2014) Margalef's mandala and phytoplankton bloom strategies. *Deep Sea Research Part II: Topical Studies in Oceanography*. **101**: 32-49.
- Xia LC, Steele JA, Cram JA, Cardon ZG, Simmons SL, Vallino JJ, Fuhrman JA, Sun F. (2011) Extended local similarity analysis (eLSA) of microbial community and other time series data with replicates. *BMC Systems Biology*. **5**(2): 1.
- Xu Y, Vick-Majors T, Morgan-Kiss R, Priscu JC, Amaral-Zettler L (2014) Ciliate Diversity, Community Structure, and Novel Taxa in Lakes of the McMurdo Dry Valleys, Antarctica. *The Biological Bulletin*. **227**: 175-190.
- Zar JH. (1999). Biostatistical Analysis, 4th Edition. (Prentice-Hall, Inc. Upper Saddle River, NJ).

Zhang L, Melø TB, Li H, Naqvi KR, Yang C. (2014) The inter-monomer interface of the major light-harvesting chlorophyll a/b complexes of photosystem II (LHCII) influences on the chlorophyll triplet distribution. *Journal of Plant Physiology*. **171**(5): 42-48.

Zimmerman EK, Cardinale BJ. (2014) Is the relationship between algal diversity and biomass in North American lakes consistent with biodiversity experiments? *Oikos*. **123**: 267-278.

APPENDICES

Appendix I

The following publication is manuscripts the author contributed to during her candidature in which she developed techniques and concepts that contributed to her thesis:

Leterme SC, **Prime E**, Mitchell J, Brown M, Ellis A. (2013). Diatom adaptability to environmental change: a case study of two *Cocconeis* species from high-salinity areas. *Diatom Research*. **28**(1): 29-35.

Diatom adaptability to environmental change: a case study of two *Cocconeis* species from high-salinity areas

SOPHIE C. LETERME^{1,2,*}, ELOISE PRIME¹, JIM MITCHELL¹, MELISSA H. BROWN¹ & AMANDA V. ELLIS³

¹School of Biological Sciences, Flinders University, Adelaide, Australia

²South Australian Research and Development Institute, Aquatic Sciences, West Beach, Australia

³Flinders Centre for Nanoscale Science and Technology, School of Chemistry and Physical Sciences, Flinders University, Adelaide, Australia

This paper investigates the impact of natural change in salinity on the morphological plasticity of diatom frustules. In particular, this study uses as an example the highly saline lagoons of the Coorong wetlands in South Australia. These wetlands have been strongly impacted by the drought in South Australia (2004–2010) which has resulted in a salinity gradient of 40 to 134 psu along the wetlands. In this framework, the impact of some environmental variables (i.e., dissolved oxygen, pH, turbidity, salinity, temperature and nutrients) was investigated on the nanoscale features characterizing the cell wall of two diatom species, *Cocconeis placentula* Ehrenberg and *C. pinnata* Gregory. The results suggest that not only salinity, but also nutrient concentration play a significant role in the morphological plasticity of the frustule of these two diatom species. It is proposed that the morphological plasticity of the diatom frustules is species-specific and related to their immediate surrounding environmental conditions.

Keywords: diatom, nanostructure, plasticity, salinity, nutrients

Introduction

Over the last two decades, there has been a growing appreciation of the role of ecologically relevant planktonic communities in aquatic ecosystems (Tréguer et al. 1995, Buesseler et al. 1998, Irigoien et al. 2002, Ianora et al. 2004, 2011). Phytoplankton communities, which are mostly composed of single-celled algae, support the basis of marine and freshwater food webs (Tanner et al. 1999, Leterme et al. 2005, Edwards et al. 2006, Huertas et al. 2011). The composition of phytoplankton communities fluctuates depending on environmental conditions, such as light, temperature, salinity, pH, nutrients and turbulence (Trigueros & Orive 2001, Leterme et al. 2005, 2006). Diatoms are typically present in marine communities; however, other microalgal groups can dominate depending on the combination of environmental conditions, as well as seasonal and climatic variability (Trigueros & Orive 2000, Bernardi Aubry et al. 2004, Leterme et al. 2005). Changes in dominant taxa (e.g., diatoms vs. flagellates) can modify entirely the trophic system (e.g., Trigueros & Orive 2001, Pedrós-Alió 2003, Mieleitner et al. 2007, Ardyna et al. 2011) and such changes will propagate up the food chain, influencing higher levels like zooplankton and fish (Edwards & Richardson 2004, Richardson & Schoeman 2004, Hays et al. 2005, Hobday et al. 2006). Only recently, attention started being paid to the processes controlling the dynamics of phytoplankton

community composition in extreme environments such as solar salterns (Estrada et al. 2004) and polar regions (Montes-Hugo et al. 2009).

The morphological integrity of the diatom frustule is based upon a siliceous backbone. It has been suggested that the silica frustules of diatoms are modified under fluctuating salinities (Parkinson & Gordon 1999, Vrieling et al. 2007, Leterme et al. 2010). In particular, Parkinson & Gordon (1999) suggested that the pore size could be a function of temperature and of the surface properties of the precipitating molecules, as well as salt. In addition, Vrieling et al. (2007) found that at lower salinity the specific surface area and pore size of *Thalassiosira punctigera* Castracane (strain CCRUGT-punct) and *T. weissflogii* Grunow (strain CCRUGT-weiss) decreased. Finally, Leterme et al. (2010) showed from *in situ* samples from the Coorong wetlands of South Australia that the pore size of *Cocconeis placentula* Ehrenberg decreased with decreasing salinity levels. These studies demonstrated the remarkable degree of morphological plasticity that diatoms possess and which might explain their ecological success in such environments.

The main objective of this study is assessing the influence of a salinity gradient on the nanoscale features of two diatom species, *C. placentula* and *C. pinnata* Gregory, from the Coorong wetland in southern Australia. In particular, this paper investigates conditions such as high salinity.

*Corresponding author. Email: sophie.leterme@flinders.edu.au

(Received 2 January 2012; accepted 9 August 2012)

ISSN 0269-249X print/ISSN 2159-8347 online

© 2013 The International Society for Diatom Research

<http://dx.doi.org/10.1080/0269249X.2012.734530>

<http://www.tandfonline.com>

Material and methods

Environmental parameters

The Coorong is a long, shallow lagoon >100 km in length which is separated from the Southern Ocean by a narrow sand dune peninsula. The salinity of the Coorong has increased dramatically because of the lack of water inflow due to the construction of barrages further up the Murray River (Nayar & Loo 2009), but also due to the recent 2004–2010 drought (Zampatti *et al.* 2010). This lagoon, parallel to the coast, is separated from the open ocean by a network of sand dunes (Webster 2005), except at the Murray River mouth. The saline waters of the Coorong receive inputs from the ocean through the Murray River mouth and are separated from the lower lakes Alexandrina and Albert by a series of barrages, which can be used to regulate the water exchange between the lakes and the sea (Fig. 1). The irregular freshwater releases through the barrages have led to decreased salinities in the northwest part of the Coorong, whereas the excess in evaporation over precipitation increases salinity along the north–south axis (Nayar & Loo 2009).

Five stations (S1–S5; Fig. 1) were monitored along the 100-km long Coorong wetlands in February, March and May 2008. At each sampling site, measurements and water sample collection were performed within sub-surface waters. Temperature, salinity and dissolved oxygen (DO) concentrations were recorded *in situ* using a

90FL-T multiparameter probe (TPS, Australia). Dissolved inorganic nutrient concentrations were determined from 100 mL filtered (Whatman GF/C) water samples, stored at -20°C in the dark and analysed within 72 h using a portable LF 2400 photometer (AquaspeX[®], Australia) according to standard colorimetric methods (Crompton 2006) for ammonium (NH_4^+) using indophenol blue, nitrite (NO_2^-) using naphthylethylene diamine, nitrate (NO_3^-) using naphthylethylene diamine after zinc reduction, phosphate (PO_4^{3-}) using ascorbic acid reduction and silicic acid ($\text{Si}(\text{OH})_4$) using heteropoly blue.

Diatom species

At each station, phytoplankton was collected using a 10- μm mesh size plankton net towed horizontally on foot to obtain concentrated samples. Ten phytoplankton replicates were collected per station and sampling date. The organic material of the diatoms was removed using sulfuric acid (Losic *et al.* 2006) and subsequently rinsed several times with distilled water prior to electron microscopical examination. Clean diatom samples were then filtered on GF/C Whatman filters and mounted onto aluminium stubs using carbon tape and sputter coated using a Cressington 208 High Resolution Sputter Coater (Cressington, UK) with a complete layer of platinum (10 nm) for observation using a field-emission scanning electron microscope (FESEM). Images were acquired using a Phillips XL30 FESEM (Philips Electronics, Andover, USA) operated at 5–10 kV. The only diatom species present on most of the samples from the Coorong wetland stations were *C. placentula* and *C. pinnata* (Fig. 2). There were no *C. placentula* recorded from stations S2 and S4 in February, and no *C. pinnata* from station S5 in March and May. Therefore, *C. placentula* was studied at only three stations in February (S1, S3, S5 with a salinity of 68, 101 and 134, respectively) and *C. pinnata* at four stations in March (m) (S1, S2, S3, S4 with a salinity of 54, 57, 91 and 109, respectively) and May (M) (S1, S2, S3, S4, with a salinity of 40, 41, 48 and 54, respectively). This sampling reflects the natural changes of salinity in the Coorong wetlands between summer and autumn.

Preparation of samples and FESEM

The architecture and distribution of the pores at the surface of the frustules was determined using FESEM (Fig. 2). From each sample, we measured 20 pores on each diatom frustule and repeated the operation on 20 more frustules for each species and at each station which corresponded to the measurement of a total of ca. 400 pores per station for each species. For each individual diatom, the size of the frustules and pores were measured from the FESEM images using MOTIC images plus 2.0 software. The size of the frustules and pores were determined by the following surface area

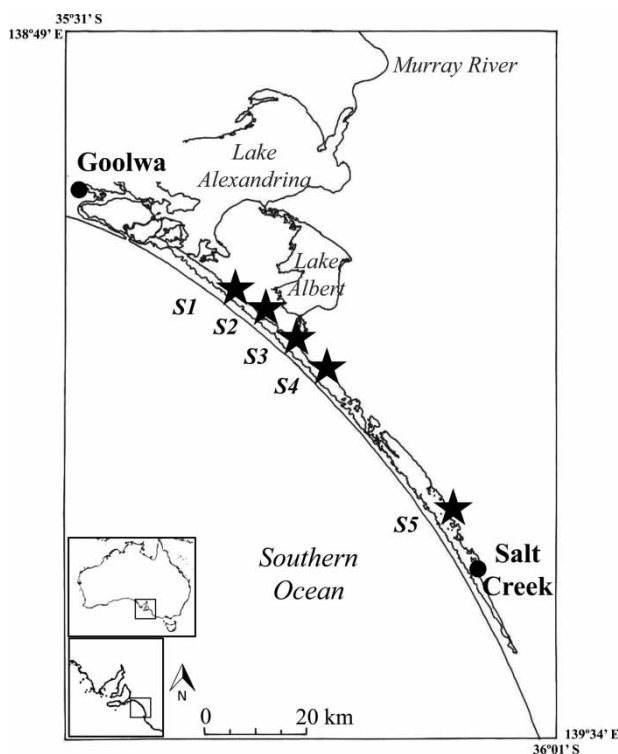


Fig. 1. Location of the five stations (S1 to S5) along the Coorong wetlands in South Australia sampled in February, March and May 2008.

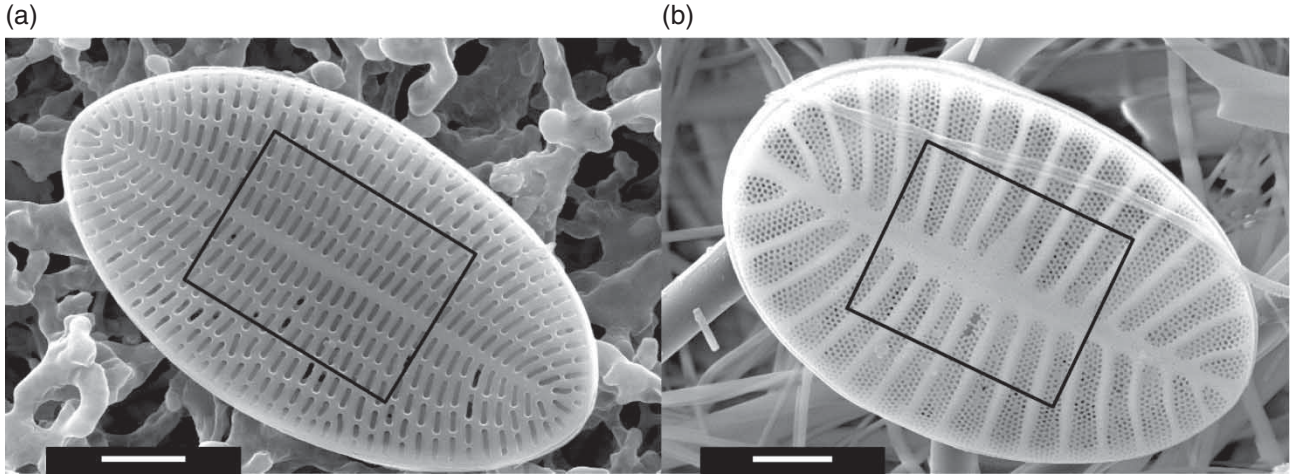


Fig. 2. FESEM image of the external valve of (A) *Cocconeis placentula* and (B) *Cocconeis pinnata*. Pore measurements were randomly selected from the same area of each diatom frustule (i.e., at the centre of the striae, where the apical and transapical axes met), indicated by a black rectangle. Scale bars = 2 μ m.

(S) equation:

$$S = \pi \times L/2 \times W/2$$

where π is a constant, L is the length of the frustule (or pore) and W is the width of the frustule (or pore). All pores were randomly selected from the same area of each diatom frustule (i.e., at the centre of the striae, where the apical and transapical axes met), for measurement in order to reduce possible variability in measurements due to the location on the frustule (Fig. 2).

Statistical analysis

As the data did not show a normal distribution (Kolmogorov–Smirnov, $p < 0.05$), comparison between stations was conducted using the Kruskal–Wallis non-parametric test with a Scheffe post hoc procedure for multiple comparisons using SPSS, v 18.0 (Zar 1999). In addition, the changes in the pore hole size (PHS) and the entire frustule surface area (FSA) of the diatoms monitored along the salinity gradient were tested through Spearman coefficient of rank correlation (Zar 1999). In order to test if the fluctuations in PHS and FSA could be explained by environmental variables, distance-based redundancy analysis (dbRDA) was used. The dbRDA method is a multivariate multiple regression of principal coordinate (PCO) axes on predictor variables where the routine finds linear combinations of the predictor variables (here the environmental parameters) that explain the greatest variability in a data cloud (here the PHS and FSA) (Anderson et al. 2008).

Results

A significant salinity increase (Spearman, $p < 0.05$) was observed which confirmed the presence of a spatial salinity gradient along the five stations of the Coorong wetlands

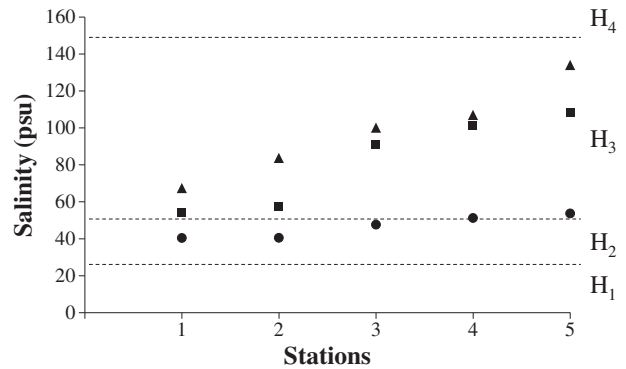


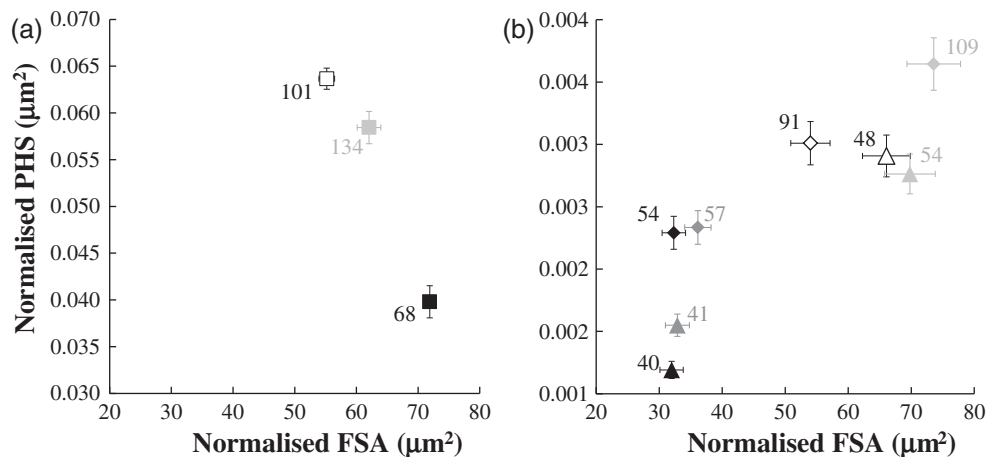
Fig. 3. Variation in subsurface salinity (S) levels at five stations along the Coorong wetlands in South Australia in February (triangle), March (box) and May (circle) 2008. Identification of four salinity-based habitats: H₁, brackish ($S < 25$); H₂, low salinity ($25 < S < 50$); H₃, high salinity ($50 < S < 150$); H₄, hypersaline ($S > 150$).

(Fig. 3). The size range of FSA and PHS recorded for both species at each salinity level is presented in Table 1. Based on 400 pore measurements at each station, the PHS of both species increased significantly along the salinity gradient (Spearman, $p < 0.05$; Fig. 4). Interestingly, a significant increase in the FSA of *C. pinnata*, as opposed to a decrease for *C. placentula*, was observed along the salinity gradient (Spearman, $p < 0.05$; Fig. 4). When the PHS and FSA of both species were compared between each station, significant differences (Kruskal–Wallis, $p < 0.05$) were observed.

The dbRDA diagrams showed clear differences in the morphology of the two species, where the *C. pinnata* cluster on the left is separated from the *C. placentula* cluster on the right (Fig. 5A,C). The dbRDA clustering explains 76.4% of the total variance in the FSA between the two species (Fig. 5A). The environmental variables responsible for the

Table 1. Size range recorded for the surface area of the frustules (FSA) and pore hole size (PHS) of *Cocconeis placentula* and *C. pinnata* for the corresponding salinity level measured at five stations along the Coorong wetlands in South Australia in February, March and May 2008.

Species	Station	Month	Salinity (psu)	FSA (μm^2)	PHS ($10^{-2} \mu\text{m}^2$)
<i>C. placentula</i>	1	February	68	37.4–179.9	2.2–10.4
	3	February	101	28.8–105.9	3.7–14.2
	5	February	134	22.0–131.7	2.0–14.3
<i>C. pinnata</i>	1	May	40	16.3–80.1	0.1–0.6
		March	54	10.7–80.1	0.1–0.4
	2	May	41	12.7–82.0	0.0–0.5
		March	57	14.5–71.3	0.1–0.4
	3	May	48	34.9–93.6	0.1–0.6
		March	91	15.3–156.8	0.1–0.6
	4	May	54	30.6–131.3	0.1–0.6
		March	109	34.2–143.6	0.2–0.8

**Fig. 4.** Scatter plots of the normalized frustule surface area (FSA) and pore hole size (PHS) (mean \pm standard error) of *C. placentula* (A) and *C. pinnata* (B) based on 400 measurements at each of the sampled station. *Cocconeis placentula* (A) was present at three stations: S1 (black), S3 (white) and S5 (light grey), and *C. pinnata* (B) at four stations: S1 (black), S2 (dark grey), S3 (white) and S4 (light grey) in March (losanges) and May (triangle). Salinity is indicated next to the data point.

clustering of the FSA data between the two species (Fig. 5A) are NH_4^+ and DO, while those responsible for the scattering of the FSA data along the y -axis are salinity and turbidity. The dbRDA clustering explains 94.7% of the total variance in the PHS between the two species (Fig. 5C). As observed for FSA, the environmental variable responsible for the clustering of PHS between the two species (Fig. 5C) is DO, while on the y -axis, NO_2^- and NH_4^+ concentrations and salinity are responsible for the clustering. When only focusing on the morphology of *C. pinnata*, the dbRDA diagram (Fig. 5B) showed clear differences in FSA, with stations 1 (mS1, MS1) and 2 (mS2, MS2) grouped together, while stations 3 (mS3, MS3) and 4 (mS4, MS4) grouped together. The dbRDA clustering explains 76.7% of the total variance in the FSA of *C. pinnata* (Fig. 5B). Salinity is responsible for the clustering of FSA between stations (Fig. 4B) while the scattering of the data cloud along the y -axis is linked to the nutrient concentrations (NO_2^- , NH_4^+ , PO_4^{3-}). Finally,

the dbRDA on the PHS of *C. pinnata* (Fig. 5D) showed data scattering along the x -axis and the environmental factors responsible for that scattering are salinity and NO_2^- . The dbRDA clustering explains 83.3% of the total variance in the PHS of *C. pinnata* (Fig. 5D). In addition, the data from S2 showed a different pattern in May (MS2) and their separation from the data cloud along the y -axis is linked to NH_4^+ . None of the scattering of data for the different morphological parameters was linked to PO_4^{3-} or silicic acid $\text{Si}(\text{OH})_4$.

Discussion

The architecture of the diatom frustules is highly species-specific and shows fundamental morphological differences including the geometric arrangement of pores (Losic *et al.* 2006). These pores allow for nutrients and other chemicals

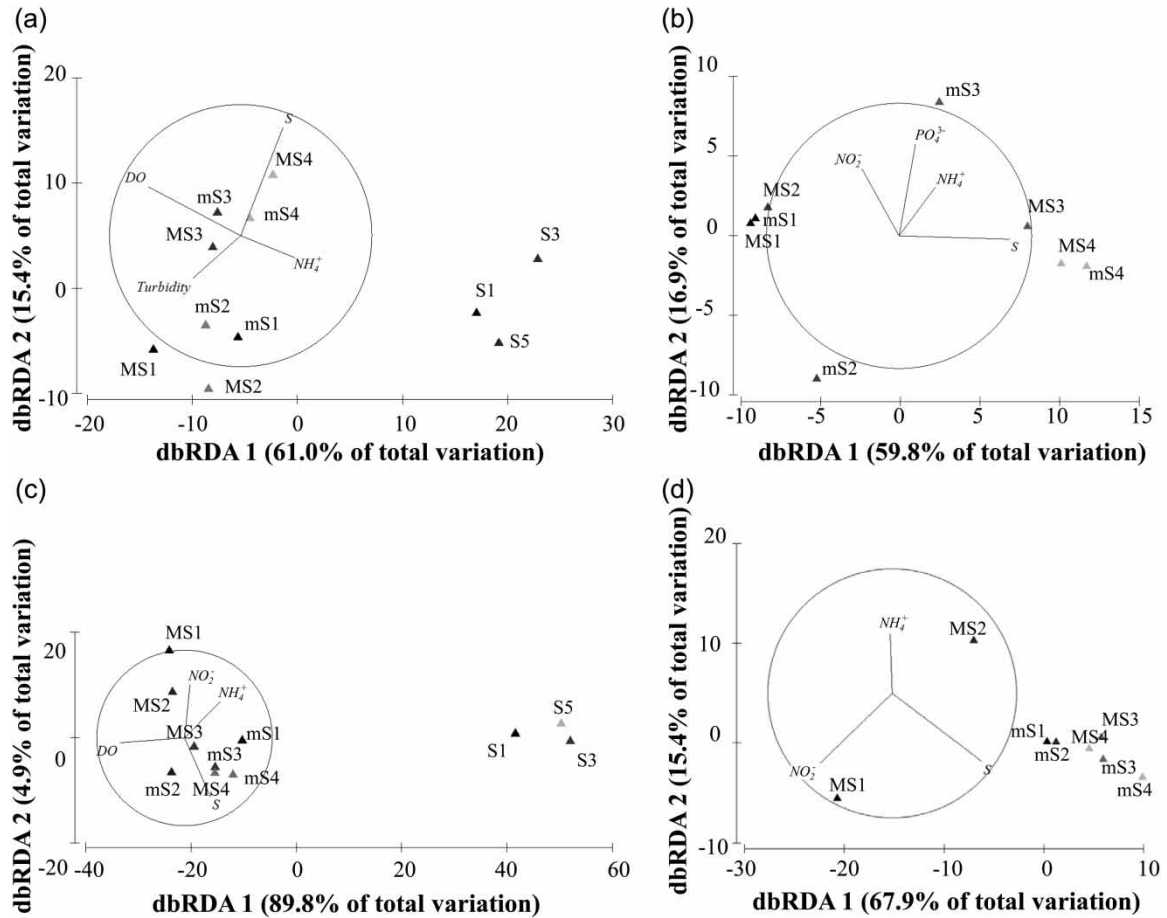


Fig. 5. Distance-based redundancy analysis diagrams representing the relationship between frustule surface area (A, B) and pore hole size (C, D), and the environmental variables, e.g., salinity (S), turbidity, dissolved oxygen (DO), and ammonium (NH_4^+), nitrite (NO_2^-) and phosphate (PO_4^{3-}) performed on both species (A, C) with *C. placentula* sampled at stations S1, S3 and S5 in February, and *C. pinnata* sampled at S1–S4 in March (m) and May (M), and then on *C. pinnata* only (B, D). The circle on each dbRDA diagram is a unit circle whose relative size and position of origin is arbitrary to the underlying plot. Each vector begins at the origin of the circle and ends in the coordinates consisting of the Spearman rank correlations between that environmental variable and each of the dbRDA axes. The length and direction of each vector indicate the strength and sign, respectively, of the relationship between that environmental variable and the dbRDA axes.

to exchange between the internal cell and the external environment and are, therefore, important features for diatom growth. Here, an increase in the PHS of *C. pinnata* and *C. placentula* with increasing salinity was observed. This change in diatom PHS has been previously demonstrated in laboratory experiments (Vrieling et al. 2007). These authors focused on narrow ranges of salinity (i.e., 20 to 33 psu), while our study shows that diatom growth may not be limited to narrow ranges of salinity as it was previously thought (Kröger 2007). In addition, the FSA of *C. pinnata* increased with increasing salinity, whereas the FSA of *C. placentula* decreased with increasing salinity (Fig. 4). This inconsistent direction of change in morphological characteristics has been previously reported by Trobajo et al. (2011) who conducted salinity experiments on various species of *Nitzschia* Hassall. Previous studies have suggested a species-specific pattern formation of the frustules dependent on their genetic basis (Zurzolo & Bowler 2001). This is in concordance

with Trobajo et al. (2004) who proposed that the effect of salinity on the morphology of pennate diatoms (e.g., *Cocconeis* Ehrenberg and *Nitzschia*) could be taxon- and/or clone-specific.

In our study, we indeed observed differences in the FSA of *C. pinnata* between sites, which would corroborate this hypothesis. For example, a clear differentiation of FSA for *C. pinnata* between S1–S2 and S3–S4 was observed (Fig. 5B), which was driven by salinity and nutrients. The physiology and morphogenesis of diatoms depend on processes linked to cell organelles such as the silica deposition vesicle (Vrieling et al. 2007). Current research indicates that salinity, light, pH, nutrients, temperature, silicate concentration, and the availability of salts and cations influence the mineralization of silica in the cell walls (Brzezinski 1985, Blank et al. 1986). Here, some of these environmental variables were considered (i.e., salinity and nutrients) and these results suggest that they influence both the FSA

and PHS of natural *C. pinnata*. Previous studies have shown that diatoms have the ability to react rapidly to environmental changes (Smith & Flocks 2010, Smol & Storermer 2010, Gerecke *et al.* 2011). In addition, Huysman *et al.* (2010) suggested that cell-cycle regulation in diatoms has evolved to adequately integrate various environmental signals. Diatoms have then been shown to possess sophisticated perception systems at a cellular level. In particular, Falcatore *et al.* (2000) showed that diatoms can detect and respond to physico-chemical changes in their environment using perception systems based on changes in cytosolic calcium concentrations. In addition, diatoms use chemical signaling for cell-cell communication to induce resistance or death of the cells depending on the stressors perceived by the cells during phytoplankton blooms (Gross 2006). Based on those findings and our work, more investigations are needed to understand the molecular and physiological adaptations behind the morphological plasticity of diatoms. In particular, more research is required to further understand how cell-cycle regulation allows for these morphological changes to occur and, in particular, how diatoms take up silica in order to regulate their resulting nanostructure. This knowledge is paramount to understanding global biochemical processes given that diatoms are seen as the main players in biogeochemical cycles (Buesseler *et al.* 1998) and are the primary cyclers of silica in the ocean (Tréguer & Pondaven 2000).

Acknowledgements

We thank D. Losic for feedback on sample preparation and FESEM methodology. We acknowledge funding of two Discovery projects from the Australian Research Council to Sophie C. Leterme and Jim G. Mitchell.

References

- ANDERSON M.J., GORLEY R.N. & CLARKE K.R. 2008. *PERMANOVA+ for PRIMER: guide to software and statistical methods*. PRIMER-E, Plymouth. 214 pp.
- ARDYNA M., GOSSELIN M., MICHEL C., POULIN M. & TREMBLAY J.-E. 2011. Environmental forcing of phytoplankton community structure and function in the Canadian High Arctic: contrasting oligotrophic and eutrophic regions. *Marine Ecology Progress Series* 442: 37–57.
- BERNARDI AUBRY E., BERTON A., BASTIANINI M., SOCAL G. & ACRI F. 2004. Phytoplankton succession in a coastal area of the NW Adriatic, over a 10-year sampling period (1990–1999). *Continental Shelf Research* 24: 97–115.
- BLANK G.S., ROBINSON D.H. & SULLIVAN C.W. 1986. Diatom mineralization of silicic acid. VIII. Metabolic requirements and the timing of protein synthesis. *Journal of Phycology* 22: 382–389.
- BRZEZINSKI M.A. 1985. The Si:C:N ratio of marine diatoms: inter-specific variability and the effect of some environmental variables. *Journal of Phycology* 21: 347–357.
- BUESSELER K., BALL L., ANDREWS J., BENITEZ-NELSON C., BELASTOCK R., CHAI F. & CHAO Y. 1998. Upper ocean export of particulate organic carbon in the Arabian Sea derived from thorium-234. *Deep-Sea Research II* 45: 2461–2487.
- CROMPTON T.R. 2006. *Analysis of seawater: a guide for the analytical and environmental chemist*. Springer-Verlag, Berlin. 510 pp.
- EDWARDS M. & RICHARDSON A.J. 2004. Impact of climate change on marine pelagic phenology and trophic mismatch. *Nature* 430: 881–884.
- EDWARDS M., JOHNS D.G., LETERME S.C., SVENDSEN E. & RICHARDSON A.J. 2006. Regional climate change and harmful algal blooms in the northeast Atlantic. *Limnology and Oceanography* 51: 820–829.
- ESTRADA M., HENRIKSEN P., GASOL J.M., CASAMAYOR E.O. & PEDRÓS-ALÍO C. 2004. Diversity of planktonic photoautotrophic microorganisms along a salinity gradient as depicted by microscopy, flow cytometry, pigment analysis and DNA-based methods. *FEMS Microbiology Ecology* 49: 281–293.
- FALCIATORE A., RIBERA D'ALCALÀ M., CROOT P. & BOWLER C. 2000. Perception of environmental signals by a marine diatom. *Science* 288: 2363–2366.
- GERECKE R., CANTONATI M., SPITALE D., STUR E. & WIEDENBRUG S. 2011. The challenges of long-term ecological research in springs in the northern and southern Alps: indicator groups, habitat diversity, and medium-term change. *Journal of Limnology, Supplement* 70: 168–187.
- GROSS L. 2006. Diatoms rely on sophisticated signaling systems for population control. *PLoS Biology* 4: e89, DOI:10.1371/journal.pbio.0040089.
- HAYS G.C., RICHARDSON A.J. & ROBINSON C. 2005. Climate change and marine plankton. *Trends in Ecology and Evolution* 20: 337–344.
- HOBDAJ A.J., OKEY T.A., POLOCZANSKA E.S., KUNZ T.J. & RICHARDSON A.J. 2006. *Impacts of climate change on Australian marine life: part C. Literature review*. Report to the Australian Greenhouse Office, Canberra, 167pp.
- HUERTAS I.E., ROUCO M., LÓPEZ-RODAS V. & COSTAS E. 2011. Warming will affect phytoplankton differently: evidence through a mechanistic approach. *Proceedings of the Royal Society, Biological Sciences* doi: 10.1098/rspb.2011.0160.
- HUYSMAN M.J.J., MARTENS C., VANDEPOELE K., GILLARD J., RAYKO E., HELJDE M., BOWLER C., INZÉ D., PEER Y.V., DE VEYLDER L. & VYVERMAN W. 2010. Genome-wide analysis of the diatom cell cycle unveils a novel type of cyclins involved in environmental signaling. *Genome Biology* 11: R17.
- IANORA A., MIRALTO A., POULET S.A., CAROTENUTO Y., BUTTINO I., ROMANO G., CASOTTI R., POHNERT G., WICHARD T., COLUCCI-D'AMATO L., TERRAZZANO G. & SMETACEK V. 2004. Aldehyde suppression of copepod recruitment in blooms of a ubiquitous planktonic diatom. *Nature* 429: 403–407.
- IANORA A., BENTLEY M.G., CALDWELL G.S., CASOTTI R., CEMBELLA A.D., ENGSTRÖM-ÖST J., HALSBAND C., SONNENSCHNEIN E., LEGRAND C., LLEWELLYN C.A., PALDAVIČIENĖ A., PILKAITYTE R., POHNERT G., RAZINKOVAS A., ROMANO G., TILLMANN U. & VAICIUTE D. 2011. The relevance of marine chemical ecology to plankton and ecosystem function: an emerging field. *Marine Drugs* 9: 1625–1648.
- IRIGOIEN X., HARRIS R.P., VERHEYE H.M., JOLY P., RUNGE J., STARR M., POND D., CAMPBELL R., SHREEVE R., WARD P., SMITH A.N., DAM H.G., PETERSON W., TIRELLI V., KOSKI

- M., SMITH T., HARBOUR D. & DAVIDSON R. 2002. Copepod hatching success in marine ecosystems with high diatom concentrations. *Nature* 419: 387–389.
- KRÖGER N. 2007. Prescribing diatom morphology: toward genetic engineering of biological nanomaterials. *Current Opinion in Chemical Biology* 11: 662–669.
- LETERME S.C., SEURONT L. & EDWARDS M. 2006. Differential contribution of diatoms and dinoflagellates to phytoplankton biomass in the NE Atlantic Ocean and the North Sea. *Marine Ecology Progress Series* 312: 57–65.
- LETERME S.C., EDWARDS M., SEURONT L., ATTRILL M.J., REID P.C. & JOHN A.W.G. 2005. Decadal basin-scale changes in diatoms, dinoflagellates, and phytoplankton colour across the North Atlantic. *Limnology and Oceanography* 50: 1244–1253.
- LETERME S.C., ELLIS A.V., MITCHELL J.G., BUSCOT M.-J., POLLET T., SCHAPIRA M. & SEURONT L. 2010. Morphological flexibility of *Cocconeis placentula* (Bacillariophyceae) nanostructure to changing salinity levels. *Journal of Phycology* 46: 715–719.
- LOŠIĆ D., ROSENGARTEN G., MITCHELL J.G. & VOELCKER N.H. 2006. Pore architecture of diatom frustules: potential nanostructured membranes for molecular and particle separations. *Journal of Nanotechnological Sciences* 6: 1–8.
- MIELEITNER J., BORSUK M., BÜRGI H.-R. & REICHERT P. 2007. Identifying functional groups of phytoplankton using data from three lakes of different trophic state. *Aquatic Sciences – Research Across Boundaries* 70: 30–46.
- MONTES-HUGO M., DONEY S.C., DUCKLOW H.W., FRASER W., MARTINSON D., STAMMERJOHN S.E. & SCHOFIELD O. 2009. Recent changes in phytoplankton communities associated with rapid regional climate change along the western Antarctic Peninsula. *Science* 323: 1470–1473.
- NAYAR S. & LOO, M.G.K. 2009. *Phytoplankton and phyto-benthic productivity along a salinity gradient in the Coorong and Murray Mouth*. CSIRO: Water for a Healthy Country National Research Flagship and South Australian Research and Development Institute (Aquatic Sciences), Adelaide. 19 pp.
- PARKINSON J. & GORDON R. 1999. Beyond micromachining: the potential of diatoms. *Trends in Biotechnology* 17: 190–196.
- PEDRÓS-ALIÓ C. 2003. Trophic ecology of solar salterns. In: *Halophilic microorganisms* (Ed. by A. Ventosa), pp. 34–48. Springer, Berlin.
- RICHARDSON A.J. & SCHOEMAN D.S. 2004. Climate impact on plankton ecosystems in the Northeast Atlantic. *Science* 305: 1609–1612.
- SMITH K.E.L. & FLOCKS J.G. 2010. *Environmental investigations using diatom microfossils*. U.S. Geological Survey Fact Sheet 2010–3115, 2 p.
- SMOL J.P. & STOERMER E.F. 2010. *The diatoms: applications for the environmental and earth sciences*. Cambridge University Press, Cambridge. 482 pp.
- TANNER R., GLENN E.P. & MOORE D. 1999. Flood chain organisms in hypersaline, industrial evaporation ponds. *Water Environment Research* 71: 494–505.
- TRÉGUER P. & PONDAVEN P. 2000. Silica control of carbon dioxide. *Nature* 406: 358–359.
- TRÉGUER P., NELSON D.M., VAN BENNEKOM A.J., DEMASTER D.J., LEYNAERT A. & QUÉGUINER B. 1995. The silica balance in the world ocean: a reestimate. *Science* 268: 375–379.
- TRIGUEROS J.M. & ORIVE E. 2000. Tidally driven distribution of phytoplankton blooms in a shallow, macrotidal estuary. *Journal of Plankton Research* 22: 969–986.
- TRIGUEROS J.M. & ORIVE E. 2001. Seasonal variations of diatoms and dinoflagellates in a shallow, temperate estuary, with emphasis on neritic assemblages. *Hydrobiologia* 444: 119–133.
- TROBAJO R., COX E.J. & QUINTANA X.D. 2004. The effects of some environmental variables on the morphology of *Nitzschia frustulum* (Bacillariophyta), in relation its use as a bioindicator. *Nova Hedwigia* 79: 433–445.
- TROBAJO R., ROVIRA L., MANN D.G. & COX E.J. 2011. Effects of salinity on growth and on valve morphology of five estuarine diatoms. *Phycological Research* 59: 83–90.
- VRIELING E.G., SUN Q., TIAN M., KOOYMAN P.J., GIESKES W.W.C., VAN SANTEN R.A. & SOMMERDIJK N.A.J.M. 2007. Salinity-dependent diatom biosilicification implies an important role of external ionic strength. *Proceedings of the National Academy of Sciences of the United States of America* 104: 10441–10446.
- WEBSTER I.T. 2005. *An overview of the hydrodynamics of the Coorong and Murray Mouth: water levels and salinity – key ecological drivers*. CSIRO Water for a Healthy Country National Research Flagship, Canberra. 23 pp.
- ZAMPATTI B.P., BICE C.M. & JENNINGS P.R. 2010. Temporal variability in fish assemblage structure and recruitment in a freshwater-deprived estuary: the Coorong, Australia. *Marine and Freshwater Research* 61: 1298–1312.
- ZAR J.H. 1999. *Biostatistical analysis*. Prentice Hall International Editions, New York. 663 pp.
- ZURZOLO C. & BOWLER C. 2001. Exploring bioinorganic pattern formation in diatoms. A story of polarized trafficking. *Plant Physiology* 127: 1339–1345.

Appendix II

The following references are conference presentations that the author contributed to during her candidature in which she developed techniques and concepts that contributed to her thesis.

Oral Presentations

1. **Prime E** (2015) Large- and Microscale Variation of Phytoplankton Communities, Oral Presentation: Flinders University Postgraduate Conference 2015. Adelaide, Australia.
2. **Prime E** (2014) Microscale Variation in the Microphytobenthos, Oral Presentation: Flinders University Postgraduate Conference 2014. Adelaide, Australia.
3. Leterme SC, **Prime E**, Ellis AV, Mitchell JG & Seuront L (2009) Morphological Flexibility of *Cocconeis sp.* Nanostructure along a Natural Salinity Gradient. Marine Connectivity, Australian Marine Science Association International Conference, 5-9 July 2009, Adelaide, Australia.
4. Leterme S.C., **Prime E.**, Ellis A.V., Mitchell J.G. & Seuront L. (2009) Morphological flexibility of *Cocconeis sp.* nanostructure along a natural salinity gradient. *AGU-ASLO-TOS Ocean Sciences Meeting, January 2009, Nice, France.*

Posters

1. **Prime E**, Newton K, Paterson J, Duan Y, Mitchell JG (2014) ‘Microscale Variation of Diatom Length in the Microphytobenthos’. Poster Presentation. International Symposium on Microbial Ecology – ISME 15. Seoul, South Korea.

2. Leterme S.C., Ellis A.V., Brown M.H., Mitchell J.G., Prime E. & Smith-Harding T. (2010) Morphological flexibility of *Cocconeis sp.* nanostructure along a natural salinity gradient. *AMSA (Australian marine Sciences Association), July 2010, Wollongong, Australia.*
3. Newton K, Chapperon C, **Prime E**, Jeffries TC, Paterson JS, van Dongen-Vogels V, Leterme S, Mitchell JG and Seuront L (2010) Elucidation of Matter and Energy Pathways in Aquatic Food Webs. Annual Scientific Meeting and Exhibition of the Australian Society for Microbiology. Sydney, Australia
4. Newton K, Chapperon C, **Prime E**, Jeffries, TC, Patterson J, van Dongen-Vogels V, Leterme S, Mitchell JG and Seuront L (2010) Differential Mortality of Bacterial Sub-populations. Poster presentation: 13th International Symposium of the International Society for Microbial Ecology. Seattle, USA
5. Newton K, Chapperon C, **Prime E**, Jeffries, TC, Patterson J, van Dongen-Vogels V, Leterme S, Mitchell JG and Seuront L (2009) Assessment of the effect of salinity on viral lysis and microzooplankton grazing on flow cytometrically-defined sub-population of heterotrophic bacteria in a coastal lagoon, The Coorong. 46th Annual Conference of the Australian Marine Sciences Association. Adelaide, Australia
6. **Prime E**, Leterme SC, Mitchell JG (2009) Diatom structures along a salinity gradient. 46th Annual Conference of the Australian Marine Sciences Association. Adelaide, Australia